UNIVERSITY OF SOUTHAMPTON

Nonlinear Surface Acoustic Waves and Applications

ALAN PAUL HARVEY

Acknowledgments

As always in the production of a thesis there are many people who deserve my most gracious thanks for their support and encouragement. I apologise for not mentioning everyone explicitly but feel that there are some that deserve special thanks.

First and foremost, thanks go to my supervisors Dr R.E. Craine and Dr S. Syngellakis for their guidance throughout the three years of my study at Southampton and the subsequent 18 months of long distance preparation. I also thank Professor D.F. Parker, Dr E.A. David, Dr Y. Cho and Dr H. Grassl for some constructive discussion *en route*.

Dr G.E. Tupholme has provided a constant source of discussion and guidance and must be thanked for urging me to finally completing the project.

I must acknowledge my colleagues at Cambridge University Press for consistently turning a blind eye to my extended use of office computers, printers and general facilities.

Finally thanks go both to my parents and to Soosan Oldroyd who have patiently put up with the irritability and general lack of consideration induced throughout the preparation of this final typescript. A greater thanks is also due to Soosan for sticking together the majority of the figures in the text.

Contents

UNIVERSITY OF SOUTHAMPTON

ABSTRACT

FACULTY OF MATHEMATICS
DEPARTMENT OF APPLIED MATHEMATICS

Doctor of Philosophy

Nonlinear Surface Acoustic Waves and Applications

by Alan Paul Harvey

The recent interest in the nonlinear propagation of surface acoustic waves has been generated by developments in acoustic wave signal processing devices. This thesis extends the multiple scales analyses of Kalyanasundaram (Int. J. Engng. Sci. 19, p.279) and Lardner (Int. J. Engng. Sci. 21, p.1331) to consider the effects of anisotropy upon the propagation characteristics of surface acoustic waves. Evolution equations are derived for the harmonic amplitudes which are then solved for cubically anisotropic materials.

The constitutive and field equations governing the deformation of a piezoelectric substrate are then derived and the analysis of anisotropic elasticity is extended to consider the propagation of surface waves on a general piezoelectric substrate. Harmonic growth and decay on the commonly used material substrate, lithium niobate, are presented and display transfer of energy between the fundamental frequency and the nonlinearly generated harmonic frequencies.

The two cases of oppositely propagating and co-directional waves are considered in the particular configurations of acoustic devices. Numerical routines are used to calculate the efficiency of the degenerate acoustic convolver and harmonic generation assessed in such devices. The interaction of harmonic frequencies of co-directional waves, known as intermodulation distortion, is explored and evolution equations derived and solved for such frequencies.

1 Introduction

It is now nearly a century since Rayleigh [1896] first proposed the existence of surface waves. The intervening years have seen interest in such waves, whose pure modes are known as Rayleigh waves, develop into a thriving area of research, not only for mathematical theoreticians but also for experimentalists in topics as diverse as non-destructive testing and signal processing.

The topic of this thesis is the particular application of surface waves on anisotropic and piezoelectric materials to the problem of signal processing in microelectronics. This problem was initially posed by Plessey, Caswell, as one of current experimental interest that required a mathematical justification. It was intended that this project should bridge the gap between the advancing nonlinear theory of surface waves and the technical innovations applied in the construction of more efficient devices.

There are essentially two backgrounds to this problem. The first is that of acoustic device development which has seen remarkable growth since its inception in the early 1970's. Most reports present results and new device designs achieved through experiment rather than theory. The second is the development of a mathematical theory yielding bounded solutions to the problem of nonlinear surface wave propagation. Much of this work has concentrated upon elastic materials and wave interaction has received little attention. We shall begin by outlining the history of acoustic devices.

There are many occasions in the the design of analogue electric devices when an electric signal is required to be inverted, delayed or encoded in some manner. This may be achieved by any number of techniques including digitization and microprocessor manipulation, however such techniques are often elaborate and costly and it is found that one of the most reliable techniques is that of acoustic wave propagation. In acoustic wave devices the input electric signal is used to generate a propagating wave in a slab of elastic material through some surface transducer. The elastic properties of the substrate are then utilised, possibly

together with interaction with other waves in the substrate, to manipulate the waveform which is then detected by a surface transducer and used to generate a modified output electric signal. Because of the availability of substrate materials and relatively low level of technology necessary for mass production, acoustic wave devices are generally cheap and easy to produce.

The propagation of acoustic waves has been utilised for signal processing since the early 1960s but was mainly confined to bulk and Love wave transmission. The most common operations required of such devices employ the nonlinearities of the material substrate to generate the sum or difference frequencies of two propagating acoustic waves. This facilitates both filtering, eliminating certain frequencies from an input spectrum, and convolution, encoding one input signal through convolution with a second known frequency. Lean and Tseng [1970] have generally been credited with the first extensive study of the nonlinear propagation of surface waves, thus illustrating their suitability for such devices. The main advantage they possess is the very low initial amplitudes necessary to produce detectable nonlinear features. This is because the energy of a surface wave is concentrated within a layer of only a few wavelengths' thickness on the surface of the material. This gives a low power loss to the device and thus a higher efficiency.

Many technological advances have been introduced to the design of acoustic devices to enhance their performance. The most critical factor is power loss to the substrate which usually occurs through the spreading of the wave on the substrate surface. This means that higher input amplitudes are necessary to propagate waves on the substrate. The use of beam compressors to focus the wave along a narrow path overcomes some of these effects, as do waveguides to channel the wave along the output transducer. Reflections at boundaries are also reduced by the inclusion of absorbers at the ends and base of the device.

The mathematical theory developed to predict the response of such devices has mainly consisted of linearised theory with small perturbations revealing the nonlinear behaviour. The most recent, Ganguly and Davis [1980], yields results comparable with experiment to within one order of magnitude. This apparent inaccuracy is accepted by most designers as statistical error and designs modified accordingly.

Lord Rayleigh first proposed the existence of waves whose amplitude decayed exponentially with depth into the material (Rayleigh [1896]). The study of Rayleigh waves was later extended to include what has become known as the "generalised" Rayleigh wave, whose amplitude exhibits exponentially damped sinusoidal decay with depth. Such waves may be found to propagate on anisotropic materials of various symmetry classes. The study of Rayleigh wave propagation on anisotropic

substrates was first considered as an outcome of seismic studies, Stoneley [1955]. The Earth's crust may be considered as a layered anisotropic medium and thus it was felt that generalised surface wave solutions may be found to propagate.

Particular anisotropic elastic symmetry groups admit many analytical decompositions to the governing field equations. This has enabled many researchers to investigate linear anisotropic elasticity on materials from the cubic, hexagonal and orthorhombic classes. Early studies, Buchwald and Davis[1963] and Synge [1956], lead to the quite general statement that surface waves could only be propagated in particular directions within crystals of these classes. This is certainly true of pure Rayleigh modes, however it has since been shown, Stroh [1962] and Currie [1974], that this conclusion arose from a false conjecture regarding the slowness vector and that generalised Rayleigh waves could propagate in all directions. Farnell [1970] used numerical techniques to show that the surface wave in fact degenerates into a bulk wave for certain directions of propagation.

The recent interest in nonlinear acoustic devices has spawned an equally virulent interest in the nonlinear propagation of surface acoustic waves. The problem of isotropic elastic surface waves was considered by Kalyanasudaram [1981]$_a$ applying a technique developed for the study of capillary waves and plate mechanics. Kalyanasundaran considered a number of wave propagation problems with specific applications to acoustic devices such as those of two oppositely propagating waves [1983] and two co-propagating waves [1981]$_b$. These papers set out general methodologies for the solution of such problems that will be utilised in this thesis. Several theoretical limitations of these papers have been pointed out and the method of solution refined by Lardner [1983, 1986] who considered the problems of propagation on both isotropic and anisotropic substrates.

A very different approach was taken by Parker and Talbot [1985] who investigated the possiblity that surface waves whose waveform remained unaltered could propagate on the surface of an isotropic substrate. Conjugate harmonic functions were employed to represent the amplitude form which were later derived through evolution equations. Such permanent form solutions have many applications in the design of efficient devices as well as in the design of transmission lines over large distances.

A coherent theory of nonlinear piezoelectricity was introduced in the pioneering paper of Toupin [1963] which set the scene for subsequent work by Nelson [1979]. These papers set out the governing field equations and constitutive relations for a deformed piezoelectric substrate in terms of the material, or reference, coordinate

system commonly used in the study of elasticity. This is of particular importance in the case of piezoelectricity since the experimental measurements are most commonly performed in the material frame by use of transducers placed in direct contact with the moving material surface. No specific consideration was given in these works to surface wave propagation however Tiersten and Baumhauer [1974] later developed a loose theory for second harmonic generation.

Bleustein and Gulyaev found experimentally that, on particular crystallographic symmetries, it was possible to propagate waves with purely transverse displacement. This was not expected from earlier experience in the propagation of elastic waves since it arises from the coupled nature of the elastic and electric field equations. Kalyanasundaram [1984] extended his analysis of Rayleigh waves to study the nonlinear propagation of so-called Bleustein–Gulyaev waves and derived coupled amplitude equations of an essentially similar form to those arising in isotropic elasticity.

Ganguly and Davis [1980] appear to have been the first to apply a "rigorous" mathematical treatment to the particular problem of nonlinear acoustic wave convolution devices, known as acoustic wave convolvers. The technique applied was a singular perturbation method and they derived the second-order surface potential which was then used to deduce estimates for the electrical efficiency of the device. The errors quoted in any acoustic device calculation are extremely high and it is generally acceptable merely to give order of magnitude results. Ganguly and Davis' results therefore compared favourably with experimental values. Cho and Yamanouchi [1987] later showed that the inaccuracy of their results was, in the most part, due to the inaccuracy of the third-order material constants used.

Much practical work related to realistic device configurations has taken place in France, Maugin [1985], Planat [1985], Planat et al [1985], who have used a number of techniques, including multiple scales and finite element methods, to solve the more complicated problems of wave excitation and waveguides in particular device applications. Whilst finite element methods give solutions satisfying the complete boundary and excitation conditions and may incorporate many features of convolver design, it is felt that very little qualitative information regarding the nonlinear processes of the crystal substrate may be gained from results obtained through this technique.

The intent of this thesis is to extend the multiple scales analysis of nonlinear surface waves presented by Kalyanasundaram [1981] and Lardner [1983] to incorporate the effects of piezoelectricity. The method of multiple scales allows bounded solutions to be obtained that are valid for relatively large propagation distances. This

theory will then be used to asses the effects of nonlinearity upon the performance of particular acoustic devices.

For the purpose of this thesis the problem will be divided into its constituent parts. Firstly we shall consider the problem of surface wave propagation on an anisotropic elastic substrate. This is a problem that has been presented in a number of papers during the course of preparation of this thesis, Lardner [1986], Lardner and Tupholme [1986] and Parker [1988]. It is included in this thesis primarily to display numerical results for particular material symmetries but also to present the notation to be used in subsequent chapters.

Secondly the problem of surface wave propagation on a piezoelectric substrate shall be investigated using the multiple scales technique developed in Chapter 3. A significant notational simplification shall be introduced, allowing the governing constitutive and field equations to be written in a form closely analogous to the equations of motion governing the deformation of a purely elastic substrate. The coupled amplitude equations derived through the method of multiple scales will then be solved using numerical techniques and harmonic amplitude growth and decay discussed. The various assumptions made to simplify the boundary representation will then be studied in detail and amplitude propagation results presented which satisfy the full boundary conditions. These results will justify the assumptions made.

The problem of two oppositely propagating surface waves under the particular restrictions required of an acoustic convolver will then be discussed and a multiple scales solution attempted. Results will be presented for the most commonly used substrate material which will duplicate the earlier results of Ganguly and Davis [1980].

Finally the nonlinear mode coupling of two co-directional waves on both piezoelectric and anisotropic elastic substrates will be considered. The problem of the interaction of harmonic frequencies leading to interference and noise in the circuit external device will be discussed and results presented for the evolution of such interactions.

2 The Basics

Before beginning an analysis of surface waves it is necessary to introduce some of the fundamental theory of elasticity and crystallography. Since the elasticity of crystals has been studied using differing approaches for isotropic, anisotropic and piezoelectric materials and by both experimentalists and theoreticians, it is also prudent to set out the notational conventions to be used in this thesis.

A general formulation of the physical properties of crystals in tensor notation is presented in Nye [1957]. Starting from the basic mathematical description of tensors, Nye introduces tensors of various ranks and their crystallographic applications are considered. Emphasis is placed upon the symmetric properties of tensors and the simplifications available through the various classes of crystallographic symmetry. This reference forms the basis for much of the material of Section 2.1 where attention is concentrated on the two classes of crystal symmetry of interest in this thesis. An outline is also given of the numerical routines used to produce the results in later chapters.

The fundamental concepts of continuum mechanics are set out in Section 2.2 and the notations to be used in later chapters are defined. The concept of two states and two coordinate systems is introduced in order that the motion of the crystal, and in particular the deformation of the boundary, does not unnecessarily complicate the statement of the field equations. This is achieved by expressing all the equations in reference, or undeformed, coordinates, that is the coordinates of each point of the material when at rest. A more detailed derivation of these equations may be found in the book by Atkin and Fox [1980] which presents the governing equations for a general deformed elastic body with no restrictions on symmetry. The stress tensor relative to the reference frame is then derived from the momentum balance equation and expressed in terms of the Gibbs' function of the substrate. The Gibbs' function can be expressed as a series function in the strain tensor and both isotropic and anisotropic media may be considered.

In Proceedings of the I.R.E. [1949] an attempt was made to set standards for the notation of the various crystallographic properties. Although succeeding in standardizing the choice of the crystallographic axes of symmetry, the article has, in general, failed to unify the notation used by researchers for the various electric, elastic and piezoelectric constants of these crystals. Bearing in mind previous work, in this thesis we use what we believe is the simplest notation for the cases considered.

2.1 CRYSTALLOGRAPHICS

In this section the notation used in crystallography is set out and the various classes of symmetry are discussed. Much of the work may be found in Nye [1957] but specific notations relevant to later discussions are also introduced. The section closes with a brief explanation of the procedures used for computation.

2.1.1 Tensors and Anisotropy

Many material parameters, such as density, may be expressed without reference to any direction and may be represented by a scalar value ρ. Other parameters, such as electric field, are direction dependent and must be specified by both magnitude and direction. Such a parameter is represented by a vector, $\mathbf{E}$, with components E_j, where $j = 1, 2, 3$, referred to a system of rectangular cartesian coordinates (x_1, x_2, x_3).

If a material is electrically isotropic, behaves the same in all directions with respect to conductivity, then the current density will be co-directional with the electric field, giving the relationship

$$j_1 = \sigma E_1 \ , \quad j_2 = \sigma E_2 \ , \quad j_3 = \sigma E_3$$

where $\mathbf{j}$ is the current density and σ the conductivity, represented by a scalar.

If we consider a material that is electrically anisotropic the current density need not be co-directional with the electric field, but may be expressed as some linear combination of the electric field components

$$\begin{aligned} j_1 &= \sigma_{11}E_1 + \sigma_{12}E_2 + \sigma_{13}E_3 \,, \\ j_2 &= \sigma_{21}E_1 + \sigma_{22}E_2 + \sigma_{23}E_3 \,, \\ j_3 &= \sigma_{31}E_1 + \sigma_{32}E_2 + \sigma_{33}E_3 \,, \end{aligned} \tag{2.1.1}$$

where σ_{ij}, the conductivity, is given by a second-order tensor. Equations (2.1.1) may be more compactly represented by

$$j_i = \sum_{k=1}^{3} \sigma_{ik} E_k \,, \qquad i = 1, 2, 3,$$

or, using Einstein's summation convention whereby a repeated suffix is summed over the values 1, 2 and 3,

$$j_i = \sigma_{ik} E_k \,. \tag{2.1.2}$$

This summation convention is used throughout this thesis for all lower case letter subscripts but, for convenience, for upper case letter subscripts it is restricted to the letters A to F.

Effects such as stress and strain are represented by second-order tensors since they not only require magnitude and direction for measurement but must also be referred to a plane of action. Thus the stress acting on the plane $x_2 = 0$ is represented by the vector

$$T_{2i} \ , \quad i = 1, 2, 3,$$

where T_{ji} denote the components of the stress tensor.

For an isotropic material the simplest stress–strain relationship would be given by

$$T_{ij} = \lambda e_{ij} + \mu e_{kk} \delta_{ij}$$

where e_{ij} is the material strain and λ and μ the isotropic elasticity constants.

For anisotropic materials the most general linear stress–strain relationship is

$$T_{ij} = c_{ijkl}\, e_{kl} \ , \tag{2.1.3}$$

where c_{ijkl} is a fourth-order tensor known as the second-order stiffness constant.

2.1.2 Symmetry

The general second-order tensor has the matrix form

$$\mathbf{S} = \begin{pmatrix} S_{11} & S_{12} & S_{13} \\ S_{21} & S_{22} & S_{23} \\ S_{31} & S_{32} & S_{33} \end{pmatrix},$$

but, under the reflective symmetry stated above the number of independent components is reduced from nine to six, giving

$$\mathbf{S} = \begin{pmatrix} S_{11} & S_{12} & S_{13} \\ S_{12} & S_{22} & S_{23} \\ S_{13} & S_{23} & S_{33} \end{pmatrix}.$$

Voight's notation represents this symmetric second-order tensor by a six-dimensional vector by subscript replacement according to the scheme

$$\begin{aligned} &S_{11} = S_1, && S_{22} = S_2, && S_{33} = S_3, \\ &S_{23} = S_{32} = S_4, && S_{13} = S_{31} = S_5, && S_{12} = S_{21} = S_6. \end{aligned}$$

An analogous simplification can be introduced for higher order tensors.

Considering equation (2.1.3), replacement of dummy subscripts reveals

$$\begin{aligned} T_{ij} &= c_{ijlk}e_{lk}, \\ &= c_{ijlk}e_{kl}, \end{aligned}$$

by the symmetry of e_{kl}. Hence, we deduce the constants c_{ijkl} must satisfy

$$c_{ijkl} = c_{ijlk}\,, \tag{2.1.4}$$

and, assuming $T_{ij} = T_{ji}$, that

$$c_{ijkl} = c_{jikl}. \tag{2.1.5}$$

Voight's notation now allows this fourth-order tensor to be represented by a second-order tensor, $c_{\alpha\beta}, \alpha, \beta = 1, 2 \ldots 6$, where

$$\begin{aligned} &c_{11} = c_{1111}\,, \quad c_{12} = c_{1122} \\ &c_{13} = c_{1133}\,, \quad c_{14} = c_{1123} = c_{1132} \\ &\quad \text{etc.} \end{aligned} \tag{2.1.6}$$

A fourth-order tensor possessing no symmetry has eighty-one independent components, but the symmetry of (2.1.6) reduces this number to thirty-six, enabling $c_{\alpha\beta}$ to be written

$$c_{\alpha\beta} = \begin{pmatrix} c_{11} & c_{12} & c_{13} & c_{14} & c_{15} & c_{16} \\ c_{21} & c_{22} & c_{23} & c_{24} & c_{25} & c_{26} \\ c_{31} & c_{32} & c_{33} & c_{34} & c_{35} & c_{36} \\ c_{41} & c_{42} & c_{43} & c_{44} & c_{45} & c_{46} \\ c_{51} & c_{52} & c_{53} & c_{54} & c_{55} & c_{56} \\ c_{61} & c_{62} & c_{63} & c_{64} & c_{65} & c_{66} \end{pmatrix}. \tag{2.1.7}$$

It will later be seen that $c_{\alpha\beta}$ posseses the further symmetry

$$c_{\alpha\beta} = c_{\beta\alpha}\,, \tag{2.1.8}$$

which reduces the number of independent values to twenty-one.

For later convenience we adopt the notation $d_{(ij)(kl)}$ used by Lardner [1986] for tensors whose components satisfy the symmetry relations

$$\begin{aligned} d_{(ij)(kl)} \equiv d_{ijkl} &= d_{klij} \\ &\neq d_{ijlk}\,, \end{aligned} \tag{2.1.9}$$

that is, when d_{ijkl} is symmetric *in* pairs not *within* pairs.

The symmetry of the fourth-order tensor given by equation (2.1.7) is that of a crystal in the triclinic class, which is the most general type of elastic material. Other materials possess higher symmetry and these crystals can be divided into various classes depending upon the type of extra symmetry they possess.

Let us now examine what is meant by the symmetry of a property. A crystal property is a relationship between two quantities measured with respect to a given set of axes. If some possible symmetry element is then applied to these axes, the quantities measured again and the relationship found to be unchanged, then the crystal is said to possess this symmetry element. The main types of symmetry considered are rotation and inversion. These may be illustrated by consideration of the representation quadric,

$$S_{ij}\, x_i\, x_j \;=\; 1,$$

where S_{ij} is a second-order tensor property of the crystal. Taking $S_{ij} = S_{ji}$,

$$S_{11}\, x_1^2 \;+\; S_{22}\, x_2^2 \;+\; S_{33}\, x_3^2 \;+\; 2\, S_{12}\, x_1\, x_2 \;+\; 2\, S_{13}\, x_1\, x_3 \;+\; 2\, S_{23}\, x_2\, x_3 \;=\; 1$$

represents the general equation of a second-degree surface. Neumann's principle, Nye [1957] , states that each element of symmetry possessed by this surface must be included in the symmetry of the crystal. It is noted here that there are as many coefficients in the above quadric as there are independent values of the second-order tensor S_{ij}.

If the quadric is referred to its principal axes, it takes the simpler form

$$S_1\, x_1^2 \;+\; S_2\, x_2^2 \;+\; S_3\, x_3^2 \;=\; 1,$$

(note that this does not reduce the number of constants since three are required to specify the position of the principal axes). Just as this quadric simplifies when referred to these axes, so does the second-order tensor, to become

$$[S_{ij}] \;=\; \begin{bmatrix} S_1 & 0 & 0 \\ 0 & S_2 & 0 \\ 0 & 0 & S_3 \end{bmatrix}.$$

Examination of the signs of S_1,S_2 and S_3 will divide these quadrics into ellipsoids, or hyperboloids of one or two sheets, see Figure 2.1.1. The principal axes of the crystal class are generally called the crystallographic axes.

The symmetry classes of interest in this thesis are cubic and trigonal. Cubic crystals possess four three-fold axes of symmetry, positioned as the four diagonals

of a cube. An n-fold axis of rotational symmetry is one about which a rotation of $2\pi/n$ leaves the crystal properties unchanged. The only quadric which possesses this symmetry is a sphere, which may be entirely defined through one parameter, the radius. This leads us to

$$S_1 = S_2 = S_3 = S\,,$$

and hence

$$[S_{ij}] = \begin{bmatrix} S & 0 & 0 \\ 0 & S & 0 \\ 0 & 0 & S \end{bmatrix}$$

referred to the principal axes.

The trigonal class possesses, in general, one three-fold axis of symmetry. A general quadric possesses three two-fold (half-revolution) axes at right angles, and three planes of symmetry, see Figure 2.1.1, and for this to have a three-fold rotation axis it must be a surface of revolution . This is sufficiently defined by two numbers, that is the lengths of the major and minor axes, giving

$$[S_{ij}] = \begin{bmatrix} S_1 & 0 & 0 \\ 0 & S_1 & 0 \\ 0 & 0 & S_3 \end{bmatrix}.$$

Similar arguments, and more direct analysis of the effects of symmetry on the physical properties, may be used for higher-order tensors. Thus, for cubic crystals, the fourth-order elasticity tensor becomes

$$[c_{\alpha\beta}] = \begin{bmatrix} c_{11} & c_{12} & c_{12} & 0 & 0 & 0 \\ c_{12} & c_{11} & c_{12} & 0 & 0 & 0 \\ c_{12} & c_{12} & c_{11} & 0 & 0 & 0 \\ 0 & 0 & 0 & c_{44} & 0 & 0 \\ 0 & 0 & 0 & 0 & c_{44} & 0 \\ 0 & 0 & 0 & 0 & 0 & c_{44} \end{bmatrix}, \tag{2.1.10}$$

whilst for trigonal crystals we have

$$[c_{\alpha\beta}] = \begin{bmatrix} c_{11} & c_{12} & c_{13} & c_{14} & 0 & 0 \\ c_{12} & c_{22} & c_{13} & -c_{14} & 0 & 0 \\ c_{13} & c_{13} & c_{33} & 0 & 0 & 0 \\ c_{14} & -c_{14} & 0 & c_{44} & 0 & 0 \\ 0 & 0 & 0 & 0 & c_{44} & -c_{14} \\ 0 & 0 & 0 & 0 & -c_{14} & c_{66} \end{bmatrix}. \tag{2.1.11}$$

A fuller description of the arguments presented above can be found in Nye [1957].

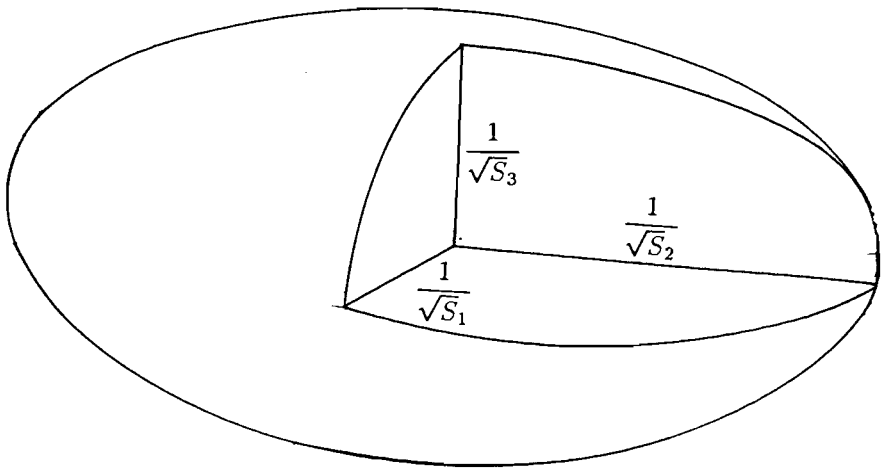

Figure 2.1.1 General representation quartic for positive S_1, S_2 and S_3

2.1.3 Rotation

When stating numerical values for the various crystal properties it must be clear to which axes these are referred. An obvious choice would be the crystallographic axes used in the previous section, and the IRE [1949] set out standards for the orientation of these axes relative to the various planes and axes of symmetry. Thus in this thesis all data for crystals is referred to a set of rectangular cartesian axes based on the principal axes, and if one wishes to consider the constants referred to another set of axes the following transformation must be performed.

Denoting the principal axes by (x_1, x_2, x_3) and our new axes by (x'_1, x'_2, x'_3), we may use Figure 2.1.2 to draw up a matrix of direction cosines,

$$\begin{array}{c} \\ x'_1 \\ x'_2 \\ x'_3 \end{array} \begin{array}{c} \begin{array}{ccc} x_1 & x_2 & x_3 \end{array} \\ \begin{pmatrix} a_{11} & a_{12} & a_{13} \\ a_{21} & a_{22} & a_{23} \\ a_{31} & a_{32} & a_{33} \end{pmatrix} \end{array} \tag{2.1.12}$$

The first subscript of the tensor a_{ij} refers to the "new" axis and the second refers to the "old" axis. A vector $\mathbf{p}$ referred to the "old" coordinate axes may then be transformed to the "new" axes, thus

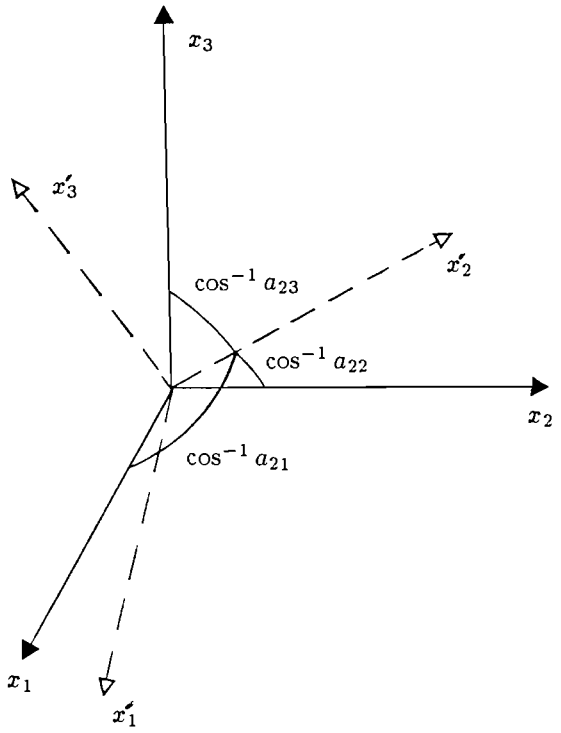

Figure 2.1.2 Transformation of axes

$$
\begin{aligned}
p'_1 &= p_1 \cos \widehat{x_1 x'_1} + p_2 \cos \widehat{x_2 x'_1} + p_3 \cos \widehat{x_3 x'_1} \,, \\
p'_2 &= p_1 \cos \widehat{x_1 x'_2} + p_2 \cos \widehat{x_2 x'_2} + p_3 \cos \widehat{x_3 x'_2} \,, \\
p'_3 &= p_1 \cos \widehat{x_1 x'_3} + p_2 \cos \widehat{x_2 x'_3} + p_3 \cos \widehat{x_3 x'_3} \,,
\end{aligned}
$$

or, using the summation convention and the direction cosine table,

$$
p'_i = a_{ij} p_j \,, \tag{2.1.13}
$$

where p'_i is the vector p_i referred to the "new" coordinate system (x'_1, x'_2, x'_3).

This concept is easily extended to higher-order tensors through consideration of the relationship

$$
p_i = S_{ij} q_j \,,
$$

where p_i and q_j are vectors and S_{ij} some second-order relational tensor. It follows from this relationship and equations (2.1.13) that

$$p'_i = a_{ij}p_j = a_{ij}S_{jk}q_k = a_{ij}S_{jk}a_{lk}q'_l$$
$$= S'_{il}q'_l ,$$

where the dash denotes a value referred to the "new" coordinate system.

Hence

$$S'_{il} = a_{ij}a_{lk}S_{jk} ,$$

or, replacing subscripts,

$$S'_{ij} = a_{ik}a_{jl}S_{kl} . \tag{2.1.14}$$

With similar arguments, the corresponding relationship for the fourth-order constants is

$$c'_{ijkl} = a_{im}a_{jn}a_{ko}a_{lp}c_{mnop} . \tag{2.1.15}$$

2.1.5 Computing

This section deals with the practical problems encountered when implementing the rotation procedures using a computer.

In setting up an analytical model of the type to be described in Chapter 3 one chooses two axes parallel to the free surface. These axes will not necessarily coincide with the principal axes of the crystal and hence the various elastic, dielectric and piezoelectric constants must be rotated to the chosen axes.

The various second- and third-order elastic constants may have, in total, eight hundred and ten non-zero values which must each be individually assigned. Together with the various electro-elastic constants there are a possible one thousand, one hundred and seventy individual values to assign. Since these are not all independent it was decided only to input the independent values. This simpler procedure is possible since each crystallographic constant must be symmetric *in* and *within* pairs and expressing them in Voight's notation thus significantly reduces the number of input values. It is also worthwhile making use of the particular classes of material symmetry to further reduce the number of independent constants. For instance, for cubic crystals the number of independent constants can be reduced to nine.

In the results discussed later in this thesis the input of constants was achieved by the following method:

1. Create an input file with the values of the independent constants and a code indicating the symmetry class.

2. The symmetry code is read and switches the programme to the appropriate routine.

3. The independent values are read in to their relevant position in an array using Voight's notation.

4. The appropriate crystal symmetry is used to "fill" the Voight's array.

5. An array routine is used to translate from the Voight's array to the full tensor array.

6. The particular orientation of axes in the problem to be considered is read in by specifying the crystal "cut" (i.e. the free surface) and the propagation direction on that surface.

7. The axes of orientation and propagation direction are used to construct the transformation matrix and the method of Section 2.1.4 used to rotate the constants.

All numerical values for the constants input into these routines must be normalised with respect to a typical value to avoid numerical errors arising from over- or under-flow numbers in repeated summations.

2.2 BASIC CONCEPTS

The mechanics of an elastic body needs to be discussed and therefore we must develop some of the tools of finite deformation theory. The key to understanding this theory is an appreciation of the dualism in the description of the two states, undeformed and deformed (or reference and current) configuration and the two sets of coordinates, material and spatial, that describe the two states respectively.

In general, as a body deforms each point within the body, $\mathcal{C}_0$, is moved, as are all points on its boundary. Thus any condition upon the boundary of the body implies knowledge of the boundary position for all time. For this reason it is convenient to introduce the concept of a "reference state", defined as the body's initial position, and to write all the governing and constitutive equations in terms of this known reference state.

A three-dimensional Euclidean space shall be considered and, for simplicity, rectangular cartesian coordinates are employed from now on.

2.2.1 Deformation

A deformation refers to a change in size, shape, orientation or location of a body without causing breakage, cracking or slippage. These latter effects cause discontinuities to occur and destroy the reversibility of the process.

Let us idealise the concept of this body by supposing it to be composed of a set of particles such that, at a given time t, each particle of the set occupies a single unique point in the region $\mathcal{C}_t$, and that each point of $\mathcal{C}_t$ is occupied by a single particle. $\mathcal{C}_t$ is known as the deformed state and is complemented by the configuration of particles at the origin of time, $\mathcal{C}_0$, known as the undeformed, or reference, state.

Denote the position vector of a particle in the undeformed state by $\mathbf{X}$, and the position vector of this same particle in the deformed state by $\mathbf{x}$. The deformation is then characterised by the transformation

$$\mathbf{x} = \mathbf{x}(\mathbf{X}, t)\,, \tag{2.2.1}$$

which maps the position $\mathbf{X}$ of each point in the undeformed region $\mathcal{C}_0$ onto its position $\mathbf{x}$ in the deformed region $\mathcal{C}_t$ at time t. The inverse transformation is defined as

$$\mathbf{X} = \mathbf{X}(\mathbf{x}, t)\,. \tag{2.2.2}$$

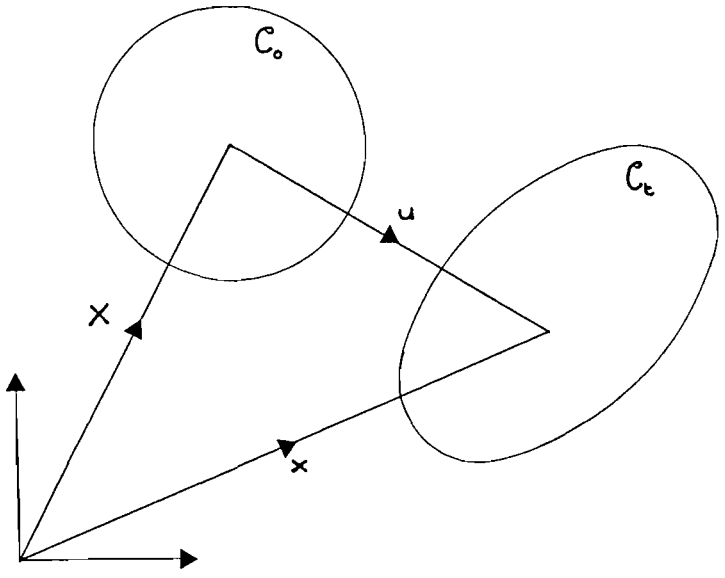

Figure 2.2.1 Displacement

These two transformations must be single-valued and many times differentiable for continuity. It is also required that the material must not be allowed to penetrate itself, thus the Jacobian J of the transformation (2.2.1) must be positive and non-zero, i.e.

$$J = \left| \frac{\partial x_i}{\partial X_A} \right| > 0 . \tag{2.2.3}$$

It is useful at this point to introduce the concept of displacement. We define the displacement vector $\mathbf{u}$ by the relation

$$\mathbf{u} = \mathbf{x} - \mathbf{X} , \tag{2.2.4}$$

with its physical significance represented in Figure 2.2.1

2.2.2 Strain

Strain is the change in size or shape resulting from changes in length or relative orientation of the body.

Consider two particles with positions $\mathbf{X}$ and $\mathbf{X} + d\mathbf{X}$ in the undeformed state, then these particles will have positions given by

$$\mathbf{x} = \mathbf{x}(\mathbf{X}, t)$$

and

$$\mathbf{x} + \mathrm{d}\mathbf{x} = \mathbf{x}(\mathbf{X} + \mathrm{d}\mathbf{X}, t)\,,$$

in the deformed state at time t.

Thus the components of the total differential $\mathrm{d}\mathbf{x}$ are given in terms of $\mathrm{d}\mathbf{X}$, by the chain rule, as

$$\mathrm{d}x_i = \frac{\partial x_i}{\partial X_A}\,\mathrm{d}X_A\,.$$

Now if the arc $\mathrm{d}x_i$ has length $\mathrm{d}s$ then the quantity $\mathrm{d}s^2$ transforms by the relation

$$\begin{aligned}\mathrm{d}s^2 &= \mathrm{d}x_i\,\mathrm{d}x_i \\ &= C_{AB}\,\mathrm{d}X_A\,\mathrm{d}X_B\,,\end{aligned}$$

where C_{AB}, defined by

$$C_{AB} = \frac{\partial x_i}{\partial X_A}\,\frac{\partial x_i}{\partial X_B}\,, \tag{2.2.5}$$

is called the Green deformation tensor, or the right Cauchy–Green strain tensor, and is a measure of the change in size and shape of the element.

There is an analogous derivation of the Cauchy deformation tensor, or left Cauchy–Green strain tensor, as the change in area of the reference state for a given current area, namely

$$B_{ij} = \frac{\partial X_A}{\partial x_i}\,\frac{\partial X_A}{\partial x_j}\,, \tag{2.2.6}$$

Finally we introduce the Green finite strain tensor, or Lagrange strain tensor, E_{AB}, by

$$E_{AB} = \frac{1}{2}\,(C_{AB} - \delta_{AB})\,. \tag{2.2.7}$$

This strain tensor is the most commonly used measure of strain.

From equation (2.2.4) we have that

$$\frac{\partial x_i}{\partial X_A} = \delta_{iB}\frac{\partial u_B}{\partial X_A} + \delta_{iA}\,, \tag{2.2.8}$$

which, together with equations (2.2.5) and (2.2.7) gives the strain in terms of displacement gradients

$$C_{AB} = u_{A,B} + u_{B,A} + u_{C,A}u_{C,B} + \delta_{AB}\,, \tag{2.2.9}$$

and

$$E_{AB} = \frac{1}{2}\left(u_{A,B} + u_{B,A} + u_{C,A}\,u_{C,B}\right). \tag{2.2.10}$$

Clearly the Lagrange strain tensor is zero under zero displacement.

2.2.3 Time Derivatives

The introduction of reference and current states means that care must be taken in stating a time derivative to ensure whether spatial or material time differentiation is implied.

A spatial time derivative is the variation of a quantity, say F, with time for a fixed point in the spatial coordinates and shall be denoted

$$\frac{\partial F(\mathrm{x},t)}{\partial t} \equiv \left.\frac{\partial F(\mathrm{x},t)}{\partial t}\right|_{\mathrm{x\ const}}. \tag{2.2.11}$$

It follows that

$$\frac{\partial \mathrm{x}}{\partial t} = 0\,.$$

A material time derivative is the variation of a quantity, F, with time for a fixed point in the material or undeformed coordinates. This may be seen as the change in F with time as observed by a rider on the mass point $\mathbf{X}$, and is denoted by

$$\frac{\mathrm{D}F(\mathbf{X},t)}{\mathrm{D}t} \equiv \dot{F}(\mathbf{X},t) \equiv \left.\frac{\partial F(\mathbf{X},t)}{\partial t}\right|_{\mathbf{X}\ \mathrm{const}}. \tag{2.2.12}$$

It immediately follows that

$$\frac{\mathrm{D}\mathbf{X}}{\mathrm{D}t} = 0\,,$$

which leads us to

$$\frac{\mathrm{D}\mathrm{x}}{\mathrm{D}t} = \frac{\mathrm{D}\mathbf{u}}{\mathrm{D}t} = \dot{\mathbf{u}}\,, \tag{2.2.13}$$

from (2.2.4). It must also be noted that the chain rule for differentiation allows us to express the material time derivative as

$$\frac{\mathrm{D}F(\mathbf{X},t)}{\mathrm{D}t} = \frac{\partial F(\mathbf{X},t)}{\partial t} + \frac{\mathrm{D}x_i}{\mathrm{D}t}\frac{\partial F(\mathbf{X},t)}{\partial x_i}\bigg|_{\mathbf{X}\text{ const}}$$
$$= \frac{\partial F}{\partial t} + \dot{u}_i \frac{\partial F}{\partial x_i}. \tag{2.2.14}$$

2.2.4 Conservation of mass

Denoting by ρ_o and ρ the reference and material state densities respectively, the principle of conservation of mass within the volumes $\mathcal{V}_0$ and $\mathcal{V}$ in $\mathcal{C}_0$ and $\mathcal{C}_t$ respectively, can be written

$$\int_{\mathcal{V}} \rho \mathrm{d}\mathcal{V} = \int_{\mathcal{V}_0} \rho_0 \, \mathrm{d}\mathcal{V}_0 . \tag{2.2.15}$$

Using the result that $d\mathcal{V} = J\, d\mathcal{V}_0$, which may be derived from equation (2.2.3), equation (2.2.15) may be represented by

$$\int_{\mathcal{V}_0} \rho J \, \mathrm{d}\mathcal{V}_0 = \int_{\mathcal{V}_0} \rho_0 \, \mathrm{d}\mathcal{V}_0 ,$$

or

$$\int_{\mathcal{V}_0} (\rho J - \rho_0) \, \mathrm{d}\mathcal{V}_0 = 0 .$$

Since the volume of integration is arbitrary, the latter integral implies that

$$\rho_0 = \rho J , \tag{2.2.16}$$

provided the integrand is continuous. Equation (2.2.16) is the law of mass conservation for our solid.

2.2.5 Conservation of momentum

Consider the volumes $\mathcal{V}_0$ and $\mathcal{V}$ in $\mathcal{C}_0$ and $\mathcal{C}_t$ to be bounded by the surfaces $\mathcal{S}_0$ and $\mathcal{S}$ respectively. Now the linear momentum of the material volume $\mathcal{V}$ may be written as

$$\int_{\mathcal{V}} \rho \dot{\mathbf{u}} \, \mathrm{d}\mathcal{V} ,$$

which may be expressed in terms of the reference volume by

$$\int_{\mathcal{V}_0} \rho J \dot{\mathbf{u}} \, \mathrm{d}\mathcal{V}_0 .$$

The rate of change of linear momentum of material volume $\mathcal{V}$ is then given by

$$\frac{\mathrm{d}}{\mathrm{d}t}\int_{\mathcal{V}_0}\rho J\,\dot{\mathbf{u}}\,\mathrm{d}\mathcal{V}_0 = \int_{\mathcal{V}_0}\left[\dot{\mathbf{u}}\,\frac{\mathrm{D}(\rho J)}{\mathrm{D}t} + \rho J\,\frac{\mathrm{D}\dot{\mathbf{u}}}{\mathrm{D}t}\right]\mathrm{d}\mathcal{V}_0\,, \tag{2.2.17}$$

since the reference volume $\mathcal{V}_0$ is fixed in time.

When ρ_0 is dependent only upon $\mathbf{X}$ it follows from equation (2.2.16) that

$$\frac{\mathrm{D}(\rho J)}{\mathrm{D}t} = \frac{\mathrm{D}(\rho_0)}{\mathrm{D}t} = 0\,. \tag{2.2.18}$$

Thus, equation (2.2.17) reduces to

$$\begin{aligned}\frac{\mathrm{d}}{\mathrm{d}t}\int_{\mathcal{V}}\rho\dot{\mathbf{u}}\,\mathrm{d}\mathcal{V} &= \int_{\mathcal{V}_0}\rho J\,\ddot{\mathbf{u}}\mathrm{d}\mathcal{V}_0 \\ &= \int_{\mathcal{V}}\rho\ddot{\mathbf{u}}\,\mathrm{d}\mathcal{V}\,.\end{aligned} \tag{2.2.19}$$

In the absence of external body forces the volume $\mathcal{V}$ is acted upon only by interatomic forces which here, as in most simple continuum theories, are represented by a vector field $\mathbf{t}(\mathbf{x},\mathbf{n})$. The latter is defined over the surface $\mathcal{S}$, of $\mathcal{V}$, where $\mathbf{n}$ is the outward normal to $\mathcal{S}$. The field $\mathbf{t}$ is known as the stress vector and with body forces absent it follows that the total force acting on $\mathcal{V}$ is given by

$$\int_{\mathcal{S}}\mathbf{t}\,(\mathbf{x},\mathbf{n})\,\mathrm{d}\mathcal{S}\,. \tag{2.2.20}$$

We may further assert that

$$\mathbf{t}\,(\mathbf{x},\mathbf{n}) = \mathbf{T}.\mathbf{n}\,, \tag{2.2.21}$$

where $\mathbf{T}$ is the Cauchy stress tensor. With the use of equation (2.2.21) and the divergence theorem, the integral (2.2.20) now becomes

$$\int_{\mathcal{V}}\mathrm{div}\,\mathbf{T}\,\mathrm{d}\mathcal{V}\,. \tag{2.2.22}$$

Taking as our principle of linear momentum the assertion that the rate of change of linear momentum is equal to the resultant force, we may write the governing equation for a deformed solid as

$$\int_{\mathcal{V}}\rho\ddot{\mathbf{u}}\,\mathrm{d}\mathcal{V} = \int_{\mathcal{V}}\mathrm{div}\,\mathbf{T}\,\mathrm{d}\mathcal{V}\,.$$

Since this must hold for all regions $\mathcal{V}$ it follows, provided the integrands are continuous, that

$$\rho\,\ddot{\mathbf{u}} = \operatorname{div}\mathbf{T}\,,$$

or

$$\rho\,\ddot{u}_i = T_{ji,j}\,, \tag{2.2.23}$$

where the summation convention is implied and "$,j$" is used to denote partial differentiation with respect to x_j.

This is the spatial form of the governing equation for a deformed elastic solid.

The moment of momentum per unit mass is given by $\mathbf{x} \times \rho\mathbf{v}$, which leads us to the total angular momentum

$$\int_{\mathcal{V}} \mathbf{x} \times \rho\mathbf{v}\,\mathrm{d}\mathcal{V}\,.$$

Now, the conservation of angular momentum asserts that the total torque exerted on the body equals the rate of change of angular momentum, thus

$$\int_{\mathcal{S}} \mathbf{x} \times \mathbf{t}\,\mathrm{d}\mathcal{S} = \frac{\mathrm{d}}{\mathrm{d}t}\int_{\mathcal{V}} \mathbf{x} \times \rho\mathbf{v}\,\mathrm{d}\mathcal{V}\,.$$

or, in subscript form,

$$\int_{\mathcal{S}} \varepsilon_{ijk} x_j t_k \mathrm{d}\mathcal{S} = \frac{\mathrm{d}}{\mathrm{d}t}\int_{\mathcal{V}} \varepsilon_{ijk} x_j \rho v_k\,\mathrm{d}\mathcal{V}\,,$$

where ε_{ijk} is the permutation symbol.
Use of the divergence theorem and the definition of the stress tensor (2.2.21) reveals

$$\int_{\mathcal{V}} \varepsilon_{ijk}\left[\frac{\partial}{\partial x_l}(x_j T_{lk}) - \rho\frac{\mathrm{D}}{\mathrm{D}t}(x_j v_k)\right]\,\mathrm{d}\mathcal{V} = 0\,.$$

Now

$$\varepsilon_{ijk}\frac{\partial}{\partial x_l}(x_j T_{lk}) = \epsilon_{ijk} T_{jk} + \varepsilon_{ijk} x_j T_{lk,l}\,,$$

and

$$\begin{aligned}\rho\epsilon_{ijk}\frac{\mathrm{D}}{\mathrm{D}t}(x_j v_k) &= \varepsilon_{ijk} x_j \rho\frac{\mathrm{D}}{\mathrm{D}t} v_k \\ &= \varepsilon_{ijk} x_j T_{lk,l}\,,\end{aligned}$$

which gives the conservation of angular momentum in the simple form

$$\int_{\mathcal{V}} \varepsilon_{ijk} T_{jk}\,\mathrm{d}\mathcal{V} = 0\,.$$

Since the volume of integration is arbitrary we now have that

$$\varepsilon_{ijk} T_{jk} = 0\,,$$

or, using the definition of ε_{ijk},

$$T_{23} - T_{32} = 0\,, \quad T_{31} - T_{13} = 0\,, \quad T_{12} - T_{21} = 0\,,$$

which may be expressed as

$$T_{ij} = T_{ji}\,.$$

2.2.6 Governing Equations in Reference Coordinates

It is important to express the governing equations (2.2.23) in reference form since it normally proves easier to solve problems when reference coordinates are used.

Consider two line elements $\mathrm{d}\mathbf{X}$ and $\mathrm{d}\mathbf{Y}$ in $\mathcal{C}_0$, which define a parallelogram of area $\mathrm{d}\mathcal{S}_0$ with unit normal $\mathbf{N}$. Likewise, the corresponding elements $\mathrm{d}\mathbf{x}$ and $\mathrm{d}\mathbf{y}$ in $\mathcal{C}_t$ define an area $\mathrm{d}\mathcal{S}$ with unit normal $\mathbf{n}$, where

$$\mathrm{d}\mathbf{X} \times \mathrm{d}\mathbf{Y} \;=\; \mathbf{N}\,\mathrm{d}\mathcal{S}_0 \tag{2.2.24}$$

and

$$\mathrm{d}\mathbf{x} \times \mathrm{d}\mathbf{y} \;=\; \mathbf{n}\,\mathrm{d}\mathcal{S}\,. \tag{2.2.25}$$

In indicial form equation (2.2.25) becomes

$$n_i \mathrm{d}\mathcal{S} \;=\; \varepsilon_{ijk}\, x_{j,B}\, x_{k,C}\, \mathrm{d}X_B\, \mathrm{d}X_C\,, \tag{2.2.26}$$

Premultiplying equation (2.2.26) by the gradient $x_{i,A}$

$$\begin{aligned} n_i\, x_{i,A}\, \mathrm{d}\mathcal{S} \;&=\; \varepsilon_{ijk}\, x_{i,A}\, x_{j,B}\, x_{k,C}\, \mathrm{d}X_B\, \mathrm{d}X_C \\ &=\; J\, \varepsilon_{ABC}\, \mathrm{d}X_B\, \mathrm{d}X_C \\ &=\; J N_A \mathrm{d}\mathcal{S}_0\,, \end{aligned} \tag{2.2.27}$$

using the definition of the Jacobian and equation (2.2.24). Multiplying equation (2.2.27) by the inverse deformation gradient $X_{A,i}$, we find that

$$n_i\, \mathrm{d}\mathcal{S} \;=\; J\, X_{A,i}\, N_A\, \mathrm{d}\mathcal{S}_0\,.$$

Recalling the definition of the Cauchy stress tensor, equation (2.2.21), it follows that

$$
\begin{aligned}
t_i \, \mathrm{d}\mathcal{S} &= T_{ji} \, n_j \, \mathrm{d}\mathcal{S} \\
&= J \, X_{A,j} \, T_{ji} \, N_A \, \mathrm{d}\mathcal{S}_0 \\
&= \sigma_{Ai} \, N_A \, \mathrm{d}\mathcal{S}_0 \, ,
\end{aligned} \tag{2.2.28}
$$

where

$$
\sigma_{Ai} = J \, X_{A,j} \, T_{ji} \, , \tag{2.2.29}
$$

defines the first Piola-Kirchoff stress tensor and is, in general, not symmetric.

Returning to the conservation of momentum principle, we may rewrite the force integral (2.2.20) as

$$
\int_{\mathcal{S}_0} \sigma_{Ai} \, N_A \, \mathrm{d}\mathcal{S}_0 \, , \tag{2.2.30}
$$

and the momentum integral (2.2.19) as

$$
\int_{\mathcal{V}_0} \rho \, J \, \frac{\mathrm{D}v_i}{\mathrm{D}t} \, \mathrm{d}\mathcal{V}_0 = \int_{\mathcal{V}_0} \rho_0 \, \frac{\mathrm{D}v_i}{\mathrm{D}t} \, \mathrm{d}\mathcal{V}_0 \, , \tag{2.2.31}
$$

giving the conservation of momentum in the form

$$
\int_{\mathcal{V}_0} \rho_0 \, \frac{\mathrm{D}v_i}{\mathrm{D}t} \, \mathrm{d}\mathcal{V}_0 = \int_{\mathcal{S}_0} \sigma_{Ai} \, N_A \, \mathrm{d}\mathcal{S}_0 \, .
$$

Use of the divergence theorem yields

$$
\int_{\mathcal{V}_0} \left[\rho_0 \, \frac{\mathrm{D}v_i}{\mathrm{D}t} - \sigma_{Ai,A} \right] \mathrm{d}\mathcal{V}_0 = 0 \, , \tag{2.2.32}
$$

from which we deduce, in the usual way, that

$$
\rho_0 \, \frac{\mathrm{D}v_i}{\mathrm{D}t} = \sigma_{Ai,A} \, ,
$$

provided these quantities are continuous. This latter equation can be written

$$
\rho_0 \, \ddot{u}_i = \sigma_{Ai,A} \, , \tag{2.2.33}
$$

which are our governing equations in the reference frame.

2.2.7 Strain Energy

The power developed by deformation of a body contained within the surface $\mathcal{S}$ may be expressed as the integral of the product of the stress on the surface and the velocity

$$\int_S t_i\, v_i \, \mathrm{d}\mathcal{S} \,. \tag{2.2.34}$$

With the use of equation (2.2.21) and the divergence theorem this integral becomes

$$\int_{\mathcal{V}} \frac{\partial}{\partial x_j}(T_{ji} v_i) \mathrm{d}\mathcal{V},$$

which may be expressed as

$$\int_{\mathcal{V}} [\, T_{ji,j}\, v_i \, + \, T_{ji}\, v_{i,j} \,] \, \mathrm{d}\mathcal{V} \,. \tag{2.2.35}$$

Now equation (2.2.23) may be written

$$\rho \frac{\mathrm{D}v_i}{\mathrm{D}t} \, = \, T_{ji,j} \quad ,$$

which may be substituted into the integral (2.2.35), yielding

$$\int_{\mathcal{V}} \left[\rho \, \frac{\mathrm{D}v_i}{\mathrm{D}t} \, v_i \, + \, T_{ji}\, v_{i,j} \right] \mathrm{d}\mathcal{V} \,,$$

or

$$\int_{\mathcal{V}} \left[\frac{\mathrm{D}}{\mathrm{D}t} (\frac{1}{2} \rho \, v_i \, v_i) \, + \, T_{ji}\, v_{i,j} \right] \mathrm{d}\mathcal{V} \,.$$

The first term in this integral can be seen to represent the power developed through kinetic energy, whilst the second term is the power derived from the stress. We now assume that the stress power is absorbed into, or derived from, some strain energy function, $\mathcal{W}$, which depends only upon deformation gradients, through the relationship

$$\frac{\mathrm{d}}{\mathrm{d}t} \int_{\mathcal{V}} \frac{\rho}{\rho_0} \, \mathcal{W} \, \mathrm{d}\mathcal{V} \, = \, \int_{\mathcal{V}} T_{ji}\, v_{i,j} \, \mathrm{d}\mathcal{V} \,. \tag{2.2.36}$$

$\mathcal{W}$ is defined to be the strain energy function for the body in $\mathcal{C}_t$ measured per unit volume of the corresponding body in $\mathcal{C}_0$, accounting for the factor ρ/ρ_0. Again this is true for arbitrary volumes $\mathcal{V}$ and so, provided the integrands are continuous, it is easily deduced from equation (2.2.36) that

$$\frac{\rho}{\rho_0} \frac{\mathrm{D}\mathcal{W}}{\mathrm{D}t} \, = \, T_{ji}\, v_{i,j} \,. \tag{2.2.37}$$

The introduction of the energy function $\mathcal{W}$ gives us what is known as Green elasticity and $\mathcal{W}$ is sometimes referred to as the Gibbs' function.

Having defined $\mathcal{W}$ to depend only upon deformation gradients, we now express it as a function of the Cauchy–Green strain tensor C_{AB}. Using the chain rule of differentiation,

$$\frac{\mathrm{D}\mathcal{W}}{\mathrm{D}t} = \frac{\partial \mathcal{W}}{\partial C_{AB}} \frac{\mathrm{D}C_{AB}}{\mathrm{D}t}, \tag{2.2.38}$$

and it can be shown, using equation (2.2.5), that

$$\begin{aligned} \frac{\mathrm{D}C_{AB}}{\mathrm{D}t} &= \frac{\mathrm{D}}{\mathrm{D}t}(x_{i,A}\, x_{i,B}) \\ &= (x_{i,A}\, x_{j,B} + x_{i,B}\, x_{j,A})\, v_{i,j}\,. \end{aligned} \tag{2.2.39}$$

Equation (2.2.37) now becomes

$$P_{ij}\, v_{i,j} = 0 \tag{2.2.40}$$

where

$$P_{ij} = T_{ji} - \frac{\rho}{\rho_0}(x_{i,A}x_{j,B} + x_{i,B}x_{j,A})\frac{\partial \mathcal{W}}{\partial C_{AB}}.$$

At any given time there are possible motions of the body for which the velocity gradients are arbitrary. Since P_{ij} is defined by deformation gradients alone, however, equation (2.2.40) implies that

$$P_{ij} = 0,$$

or, equivalently

$$T_{ji} = \frac{\rho}{\rho_0}(x_{i,A}\, x_{j,B} + x_{i,B}\, x_{j,A})\frac{\partial \mathcal{W}}{\partial C_{AB}}. \tag{2.2.41}$$

Using the symmetry of C_{AB} the above reduces to

$$T_{ji} = \frac{\rho}{\rho_0} x_{i,A}\, x_{j,B} \left(\frac{\partial \mathcal{W}}{\partial C_{AB}} + \frac{\partial \mathcal{W}}{\partial C_{BA}}\right). \tag{2.2.42}$$

Equations (2.2.42) and (2.2.29) combine to give

$$\sigma_{Ai} = x_{i,B} \left(\frac{\partial \mathcal{W}}{\partial C_{AB}} + \frac{\partial \mathcal{W}}{\partial C_{BA}}\right). \tag{2.2.43}$$

If we ensure that $\mathcal{W}$ is expressed as a symmetric function of C_{AB} the latter equation becomes

$$\sigma_{Ai} = 2\, x_{i,B} \frac{\partial \mathcal{W}}{\partial C_{AB}},$$

or, with use of equation (2.2.7),

$$\sigma_{Ai} = x_{i,B} \frac{\partial \mathcal{W}}{\partial E_{AB}}, \tag{2.2.44}$$

with the same restriction that $\mathcal{W}$ must be expressed as a symmetric function of E_{AB}.

The precise form of the strain energy function depends on the particular material chosen and thus detailed discussion of its properties shall be left to subsequent chapters. Here it is simply noted that for an adiabatic elastic material $\mathcal{W}$ may be expanded as a Taylor's series in the Lagrangian strain, where the coefficients are called the elasticity constants, whilst for the piezoelectric material considered in Chapter 4 $\mathcal{W}$ must be expanded as a series in both the strain and electric field.

Equations (2.2.33) and (2.2.44) represent the governing equations and constitutive equations for a deformed anisotropic elastic solid. In their derivation no material symmetry has been assumed. The introduction of a particular form for the strain energy function will describe the solid and complete the system of equations.

3 Anisotropic Elasticity

The propagation of elastic waves on the surface of a traction-free half-space has been extensively investigated since Rayleigh [1896] predicted their existence in 1896.

The work of Rayleigh for an isotropic linearly elastic material was extended to anisotropic materials by Stonely [1955] who investigated the propagation of surface waves on the Basal plane (a particular crystallographic configuration) of cubic crystals. This symmetry class and orientation were chosen since the momentum balance equations (2.2.33) degenerate to an algebraically solvable system. Stonely considered only "pure" Rayleigh wave modes, that is those possessing amplitudes that decay exponentially with depth and neglected a whole class of solutions now accepted as "generalised" Rayleigh waves in which the decay of the amplitude with depth is of damped sinusoidal form. These latter solutions were obtained by Buchwald [1963] who achieved the results through consideration of the slowness surfaces.

Buchwald, like Stonely, found regions in which he claimed surface waves could not propagate. This proposition was backed up by the numerical results of Gazis et al [1960] and the theoretical work of Synge [1957], who deduced that the slowness characteristic polynomial is complex and thus only admits complex solutions leading to waves with attenuation in the direction of propagation. The existence of "forbidden zones" was shown to be false by Stroh [1962] and, later, Currie [1974], who proved that the slowness characteristic polynomial in fact reduces to a purely real equation and therefore a surface wave may always propagate. Farnell [1970] used numerical search procedures to find the admissible surface wave speeds for various crystals and configurations and to examine the form of the solutions obtained. He showed that the surface wave in fact degenerates into a bulk wave satisfying the surface boundary conditions for particular crystal configurations and he also examined the behaviour of the so-called "pseudo"-surface wave which decays with propagation distance.

More recently there has been growing interest in the propagation of nonlinear waves on elastic half-spaces. Kalyanasundaram [1981] presented a periodic waveform solution for propagation in a half-space of quadratically nonlinear isotropic elastic material using the method of multiple scales, a technique developed to eliminate secular terms in the nonlinear solutions and previously applied to dispersive wave problems, Kakutani et al [1974]. This technique is discussed in detail in the books by Nayfeh [1973] and Bender and Orszag [1974]. Kalyanasundaram's application of the technique, however, suffered from the limitation that the secular terms of interest were y-dependent and no condition was derived for their elimination. Subsequent papers by Kalyanasundaram considering the interactions of opposite propagating waves, [1983], and co-directional waves, [1981], suffered from similar analytical shortcomings.

The limitations of Kalyanasundaram's approach were noted and corrected by David [1985] and also, in a series of papers, by Lardner that considered elastic wave propagation [1983], harmonic generation [1984] and shock development [1985]. Lardner extended Kalyanasundaram's application of the multiple scales technique to include "slow" parameters in the y-direction in order to eliminate the secular terms. The form of solution considered by Lardner involved an integral over all available wavenumbers and therefore allows for the input signal to be much more general than a pure sinusoidal one. This approach, as Kalyanasundaram's, lead to infinite systems of coupled amplitude equations which were truncated and solved for the material fused quartz.

A different approach was adopted by Parker and Talbot [1985] who used harmonic conjugate functions to represent the linear Rayleigh wave and thus were able to consider any form of input wave. This method enables the surface elevation of waves which propagate without distortion to be characterised as those satisfying a certain nonlinear functional equation. Through the use of this method Parker and Talbot found non-distorting waveforms which travel at speeds other than the Rayleigh wave speed.

The effects of anisotropy upon the nonlinear propagation of surface waves were first considered by Lardner [1986]. A technique directly analogous to that applied to isotropic materials (Lardner [1983]) was utilised, taking into account the strain energy expansion for an anisotropic material. The characteristic equation obtained apparently yields no algebraic solutions and thus no closed-form analytical representation for the coupled amplitude equations has been found. In a later paper, Lardner and Tupholme [1986], present numerical solutions based upon the method of Lardner [1986] for the particular case of cubic, $m3m$, symmetry and a simple sinusoidal signalling condition was considered.

Parker [1988] extended the analysis of Parker and Talbot [1985] to include the effects of anisotropy and to consider the non-distorting waveforms admitted by anisotropic materials. This technique was further extended to include the spreading of surface waves on the two-dimensional surface of a semi-infinite substrate in Parker and David [1989].

It is noted here that much of the work quoted above section has been published in the past four years and that, in view of this fact, the work presented in this particular chapter of the thesis, whilst not original in content, was developed independently of the previously stated analyses. The notations used have developed over the period 1985–88, although some modifications have taken place in view of the recently published papers of Lardner[1986], Lardner and Tupholme [1986] and Parker [1988].

3.1 CONSTITUTIVE EQUATIONS

The constitutive relations for a general elastic substrate have been derived in Section 2.2.7 in terms of the strain energy, or Gibbs' function. In this section the form of the strain energy is given for a general anisotropic elastic material. This shall then be used, with suitable tensorial symmetry, to derive the momentum balance equations for a deformed elastic solid.

3.1.1 Strain Energy

The strain energy used in Chapter 2 must be expressed as a symmetric function of the Lagrange strain. First we expand $\mathcal{W}$ as a Taylor's series

$$\mathcal{W} = c^{(0)} + c^{(1)}_{AB}\, E_{AB} + \frac{1}{2} c^{(2)}_{ABCD}\, E_{AB}\, E_{CD} + \frac{1}{6} c^{(3)}_{ABCDEF}\, E_{AB}\, E_{CD}\, E_{EF} + \ldots , \tag{3.1.1}$$

where the coefficients $c^{(1)}_{AB}$, $c^{(2)}_{ABCD}$ and $c^{(3)}_{ABCDEF}$ are defined through the relations

$$\begin{aligned}
c^{(0)} &= \mathcal{W}|_{E_{AB}=0} \\
c^{(1)}_{AB} &= \left.\frac{\partial \mathcal{W}}{\partial E_{AB}}\right|_{E_{AB}=0} \\
c^{(2)}_{ABCD} &= \left.\frac{\partial^2 \mathcal{W}}{\partial E_{AB}\, \partial E_{CD}}\right|_{E_{AB}=0} \\
c^{(3)}_{ABCDEF} &= \left.\frac{\partial^3 \mathcal{W}}{\partial E_{AB} \partial E_{CD} \partial E_{EF}}\right|_{E_{AB}=0}
\end{aligned}$$

If we take the unstrained state as the reference state for $\mathcal{W}$, $c^{(0)} = 0$, and from equation (3.1.1) we define $\mathcal{W}$ through

$$\mathcal{W} = c^{(1)}_{AB}\, E_{AB} + \frac{1}{2} c^{(2)}_{ABCD}\, E_{AB}\, E_{CD} + \frac{1}{6} c^{(3)}_{ABCDEF}\, E_{AB}\, E_{CD}\, E_{EF} . \tag{3.1.2}$$

The coefficients of equation (3.1.2) are known as the first-, second- and third-order elastic constants respectively and are analogous to Lamé's constants of isotropic elasticity. The Taylor's series has been truncated at cubic order mainly because numerical values for the higher-order constants are unavailable.

The Lagrange strain is a symmetric second-order tensor and we may thus write

$$\mathcal{W} = c^{(1)}_{BA}\, E_{AB} + \frac{1}{2} c^{(2)}_{ABCD}\, E_{AB}\, E_{CD} + \frac{1}{6} c^{(3)}_{ABCDEF}\, E_{AB}\, E_{CD}\, E_{EF} , \tag{3.1.3}$$

by replacement of the dummy subscripts in the first term on the right hand side of equation (3.1.2).

Comparison of equations (3.1.2) and (3.1.3) shows that the first-order coefficients must satisfy

$$c^{(1)}_{AB} = c^{(1)}_{BA}\,.$$

A similar replacement of subscripts for the second- and third-order coefficients leads to the relations

$$c^{(2)}_{ABCD} = c^{(2)}_{BACD} = c^{(2)}_{ABDC} \tag{3.1.4}$$

and

$$c^{(3)}_{ABCDEF} = c^{(3)}_{BACDEF} = c^{(3)}_{ABDCEF} = c^{(3)}_{ABCDFE}\,. \tag{3.1.5}$$

The symmetry of the strain energy with respect to the Lagrange strain imposed in Chapter 2 leads us to the further conditions

$$c^{(2)}_{ABCD} = c^{(2)}_{CDAB} \tag{3.1.6}$$

and

$$c^{(3)}_{ABCDEF} = c^{(3)}_{CDABEF} = c^{(3)}_{ABEFCD}\,, \tag{3.1.7}$$

which, together with the conditions (3.1.4) and (3.1.5), may be represented by

$$\begin{aligned} c^{(1)}_{AB} &= c^{(1)}_{BA} \\ c^{(2)}_{ABCD} &= c^{(2)}_{BACD} = c^{(2)}_{CDAB} \\ c^{(3)}_{ABCDEF} &= c^{(3)}_{BACDEF} = c^{(3)}_{CDABEF} = c^{(3)}_{ABEFCD}\,. \end{aligned} \tag{3.1.8}$$

3.1.2 Piola-Kirchhoff Stress

Recall that equation (2.2.44) gives the Piola-Kirchhoff stress tensor in terms of the strain energy function as

$$\sigma_{Ai} = x_{i,B}\,\frac{\partial \mathcal{W}}{\partial E_{AB}}\,. \tag{3.1.9}$$

On substituting the series expansion (3.1.2) for $\mathcal{W}$ into equation (3.1.9), the Piola-Kirchhoff stress tensor can be calculated in terms of the Lagrangian strain.

Taking the second term in the series expansion for $\mathcal{W}$, for illustrative purposes, and assuming this terms makes a contribution $\mathcal{T}_2$ in σ_{Ai}, it follows that

$$
\begin{aligned}
\mathcal{T}_2 &= x_{i,B}\,\frac{\partial}{\partial E_{AB}}\left[\frac{1}{2}\,c^{(2)}_{CDEF}\,E_{CD}\,E_{EF}\right] \\
&= x_{i,B}\,c^{(2)}_{ABCD}\,E_{CD}\,, \qquad \text{using } c^{(2)}_{ABCD} = c^{(2)}_{CDAB}\,, \\
&= x_{i,B}\,c^{(2)}_{ABCD}\left[\frac{1}{2}u_{C,D} + \frac{1}{2}\,u_{D,C} + \frac{1}{2}\,u_{E,C}\,u_{E,D}\right], \qquad (3.1.10)
\end{aligned}
$$

with the use of equation (2.2.10). On further manipulation and using the symmetries (3.1.8)

$$
\begin{aligned}
\mathcal{T}_2 &= (u_{i,B} + \delta_{iB})\,c^{(2)}_{ABCD}\left[\frac{1}{2}\,u_{C,D} + \frac{1}{2}\,u_{D,C} + \frac{1}{2}\,u_{E,C}\,u_{E,D}\right] \\
&= \delta_{iB}\,c^{(2)}_{ABCD}\,u_{C,D} + \frac{1}{2}\,c^{(2)}_{ABCD}\,u_{i,B}\,u_{C,D} + \frac{1}{2}\,c^{(2)}_{ABCD}\,u_{i,B}\,u_{D,C} \\
&\quad + \frac{1}{2}\,c^{(2)}_{ABCD}\,u_{i,B}\,u_{E,C}\,u_{E,D} + \frac{1}{2}\,\delta_{iB}\,c^{(2)}_{ABCD}\,u_{E,C}\,u_{E,D} \qquad (3.1.11)
\end{aligned}
$$

Repeating this process for other terms in the expansion yields the constitutive relation

$$
\begin{aligned}
\sigma_{Ai} &= \delta_{iB}\,c^{(1)}_{AB} + c^{(1)}_{AB}\,u_{i,B} + \delta_{iB}\,c^{(2)}_{ABCD}\,u_{C,D} + \frac{1}{2}\,c^{(2)}_{ABCD}\,u_{i,B}\,u_{C,D} \\
&\quad + \frac{1}{2}\,c^{(2)}_{ABCD}\,u_{i,B}\,u_{D,C} + \frac{1}{2}\,\delta_{iB}\,c^{(2)}_{ABCD}\,u_{E,C}\,u_{E,D} \\
&\quad + \frac{1}{2}\,\delta_{iB}\,c^{(3)}_{ABCDEF}\,u_{C,D}\,u_{E,F} + \mathrm{O}\Big((u_{A,B})^3\Big) \qquad (3.1.12)
\end{aligned}
$$

The latter expression for σ may be somewhat simplified by noting that all derivatives are with respect to the reference frame. We can therefore, without loss of generality, allow the elastic coefficients to have lower case subscripts. It follows that

$$
\begin{aligned}
\sigma_{Ai} &= c^{(1)}_{Ai} + c^{(1)}_{AB}\,u_{i,B} + c^{(2)}_{AiCD}\,u_{C,D} + \frac{1}{2}c^{(2)}_{ABCD}\,u_{i,B}\,u_{C,D} \\
&\quad + \frac{1}{2}c^{(2)}_{ABDC}\,u_{i,B}\,u_{C,D} + \frac{1}{2}c^{(2)}_{AiCD}\,u_{E,C}\,u_{E,D} \\
&\quad + \frac{1}{2}c^{(3)}_{AiCDEF}\,u_{C,D}\,u_{E,F} + \mathrm{O}\Big((u_{A,B})^3\Big) \\
&= c^{(1)}_{Ai} + c^{(1)}_{AB}\,u_{i,B} + c^{(2)}_{AiCD}\,u_{C,D}
\end{aligned}
$$

$$+ \frac{1}{2}\left[\delta_{iC}\, c^{(2)}_{ADEF} + \delta_{iE}\, c^{(2)}_{AFDC} + \delta_{EC}\, c^{(2)}_{AiDF}\right] u_{C,D}\, u_{E,F}$$

$$+ \frac{1}{2} c^{(3)}_{AiCDEF}\, u_{C,D}\, u_{E,F} + \mathrm{O}\left((u_{A,B})^3\right)$$

$$= c^{(1)}_{Ai} + c^{(1)}_{AB}\, u_{i,B} + c^{(2)}_{AiCD}\, u_{C,D}$$

$$+ d_{iACDEF}\, u_{C,D}\, u_{E,F} + \mathrm{O}\left((u_{A,B})^3\right), \tag{3.1.13}$$

where d_{iACDEF}, defined by

$$d_{iACDEF} = \frac{1}{2}\left[\delta_{iC}\, c^{(2)}_{ADEF} + \delta_{iE}\, c^{(2)}_{AFDC} + \delta_{EC}\, c^{(2)}_{AiDF} + c^{(3)}_{AiCDEF}\right], \tag{3.1.14}$$

is called a quasi-third-order elasticity constant.

On replacement of dummy suffices with use of the symmetries (3.1.8), equation (3.1.14) reduces to

$$d_{ijklmn} = \frac{1}{2}\left[\delta_{ik}\, c^{(2)}_{jlmn} + \delta_{im}\, c^{(2)}_{jnlk} + \delta_{km}\, c^{(2)}_{ijln} + c^{(3)}_{ijklmn}\right], \tag{3.1.15}$$

equivalent to equation (5) in Lardner [1986]. Recalling the symmetry relations (3.1.8) and the notation introduced in Chapter 2, it is easily seen from the above that the symmetry of d_{ijklmn} is shown through $d_{(ij)(kl)(mn)}$.

Assuming that the material is unstressed when the displacement gradients are zero, we require

$$c^{(1)}_{Ai} = 0\,.$$

Equation (3.1.13) then becomes

$$\sigma_{Ai} = c_{AiCD}\, u_{C,D} + d_{iACDEF}\, u_{C,D}\, u_{E,F} + o((u_{A,B})^3), \tag{3.1.16}$$

where for convenience, the superscript $^{(2)}$ is dropped from the second-order elasticity constant.

We have already stated that σ_{Ai} is not generally symmetric and it is seen from equation (3.1.15) that the third-order term is not symmetric within the first two subscripts.

3.1.3 Equations of motion

Equation (3.1.16) may now be substituted into the momentum balance equation (2.2.33) to give

$$\rho_0 \ddot{u}_i = c_{AiCD}\, u_{C,DA} + d_{iACDEF}\, u_{C,DA}\, u_{E,F} + d_{iACDEF}\, u_{C,D}\, u_{E,FA}\,, \qquad (3.1.17)$$

which can be rewritten as

$$\rho_0 \ddot{u}_i = c_{iACD}\, u_{C,DA} + 2d_{iACDEF}\, u_{C,DA}\, u_{E,F}\,, \qquad (3.1.18)$$

using the symmetries of the second- and quasi–third-order elasticity tensor.

3.1.4 Boundary Conditions

The momentum balance equations have been derived for a deformed elastic substrate, referred to a general rectangular cartesian coordinate system (x_1, x_2, x_3) without discussing the orientation of the substrate. We restrict attention to surface waves propagating on an infinite flat surface and hence consider the material to lie, in its reference configuration, in the half space $\{-\infty < X_1 < \infty,\ -\infty < X_2 \leq 0,\ -\infty < X_3 < \infty\}$.

The only boundary to be considered is thus $X_2 = 0$, for $-\infty < X_1 < \infty$, $-\infty < X_3 < \infty$. The condition normally imposed upon this surface is that it must be stress free, since the upper half-space is assumed to be a vacuum. Referring to our definitions of the Cauchy stress tensor and the Piola-Kirchhoff stress tensor, equations (2.2.21), (2.2.28) and (2.2.29), this implies that

$$\sigma_{2i} = 0 \qquad \text{on } X_2 = 0\,, \qquad (3.1.19)$$

which can be rewritten, with the aid of equation (3.1.16) and dropping higher order terms, as

$$c_{2iCD}\, u_{C,D} + d_{i2CDEF}\, u_{C,D}\, u_{E,F} = 0\,,$$

or, using the symmetry of the second-order elasticity tensor,

$$c_{i2CD}\, u_{C,D} + d_{i2CDEF}\, u_{C,D}\, u_{E,F} = 0\,. \qquad (3.1.20)$$

3.2 NON-DIMENSIONALISING

If we consider equation (3.1.18), each term has the dimensions

$$\frac{\mathrm{M}}{\mathrm{L}^3}\frac{\mathrm{L}}{\mathrm{T}^2} = \frac{\mathrm{M}}{\mathrm{L}^2\mathrm{T}^2}.$$

However, in general, the material density will be $\mathrm{O}(10^3)$ kg/m^3, with the linear stress driving term having the magnitude of the second-order elasticity constant, typically $\mathrm{O}(10^{11})$ N/m^2. It is then clearly seen that the terms will be of greatly different magnitude. This could cause problems in numerical routines since the ratio of two greatly different terms may be too large or small to register on the computer. For this reason each term is non-dimensionalised with respect to some typical value to become $\mathrm{O}(1)$–$\mathrm{O}(10^2)$.

All elasticity constants are typically $\mathrm{O}(10^{11})$ N/m^2 and we therefore may choose one of the second-order constants as the non-dimensionalising constant c_a. Here we choose $c_a = c_{44}$, as a consequence, we replace c_{ijkl} and d_{ijklmn} by

$$\begin{aligned} c'_{ijkl} &= \frac{c_{ijkl}}{c_a} \\ d'_{ijklmn} &= \frac{d_{ijklmn}}{c_a}, \end{aligned} \tag{3.2.1}$$

where a dash denotes a non-dimensionalised quantity.

All distance measurements may be non-dimensionalised with respect to the wavelength of the wave, or $1/k_0$, where k_0 is the wavenumber of the fundamental wave. Thus we introduce the non-dimensional quantities u'_i, x', y' and z' through the relations

$$\begin{aligned} u'_i &= k_0\, u_i\,, \\ x' &= k_0\, x\,, \\ y' &= k_0\, y\,, \\ z' &= k_0\, z\,, \end{aligned} \tag{3.2.2}$$

If the wave is travelling at speed c, the frequency of the wave is $k_0 c$, and this may be used to non-dimensionalise the time t, through

$$t' = k_0\, c\, t\,. \tag{3.2.3}$$

Finally, by inspection of equations (3.1.18), a non-dimensional density is defined through

$$\rho' = \frac{c^2}{c_a}\rho_0 \,. \tag{3.2.4}$$

These substitutions, together with the replacements $u_i \rightarrow \epsilon u_i$, made in order that we may keep track of the various orders of terms involved, mean that the forms of equations (3.1.18) and (3.1.19) become

$$\rho' \ddot{u}'_i = c'_{ijkl}\, u'_{k,lj} + 2\epsilon d'_{ijklmn}\, u'_{k,l}\, u'_{m,nj} \,, \tag{3.2.5}$$

and

$$0 = c'_{i2kl}\, u'_{k,l} + \epsilon d'_{i2klmn}\, u'_{k,l}\, u'_{m,n} \,, \tag{3.2.6}$$

where all derivatives are with respect to the reference frame although lower case subscripts are used throughout for ease of notation. For later convenience all dashes will henceforth be dropped from the non-dimensional equations (3.2.5) and (3.2.6).

3.3 SOLUTION

In this section we shall investigate solutions to the quadratically nonlinear equations (3.2.5) subject to the boundary conditions (3.2.6). A standard perturbation expansion may be used, but a simple example below reveals how such a technique produces non-uniformities of solution when applied to surface waves. This leads us to the method of multiple scales which yields a far-field solution and uses the possible non-uniformities to derive further information about the linear amplitude. The main advantage of this approach is that the nonlinear system need not be completely solved in order to provide a correction to the linear solution.

Applying the method of multiple scales gives an infinite system of coupled partial differential equations which, after some simplification and truncation, can be solved by numerical techniques.

3.3.1 An example

Let us consider the single illustrative equation considered in Bender and Orszag [1978], of an essentially similar form to equation (3.2.5),

$$\frac{d^2u}{dy^2} + u = -\epsilon u^3 , \tag{3.3.1}$$

where ϵ is some small parameter. Suppose we seek a solution to equation (3.3.1) subject to the boundary conditions $u = 1$ and $u_y = 0$, both on $y = 0$. A straightforward perturbation expansion of u with respect to ϵ gives

$$u = u^{(1)} + \epsilon u^{(2)} + \dots , \tag{3.3.2}$$

and substitution into equation (3.3.1) yields

$$\frac{d^2u^{(1)}}{dy^2} + u^{(1)} = 0 \quad ; \quad u^{(1)} = 1 \text{ and } \frac{du^{(1)}}{dy} = 0 \text{ on } y = 0 , \tag{3.3.3}$$

and

$$\frac{d^2u^{(2)}}{dy^2} + u^{(2)} = -u^{(1)^3} \quad ; \quad u^{(2)} = 0 \text{ and } \frac{du^{(2)}}{dy} = 0 \text{ on } y = 0 , \tag{3.3.4}$$

at first- and second-order in ϵ respectively.

A solution to the homogeneous equation (3.3.3) that satisfies the appropriate boundary conditions is

$$u^{(1)} = \cos y . \tag{3.3.5}$$

When substituted into equation (3.3.3) this yields the inhomogeneous equation

$$\frac{d^2u^{(2)}}{dy^2} + u^{(2)} = - \quad \cos^3 y$$

$$= - \quad \left[\frac{1}{4}\cos 3y + \frac{3}{4}\cos y\right], \tag{3.3.6}$$

which must be solved subject to the boundary conditions

$$u^{(2)} = 0 \quad \text{and} \quad \frac{du^{(2)}}{dy} = 0 \quad \text{on} \quad y = 0. \tag{3.3.7}$$

The solution to equations (3.3.7) and (3.3.6) consists of a complementary function and a particular integral. Now the complementary function (CF) is the solution to the homogeneous form of equation (3.3.6), which is exactly the first-order equation (3.3.3), leading to

$$u^{(2)}_{\text{CF}} = A\cos y + B\sin y, \tag{3.3.9}$$

with the constants A and B undefined. The particular integral (PI) is obtained by inspection of the right hand side of equation (3.3.6). However, the form of the CF restricts us to a PI of the form

$$u^{(2)}_{\text{PI}} = Cy\sin y + D\cos 3y, \tag{3.3.10}$$

with the constants C and D to be found by substitution. The second-order solution finally becomes

$$u^{(2)} = A\cos y + B\sin y - \frac{3}{8}y\sin y + \frac{1}{32}\cos 3y,$$

which, after application of the boundary conditions gives

$$u^{(2)} = -\frac{1}{32}\cos y - \frac{3}{8}y\sin y + \frac{1}{32}\cos 3y. \tag{3.3.11}$$

This is the solution at order ϵ and should be O(1) with respect to ϵ. It is seen however that the second term in this solution, known as the secular term, grows linearly with y and that it is no longer of O(1) for values of y of $O(1/\epsilon)$. To emphasise this point, the solution for u can be written

$$u = \cos y - \left[\frac{\epsilon}{32}\cos y + \frac{3}{8}(\epsilon y)\sin y - \frac{\epsilon}{32}\cos 3y\right] + O(\epsilon^2), \tag{3.3.12}$$

and in order that this expansion is valid the square bracketed term must be $O(\epsilon)$. This is clearly not true for the secular term for values of y of $O(1/\epsilon)$. This expansion is therefore valid only for small $y \ll \epsilon$, the "near-field", but breaks down before y becomes $O(1/\epsilon)$.

In the study of nonlinear elasticity in this thesis we are considering a semi-infinite material and shall impose conditions upon the deformation at infinite depth. In order to ensure that such conditions are satisfied it is necessary for us to eliminate any secular terms in the solution.

The method of multiple scales achieves this objective by introducing slow scales, that allow derivatives of linear terms to appear in the nonlinear system. These terms are of a similar form to those giving rise to the secular terms and thus may be used to effectively "cancel out" the effect of the secular terms.

First we introduce the "slow" variable $\eta = \epsilon y$ and allow u to depend upon η through the perturbation expansion

$$u = u^{(1)}(y,\eta) + \epsilon u^{(2)}(y,\eta) + \dots , \tag{3.3.13}$$

which may be substituted into equation (3.3.1) to give

$$\frac{\partial^2 u^{(1)}}{\partial y^2} + u^{(1)} = 0 \quad ; \quad u^{(1)} = 1 \text{ and } \frac{\partial u^{(1)}}{\partial y} = 0 \text{ on } y = 0 , \tag{3.3.14}$$

and

$$\frac{\partial^2 u^{(2)}}{\partial y^2} + u^{(2)} = -u^{(1)^3} - 2\frac{\partial^2 u^{(1)}}{\partial y \partial \eta} \quad ; \quad u^{(2)} = 0 \text{ and } \frac{\partial u^{(2)}}{\partial y} = -\frac{\partial u^{(1)}}{\partial \eta} \text{ on } y = 0 , \tag{3.3.15}$$

at first- and second-order in ϵ respectively. The derivative with respect to the slow variable arises from the chain-rule relation

$$\frac{du}{dy} = \frac{\partial u^{(1)}}{\partial y} + \epsilon \left(\frac{\partial u^{(1)}}{\partial \eta} + \frac{\partial u^{(2)}}{\partial y} \right) + \dots .$$

The most general solution to the differential equation (3.3.14) may be taken as

$$u^{(1)} = A(\eta) \mathrm{e}^{\mathrm{i}y} + \bar{A}(\eta) \mathrm{e}^{-\mathrm{i}y} \tag{3.3.16}$$

where the superposed bar denotes the complex conjugate. Substitution of this solution into equation (3.3.15) gives

$$\frac{\partial^2 u^{(2)}}{\partial y^2} + u^{(2)} = -\left[3A^2\bar{A} + 2\mathrm{i}\frac{\partial A}{\partial \eta} \right] \mathrm{e}^{\mathrm{i}y} - \left[3\bar{A}^2 A - 2\mathrm{i}\frac{\partial \bar{A}}{\partial \eta} \right] \mathrm{e}^{-\mathrm{i}y} + A^3 \mathrm{e}^{3\mathrm{i}y} + \bar{A}^3 \mathrm{e}^{-3\mathrm{i}y} . \tag{3.3.17}$$

It is clear that the square bracketed terms will lead to secular terms of the form $y\mathrm{e}^{\mathrm{i}y}$ in the second-order solution. These may be eliminated through the conditions

$$\left[3A^2\bar{A} + 2\mathrm{i}\frac{\partial A}{\partial \eta}\right] = 0 \tag{3.3.18}$$

and

$$\left[3\bar{A}^2 A - 2\mathrm{i}\frac{\partial \bar{A}}{\partial \eta}\right] = 0\,,$$

which may be seen to be conjugates.

The modulus–argument decomposition

$$A(\eta) = R(\eta)\mathrm{e}^{\mathrm{i}\theta(\eta)}$$

may now be combined with equation (3.3.18), to reveal

$$\frac{dR}{d\eta} = 0\,,$$

and

$$\frac{d\theta}{d\eta} = \frac{3}{2}R^2\,,$$

yielding the representation

$$A(\eta) = R(0)\mathrm{e}^{\mathrm{i}\theta(0)} + 3\mathrm{i}R^2(0)\eta/2$$

and thus

$$u^{(1)} = 2R(0)\cos\left[\theta(0) + \frac{3}{2}R^2(0)\eta + y\right]\,. \tag{3.3.19}$$

The boundary conditions (3.3.14) now imply that

$$R(0) = \frac{1}{2}\,, \quad \text{and} \quad \theta(0) = 0\,,$$

yielding

$$u^{(1)} = \cos\left(1 + \frac{3}{8}\epsilon\right)y\,. \tag{3.3.20}$$

The representation (3.3.20) is clearly bounded for all y and may be considered as a perturbation about the first-order solution. It is a better approximation to the exact solution however the "phase shift", $\frac{3}{8}\epsilon$, becomes noticeable for values of y of $\mathrm{O}(1/\epsilon)$, or η of $\mathrm{O}(1)$ which may clearly be seen from the figures in Bender and Orszag [1974]. Secular terms of the form $y\mathrm{e}^y$ have been eliminated from the first-order solution through this technique, however second-order secular terms may still arise. We may therefore say that the multiple scales solution provides a bounded solution for u valid in the "far field" to values of y of $\mathrm{O}(1/\epsilon^2)$.

3.3.2 Multiple Scales Expansion

To apply the multiple scales technique to the three dependent variable problem (3.2.5) and (3.2.6) we define slow variables ξ, η and τ by

$$\begin{aligned} \xi &= \epsilon x\,, \\ \eta &= \epsilon y\,, \\ \tau &= \epsilon t\,. \end{aligned}$$

The displacement u_i is now allowed to depend upon distance, time and the slow variables ξ, η and τ, through the expansion

$$u_j = u_j^{(1)}(x,y,t,\xi,\eta,\tau) + \epsilon\, u_j^{(2)}(x,y,t,\xi,\eta,\tau) + \ldots\,. \tag{3.3.21}$$

On substituting into equations (3.2.5) and (3.2.6) and collecting together corresponding terms in powers of ϵ, one obtains the two systems

$$\rho\, \ddot{u}_i^{(1)} - c_{ijkl}\, u_{k,lj}^{(1)} = 0\,, \tag{3.3.22}$$

subject to

$$c_{i2kl}\, u_{k,l}^{(1)} = 0 \tag{3.3.23}$$

on $y = \eta = 0$, and

$$\begin{aligned} \rho\, \ddot{u}_i^{(2)} - c_{ijkl}\, u_{k,lj}^{(2)} &= (c_{i1kl} + c_{ilk1})\, u_{k,l\xi}^{(1)} + (c_{i2kl} + c_{ilk2})\, u_{k,l\eta}^{(1)} \\ &\quad - 2\rho\, \dot{u}_{i,\tau}^{(1)} + 2d_{ijklmn}\, u_{k,l}^{(1)}\, u_{m,nj}^{(1)}\,, \end{aligned} \tag{3.3.24}$$

subject to

$$c_{i2kl}\, u_{k,l}^{(2)} = -\, c_{i2k1}\, u_{k,\xi}^{(1)} - c_{i2k2}\, u_{k,\eta}^{(1)} - d_{i2klmn}\, u_{k,l}^{(1)}\, u_{m,n}^{(1)} \tag{3.3.25}$$

on $y = \eta = 0$.

The homogeneous linear system (3.3.22) is solved subject to the linear boundary conditions (3.3.23) and its solution is then substituted into the inhomogeneous second-order system (3.3.24) and (3.3.25).

3.3.3 First-order System

A solution to equation (3.3.22) satisfying the boundary conditions (3.3.23) is now sought. Having defined the surface of the substrate to be $y = 0$, we seek a solution representing a plane wave propagating in the positive x-direction. Thus we look for a solution of the form

$$u_j^{(1)} = a_j(y,\xi,\eta,\tau)\,\mathrm{e}^{\mathrm{i}(x-t)} + \text{c.c.}\,, \tag{3.3.26}$$

since the variables have been non-dimensionalised with respect to the wavelength and frequency. The quantity "c.c." denotes the complex conjugate of the function and it appears to ensure that the displacement $u_i^{(1)}$ is real and since the conjugate of any solution to a differential equation with real coefficients is also a solution to the same equation.

The restriction to consideration of x-propagating waves rather than the more general formulation

$$u_j^{(1)} = a_j(y\,,\,\xi,\eta,\tau)\,\mathrm{e}^{\mathrm{i}(kx+lz-t)} + \text{c.c.}\,,$$

allowing consideration of propagation in any direction on the surface $y = 0$, simplifies some of the ensuing analysis. A more detailed numerical study of symmetry decompositions and the effects of consideration of the "slowness surface" defined by k and l in the above representation will be presented in Section 3.4.

Substituting the representation (3.3.26) into the equations of motion (3.3.22) yields the equations

$$\rho\,\delta_{ik}\,a_k + c_{i2k2}\,a_{k,yy} + \mathrm{i}(c_{i2k1} + c_{i1k2})\,a_{k,y} - c_{i1k1}\,a_k = 0\,. \tag{3.3.27}$$

In order that the displacements $u_j^{(1)}$ represent a surface wave, their magnitude must decrease with depth. If the slowly varying amplitudes a_j have the representation

$$a_j(y,\xi,\eta,\tau) = A(\xi,\eta,\tau)\,a_j\,\mathrm{e}^{\mathrm{i}sy}\,, \tag{3.3.28}$$

then the displacement decays with depth only if $\Im(s) < 0$, where $\Im$ represents the imaginary part of a number.

On substituting equation (3.3.28) into equation (3.3.27) the following matrix equation for a_j and s is obtained:

$$\mathrm{L}_{ik}(s)\,a_k = 0\,, \tag{3.3.29}$$

where

$$\mathrm{L}_{ik}(s) = c_{i2k2}\,s^2 + (c_{i2k1} + c_{i1k2})\,s + c_{i1k1} - \rho\,\delta_{ik}\,. \tag{3.3.30}$$

It is noted here that the matrix L_{ik} is symmetric through the symmetry of the elasticity constants c_{ijkl}.

To ensure that equation (3.3.29) has a non-trivial solution it is necessary that

$$|\mathrm{L}_{ik}(s)| = 0\,, \tag{3.3.31}$$

which represents a sixth-order polynomial in s with real coefficients. This equation will have six roots which will either be real or appear as pairs of complex conjugates (in all possible combinations). Our decay condition upon s means that we are only interested in the complex roots. The coefficients of the polynomial (3.3.31) are not completely defined since they involve the nondimensional parameter ρ which, because of its definition (3.2.4), depends upon the unknown surface wavespeed. This parameter ρ may be chosen to lie within a range that leads to three pairs of complex conjugate roots. Clearly three roots can then be chosen to satisfy the decay condition, one from each pair. These roots are denoted by $s^{(n)}$, $n = 1, 2, 3$, and the corresponding eigenvector solutions to equation (3.3.29) by $a_j^{(n)}$.

Our first-order solution now takes the form of a summation over these three admissible surface modes

$$u_j^{(1)} = \sum_{n=1}^{3} A^{(n)}(\xi, \eta, \tau) a_j^{(n)} \, \mathrm{e}^{\mathrm{i}s^{(n)}y} \, \mathrm{e}^{\mathrm{i}(x-t)} + \text{c.c.}\,. \tag{3.3.32}$$

This solution must now satisfy the boundary conditions (3.3.23), which yield the matrix equation

$$\sum_{n=1}^{3} \mathrm{M}_{in} \, A^{(n)} = 0 \tag{3.3.33}$$

where

$$\mathrm{M}_{in} = (c_{i2k1} + c_{i2k2}\, s^{(n)})\, a_k^{(n)}\,. \tag{3.3.34}$$

The set of equations (3.3.33) must also have a non-trivial solution, giving rise to the condition

$$|\mathrm{M}_{in}| = 0\,. \tag{3.3.35}$$

The only quantity appearing in $|\mathrm{M}_{in}|$ yet to be determined is ρ. In general ρ cannot be found algebraically but it can be found numerically using an iterative process described in more detail later in this chapter.

The method of multiple scales allows us to inspect the second-order system to obtain coupled partial differential equations for the slowly varying amplitudes $A^{(n)}$. In order to obtain this system however, we must include in the first-order solution

all harmonics generated by the nonlinearities. Thus we must extend the linear solution (3.3.32) to be a summation over every harmonic:

$$u_j^{(1)} = \sum_{K=1}^{\infty} \sum_{n=1}^{3} A_K^{(n)}(\xi, \eta, \tau)\, a_j^{(n)}\, \mathrm{e}^{\mathrm{i}Ks^{(n)}y}\, \mathrm{e}^{\mathrm{i}K(x-t)} + \mathrm{c.c}\,, \tag{3.3.36}$$

where we shall call K the harmonic number. Clearly the introduction of the wavenumber K does not affect the determination of $s^{(n)}$ and ρ.

Finally it is necessary to find the expression for the surface displacement by choosing $\beta^{(n)}$ to be a particular solution to equation (3.3.33), thus satisfying

$$\sum_{n=1}^{3} \mathrm{M}_{in}\, \beta^{(n)} = 0 \tag{3.3.37}$$

in which case the surface displacement of the wave can be written

$$u_j^{(1)}(0) = \sum_{K=1}^{\infty} \sum_{n=1}^{3} \gamma_K(\xi, \tau)\, \beta^{(n)}\, a_j^{(n)}\, \mathrm{e}^{\mathrm{i}K(x-t)} + \mathrm{c.c.}\,, \tag{3.3.38}$$

where γ_K is the slowly varying surface amplitude. As discussed earlier the appearance of the complex conjugate of the summation ensures that the surface displacement $u_j^{(1)}$ is real.

3.3.4 Second-order System

The next stage in the solution procedure is to substitute the expression (3.3.36) into the second-order equations (3.3.24) and (3.3.25)

The quadratic terms on the right hand side of equation (3.3.24) give us the product of two infinite summations,

$$\begin{aligned} Q &= d_{ijklmn}\, u_{k,l}\, u_{m,nj} \\ &= d_{ijklmn} \left[\sum_{K=1}^{\infty} \sum_{m=1}^{3} \mathrm{i}K\delta_l^{(m)}\, A_K^{(m)}\, a_k^{(m)}\, \mathrm{e}^{\mathrm{i}Ks^{(m)}y} \mathrm{e}^{\mathrm{i}K(x-t)} + \mathrm{c.c.} \right] \\ &\quad \times \left[- \sum_{L=1}^{\infty} \sum_{n=1}^{3} L^2\, \delta_n^{(n)} \delta_j^{(n)}\, A_L^{(n)}\, a_m^{(n)}\, \mathrm{e}^{\mathrm{i}Ls^{(n)}y} \mathrm{e}^{\mathrm{i}L(x-t)} + \mathrm{c.c.} \right] \end{aligned} \tag{3.3.39}$$

where

$$\delta_1^{(n)} = 1 \quad , \quad \delta_2^{(n)} = s^{(n)} \quad , \quad \delta_3^{(n)} = 0\,.$$

These products may be simplified to double summations using the following procedure.

The summations may be represented by

$$\left[\sum_{K=1}^{\infty} A_K \, \mathrm{e}^{\mathrm{i}K} + \text{c.c.}\right] \times \left[\sum_{L=1}^{\infty} B_L \, \mathrm{e}^{\mathrm{i}L} + \text{c.c.}\right].$$

It is not difficult to see that four types of product will result, having the exponential forms

(i) $\displaystyle\sum_{K=1}^{\infty}\sum_{L=1}^{\infty} \mathrm{e}^{\mathrm{i}(K+L)}$

(ii) $\displaystyle\sum_{K=1}^{\infty}\sum_{L=1}^{\infty} \mathrm{e}^{\mathrm{i}(-K-L)}$

(iii) $\displaystyle\sum_{K=1}^{\infty}\sum_{L=1}^{\infty} \mathrm{e}^{\mathrm{i}(K-L)}$

(iv) $\displaystyle\sum_{K=1}^{\infty}\sum_{L=1}^{\infty} \mathrm{e}^{\mathrm{i}(-K+L)}$

Clearly (ii) is the conjugate of (i) which naturally leads us to the representation

$$\sum_{M=2}^{\infty} \mathrm{e}^{\mathrm{i}M} + \text{c.c.},$$

where $K = M - L$. Since we have taken $K \geq 1$, which implies that $L < M$, type (i) and (ii) terms can be written

$$\sum_{M=2}^{\infty}\sum_{L=1}^{M-1} A_{M-L}\, B_L \, \mathrm{e}^{\mathrm{i}M} + \text{c.c.}.$$

Returning to the original quadratic expression (3.3.39), type (i) and (ii) terms yield

$$\mathcal{Q}_1 = -\sum_{M=2}^{\infty}\sum_{L=1}^{M-1}\sum_{m=1}^{3}\sum_{n=1}^{3} \mathrm{i}\,(M-L)L^2\, d_{ijklmn}\, \delta_l^{(m)}\delta_n^{(n)}\delta_j^{(n)}\, A_{M-L}^{(m)}\, A_L^{(n)}\, a_k^{(m)}\, a_m^{(n)} \times \mathrm{e}^{\mathrm{i}[(M-L)s^{(m)} + Ls^{(n)}]y} \mathrm{e}^{\mathrm{i}M(x-t)} + \text{c.c.}, \tag{3.3.40}$$

Type (iii) and (iv) terms may be similarly grouped and have the representation

$$\sum_{M=0}^{\infty} \mathrm{e}^{\mathrm{i}M} + \text{c.c.},$$

where the inclusion of the terms $M = 0$ and $M = 1$ is noted, but $M = 0$ shall be treated as a simplification of the general case in later expressions.
For type (iii) terms $L = K - M$ and hence $M < K$, whilst for type (iv) terms $K = L - M$ and hence $M < L$.

Thus the two types of term may be represented by

$$\sum_{M=1}^{\infty} \sum_{K=M+1}^{\infty} A_K \bar{B}_{K-M} \mathrm{e}^{\mathrm{i}M} + \text{c.c.},$$

and

$$\sum_{M=1}^{\infty} \sum_{L=M+1}^{\infty} \bar{A}_{L-M} B_L \mathrm{e}^{\mathrm{i}M} + \text{c.c.}.$$

These may be combined as a single term

$$\sum_{M=1}^{\infty} \sum_{K=M+1}^{\infty} [\bar{A}_{K-M} B_K + A_K \bar{B}_{K-M}] \mathrm{e}^{\mathrm{i}M} \text{ c.c.}.$$

Again returning to the original quadratic expression (3.3.39) we find that type (iii) and (iv) terms yield

$$\begin{aligned} \mathcal{Q}_2 = & \sum_{M=1}^{\infty} \sum_{L=M+1}^{\infty} \sum_{m=1}^{3} \sum_{n=1}^{3} [-\mathrm{i}(L-M)^2 L\, d_{ijklmn}\, \delta_l^{(m)} \bar{\delta}_n^{(n)} \bar{\delta}_j^{(n)}\, A_L^{(m)}\, \bar{A}_{L-M}^{(n)}\, a_k^{(m)}\, \bar{a}_m^{(n)} \\ & \times \mathrm{e}^{\mathrm{i}[Ls^{(m)} - (L-M)\bar{s}^{(n)}]y} \mathrm{e}^{\mathrm{i}M(x-t)}] \\ & + \sum_{M=1}^{\infty} \sum_{L=M+1}^{\infty} \sum_{m=1}^{3} \sum_{n=1}^{3} [\mathrm{i}(L-M)L^2\, d_{ijklmn}\, \bar{\delta}_l^{(n)} \delta_n^{(m)} \delta_j^{(m)}\, \bar{A}_{L-M}^{(n)}\, A_L^{(m)}\, \bar{a}_k^{(n)}\, a_m^{(m)} \\ & \times \mathrm{e}^{\mathrm{i}[Ls^{(m)} - (L-M)\bar{s}^{(n)}]y} \mathrm{e}^{\mathrm{i}M(x-t)}] + \text{c.c.}, \end{aligned}$$

which simplifies to

$$\begin{aligned} \mathcal{Q}_2 = & \sum_{M=1}^{\infty} \sum_{L=M+1}^{\infty} \sum_{m=1}^{3} \sum_{n=1}^{3} \mathrm{i}\, d_{ijklmn}\, A_L^{(m)}\, \bar{A}_{L-M}^{(n)} \left[-L(L-M)^2\, \delta_l^{(m)} \bar{\delta}_n^{(n)} \bar{\delta}_j^{(n)}\, a_k^{(m)}\, \bar{a}_m^{(n)} \right. \\ & \left. + L^2(L-M)\, \bar{\delta}_l^{(n)} \delta_n^{(m)} \delta_j^{(m)}\, \bar{a}_k^{(n)}\, a_m^{(m)} \right] \mathrm{e}^{\mathrm{i}[Ls^{(m)} - (L-M)\bar{s}^{(n)}]y} \mathrm{e}^{\mathrm{i}M(x-t)} + \text{c.c.}. \end{aligned} \tag{3.3.41}$$

On evaluating all the necessary products, the equations of motion (3.3.24) can be expressed

$$\rho\,\ddot{u}_i^{(2)} - c_{ijkl}\,u_{k,lj}^{(2)} = \left(\sum_{K=1}^{\infty}\sum_{n=1}^{3}\left(F_{iK1}^{(n)}(y)\,A_{K,\xi}^{(n)} + F_{iK2}^{(n)}(y)\,A_{K,\eta}^{(n)} + F_{iK3}^{(n)}(y)\,A_{K,\tau}^{(n)}\right)\mathrm{e}^{\mathrm{i}K(x-t)}\right.$$
$$+ \sum_{K=1}^{\infty}\sum_{L=1}^{K-1}\sum_{n=1}^{3}\sum_{m=1}^{3} H_{iKL}^{(m,n)}(y)\,A_{K-L}^{(n)}\,A_L^{(m)}\,\mathrm{e}^{\mathrm{i}K(x-t)}$$
$$+ \sum_{K=1}^{\infty}\sum_{L=K+1}^{\infty}\sum_{n=1}^{3}\sum_{m=1}^{3} G_{iKL}^{(m,n)}(y)\,\bar{A}_{L-K}^{(n)}\,A_L^{(m)}\,\mathrm{e}^{\mathrm{i}K(x-t)}$$
$$\left. + \sum_{K=1}^{\infty}\sum_{n=1}^{3}\sum_{m=1}^{3} Q_{iK}^{(m,n)}(y)\,A_K^{(m)}\,\bar{A}_K^{(n)}\right) + \text{c.c.} \qquad (3.3.42)$$

which must be solved subject to

$$c_{i2kl}\,u_{k,l}^{(2)} = \left(\sum_{K=1}^{\infty}\sum_{n=1}^{3}\left(f_{i1}^{(n)}\,A_{K,\xi}^{(n)} + f_{i2}^{(n)}\,A_{K,\eta}^{(n)}\right)\mathrm{e}^{\mathrm{i}K(x-t)}\right.$$
$$+ \sum_{K=1}^{\infty}\sum_{L=1}^{K-1}\sum_{n=1}^{3}\sum_{m=1}^{3} h_{iKL}^{(m,n)}\,A_{K-L}^{(n)}\,A_L^{(m)}\,\mathrm{e}^{\mathrm{i}K(x-t)}$$
$$+ \sum_{K=1}^{\infty}\sum_{L=K+1}^{\infty}\sum_{n=1}^{3}\sum_{m=1}^{3} g_{iKL}^{(m,n)}\,\bar{A}_{L-K}^{(n)}\,A_L^{(m)}\,\mathrm{e}^{\mathrm{i}K(x-t)}$$
$$\left. + \sum_{K=1}^{\infty}\sum_{n=1}^{3}\sum_{m=1}^{3} q_{iK}^{(m,n)}\,A_K^{(m)}\,\bar{A}_K^{(n)}\right) + \text{c.c.}\,. \qquad (3.3.43)$$

on $y = \eta = 0$. Here it is noted that type (iii) and (iv) terms independent of x and t have been separated. Expressions for the functions $F_{iK1}^{(n)}(y)$, $F_{iK2}^{(n)}(y)$, $F_{iK3}^{(n)}(y)$, $G_{iKL}^{(m,n)}(y)$, $H_{iKL}^{(m,n)}(y)$, $f_{i1}^{(n)}$, $f_{i2}^{(n)}$, $g_{iKL}^{(m,n)}$ and $h_{iKL}^{(m,n)}$ that appear in (3.3.42) and (3.3.43) are now stated.

The coefficients of the terms linear in the amplitudes are easily calculated to be

$$F_{iKw}^{(n)}(y) = \mathrm{i}\,K((c_{iwj2} + c_{i2jw})s^{(n)} + (c_{iwj1} + c_{i1jw}))\,a_j^{(n)}\,\mathrm{e}^{\mathrm{i}Ks^{(n)}y}\,, \qquad w = 1,2\,, \qquad (3.3.44)_1$$

$$F_{iK3}^{(n)}(y) = 2\mathrm{i}\,K\rho a_i^{(n)}\,\mathrm{e}^{\mathrm{i}Ks^{(n)}y}\,, \qquad (3.3.44)_2$$

and

$$f_{jw}^{(n)} = -c_{j2kw}\,a_k^{(n)}\,, \qquad w = 1,2\,. \qquad (3.3.44)_3$$

Whilst referring to the expressions (3.3.40) and (3.3.41) allows the terms that are quadratic in the amplitudes to be expressed

$$H_{iKL}^{(m,n)}(y) = -2\mathrm{i}\,L^2(K-L)\,d_{ijklmn}\,\delta_l^{(n)}\,\delta_n^{(m)}\,\delta_j^{(m)}\,a_k^{(n)}\,a_m^{(m)}\,\mathrm{e}^{\mathrm{i}[Ls^{(m)}+(K-L)s^{(n)}]y}\,, \tag{3.3.44}_4$$

$$G_{iKL}^{(m,n)}(y) = 2\mathrm{i}\,d_{ijklmn}\,\Big(L^2(L-K)\,\bar{\delta}_l^{(n)}\,\delta_n^{(m)}\,\delta_j^{(m)}\,\bar{a}_k^{(n)}\,a_m^{(m)} - L(L-K)^2\,\delta_l^{(m)}\,\bar{\delta}_n^{(n)}\,\bar{\delta}_j^{(n)}\,a_k^{(m)}\,\bar{a}_m^{(n)}\Big)\,\mathrm{e}^{\mathrm{i}[Ls^{(m)}-(L-K)\bar{s}^{(n)}]y}\,, \tag{3.3.44}_5$$

$$Q_{iK}^{(m,n)}(y) = 2\mathrm{i}d_{ijklmn}K^3\left(\bar{\delta}_l^{(n)}\delta_n^{(m)}\delta_j^{(m)}\bar{a}_k^{(n)}a_m^{(m)}\right)\mathrm{e}^{\mathrm{i}K[s^{(m)}-\bar{s}^{(n)}]y}, \tag{3.3.44}_6$$

$$g_{iKL}^{(m,n)} = -2L(L-K)\,d_{i2klmn}\,\bar{\delta}_l^{(n)}\,\delta_n^{(m)}\,\bar{a}_k^{(n)}\,a_m^{(m)}\,, \tag{3.3.44}_7$$

$$h_{iKL}^{(m,n)} = -L(L-K)\,d_{i2klmn}\,\delta_l^{(n)}\,\delta_n^{(m)}\,a_k^{(n)}\,a_m^{(m)}\,, \tag{3.3.44}_8$$

and

$$q_{iK}^{(m,n)} = -\,K^2\,d_{i2klmn}\,\bar{\delta}_l^{(n)}\,\delta_n^{(m)}\,\bar{a}_k^{(n)}\,a_m^{(m)}\,, \tag{3.3.44}_9$$

Equation (3.3.42) represents a system of inhomogeneous equations and the solution therefore consists of the sum of a complementary function and a particular integral. It is clear, therefore, that the general solution to (3.3.42) takes the form

$$\begin{aligned} u_j^{(2)} = {} & \sum_{K=1}^{\infty}\sum_{n=1}^{3} b_{jK}^{(n)}\,\mathrm{e}^{\mathrm{i}Ks^{(n)}y}\mathrm{e}^{\mathrm{i}K(x-t)} + \sum_{K=1}^{\infty}\sum_{m=1}^{3}\sum_{n=1}^{3} r_{jK}^{(m,n)}\,\mathrm{e}^{\mathrm{i}KT_{0K}^{(m,n)}y} \\ & + \sum_{K=1}^{\infty}\sum_{L=1}^{K-1}\sum_{m=1}^{3}\sum_{\substack{n=1\\ n\neq m}}^{3} R_{jKL}^{(m,n)}\,\mathrm{e}^{\mathrm{i}KP_{KL}^{(m,n)}y}\mathrm{e}^{\mathrm{i}K(x-t)} \\ & + \sum_{K=1}^{\infty}\sum_{L=K+1}^{\infty}\sum_{m=1}^{3}\sum_{n=1}^{3} S_{jKL}^{(m,n)}\,\mathrm{e}^{\mathrm{i}KT_{KL}^{(m,n)}y}\mathrm{e}^{\mathrm{i}K(x-t)}\,, \end{aligned} \tag{3.3.45}$$

where

$$P_{KL}^{(m,n)} = \left(Ls^{(m)} + (K-L)s^{(n)}\right)/K$$

$$T_{KL}^{(m,n)} = \left(Ls^{(m)} - (L-K)\bar{s}^{(n)}\right)/K\,, \tag{3.3.46}$$

and the restriction of the summation over n in the third term of the representation (3.3.45) is because the eliminated terms appear in the first term of the representation.

Firstly let us consider those terms in the representation (3.3.45) dependent on x and t. Upon substituting the representation (3.3.45) into the boundary conditions (3.3.42) it follows from comparison of the relevant coefficients that

$$K^2\,\mathrm{L}_{ij}(s^{(n)})\,b_{jK}^{(n)} = W_{iK}^{(n)} \tag{3.3.47}$$

$$K^2\,\mathrm{L}_{ij}(P_{KL}^{(m,n)})\,R_{jKL}^{(m,n)} = H_{iKL}^{(m,n)}(0)\,A_{K-L}^{(n)}\,A_L^{(m)} \tag{3.3.48}$$

$$K^2\,\mathrm{L}_{ij}(T_{KL}^{(m,n)})\,S_{jKL}^{(m,n)} = G_{iKL}^{(m,n)}(0)\,\bar{A}_{L-K}^{(n)}\,A_L^{(m)}\,, \tag{3.3.49}$$

where

$$W_{iK}^{(n)} = F_{iK1}^{(n)}(0)\,A_{K,\xi}^{(n)} + F_{iK2}^{(n)}(0)\,A_{K,\eta}^{(n)} + F_{iK3}^{(n)}(0)\,A_{K,\tau}^{(n)} + \sum_{L=1}^{K-1} H_{iKL}^{(n,n)}(0)\,A_{K-L}^{(n)}\,A_L^{(n)}\,. \tag{3.3.50}$$

Equations (3.3.47), (3.3.48) and (3.3.49) represent matrix equations in the coefficients $b_{jK}^{(n)}$, $R_{jKL}^{(m,n)}$ and $S_{jKL}^{(m,n)}$, respectively. If we define $\mathrm{L}_{ij}^{-1}(s)$ to be the inverse of $\mathrm{L}_{ij}(s)$ whenever $\mathrm{L}_{ij}(s)$ is non-singular and zero where it is not, the solutions of equations (3.3.48) and (3.3.49) are

$$R_{jKL}^{(m,n)} = \frac{1}{K^2}\,\mathrm{L}_{ij}^{-1}(P_{KL}^{(m,n)})\,H_{iKL}^{(m,n)}(0)\,A_{K-L}^{(n)}\,A_L^{(m)} \tag{3.3.51}$$

and

$$S_{jKL}^{(m,n)} = \frac{1}{K^2}\,\mathrm{L}_{ij}^{-1}(T_{KL}^{(m,n)})\,G_{iKL}^{(m,n)}(0)\,\bar{A}_{L-K}^{(n)}\,A_L^{(m)}\,. \tag{3.3.52}$$

In fact $\mathrm{L}_{ij}(P_{KL}^{(m,n)})$ and $\mathrm{L}_{ij}(T_{KL}^{(m,n)})$ are always non-singular since $T_{KL}^{(m,n)} \neq s^{(l)}$ for any m, n, K or L and $P_{KL}^{(m,n)} \neq s^{(l)}$ provided $n \neq m$ for any K or L, and $s^{(l)}$ are the only values giving singular $\mathrm{L}_{ij}(s)$.

The singularity of $\mathrm{L}_{ij}(s^{(n)})$, however, and the satisfying of (3.3.47) requires that, to ensure consistency, we impose the condition

$$a_j^{(n)} W_{jK}^{(n)} = 0\,. \tag{3.3.53}$$

This consistency condition may be expressed as

$$\Gamma_K^{(n)} A_{K,\xi}^{(n)} + \Delta_K^{(n)} A_{K,\eta}^{(n)} + \Theta_K^{(n)} A_{K,\tau}^{(n)} + \sum_{L=1}^{K-1} \Lambda_{KL}^{(n)} A_{K-L}^{(n)} A_L^{(n)} = 0\,, \tag{3.3.54}$$

where

$$\begin{aligned}
\Gamma_K^{(n)} &= a_j^{(n)} F_{jK1}^{(n)}(0)\,,\\
\Delta_K^{(n)} &= a_j^{(n)} F_{jK2}^{(n)}(0)\,,\\
\Theta_K^{(n)} &= a_j^{(n)} F_{jK3}^{(n)}(0)\,,\\
\Lambda_{KL}^{(n)} &= a_j^{(n)} H_{jKL}^{(n,n)}(0)\,.
\end{aligned} \tag{3.3.55}$$

Equation (3.3.54) represents an infinite system of coupled partial differential equations in the amplitudes $A_K^{(n)}$. The equations are valid everywhere within the material and clearly hold in the limits $y \to 0$ and $\eta \to 0$, as the free surface is approached.

The condition (3.3.54) also ensures that the nonlinear terms do not give rise to secular terms in the particular integral by setting the kernel of these terms to zero and is analogous to equation (3.3.18) in the earlier example.

Returning to those terms independent of x and t in the expression (3.3.45), we find, from substituting (3.3.45) into equations (3.3.42) and comparing coefficients, that

$$-c_{i2k2} r_{kK}^{(m,n)} \left(\mathrm{i}KT_{0K}^{(m,n)}\right)^2 = Q_{iK}^{(m,n)}(0) A_K^{(m)} \bar{A}_K^{(n)}\,,$$

or

$$c_{i2k2} r_{kK}^{(m,n)} = \frac{-Q_{iK}^{(m,n)}(0) A_K^{(m)} \bar{A}_K^{(n)}}{\left(\mathrm{i}KT_{0K}^{(m,n)}\right)^2}\,. \tag{3.3.56}$$

Now, from $(3.3.44)_6$ and (3.3.46),

$$\frac{Q_{iK}^{(m,n)}(0)}{\mathrm{i}KT_{0K}^{(m,n)}} = \frac{2K^2 d_{ijklmn}\left(\bar{\delta}_l^{(n)}\delta_n^{(m)}\delta_j^{(m)}\bar{a}_k^{(n)}a_m^{(m)} - \delta_l^{(m)}\bar{\delta}_n^{(n)}\bar{\delta}_j^{(n)}a_k^{(m)}\bar{a}_m^{(n)}\right)}{\left(s^{(m)} - \bar{s}^{(n)}\right)}$$
$$= \frac{2K^2\, d_{i1klmn}\left(\bar{\delta}_l^{(n)}\,\delta_n^{(m)}\bar{a}_k^{(n)}a_m^{(m)} - \delta_l^{(m)}\bar{\delta}_n^{(n)}a_k^{(m)}\bar{a}_m^{(n)}\right)}{\left(s^{(m)} - \bar{s}^{(n)}\right)}$$
$$+ \frac{2K^2 d_{i2klmn}\left(\bar{\delta}_l^{(n)}\delta_n^{(m)}s^{(m)}\bar{a}_k^{(n)}a_m^{(m)} - \delta_l^{(m)}\bar{\delta}_n^{(n)}\bar{s}^{(n)}a_k^{(m)}\bar{a}_m^{(n)}\right)}{\left(s^{(m)} - \bar{s}^{(n)}\right)},$$

which, upon replacement of dummy subscripts, may be written as

$$\frac{Q_{iK}^{(m,n)}(0)}{\mathrm{i}KT_{0K}^{(m,n)}} = 2K^2 d_{i2klmn}\left(\bar{\delta}_l^{(n)}\delta_n^{(m)}\bar{a}_k^{(n)}a_m^{(m)}\right)$$
$$= -q_{iK}^{(m,n)}.$$

Therefore (3.3.56) leads to the condition

$$c_{i2k2}r_{kK}^{(m,n)} = \frac{q_{iK}^{(m,n)}A_K^{(m)}\bar{A}_K^{(n)}}{\mathrm{i}KT_{0K}^{(m,n)}}. \tag{3.3.57}$$

Substitution of the representation into the boundary condition (3.3.43) and similar comparison of coefficients leads to the relationship

$$c_{i2k2}r_{kK}^{(m,n)}\mathrm{i}KT_{0K}^{(m,n)} = \quad q_{iK}^{(m,n)}A_K^{(m)}\bar{A}_K^{(n)}. \tag{3.3.58}$$

Clearly from (3.3.57) any solution for the non-propagating terms identically satisfies the boundary conditions. We may therefore neglect such terms in the ensuing analysis.

It now remains to define the coefficients $b_{jK}^{(n)}$ in the representation (3.3.45). The singular operator matrix $\mathrm{L}_{ij}(s^{(n)})$ cannot be inverted but it is possible to find an inverse that is restricted to the subspace orthogonal to its eigenvector $a_j^{(n)}$. This will enable us to express $b_{jK}^{(n)}$ as a sum of two terms, one parallel to $a_j^{(n)}$ and the other orthogonal to it.

This partial inverse matrix, $\mathrm{U}_{ij}^{(n)}$, must satisfy the condition

$$\mathrm{U}_{ij}^{(n)}\,\mathrm{L}_{jk}(s^{(n)})\,\zeta_k^{(n)} = \zeta_i^{(n)}, \tag{3.3.59}$$

where $\zeta_k^{(n)}$ is any vector orthogonal to $a_j^{(n)}$.

The matrix $\mathrm{L}_{ij}(s^{(n)})$ has three eigenvalues and three corresponding eigenvectors. The eigenvector $a_j^{(n)}$ corresponds to a zero eigenvalue whilst we denote the remaining two eigenvectors by $a_{jP}^{(n)}$, corresponding to the eigenvalues $\lambda_P^{(n)}$, $P = 1$, 2, respectively. Since $\mathrm{L}_{ij}(s^{(n)})$ is symmetric, the three eigenvectors must be orthogonal and hence any vector orthogonal to $a_j^{(n)}$ may be expressed as a linear combination of the eigenvectors $a_{jP}^{(n)}$, $P = 1$, 2. Thus the condition (3.3.59) may be re-written as

$$\mathrm{U}_{ij}^{(n)}\,\mathrm{L}_{jk}(s^{(n)})\,a_{kP}^{(n)} = a_{iP}^{(n)}, \qquad P = 1,2. \tag{3.3.60}$$

Now, using the symmetry of $\mathrm{L}_{ij}(s^{(n)})$ and the eigenvector definition,

$$\begin{aligned} a_{jP}^{(n)}\,\mathrm{L}_{jk}(s^{(n)}) &= \lambda_P^{(n)}\,a_{kP}^{(n)}, \\ a_{jP}^{(n)}\,\mathrm{L}_{jk}(s^{(n)})\,a_{kP}^{(n)} &= \lambda_P^{(n)}\,a_{kP}^{(n)}\,a_{kP}^{(n)}, \\ \left(a_{iP}^{(n)}\,a_{jP}^{(n)}\right)\,\mathrm{L}_{jk}(s^{(n)})\,a_{kP}^{(n)} &= \left(\lambda_P^{(n)}\,a_{kP}^{(n)}\,a_{kP}^{(n)}\right)\,a_{iP}^{(n)}. \end{aligned} \tag{3.3.61}$$

Bearing in mind the relation (3.3.61) it is obvious that equation (3.3.60) is satisfied if

$$\mathrm{U}_{ij}^{(n)} = \sum_{P=1}^{2} \frac{a_{iP}^{(n)}\,a_{jP}^{(n)}}{\lambda_P^{(n)}\,a_{kP}^{(n)}\,a_{kP}^{(n)}}. \tag{3.3.62}$$

Applying this matrix to equation (3.3.47) yields

$$b_{jK}^{(n)} = \chi_K^{(n)}\,a_j^{(n)} + \frac{1}{K^2}\,\mathrm{U}_{ji}^{(n)}\,W_{iK}^{(n)}, \tag{3.3.63}$$

since $\mathrm{U}_{ij}^{(n)} a_i^{(n)} = 0$ by the orthogonality of the eigenvectors, thus removing any element of $W_{iK}^{(n)}$ parallel to $a_i^{(n)}$.

Substitution of the full solution (3.3.45) into the boundary conditions (3.3.43), yields

$$\begin{aligned} &\sum_{n=1}^{3}(\mathrm{i}K)\left(c_{i2j2}s^{(n)} + c_{i2j1}\right)\,b_{jK}^{(n)} = \\ &-\sum_{n=1}^{3}\sum_{m=1}^{3}\left[\sum_{L=1}^{K-1}(\mathrm{i}K)\left(c_{i2j2}P_{KL}^{(m,n)} + c_{i2j1}\right)\,R_{jKL}^{(m,n)} + \sum_{L=K+1}^{\infty}(\mathrm{i}K)\left(c_{i2j2}T_{KL}^{(m,n)} + c_{i2j1}\right)\,S_{jKL}^{(m,n)}\right] \\ &+\sum_{n=1}^{3}\left[f_{i1}^{(n)}\,A_{K,\xi}^{(n)} + f_{i2}^{(n)}\,A_{K,\eta}^{(n)} + \sum_{m=1}^{3}\sum_{L=1}^{K-1} h_{iKL}^{(m,n)}\,A_{K-L}^{(n)}\,A_L^{(m)} + \sum_{m=1}^{3}\sum_{L=K+1}^{\infty} g_{iKL}^{(m,n)}\,\bar{A}_{L-K}^{(n)}\,A_L^{(m)}\right], \end{aligned} \tag{3.3.64}$$

on $y = \eta = 0$.

With the use of equations (3.3.51), (3.3.52), and (3.3.63), the above leads to the following matrix equation for the coefficients $\chi_K^{(n)}$,

$$(\mathrm{i}K)\sum_{n=1}^{3}\mathrm{M}_{in}\,\chi_K^{(n)} = \sum_{n=1}^{3}\frac{1}{(\mathrm{i}K)}\left(c_{i2j2}s^{(n)} + c_{i2j1}\right)\mathrm{U}_{jl}^{(n)}\,W_{lK}^{(n)}$$

$$+\sum_{n=1}^{3}\sum_{m=1}^{3}\left[\sum_{L=1}^{K-1}\frac{1}{(\mathrm{i}K)}\left(c_{i2j2}P_{KL}^{(m,n)} + c_{i2j1}\right)\mathrm{L}_{jl}^{-1}(P_{KL}^{(m,n)})\,H_{lKL}^{(m,n)}(0)\,A_{K-L}^{(n)}\,A_L^{(m)}\right.$$

$$\left.+\sum_{L=K+1}^{\infty}\frac{1}{(\mathrm{i}K)}\left(c_{i2j2}T_{KL}^{(m,n)} + c_{i2j1}\right)\mathrm{L}_{jl}^{-1}(T_{KL}^{(m,n)})\,G_{lKL}^{(m,n)}(0)\,\bar{A}_{L-K}^{(n)}\,A_L^{(m)}\right]$$

$$+\sum_{n=1}^{3}\left[f_{i1}^{(n)}\,A_{K,\xi}^{(n)} + f_{i2}^{(n)}\,A_{K,\eta}^{(n)} + \sum_{m=1}^{3}\sum_{L=1}^{K-1}h_{iKL}^{(m,n)}\,A_{K-L}^{(n)}\,A_L^{(m)} + \sum_{m=1}^{3}\sum_{L=K+1}^{\infty}g_{iKL}^{(m,n)}\,\bar{A}_{L-K}^{(n)}\,A_L^{(m)}\right], \tag{3.3.65}$$

on $y = \eta = 0$.

In view of equation (3.3.35), the matrix M_{in} is singular and the equations (3.3.65) are dependent. Thus, on premultiplying equation (3.3.65) by any particular solution to $\lambda_i\mathrm{M}_{in} = 0$, the consistency condition

$$\sum_{n=1}^{3}\frac{1}{(\mathrm{i}K)}\lambda_i\left(c_{i2j2}s^{(n)} + c_{i2j1}\right)\mathrm{U}_{jl}^{(n)}\left(F_{lK1}^{(n)}(0)\,A_{K,\xi}^{(n)} + F_{lK2}^{(n)}(0)\,A_{K,\eta}^{(n)} + F_{lK3}^{(n)}(0)\,A_{K,\tau}^{(n)}\right.$$

$$\left.+\sum_{L=1}^{K-1}H_{lKL}^{(n,n)}(0)\,A_{K-L}^{(n)}\,A_L^{(n)}\right)$$

$$+\sum_{n=1}^{3}\sum_{m=1}^{3}\left[\sum_{L=1}^{K-1}\frac{1}{(\mathrm{i}K)}\lambda_i\left(c_{i2j2}P_{KL}^{(m,n)} + c_{i2j1}\right)\mathrm{L}_{jl}^{-1}(P_{KL}^{(m,n)})\,H_{lKL}^{(m,n)}(0)\,A_{K-L}^{(n)}\,A_L^{(m)}\right.$$

$$\left.+\sum_{L=K+1}^{\infty}\frac{1}{(\mathrm{i}K)}\lambda_i\left(c_{i2j2}T_{KL}^{(m,n)} + c_{i2j1}\right)\mathrm{L}_{jl}^{-1}(T_{KL}^{(m,n)})\,G_{lKL}^{(m,n)}(0)\,\bar{A}_{L-K}^{(n)}\,A_L^{(m)}\right]$$

$$+\sum_{n=1}^{3}\lambda_i\left[f_{i1}^{(n)}\,A_{K,\xi}^{(n)} + f_{i2}^{(n)}\,A_{K,\eta}^{(n)} + \sum_{m=1}^{3}\sum_{L=1}^{K-1}h_{iKL}^{(m,n)}\,A_{K-L}^{(n)}\,A_L^{(m)} + \sum_{m=1}^{3}\sum_{L=K+1}^{\infty}g_{iKL}^{(m,n)}\,\bar{A}_{L-K}^{(n)}\,A_L^{(m)}\right]$$

$$= 0\,, \tag{3.3.66}$$

on $y = \eta = 0$, is obtained. This condition may be simplified with the use of equations (3.3.38) and (3.3.54) to substitute for the slow y derivative to give

$$\sum_{n=1}^{3}\Bigg\{\Big(\frac{\lambda_i}{(\mathrm{i}K)}\left(c_{i2j2}s^{(n)}+c_{i2j1}\right)\mathrm{U}_{jl}^{(n)}F_{lK1}^{(n)}(0)+\lambda_i f_{i1}^{(n)}\Big)$$

$$-\frac{\Gamma_K^{(n)}}{\Delta_K^{(n)}}\Big(\frac{\lambda_i}{(\mathrm{i}K)}\left(c_{i2j2}s^{(n)}+c_{i2j1}\right)\mathrm{U}_{jl}^{(n)}F_{lK2}^{(n)}(0)+\lambda_i f_{i2}^{(n)}\Big)\Bigg\}\beta^{(n)}\gamma_{K,\xi}$$

$$+\sum_{n=1}^{3}\Bigg\{\frac{\lambda_i}{(\mathrm{i}K)}\left(c_{i2j2}s^{(n)}+c_{i2j1}\right)\mathrm{U}_{jl}^{(n)}\Big(F_{lK3}^{(n)}(0)-\frac{\Theta_K^{(n)}}{\Delta_K^{(n)}}F_{lK2}^{(n)}(0)\Big)$$

$$-\lambda_i f_{i2}^{(n)}\frac{\Theta_K^{(n)}}{\Delta_K^{(n)}}\Bigg\}\beta^{(n)}\gamma_{K,\tau}=$$

$$-\sum_{L=1}^{K-1}\sum_{n=1}^{3}\Bigg\{\sum_{m=1}^{3}\Bigg[\frac{\lambda_i}{(\mathrm{i}K)}\left(c_{i2j2}P_{KL}^{(m,n)}+c_{i2j1}\right)\mathrm{L}_{jl}^{-1}(P_{KL}^{(m,n)})\,H_{lKL}^{(m,n)}(0)+\lambda_i h_{iKL}^{(m,n)}\Bigg]\beta^{(m)}$$

$$-\Bigg[\frac{\lambda_i}{(\mathrm{i}K)}\left(c_{i2j2}s^{(n)}+c_{i2j1}\right)\mathrm{U}_{jl}^{(n)}F_{lK2}^{(n)}(0)+\lambda_i f_{i2}^{(n)}\Bigg]\frac{\Lambda_{KL}^{(n)}}{\Delta_K^{(n)}}\beta^{(n)}$$

$$+\Bigg[\frac{\lambda_i}{(\mathrm{i}K)}\left(c_{i2j2}s^{(n)}+c_{i2j1}\right)\mathrm{U}_{jl}^{(n)}H_{lKL}^{(m,n)}(0)\,\beta^{(n)}\Bigg]\Bigg\}\beta^{(n)}\gamma_{K-L}\,\gamma_L$$

$$-\sum_{L=K+1}^{\infty}\sum_{n=1}^{3}\sum_{m=1}^{3}\Bigg[\frac{\lambda_i}{(\mathrm{i}K)}\left(c_{i2j2}T_{KL}^{(m,n)}+c_{i2j1}\right)\mathrm{L}_{jl}^{-1}(T_{KL}^{(m,n)})\,G_{lKL}^{(m,n)}(0)$$

$$+\lambda_i g_{iKL}^{(m,n)}\Bigg]\beta^{(m)}\bar{\beta}^{(n)}\bar{\gamma}_{L-K}\,\gamma_L\,. \tag{3.3.67}$$

Now

$$\mathrm{U}_{jk}^{(n)}F_{kK3}^{(n)}(0)=0 \tag{3.3.68}$$

follows from equations $(3.3.44)_2$ and (3.3.62) and, using equations (3.3.67) and (3.3.68), it is deduced that

$$N_K\,\gamma_{K,\xi}+P_K\,\gamma_{K,\tau}-\sum_{L=1}^{K-1}\Pi_{KL}\,\gamma_{K-L}\,\gamma_L-\sum_{L=K+1}^{\infty}\Delta_{KL}\,\bar{\gamma}_{L-K}\,\gamma_L=0\,, \tag{3.3.69}$$

where

$$N_K=\sum_{n=1}^{3}\Bigg\{\Big(\frac{\lambda_i}{(\mathrm{i}K)}\left(c_{i2j2}s^{(n)}+c_{i2j1}\right)\mathrm{U}_{jl}^{(n)}F_{lK1}^{(n)}(0)+\lambda_i f_{i1}^{(n)}\Big)$$

$$- \frac{\Gamma_K^{(n)}}{\Delta_K^{(n)}} \Big(\frac{\lambda_i}{(\mathrm{i}K)} \left(c_{i2j2} s^{(n)} + c_{i2j1} \right) \mathrm{U}_{jl}^{(n)} F_{lK2}^{(n)}(0) + \lambda_i f_{i2}^{(n)} \Big) \Bigg\} \beta^{(n)} \tag{3.3.70}$$

$$P_K = - \sum_{n=1}^{3} \left\{ \frac{\lambda_i}{(\mathrm{i}K)} \left(c_{i2j2} s^{(n)} + c_{i2j1} \right) \mathrm{U}_{jl}^{(n)} F_{lK2}^{(n)}(0) \frac{\Theta_K^{(n)}}{\Delta_K^{(n)}} + \lambda_i f_{i2}^{(n)} \frac{\Theta_K^{(n)}}{\Delta_K^{(n)}} \right\} \beta^{(n)} \tag{3.3.71}$$

$$\begin{aligned} \Pi_{KL} = - \sum_{n=1}^{3} \sum_{m=1}^{3} \Bigg[& \frac{\lambda_i}{(\mathrm{i}K)} \left(c_{i2j2} P_{KL}^{(m,n)} + c_{i2j1} \right) \mathrm{L}_{jl}^{-1}(P_{KL}^{(m,n)}) H_{lKL}^{(m,n)}(0) \\ & + \lambda_i h_{iKL}^{(m,n)} \Bigg] \beta^{(m)} \beta^{(n)} \\ + \sum_{n=1}^{3} \Bigg\{ & \Bigg[\frac{\lambda_i}{(\mathrm{i}K)} \left(c_{i2j2} s^{(n)} + c_{i2j1} \right) \mathrm{U}_{jl}^{(n)} F_{lK2}^{(n)}(0) + \lambda_i f_{i2}^{(n)} \Bigg] \frac{\Lambda_{KL}^{(n)}}{\Delta_K^{(n)}} \\ & - \frac{\lambda_i}{(\mathrm{i}K)} \left(c_{i2j2} s^{(n)} + c_{i2j1} \right) \mathrm{U}_{jl}^{(n)} H_{lKL}^{(m,n)}(0) \Bigg\} \beta^{(n)} \beta^{(n)} \end{aligned} \tag{3.3.72}$$

and

$$\begin{aligned} \Delta_{KL} = - \sum_{n=1}^{3} \sum_{m=1}^{3} \Bigg[& \frac{\lambda_i}{(\mathrm{i}K)} \left(c_{i2j2} T_{KL}^{(m,n)} + c_{i2j1} \right) \mathrm{L}_{jl}^{-1}(T_{KL}^{(m,n)}) G_{lKL}^{(m,n)}(0) \\ & + \lambda_i g_{iKL}^{(m,n)} \Bigg] \beta^{(m)} \bar{\beta}^{(n)} . \end{aligned} \tag{3.3.73}$$

Returning to equations (3.3.44) and (3.3.55), it is seen that

$$\begin{aligned} \Gamma_K^{(n)} + s^{(n)} \Delta_K^{(n)} &= a_j^{(n)} \left[F_{jK1}^{(n)}(0) + s^{(n)} F_{jK2}^{(n)}(0) \right] \\ &= a_j^{(n)} \Big[\left(c_{j1k2} + c_{j2k1} \right) s^{(n)} + 2c_{j1k1} + 2c_{j2k2} s^{(n)^2} \\ &\quad + \left(c_{j1k2} + c_{j2k1} \right) s^{(n)} \Big] (\mathrm{i}K) a_k^{(n)} \\ &= 2a_j^{(n)} (\mathrm{i}K) \left[\left(c_{j1k2} + c_{j2k1} \right) s^{(n)} + c_{j1k1} + c_{j2k2} s^{(n)^2} \right] a_k^{(n)} \\ &= 2a_j^{(n)} (\mathrm{i}K) \left[\mathrm{L}_{jk}(s^{(n)}) + \rho \delta_{jk} \right] a_k^{(n)} \\ &= 2a_j^{(n)} (\mathrm{i}K) a_j^{(n)} \rho , \end{aligned}$$

or, using $(3.3.44)_2$ and $(3.3.55)_3$,

$$\Gamma_K^{(n)} + s^{(n)}\Delta_K^{(n)} = \Theta_K^{(n)}. \tag{3.3.74}$$

This may be used in equation (3.3.71) to give

$$\begin{aligned} P_K &= -\sum_{n=1}^{3}\left[\frac{\lambda_i}{(iK)}\left(c_{i2j2}s^{(n)} + c_{i2j1}\right)\mathrm{U}_{jl}^{(n)}\,F_{lK2}^{(n)}(0) + \lambda_i\, f_{i2}^{(n)}\right]\beta^{(n)}\,\frac{\Gamma_K^{(n)} + s^{(n)}\Delta_K^{(n)}}{\Delta_K^{(n)}} \\ &= -\sum_{n=1}^{3}\left[\frac{\lambda_i}{(iK)}\left(c_{i2j2}s^{(n)} + c_{i2j1}\right)\mathrm{U}_{jl}^{(n)}\,F_{lK2}^{(n)}(0) + \lambda_i\, f_{i2}^{(n)}\right]\beta^{(n)}\,\frac{\Gamma_K^{(n)}}{\Delta_K^{(n)}} \\ &\quad - \sum_{n=1}^{3}\left[\frac{\lambda_i}{(iK)}\left(c_{i2j2}s^{(n)} + c_{i2j1}\right)\mathrm{U}_{jl}^{(n)}\,F_{lK2}^{(n)}(0) + \lambda_i\, f_{i2}^{(n)}\right]\beta^{(n)}\,s^{(n)}. \end{aligned} \tag{3.3.75}$$

It directly follows from proof of equation (3.3.74) that

$$F_{iK1}^{(n)}(0) + s^{(n)}\,F_{iK2}^{(n)}(0) = F_{iK3}^{(n)}(0),$$

or

$$s^{(n)}\,F_{iK2}^{(n)}(0) = -F_{iK1}^{(n)}(0) + F_{iK3}^{(n)}(0),$$

and thus equation (3.3.74) becomes

$$\begin{aligned} P_K &= -\sum_{n=1}^{3}\left[\frac{\lambda_i}{(iK)}\left(c_{i2j2}s^{(n)} + c_{i2j1}\right)\mathrm{U}_{jl}^{(n)}\,F_{lK2}^{(n)}(0) + \lambda_i\, f_{i2}^{(n)}\right]\beta^{(n)}\,\frac{\Gamma_K^{(n)}}{\Delta_K^{(n)}} \\ &\quad + \sum_{n=1}^{3}\left[\frac{\lambda_i}{(iK)}\left(c_{i2j2}s^{(n)} + c_{i2j1}\right)\mathrm{U}_{jl}^{(n)}\,F_{lK1}^{(n)}(0) - \lambda_i\, s^{(n)}\, f_{i2}^{(n)}\right]\beta^{(n)}. \end{aligned}$$

From equation (3.3.37) we may derive that

$$\sum_{n=1}^{3} s^{(n)}\, f_{i2}^{(n)}\,\beta^{(n)} = -\sum_{n=1}^{3} f_{i1}^{(n)}\,\beta^{(n)}$$

giving

$$\begin{aligned} P_K &= -\sum_{n=1}^{3}\left[\frac{\lambda_i}{(iK)}\left(c_{i2j2}s^{(n)} + c_{i2j1}\right)\mathrm{U}_{jl}^{(n)}\,F_{lK2}^{(n)}(0) + \lambda_i\, f_{i2}^{(n)}\right]\beta^{(n)}\,\frac{\Gamma_K^{(n)}}{\Delta_K^{(n)}} \\ &\quad + \sum_{n=1}^{3}\left[\frac{\lambda_i}{(iK)}\left(c_{i2j2}s^{(n)} + c_{i2j1}\right)\mathrm{U}_{jl}^{(n)}\,F_{lK1}^{(n)}(0) + \lambda_i\, f_{i1}^{(n)}\right]\beta^{(n)}, \\ &= N_K. \end{aligned} \tag{3.3.76}$$

Finally, equations (3.3.69) and (3.3.76) combine to give

$$\gamma_{K,\xi} + \gamma_{K,\tau} = \sum_{L=1}^{K-1} \Pi'_{KL}\, \gamma_{K-L}\, \gamma_L + \sum_{L=K+1}^{\infty} \Delta'_{KL}\, \bar{\gamma}_{L-K}\, \gamma_L\,, \tag{3.3.77}$$

where

$$\begin{aligned} \Pi'_{KL} &= \frac{\Pi_{KL}}{N_K} \\ \Delta'_{KL} &= \frac{\Delta_{KL}}{N_K}\,. \end{aligned} \tag{3.3.78}$$

The coefficients (3.3.78) are entirely determined by the third-order elasticity constants and the various eigenvectors found in the derivation of the first-order solution. It is therefore useful to return to the linear equations and inspect the effects of crystallographic symmetry upon the form of the linear solution. This topic is discussed in the following section.

3.4 PARTICULAR LINEAR SOLUTIONS

The linear solution discussed in Section 3.3.3 depends upon the symmetry of the elastic material being considered. The class of symmetry most often investigated is cubic, $m3m$, for which the elastic constant c_{ijkl} in Voight's form, is given by

$$c_{\alpha\beta} = \begin{pmatrix} c_{11} & c_{12} & c_{12} & 0 & 0 & 0 \\ c_{12} & c_{11} & c_{12} & 0 & 0 & 0 \\ c_{12} & c_{12} & c_{11} & 0 & 0 & 0 \\ 0 & 0 & 0 & c_{44} & 0 & 0 \\ 0 & 0 & 0 & 0 & c_{44} & 0 \\ 0 & 0 & 0 & 0 & 0 & c_{44} \end{pmatrix}.$$

Lardner and Tupholme [1986] have shown that for a crystal of this class, with the free surface along a plane of symmetry and for wave propagation along an axis of symmetry, the characteristic polynomial takes the form

$$\begin{aligned} |\mathrm{L}_{ij}(s)| &= \left[s^2 - \left(\frac{\rho - c_{44}}{c_{44}}\right)\right][c_{11}c_{44}s^4 + (c_{44}^2 + c_{11}^2 - (c_{11} + c_{44})\rho - (c_{12} + c_{44})^2)s^2 \\ &\quad + (c_{44} - \rho)(c_{11} - \rho)] \qquad (3.4.1) \\ &= 0\,, \end{aligned}$$

which yields the modal solutions as

$$s^2 = \frac{\rho - c_{44}}{c_{44}}\,, \qquad (3.4.2)$$

where $\rho \leq c_{44}$, and the solutions to a quadratic equation in s^2. Three of the six roots for s satisfy the decay condition ($\Im(s) < 0$), and may be used to derive the three associated eigenvectors and hence the boundary determinant

$$B = |\mathrm{M}_{in}|\,.$$

The chosen modal roots are not known explicitly, however their sum and product are known through the relationship between roots of a quadratic. Use of this relationship reveals that this boundary determinant is zero only when

$$\rho = c_{44} \qquad (3.4.3)$$

or

$$p^2[(\delta - 1)^2 + r(1 - r - p^2)]^2 - (1 - p^2)^2[r(r - 1 + p^2)] = 0\,, \qquad (3.4.4)$$

where the quantities p, δ and r are defined by

$$
\begin{aligned}
p^2 &= 1 - \frac{\rho}{c_{44}} \\
\delta &= \frac{c_{12} + c_{44}}{c_{44}} \\
r &= \frac{c_{11}}{c_{44}} .
\end{aligned}
\tag{3.4.5}
$$

It is obvious from equation (3.4.2) that the case (3.4.3) leads to a wavespeed and eigenvectors consistent with a transverse bulk wave, whilst the conditions (3.4.4), however, yield the wavespeed of a surface wave.

Suppose that the direction of propagation is rotated to an angle θ away from the axis of symmetry, whilst the plane of symmetry remains the free surface. In this situation the rotation matrix

$$
a_{ij} = \begin{pmatrix} \cos\theta & 0 & \sin\theta \\ 0 & 1 & 0 \\ -\sin\theta & 0 & \cos\theta \end{pmatrix},
\tag{3.4.6}
$$

may be applied, in accordance with the scheme of Section 2.1.4, to the elastic constants to deduce that the rotated constant c_{ijkl}, in Voights notation, is

$$
c_{\alpha\beta} = \begin{pmatrix} c'_{11} & c'_{12} & c'_{13} & 0 & c'_{15} & 0 \\ c'_{12} & c'_{22} & c'_{13} & 0 & 0 & 0 \\ c'_{13} & c'_{13} & c'_{11} & 0 & c'_{35} & 0 \\ 0 & 0 & 0 & c'_{44} & 0 & 0 \\ c'_{15} & 0 & c'_{35} & 0 & c'_{55} & 0 \\ 0 & 0 & 0 & 0 & 0 & c'_{44} \end{pmatrix},
\tag{3.4.7}
$$

where

$$
\begin{aligned}
c'_{11} &= (1 - \cos 4\theta)(c_{11} + c_{12} + 2c_{44})/4 + (1 + \cos 4\theta)c_{11}/2 \\
c'_{22} &= c_{11} \\
c'_{12} &= c_{12} \\
c'_{13} &= (1 - \cos 4\theta)(c_{11} - c_{12} - 2c_{44})/4 + c_{12} \\
c'_{15} &= \sin 4\theta(c_{11} - c_{12} - 2c_{44})/4 \\
c'_{55} &= (1 - \cos 4\theta)(c_{11} - c_{12} - 2c_{44})/4 + (\cos 4\theta)\, c_{44} \\
c'_{44} &= c_{44} \\
c'_{35} &= -c'_{15} ,
\end{aligned}
\tag{3.4.8}
$$

The expressions (3.4.8) were obtained on a computer using REDUCE, the algebraic computing package, although they are not difficult to obtain by direct calculation.

It is useful to note at this point the appearance of the factor $\eta = (c_{11} - c_{12})/2c_{44}$ in the expressions for the rotated constants. If we set $\eta = 1$, it may be seen that

$$\begin{aligned} c'_{11} &= c_{11} \\ c'_{13} &= c_{12} \\ c'_{15} &= 0 \\ c'_{55} &= c_{44} \end{aligned}$$

which are all independent of θ. In fact materials satisfying $\eta = 1$ are linearly isotropic. The parameter η can therefore be utilised as a linear isotropy factor, and cubic elastic crystals can be separated into two sub-classes, $\eta < 1$ and $\eta > 1$.

The elastic constants defined through equation (3.4.8) enable the characteristic polynomial to be rewritten in the form

$$\begin{aligned} &[(c'_{44}\,s^2 + c'_{11} - \rho)(c'_{22}\,s^2 + c'_{44} - \rho) - (c'_{44} + c'_{12})^2\,s^2\,]\,[c'_{44}\,s^2 + c'_{55} - \rho] \\ &\quad - {c'_{15}}^2\,(c'_{22}\,s^2 + c'_{44} - \rho) = 0\,, \end{aligned} \tag{3.4.9}$$

which is cubic in s^2.

The above equation may be solved analytically using REDUCE and the appropriate solutions selected. The eigenvectors and eigenvalues for the linear problem, along with the boundary determinant may then be expressed algebraically. It was found, however, that these expressions were extremely lengthy with no obvious decomposition. More importantly there appeared to be no straightforward dependence of the boundary determinant upon the angle of rotation.

Synge [1956] considered the more general linear partial wave representation

$$u_j^{(1)} = A_j e^{i(s_i x_i - t)}\,,$$

in which s represents the slowness vector. Substitution of this representation into the equations of motion (3.3.22) leads to the characteristic equation (or slowness equation) in the form

$$(\rho\delta_{ik} - c_{ijkl}s_j s_l)A_k = 0\,.$$

For consideration of surface waves in the present configuration the values of s_1 and s_3 must be real, whilst s_2 must have a negative imaginary part. Taking

the parameters s_1 and s_3 to represent Cartesian coordinates, the slowness surface for s_2 represented by the slowness equation may be plotted. Values of s_2 lying within certain regions of this surface may be shown to satisfy the decay conditions necessary for a surface wave. Synge deduced that the slowness surface admitted surface wave solutions only for certain directions of propagation on the material surface (or pairs of vector coordinates (s_1, s_3)). This conclusion, however, was derived under the condition that the s_i are all distinct, which is certainly never true for the isotropic limit. Currie [1970] later showed this conjecture to be false and derived a more general formulation for the slowness equation.

For the purpose of this thesis we shall restrict our attention to propagation in particular directions on the material surface. Farnell [1979] considered various cuts of cubic crystals and found that, on a plane of mirror symmetry, the surface wave degenerated to a bulk wave at 45° away from the axis of symmetry. Thus, taking $\theta = 45°$, equation (3.4.9) becomes

$$r\,s^4 + [\tfrac{1}{2}r(r+\delta-1) + r\,p^2 + p^2 - \delta^2]\,s^2 + p^2[\tfrac{1}{2}(r+\delta-1) + p^2] = 0 \qquad (3.4.10)$$

and

$$s^2 = \tfrac{1}{2}(\delta + 1 - r) - p^2\,. \qquad (3.4.11)$$

The three values of s yielding decaying amplitudes as y increases lead to a boundary determinant, B, in the form

$$B = \Big[r(r-1)p^6 + \big[2r(r-\delta)\delta - \tfrac{1}{2}r(r-\delta-1)(1-2r)\big]p^4 + \Big[\Big((1-\delta)^2 - \tfrac{1}{2}r(r+\delta-1)\Big)^2 + r(r+\delta-2)\Big]p^2 - \tfrac{1}{2}r(r+\delta-1)\Big]\Big[\tfrac{1}{2}(\delta+1-r) - p^2\Big]\,. \qquad (3.4.12)$$

This determinant is clearly zero either when p^2 satisfies a cubic equation, or

$$p^2 = \tfrac{1}{2}(\delta + 1 - r)\,. \qquad (3.4.13)$$

As in Lardner and Tupholme [1986], the solution (3.4.13) corresponds to a bulk wave satisfying the surface wave boundary conditions. Moreover, the cubic equation yields two admissible modes with the appropriate decay, but a third mode which does not decay with depth. This latter mode need not be excluded however, since the element of the eigenvector $\beta^{(n)}$ corresponding to this mode may be set to zero.

In general, therefore, for the chosen orientation of material and direction of propagation a surface wave and a bulk wave can propagate, both satisfying the boundary

conditions. The surface wave, however, exists only for this particular crystal configuration. Small deviations away from this particular direction of propagation introduce a small complex part to the boundary determinant B, and then the value of the boundary determinant can only be equated to zero by introducing a complex wavenumber. The surface wave will therefore decay both with depth *and* distance in the direction of propagation and is commonly called a pseudo–surface wave. The bulk wave however exhibits decay with depth at all small angles away from the 45° direction and becomes a surface wave.

To examine the behaviour at angles between $\theta = 0°$ and $\theta = 45°$ Farnell [1974] outlines a search procedure based on the Golden Section, using the parameter ρ as the independent variable. This technique may be summarised as follows:

A value is assigned to ρ and the resulting characteristic equation solved numerically. The appropriate roots are then used to obtain a value for the boundary determinant B. This process is carried out for four values of ρ, namely ρ_1, ρ_2, ρ_3 and ρ_4, chosen such that their enclosing set, here called the range, encloses the true value of ρ (an estimate of ρ may be obtained by consideration of the bulk wave). The four points are chosen to lie in the Golden Ratio when plotted on a linear scale, see Figure 3.4.1.

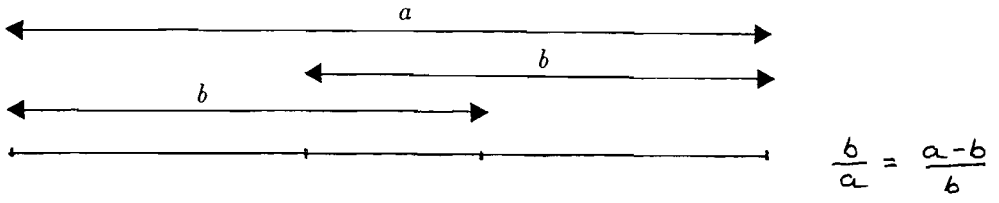

Figure 3.4.1 The Golden Section

The set of points enclosing the minimum value of B, called the minimum set, may then be chosen by examining the value of B at each of the four evaluated points. The minimum set will be either $\{\rho_1, \rho_3\}$ or $\{\rho_2, \rho_4\}$, and a fifth point at which to evaluate B may now be positioned within the appropriate set. This point can clearly be placed to lie in the Golden Ratio with the remaining three points in the set, see Figure 3.4.1, and again the minimum set is located.

Repeated use of this process gradually reduces the width of the minimum set until either it becomes less than the tolerance placed on the parameter ρ or the determinant B is found to be sufficiently close to zero at one of the evaluated points.

One of the major disadvantages of the Golden Ratio process is that the rate of convergence is fixed, since one always reduces the width of the minimum set by a fixed ratio.

A more efficient technique would obviously be one in which the width of the minimum set could be reduced by a variable amount. One proceeds as for the Golden Section technique, however the four points are placed equidistantly in the range. Again the minimum set is located, however the fifth point is positioned according to the algorithm

$$\rho' = \frac{(\rho_2 - \rho_1)B_1}{(B_1 + B_2)} + \rho_1$$

where the two extreme points of the minimum set are assumed to be ρ_1 and ρ_2 ($\rho_2 > \rho_1$), with their respective boundary determinant values represented by B_1 and B_2. Thus the fifth point is positioned closest to the true root and the width of the minimum set reduced. This algorithm is then repeated until the range becomes less than the tolerance of the parameter ρ.

The two methods described above are shown diagramatically in Figures 3.4.2 and 3.4.3.

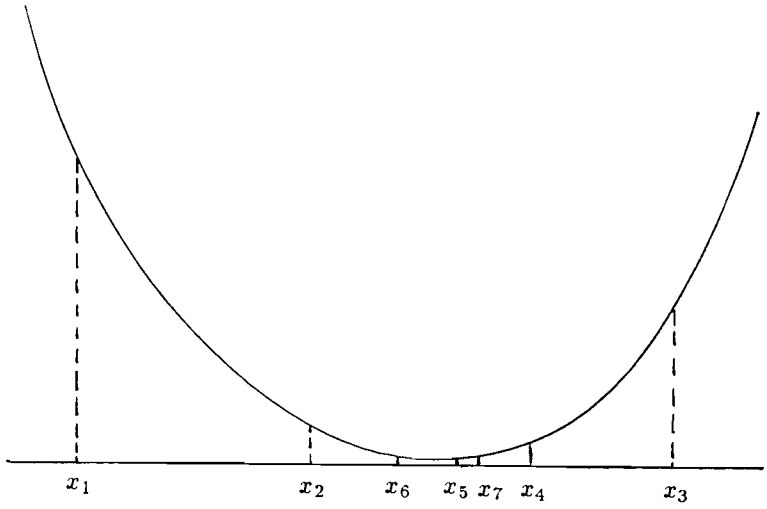

Figure 3.4.2 An example of the Golden Section iterative procedure

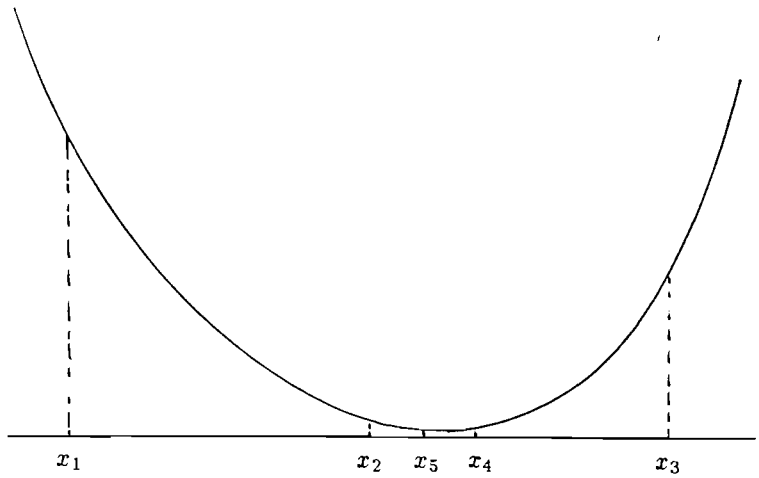

Figure 3.4.3 An example of the iterative procedure used in this thesis

It was found in general that the second method converged at a much faster rate than the first, although both methods were highly sensitive to the initial conditioning of the parameters.

It is now possible, with the use of the numerical routines outlined in this section and those presented in Chapter 2 for the rotation of the crystallographic axes, to numerically find the value of the parameter ρ and hence the surface wavespeed. The eigenvectors of the linear solution may then be evaluated and these allow us to examine the nature of the solution.

The above numerical search routines have been tested on several of the materials examined by Farnell [1974], for both types of cubic crystal ($\eta < 1$ and $\eta > 1$, where η is the isotropy factor). Graphs of the calculated values of the surface wavespeeds for two different cubically anisotropic materials are shown in Figures 3.4.4 and 3.4.5. It is easily seen that the graphs exactly reproduce the results in Farnell [1974] and our results reproduce the development of the bulk wave satisfying the boundary conditions at the particular angle of 45° away from the axis of symmetry. The reproduction of Farnell's results is a partial justification of our rotation and search techniques.

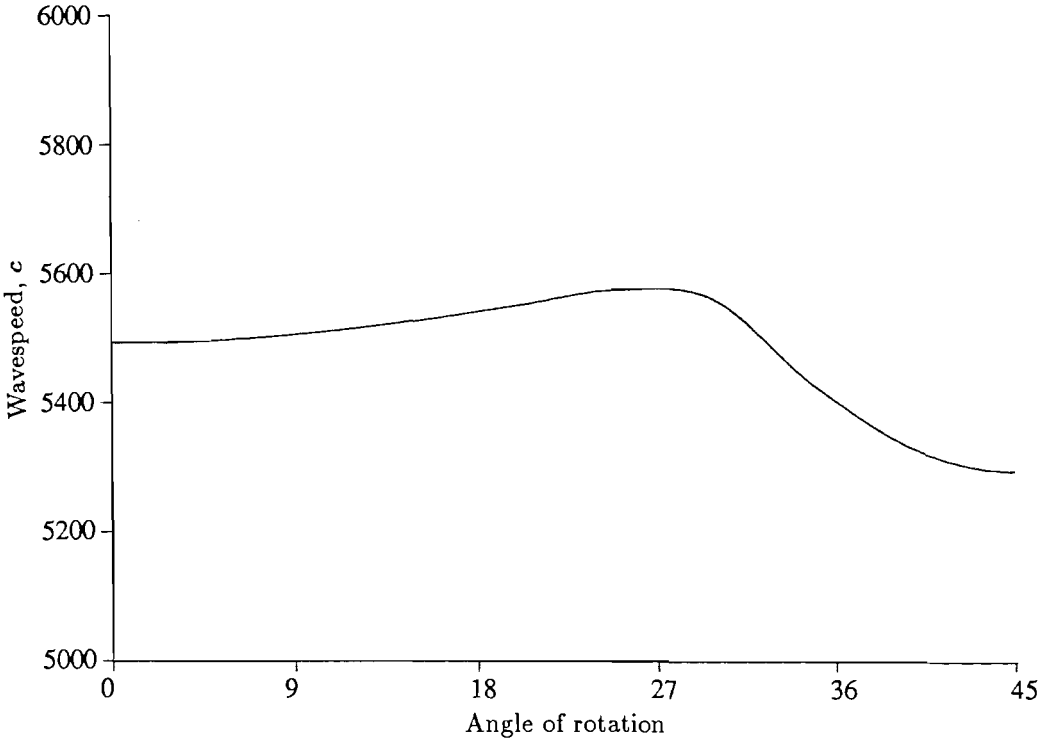

Figure 3.4.4 Surface wavespeed for various angles of propagation away from the X-axis on a Y-cut surface of MgO

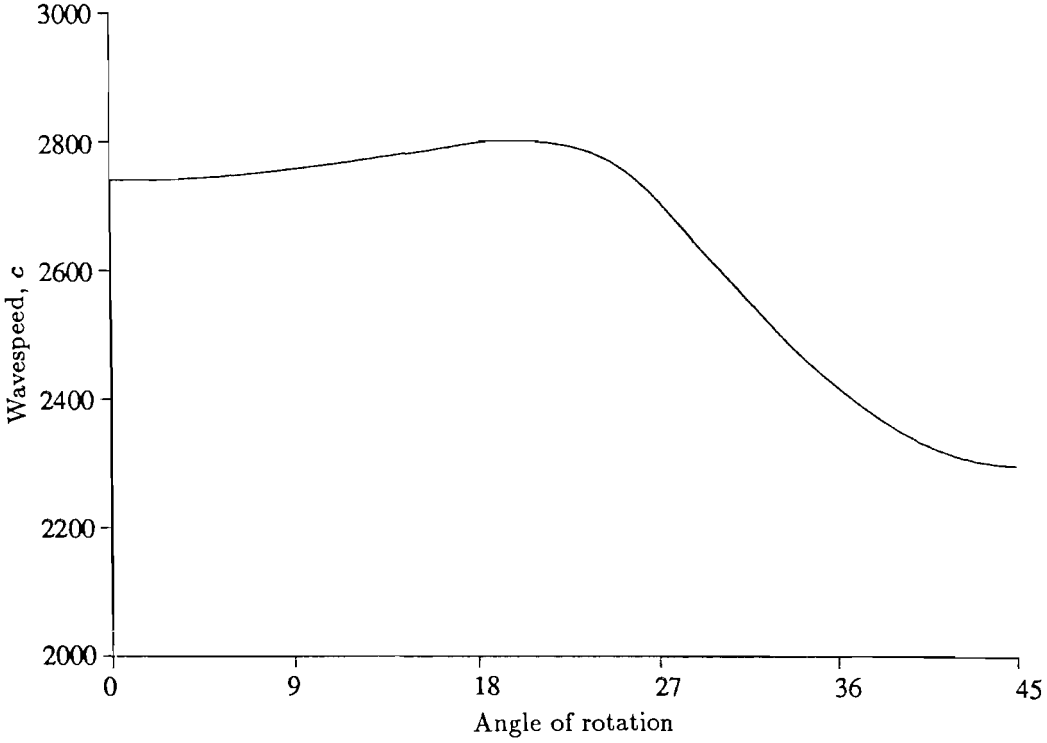

Figure 3.4.5 Surface wavespeed for various angles of propagation away from the X-axis on a Y-cut surface of Nickel

3.5 RESULTS AND DISCUSSION

The equations (3.3.77) represent an infinite system of coupled partial differential equations in the surface amplitude, and are called coupled amplitude equations. We are now in a position to present solutions to the coupled amplitude equations for an anisotropic elastic material of general symmetry.

When only the first two harmonics are retained the system (3.3.77) reduces to two partial differential equations in the amplitudes of the two harmonics

$$\begin{aligned} \gamma_{1,\xi} + \gamma_{1,\tau} &= 0 \\ \gamma_{2,\xi} + \gamma_{2,\tau} &= \Pi'_{21}\,\gamma_1\,\gamma_1 \,. \end{aligned} \tag{3.5.1}$$

Kalyanasundaram [1981] has shown that, in the isotropic case, this greatly simplified system may be solved by decomposition of the complex amplitude into modulus argument form

$$\gamma_K = \rho_K(\xi,\tau)\,e^{i\theta_K(\xi,\tau)} \,. \tag{3.5.2}$$

This method of solution works due to the homogeneous nature of equation $(3.5.1)_1$ and because the coefficients of the terms on the right hand side are purely real. The method of solution breaks down for the anisotropic case because all coefficients become complex. The method also breaks down for larger systems including higher harmonics because no equation is homogeneous.

Taking a monochromatic wave source, that is a time independent source, the slow time dependence of the surface amplitude may be neglected, reducing the partial differential equation (3.3.77) to the ordinary differential equation

$$\frac{d\gamma_K}{d\xi} = \sum_{L=1}^{K-1} \Pi'_{KL}\,\gamma_{K-L}\,\gamma_L + \sum_{L=K+1}^{\infty} \Delta'_{KL}\,\bar{\gamma}_{L-K}\,\gamma_L \,. \tag{3.5.3}$$

This ODE now admits a finite difference method solution of the type

$$\frac{\gamma_K(\xi+\Delta\xi) - \gamma_K(\xi-\Delta\xi)}{2\Delta\xi} = \sum_{L=1}^{K-1} \Pi'_{KL}\,\gamma_{K-L}(\xi)\,\gamma_L(\xi) + \sum_{L=K+1}^{\infty} \Delta'_{KL}\,\bar{\gamma}_{L-K}(\xi)\,\gamma_L(\xi) \,, \tag{3.5.4}$$

where $\Delta\xi$ is the mesh size, see David [1985]. In order to produce a closed system of equations the infinite summation must obviously be truncated at some selected number of harmonics. This numerical procedure is used to derive the results in this section.

Clearly the infinite summation in (3.5.4) must be truncated before solving the system and Figures 3.5.1 to 3.5.4 illustrate the effects of including increasing numbers of harmonics when solving equation (3.5.4) for an unrotated (Y-) cut of the material magnesium oxide considered earlier by Lardner and Tupholme [1986]. Only the first three harmonics are displayed for clarity of presentation. Figure 3.5.1 displays the amplitude growth and decay with propagation distance for two harmonics, 3.5.2 for three harmonics, 3.5.3 for ten harmonics and 3.5.4 for thirty-two harmonics. It can be seen that the plot of the second harmonic changes very little between Figures 3.5.2 and 3.5.3, that is upon inclusion of the tenth harmonic, and likewise there is very little change in the plot of the third harmonic between Figures 3.5.3 and 3.5.4. Due to the nature of equations (3.5.4) it can be seen that truncation of the harmonic series at $K = n$ will lead to unreliable solutions for the nth harmonic whilst the lower harmonics will converge towards their true values. The value of n is given on each of the figures in this section.

Examination of equations (3.5.4) and in particular the expressions for the coefficients (3.3.44), reveals that the right hand sides of equations (3.5.4) are of order n^3 whilst the left hand sides are of order 1. This becomes important when considering systems of say 30 harmonics, where the right hand sides will be of order 10^3. This provides an explanation for the slightly "turned-up" end of the plot of the third harmonic in Figure 3.5.4. Here the highest harmonics are obviously exploding to unrealistic values which gradually feed back through the system and will eventually invalidate the results for larger propagation distances.

As discussed earlier the method of multiple scales in fact provides results valid to values of $\xi \sim 1/\epsilon$ and reliable up to $\xi = 1$, and it has been found that restriction of the slow variable to the range $0 \leq \xi \leq 1$ provides results that conserve energy even for fairly large numbers of harmonics. In general results in this section are presented for values of ξ lying in the range $0 \leq \xi \leq 1$ and, since we are interested only in the first three harmonics, we shall truncate the harmonic series at $n = 10$.

As an exception to this rule, Figure 3.5.5 presents the results obtained by taking the system (3.5.4) and truncating at $K = 3$. The wave here is allowed to propagate up to $\xi = 10$ and illustrates the possible bounded nature of this system, but closer examination of the precise system of equations, including expansion of the coefficients involved to investigate possible analytical relationships between them, proved inconclusive. This graph gives an excellent illustration of the continuous transfer of energy between the various harmonics noted by Kalyanasundaram [1981] and Lardner and Tupholme [1986].

Figure 3.5.6 displays the behaviour of the first three harmonics when the direction of propagation on the surface of the material magnesium oxide is rotated away from the material axis by 20° and then a further 20° for Figure 3.5.7. It is seen that the decay decreases away from the axis of symmetry.

Figures 3.5.8 and 3.8.9 show the amplitude decay for X- and Z-cut magnesium oxide for comparison. These are identical to the results for the unrotated Y-cut which is obvious upon consideration of the positioning of the axes of symmetry. This reproduction of results again partially justifies our rotation procedures. Figure 3.5.10 displays results for propagation along a cut of the crystal chosen at random for its potential lack of symmetry.

Results for two different cubic elastic materials, copper and nickel, are presented in Figures 3.5.11 and 3.5.12 and these demonstrate the similarity in behaviour for the propagation of surface waves in the various subgroups of cubic crystals outlined in Section 3.4. Rotations away from the axis of symmetry are presented in Figures 3.5.13 and 3.5.14.

Before drawing any conclusions from these graphs, let us now consider perhaps the simplest form of solution to equations (3.5.3), namely a series solution in ξ, which we would expect to be valid for small values of ξ. Hence we consider the surface amplitude $\tilde{\gamma}_K = \gamma_K/a$, where a is the nondimensional initial amplitude of the fundamental, to take the form

$$\tilde{\gamma}_K = w_K^{(0)} + w_K^{(1)}\xi_1 + w_K^{(2)}\xi_1^2 + w_K^{(3)}\xi_1^3 + \dots \,, \tag{3.5.5}$$

where $\xi_1 = a\xi$.

Substituting the representation (3.5.5) into the coupled amplitude equations (3.3.53) and considering increasing numbers of harmonics it may easily be shown that, for the signalling condition

$$\begin{aligned} \tilde{\gamma}_1 &= 1 \\ \tilde{\gamma}_K &= 0\,, \quad K \geq 2\,, \end{aligned} \tag{3.5.6}$$

the coefficients are given by

$$
\begin{aligned}
w_1^{(0)} &= 1 \\
w_1^{(1)} &= 0 \\
w_1^{(2)} &= \Pi'_{12}\Delta'_{21}/2 \\
w_2^{(0)} &= 0 \\
w_2^{(1)} &= \Pi'_{12} \\
w_2^{(2)} &= 0 \\
w_2^{(3)} &= {\Pi'_{12}}^2\Delta'_{21}/3 + \Pi'_{12}(\Pi'_{13} + \Pi'_{23})\Delta'_{32}/6 \\
w_3^{(0)} &= 0 \\
w_3^{(1)} &= 0 \\
w_3^{(2)} &= \Pi'_{12}(\Pi'_{13} + \Pi'_{23})/2 .
\end{aligned}
\tag{3.5.7}
$$

Whilst only valid for small values of ξ_1, this series solution gives some insight into the initial growth and decay of the fundamental wave and its various harmonics. More significantly, the parameters $w_1^{(2)}$ and $w_2^{(1)}$, representing the quadratic decay of the fundamental and the linear growth of the second harmonic respectively, may be used to assess the change in the rates of growth and decay of the amplitudes of the leading harmonics for varying cuts and directions of propagation in different crystals.

A graph of the variation of the parameters $w_1^{(2)}$, $w_2^{(1)}$, $w_2^{(3)}$ and $w_3^{(2)}$ with direction of propagation is given in Figure 3.5.15. This figure shows clearly the decrease in the amplitude decay of the fundamental and the corresponding decrease in the growth of the higher harmonics as the direction of propagation rotates away from the axis of symmetry. The shape of this graph appears to bear little resemblance to what one would expect upon consideration of the continuous change in the values of the various second- and third-order constants illustrated through equations (3.4.8). This leads one to suppose that it would be useful to have some parameter to measure the "level" of anisotropy of a particular cut and orientation. Consideration of the variation of the growth and decay coefficients with such a parameter may lead to some greater insight into the dependence of surface wave evolution upon material symmetry.

For the purposes of acoustic device design, the growth of one particular harmonic must be either minimised or maximised and thus the choice would be that surface and propagation direction for which the value of the appropriate growth or decay parameter is minimum or maximum. Our plot of the values of the growth and

decay parameters for various angles of propagation would indicate that orientations of high symmetry lead to fast growth and decay, whilst those of low symmetry lead to slow growth and decay. It is not possible to be more precise and no wholly conclusive results may be drawn from the graphs presented since, as we have already mentioned, the nonlinear constants available are subject to extreme errors.

Key to Figures

- ■ Fundamental amplitude, $\tilde{\gamma}_1$.
- □ Second harmonic amplitude, $\tilde{\gamma}_2$.
- ▲ Third harmonic amplitude, $\tilde{\gamma}_3$.
- △ Fourth harmonic amplitude, $\tilde{\gamma}_4$ (where shown).

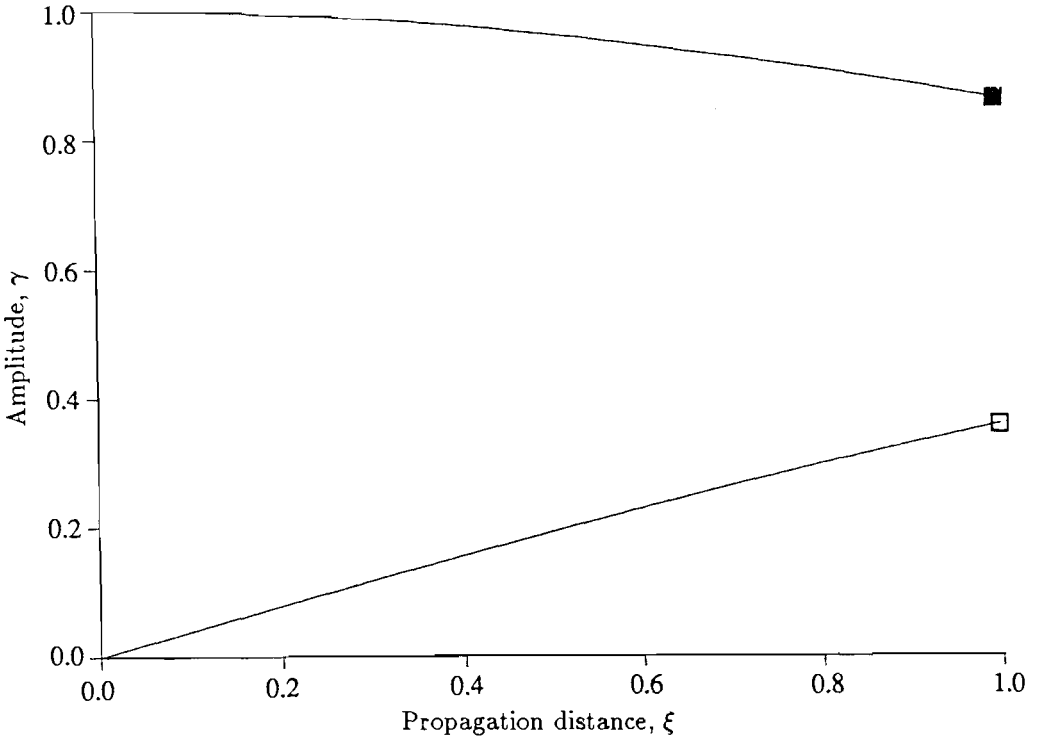

Figure 3.5.1 Growth and decay of the amplitudes $\tilde{\gamma}_K$ with propagation distance ξ_1 for X-propagation on Y-cut MgO, (2 harmonics)

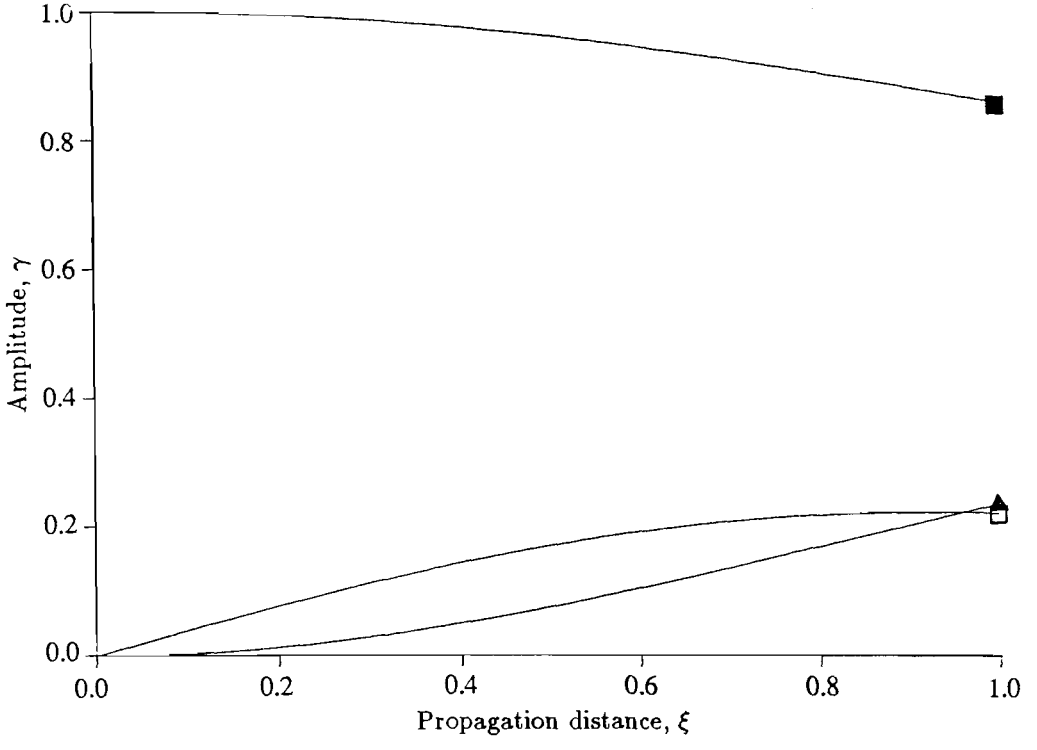

Figure 3.5.2 Growth and decay of the amplitudes $\tilde{\gamma}_K$ with propagation distance ξ_1 for X-propagation on Y-cut MgO, (3 harmonics)

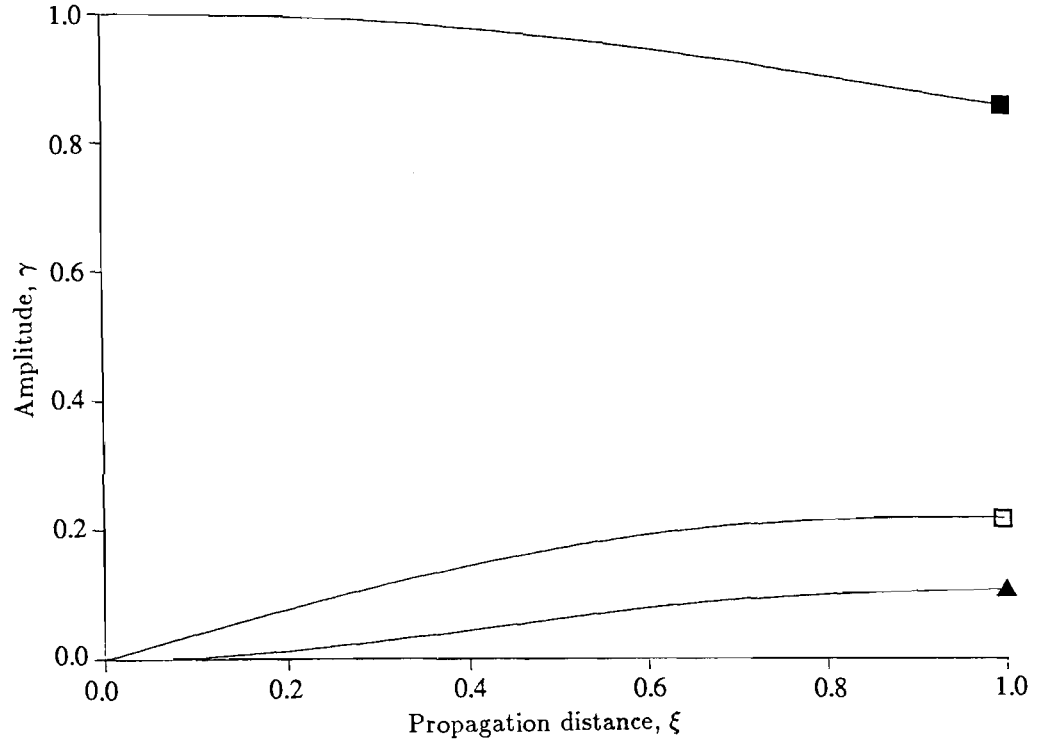

Figure 3.5.3 Growth and decay of the amplitudes $\tilde{\gamma}_K$ with propagation distance ξ_1 for X-propagation on Y-cut MgO, (10 harmonics)

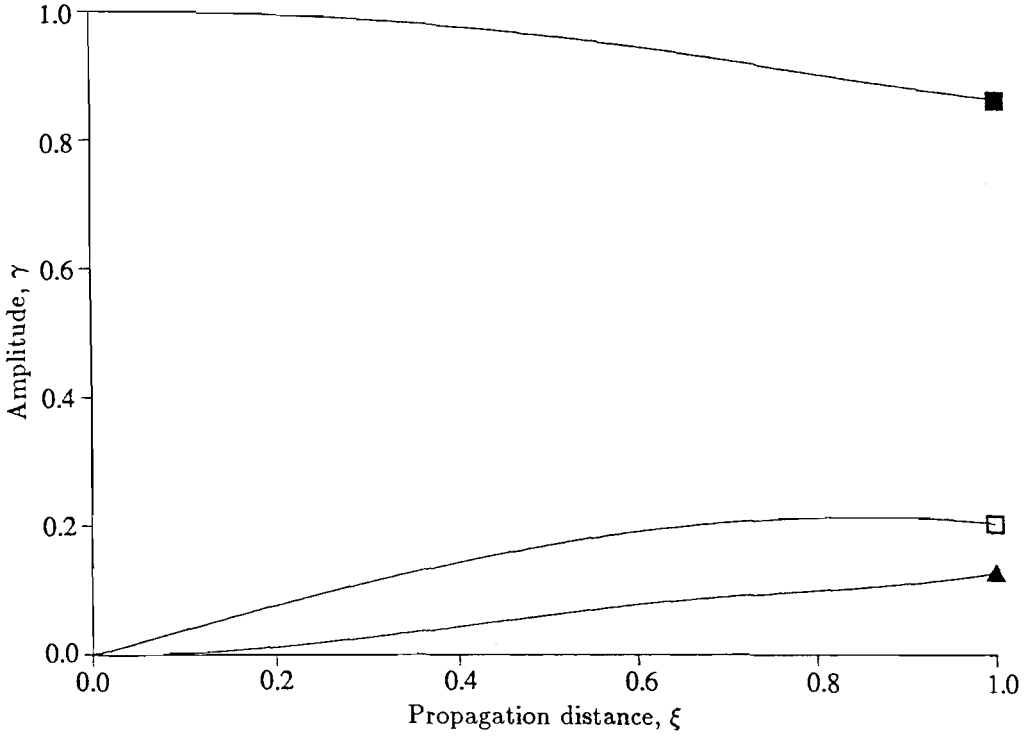

Figure 3.5.4 Growth and decay of the amplitudes $\tilde{\gamma}_K$ with propagation distance ξ_1 for X-propagation on Y-cut MgO, (32 harmonics)

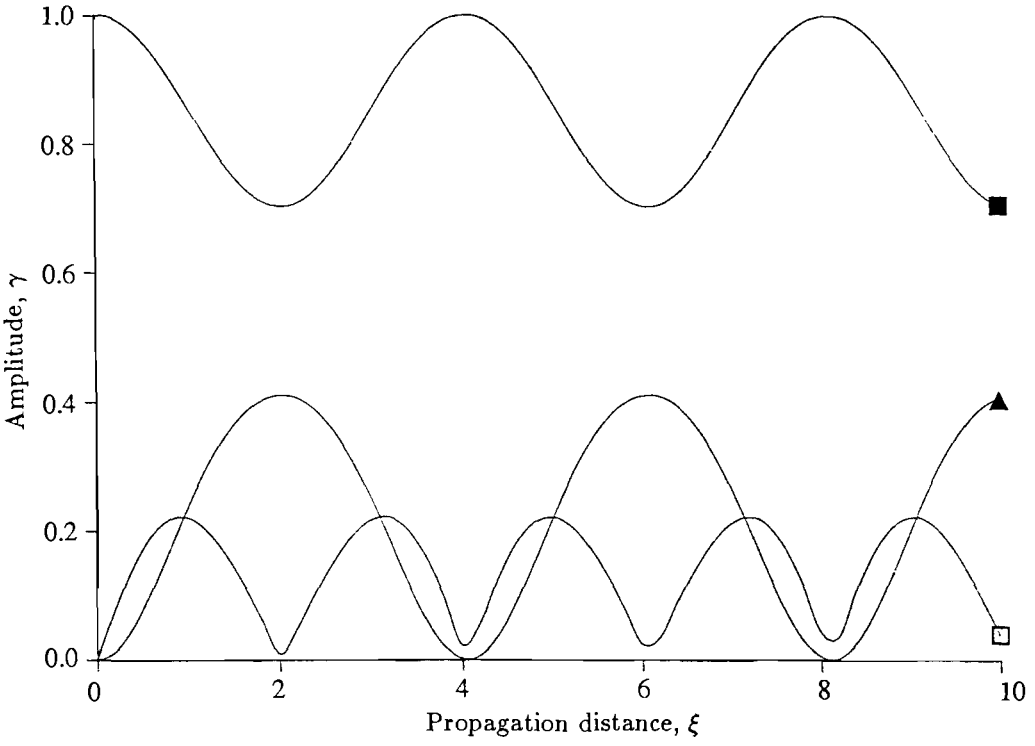

Figure 3.5.5 Growth and decay of the amplitudes $\tilde{\gamma}_K$ with propagation distance ξ_1 for X-propagation on Y-cut MgO, (3 harmonics)

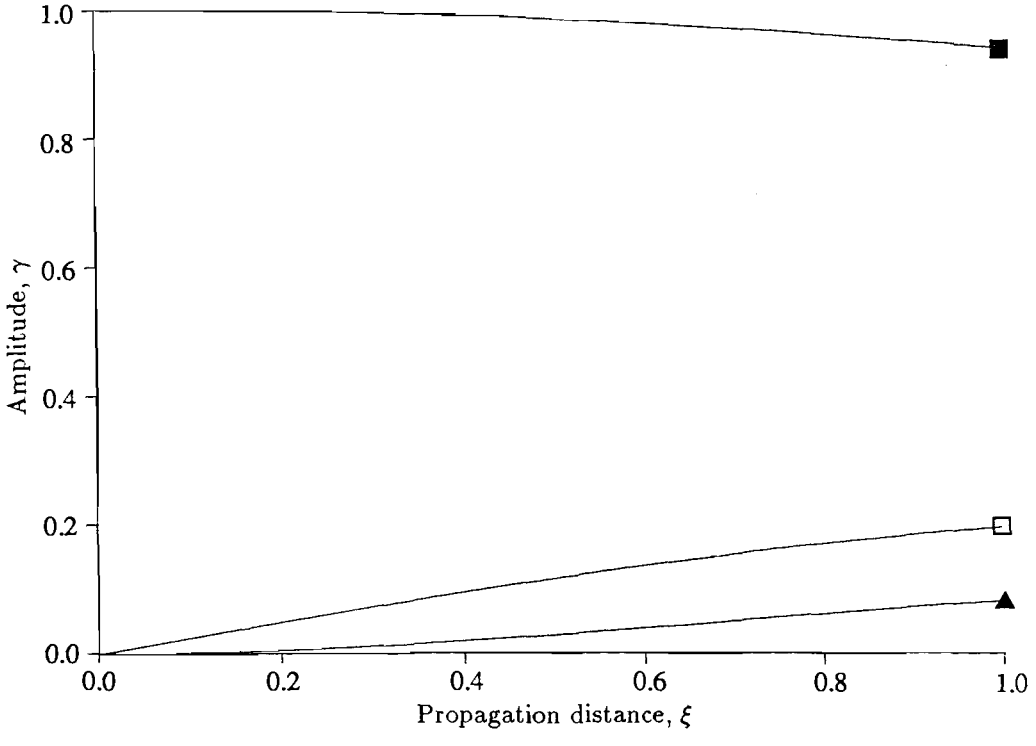

Figure 3.5.6 Growth and decay of the amplitudes $\tilde{\gamma}_K$ with propagation distance ξ_1 for propagation 20° from X-axis on Y-cut MgO, (10 harmonics)

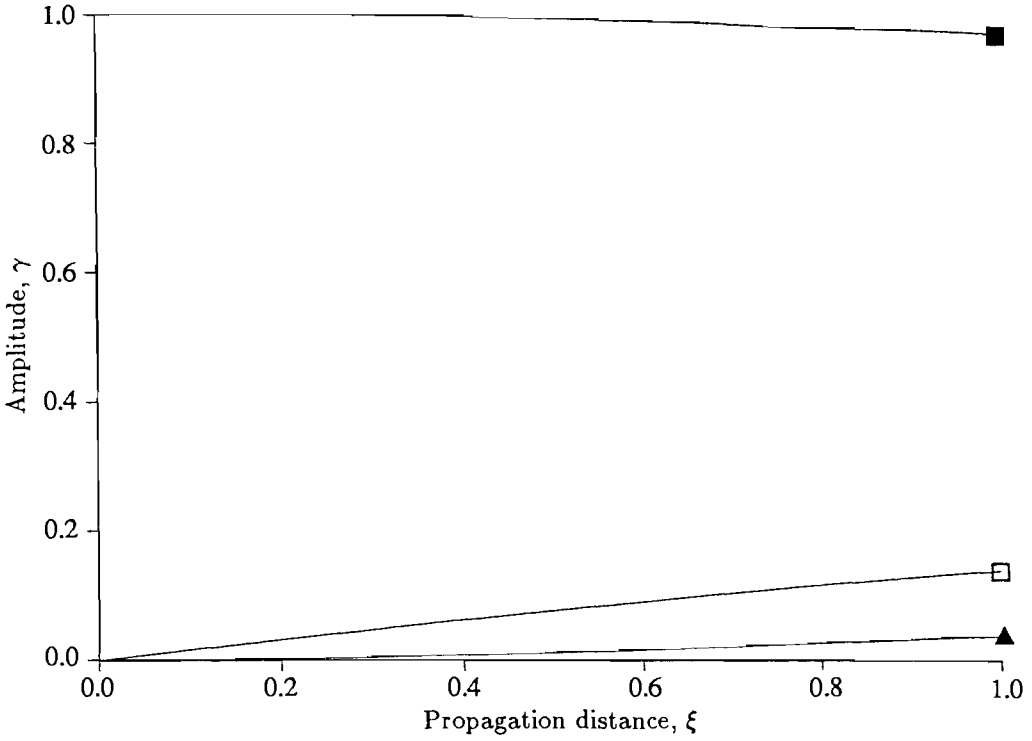

Figure 3.5.7 Growth and decay of the amplitudes $\tilde{\gamma}_K$ with propagation distance ξ_1 for propagation 40° from X-axis on Y-cut MgO, (10 harmonics)

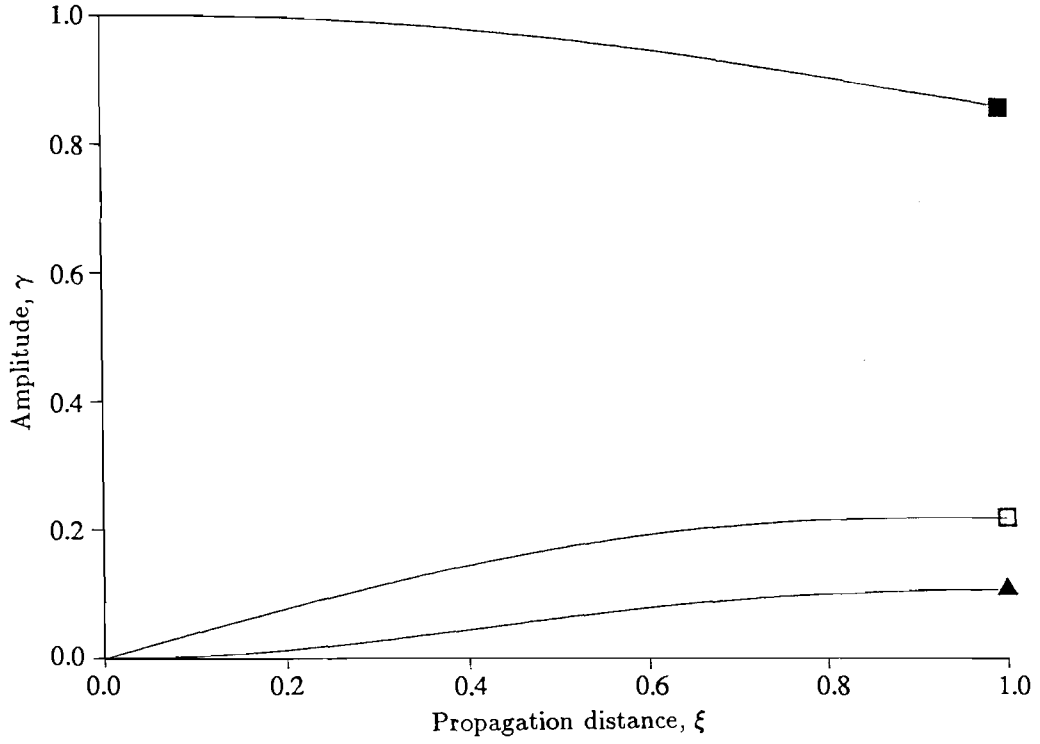

Figure 3.5.8 Growth and decay of the amplitudes $\tilde{\gamma}_K$ with propagation distance ξ_1 for Z-propagation on X-cut MgO, (10 harmonics)

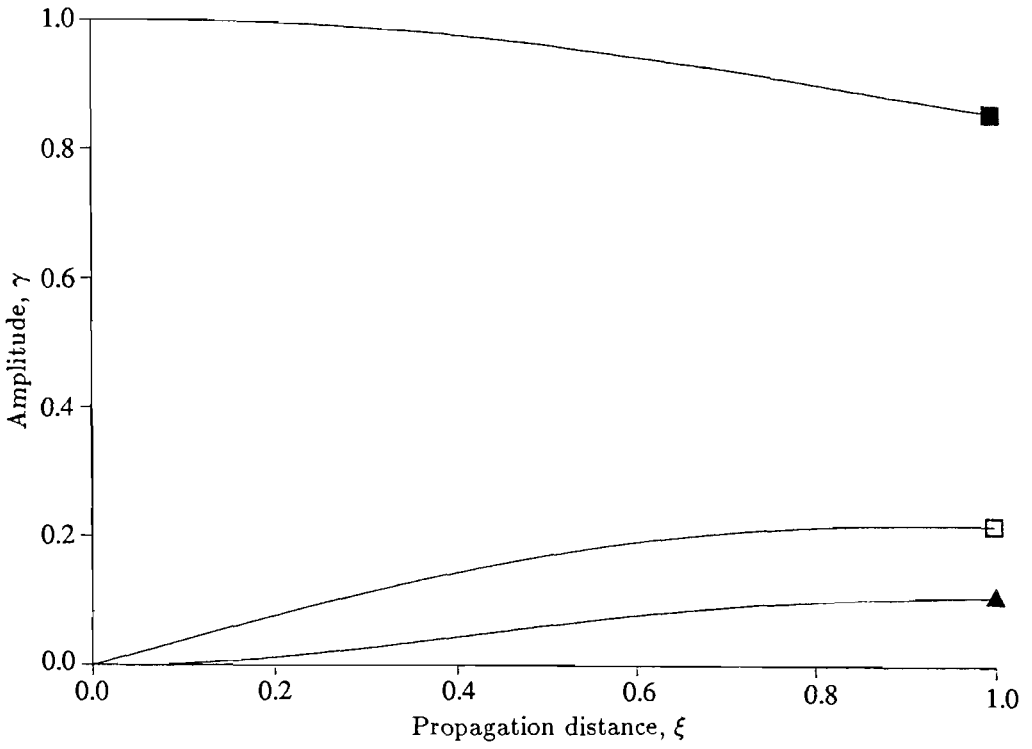

Figure 3.5.9 Growth and decay of the amplitudes $\tilde{\gamma}_K$ with propagation distance ξ_1 for X-propagation on Z-cut MgO, (10 harmonics)

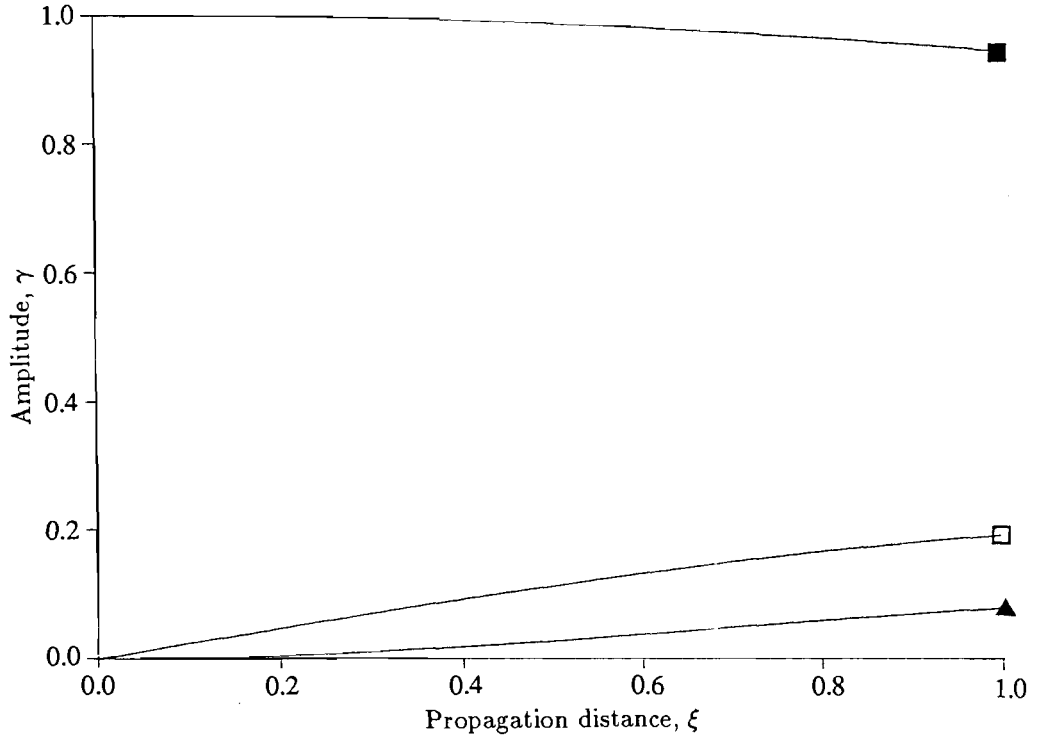

Figure 3.5.10 Growth and decay of the amplitudes $\tilde{\gamma}_K$ with propagation distance ξ_1 for propagation on a random cut of MgO, (10 harmonics)

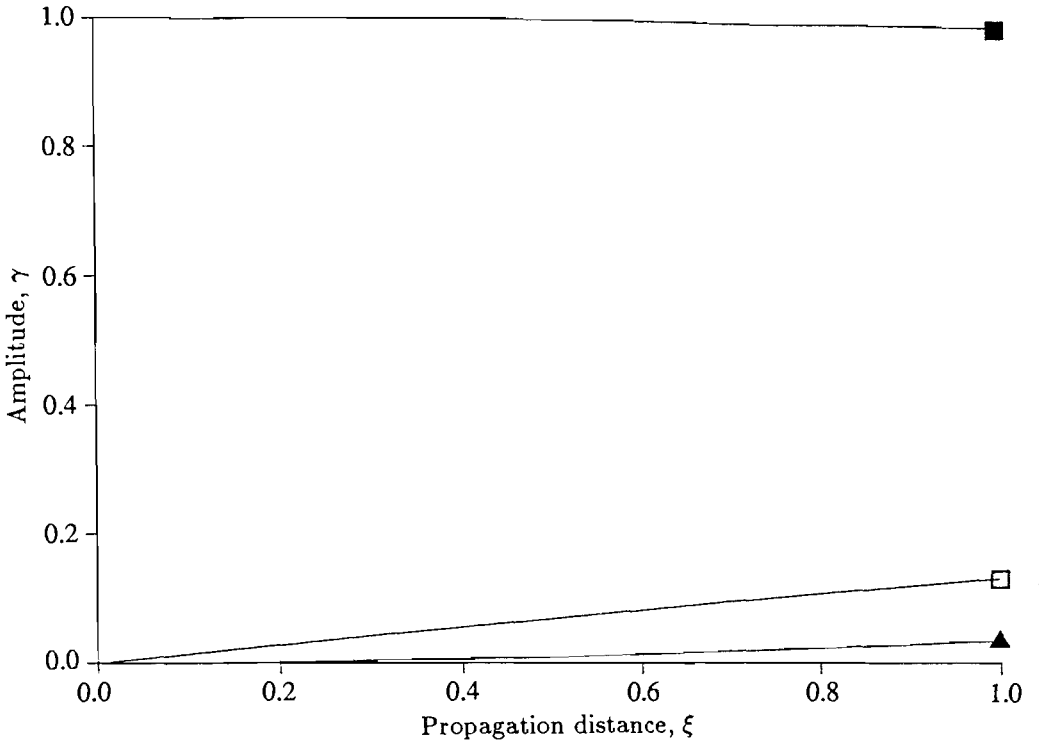

Figure 3.5.11 Growth and decay of the amplitudes $\tilde{\gamma}_K$ with propagation distance ξ_1 for X-propagation on Y-cut Copper, (10 harmonics)

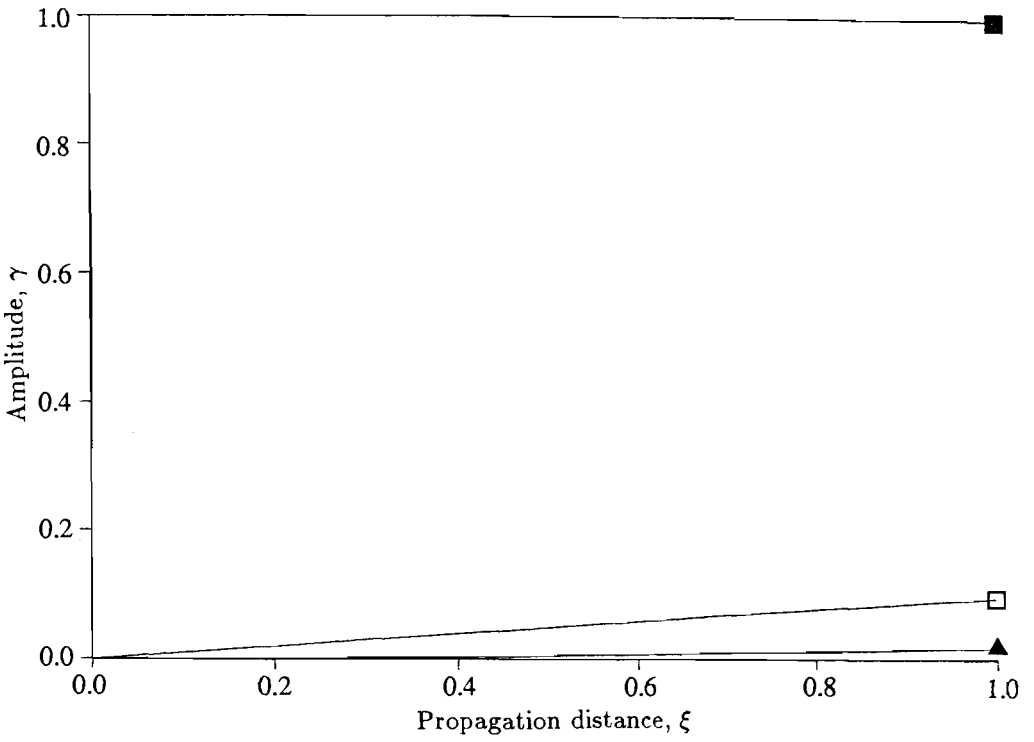

Figure 3.5.12 Growth and decay of the amplitudes $\tilde{\gamma}_K$ with propagation distance ξ_1 for X-propagation on Y-cut Nickel, (10 harmonics)

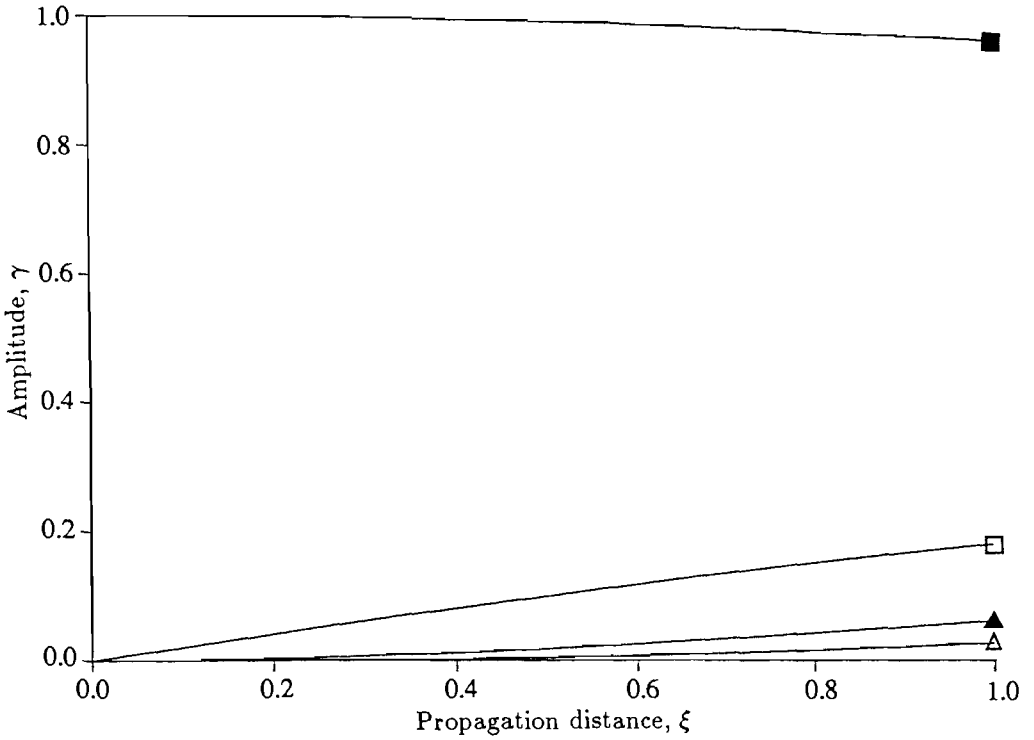

Figure 3.5.13 Growth and decay of the amplitudes $\tilde{\gamma}_K$ with propagation distance ξ_1 for propagation 20° away from the X-axis on Y-cut Copper, (10 harmonics)

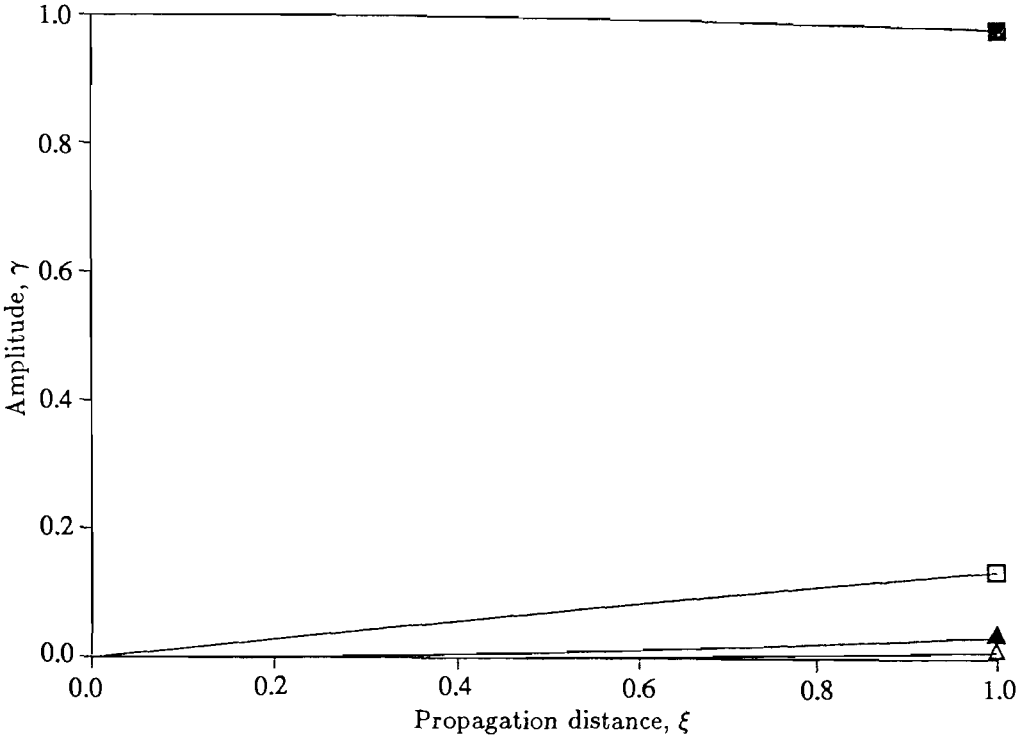

Figure 3.5.14 Growth and decay of the amplitudes $\tilde{\gamma}_K$ with propagation distance ξ_1 for propagation 20° away from the X-axis on Y-cut Nickel, (10 harmonics)

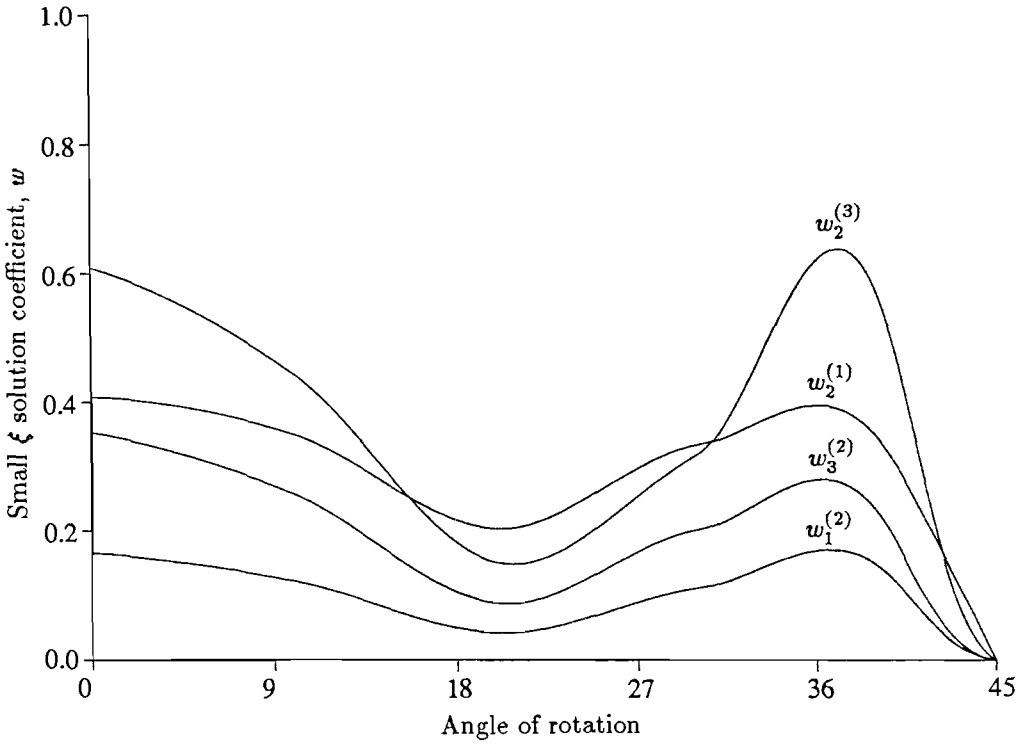

Figure 3.5.15 $w_1^{(2)}$, $w_2^{(1)}$,$w_2^{(3)}$ and $w_3^{(2)}$ for angles of propagation away from the X-axis on Y-cut MgO

4 Piezoelectricity

The propagation of waves in anisotropic materials has been studied in recent years in response to the growing interest in acoustic wave devices such as convolvers, filters and delay lines. Although much of the recent work has concentrated upon anisotropic elastic materials, most acoustic devices utilise the electro–elastic coupling of piezoelectric crystals such as lithium niobate and lithium tantalate. The study of piezoelectric surface waves is not dissimilar to the study of elastic waves on anisotropic media and it is possible to build upon the analysis of the previous chapter.

Following the work of Toupin [1963], a survey of nonlinear piezoelectricity is given in the book by Nelson [1979]. No specific consideration to surface waves is given in the text however, although a general derivation of the field equations governing the deformation of a piezoelectric substrate is presented. The reference provides much of the basic material for the first two sections of this chapter.

Campbell and Jones [1968] presented an early analysis of linear piezoelectric surface waves. The linearised equations of motion were solved by substitution of the appropriate surface waveform and numerical routines used to obtain plots of surface wavespeed for various crystallographic cuts of lithium niobate. These results were used to predict the linear electro–elastic coupling factor which, it is claimed, is related to the nonlinear electro–elastic coupling factor which may be used to assess the efficiency of a particular crystal orientation for use in acoustic devices.

Taylor and Crampin [1978] derived an elegant notational simplification allowing the linear field equations to be greatly simplified and written in a form closely similar to the anisotropic elastic case. This was achieved by extending the displacement vector to four components by including the electric potential and introducing similar extensions to the elasticity constants. Their method is extremely useful but there are a number of minor errors in the execution of their technique which shall be discussed later in this chapter. Extensions of their technique to the nonlinear

case shall be discussed in Section 4.4 , see also Tupholme and Harvey [1988] and Parker and David [1989].

A complete study of nonlinear piezoelectric waves was first presented by Tiersten and Baumhauer [1974]. In this paper the parametric excitation of second harmonics in a piezoelectric substrate of general symmetry was considered. The technique applied was essentially a perturbation of the linear solution. However the second-order solution they obtained contained amplitude functions which were then chosen so that the solution satisfied the surface boundary conditions. Their method is not satisfactory since it is not then clear that the solutions obtained through this technique in fact satisfy the governing field equations. Also, the free-space electric field effects above the crystal require consideration of geometric nonlinearities and Tiersten and Baumhauer assumed a Taylor's series expansion about the reference surface. This leads to certain inconsistencies in the regions of validity of the governing equations which shall be dealt with in Chapter 5.

Kalyanasundaram [1984] extended his multiple scales analysis of nonlinear isotropic elasticity to consider the propagation of electro-elastic waves on the surface of certain piezoelectric substrates of hexagonal symmetry. It is possible to propagate waves of purely transverse displacement coupled to the electric field on such substrates. These waves were initially observed experimentally and have become known as Bleustein–Gulyaev waves.

The present chapter intends to present a derivation from first principles of the constitutive relations and governing field equations for a deformed piezoelectric substrate. The notational simplifications of Taylor and Crampin [1973] shall then be extended to the nonlinear problem (see Tupholme and Harvey [1988]) and the multiple scales technique of Chapter 3 is applied. Coupled amplitude equations are derived and numerical routines are employed to provide graphs of the growth and decay of the amplitudes of the harmonics comprising the surface wave.

4.1 STRESS AND ELECTRIC FIELD

In Chapter 2 the constitutive relations for a general elastic material were derived in terms of the strain energy, or Gibb's function. In this section the corresponding energy function for a piezoelectric material, referred to as the electric enthalpy, is defined and the constitutive relations appropriate for a discussion of the deformation of the piezoelectric material are derived. Maxwell's equations are stated and the momentum balance equation is used to give the governing field equations for a deformed solid.

The concept of electric field is here introduced through Maxwell's equations, Nelson [1979], and the induced force is used to define the electric displacement vector in terms of the electric enthalpy.

In a piezoelectric substrate under the quasistatic approximation, the electric field, $\mathbf{E}$, and polarisation, $\mathbf{P}$, satisfy Maxwell's equations to give

$$\epsilon_0 \nabla \cdot \mathbf{E} = -\nabla \cdot \mathbf{P} = q, \tag{4.1.1}$$

where q is the electric charge and ϵ_0 the vacuum permittivity.

Defining the electric displacement vector through

$$\mathbf{D} = \epsilon_0 \mathbf{E} + \mathbf{P}, \tag{4.1.2}$$

then allows equation (4.1.1) to be written

$$\nabla \cdot \mathbf{D} = 0. \tag{4.1.3}$$

Under the quasi-static approximation we may assume there is no magnetic induction. This assumption yields, via the Maxwell-Lorentz equation, Nelson [1979],

$$\nabla \times \mathbf{E} = 0,$$

which admits the representation

$$\mathbf{E} = -\nabla \phi,$$

or

$$E_j = -\phi_{,j}, \tag{4.1.4}$$

where ϕ is called the scalar electric potential.

The force per unit volume developed from the electric field, Maugin [1985], is given by

$$\mathbf{f} = (\mathbf{P}.\nabla)\mathbf{E},$$

which leads to the electric power per unit volume in the form

$$\mathcal{P} = f_i v_i + \rho E_i \frac{\mathrm{D}}{\mathrm{D}t}\left(\frac{P_i}{\rho}\right) \tag{4.1.5}$$

where the second term arises through consideration of the power developed by the body as a whole.

Now the Cauchy stress, $\mathbf{T}$, is not symmetric in the case of nonlinear piezoelectricity and thus we may write

$$T_{ij} = T_{\{ij\}} + T_{[ij]}$$

where the braces and square brackets are used to denote the symmetric and skew part respectively of a non-symmetric tensor. Since the skew part arises from the electric polarization, we have that (Maugin [1985])

$$T_{[ji]} = E_{[j} P_{i]}.$$

From the first law of thermodynamics the total power may be written as

$$\frac{\mathrm{D}}{\mathrm{D}t}\int_{\mathcal{V}} \rho(\tfrac{1}{2} v_i v_i + e)\, d\mathcal{V} = \int_{\mathcal{V}} \mathcal{P}\, d\mathcal{V} + \int_{\mathcal{S}} v_i T_{ji} n_j\, d\mathcal{S}$$

where e is the energy of the body, less the kinetic energy. This yields in local form

$$\rho v_i \dot{v}_i + \rho \dot{e} = \mathcal{P} + v_{i,j} T_{ji} + v_i T_{ji,j}. \tag{4.1.6}$$

The equation of motion (2.2.23), for a piezoelectric substrate, must include the power generated by the electric field and may thus be written in the form

$$\rho \dot{v}_i = T_{ji,j} + f_i$$

which gives

$$\rho v_i \dot{v}_i = v_i T_{ji,j} + v_i f_i. \tag{4.1.7}$$

Now (4.1.5), (4.1.6) and (4.1.7) may be combined to reveal that

$$\rho \dot{e} = v_{i,j} T_{ji} + \rho E_i \frac{\mathrm{D}}{\mathrm{D}t}\left(\frac{P_i}{\rho}\right) \tag{4.1.8}$$

If we now let

$$\hat{e} = e - \frac{E_i P_i}{\rho} \tag{4.1.9}$$

we have, from (4.1.8), that

$$\rho\frac{\mathrm{D}\hat{e}}{\mathrm{D}t} = v_{i,j}T_{ji} - P_i\dot{E}_i. \tag{4.1.10}$$

We may define a reference frame polarization vector through

$$\mathrm{P}_A = JX_{A,i}P_i \tag{4.1.11}$$

and a measure of the reference frame electric field through

$$\mathcal{E}_A = E_i x_{i,A} = -\phi_{,A}, \tag{4.1.12}$$

and so

$$\frac{\mathcal{E}_A\mathrm{P}_A}{\rho_0} = \frac{E_iP_i}{\rho}.$$

Now

$$\begin{aligned}\dot{E}_i &= \frac{\mathrm{D}}{\mathrm{D}t}(\mathcal{E}_A X_{A,i}) = \dot{\mathcal{E}}_A X_{A,i} + \mathcal{E}_A\frac{\mathrm{D}}{\mathrm{D}t}(X_{A,i}) \\ &= \dot{\mathcal{E}}_A X_{A,i} - \mathcal{E}_A X_{A,j}v_{j,i},\end{aligned} \tag{4.1.13}$$

hence (4.1.10) becomes

$$\begin{aligned}\rho\frac{\mathrm{D}\hat{e}}{\mathrm{D}t} &= v_{i,j}T_{ji} - P_i\dot{\mathcal{E}}_A X_{A,i} + P_i\mathcal{E}_A X_{A,j}v_{j,i} \\ &= v_{i,j}T_{ji} - \frac{\rho}{\rho_0}\mathrm{P}_A\dot{\mathcal{E}}_A + E_jP_iv_{j,i}\end{aligned} \tag{4.1.14}$$

Defining

$$D_{ij} = v_{\{i,j\}} \qquad \text{and} \qquad \Omega_{ij} = v_{[ij]}$$

we may write

$$\begin{aligned}\rho\frac{\mathrm{D}\hat{e}}{\mathrm{D}t} &= D_{ij}T_{\{ji\}} + \Omega_{ij}E_{[j}P_{i]} - \frac{\rho}{\rho_0}\mathrm{P}_A\dot{\mathcal{E}}_A + E_{\{j}P_{i\}}D_{ij} + E_{[j}P_{i]}\Omega_{ji} \\ &= D_{ij}\left(T_{\{ij\}} + E_{\{j}P_{i\}}\right) - \frac{\rho}{\rho_0}\mathrm{P}_A\dot{\mathcal{E}}_A \\ &= D_{ij}S_{ij} - \frac{\rho}{\rho_0}\mathrm{P}_A\dot{\mathcal{E}}_A,\end{aligned} \tag{4.1.16}$$

where S_{ij} is the symmetric stress tensor

Now, from (2.2.39),

$$\frac{\mathrm{D}E_{AB}}{\mathrm{D}t} = x_{i,A}x_{j,B}D_{ij}$$

and thus

$$\begin{aligned}S_{ij}D_{ij} &= S_{ij}X_{A,i}X_{B,j}\dot{E}_{AB} \\ &= \frac{\rho}{\rho_0}X_{B,j}\sigma_{Aj}\dot{E}_{AB},\end{aligned} \tag{4.1.17}$$

where $\sigma_{Aj} = JX_{A,i}S_{ij}$ is the symmetric Piola–Kirchhoff stress tensor.

Substituting (4.1.17) into (4.1.16) we have

$$\frac{\mathrm{D}\mathcal{W}}{\mathrm{D}t} = X_{B,j}\sigma_{Aj}\dot{E}_{AB} - \mathrm{P}_A\dot{\mathcal{E}}_A \tag{4.1.18}$$

where $\mathcal{W} = \rho_0\hat{\mathrm{e}}$ is the electric enthalpy.

Throughout this chapter we shall make the assumption that free-space electric field effects may be neglected. This leads to the simplification

$$\mathrm{D}_A = \mathrm{P}_A, \tag{4.1.19}$$

where

$$\mathrm{D}_A = JX_{A,i}D_i,$$

and we may then write, directly from (4.1.18),

$$\sigma_{Ai} = x_{i,B}\frac{\partial\mathcal{W}}{\partial E_{AB}} \tag{4.1.20}$$

and

$$\mathrm{D}_A = -\frac{\partial\mathcal{W}}{\partial\mathcal{E}_A}. \tag{4.1.21}$$

The assumption (4.1.19) will be considered in greater detail in Chapter 5 where the full efects of the free-space electric field and boundary continuity will be considered.

4.2 ELECTRIC ENTHALPY

In Section 3.1 we expanded the strain energy function as a series in the independent variable E_{AB}. In the previous section the Piola-Kirchhoff stress tensor and electric displacement vector were expressed as functions of the electric enthalpy, the piezoelectric analogy to the strain energy, and we assumed the enthalpy to be a function of both the Lagrangian strain and the electric field vector. Expanding the electic enthalpy as a series in both independent variables therefore leads to the expression

$$\begin{aligned}\mathcal{W} = {} & c^{(0)} + c^{(0)}_{AB}E_{AB} + \tfrac{1}{2}c^{(2)}_{ABCD}E_{AB}E_{CD} + \tfrac{1}{6}c^{(3)}_{ABCDEF}E_{AB}E_{CD}E_{EF} \\ & - \epsilon^{(1)}_{m}\mathcal{E}_{m} - \tfrac{1}{2}\epsilon^{(2)}_{mn}\mathcal{E}_{m}\mathcal{E}_{n} - \tfrac{1}{6}\epsilon^{(3)}_{mnp}\mathcal{E}_{m}\mathcal{E}_{n}\mathcal{E}_{p} - e^{(2)}_{mAB}\mathcal{E}_{m}E_{AB} \\ & - \tfrac{1}{2}e^{(3)}_{mABCD}\mathcal{E}_{m}E_{AB}E_{CD} - \tfrac{1}{2}l_{mnAB}\mathcal{E}_{m}\mathcal{E}_{n}E_{AB}\,, \end{aligned} \tag{4.2.1}$$

where only terms up to cubic order in strain and electric field are included. It is clear from the representation (4.2.1) that the coefficients may be expressed as derivatives of the electric enthalpy through

$$\begin{aligned} c^{(0)} &= \mathcal{W}|_{E_{AB}=0} \\ c^{(1)}_{AB} &= \left.\frac{\partial \mathcal{W}}{\partial E_{AB}}\right|_{E_{AB}=0} \\ c^{(2)}_{ABCD} &= \left.\frac{\partial^2 \mathcal{W}}{\partial E_{AB}\partial E_{CD}}\right|_{E_{AB}=0} \\ c^{(3)}_{ABCDEF} &= \left.\frac{\partial^3 \mathcal{W}}{\partial E_{AB}\partial E_{CD}\partial E_{EF}}\right|_{E_{AB}=0} \\ \epsilon^{(1)}_{m} &= -\left.\frac{\partial \mathcal{W}}{\partial \mathcal{E}_{m}}\right|_{\mathcal{E}_{m}=0} \\ \epsilon^{(2)}_{mn} &= -\left.\frac{\partial^2 \mathcal{W}}{\partial \mathcal{E}_{m}\partial \mathcal{E}_{n}}\right|_{\mathcal{E}_{m}=0} \\ \epsilon^{(3)}_{mnp} &= -\left.\frac{\partial^3 \mathcal{W}}{\partial \mathcal{E}_{m}\partial \mathcal{E}_{n}\partial \mathcal{E}_{p}}\right|_{\mathcal{E}_{m}=0} \\ e^{(2)}_{mAB} &= -\left.\frac{\partial^2 \mathcal{W}}{\partial \mathcal{E}_{m}\partial E_{AB}}\right|_{\mathcal{E}_{m}=E_{AB}=0} \\ e^{(3)}_{mABCD} &= -\left.\frac{\partial^3 \mathcal{W}}{\partial \mathcal{E}_{m}\partial E_{AB}\partial E_{CD}}\right|_{\mathcal{E}_{m}=E_{AB}=0} \\ l_{mnAB} &= -\left.\frac{\partial^3 \mathcal{W}}{\partial \mathcal{E}_{m}\partial \mathcal{E}_{n}\partial E_{AB}}\right|_{\mathcal{E}_{m}=E_{AB}=0} \end{aligned} \tag{4.2.2}$$

where the coefficients $c^{(1)}_{AB}$, $c^{(2)}_{ABCD}$ $c^{(3)}_{ABCDEF}$, $\epsilon^{(1)}_{m}$, $\epsilon^{(2)}_{mn}$, $\epsilon^{(3)}_{mnp}$, $e^{(2)}_{mAB}$, $e^{(3)}_{mABCD}$ and l_{mABCD} are known as the first-, second- and third-order elastic constants, first-, second- and third-order dielectric constants, second- and third-order piezoelectric constants and electrostrictive constants respectively.

We impose the constraint that the electric enthalpy must be zero in the absence of strain and electric field. This is consistent with there being no power generated under such conditions and leads to the relation

$$c^{(0)} = 0\,.$$

Replacement of the dummy subscripts in the expression (4.2.1) reveals the obvious symmetry relations

$$\begin{aligned}
c^{(2)}_{ABCD} &= c^{(2)}_{CDAB} \\
c^{(3)}_{ABCDEF} &= c^{(3)}_{CDABEF} = c^{(3)}_{ABEFCD} \\
\epsilon^{(2)}_{mn} &= \epsilon^{(2)}_{nm} \\
\epsilon^{(3)}_{mnp} &= \epsilon^{(3)}_{nmp} = \epsilon^{(3)}_{mpn} \\
e^{(3)}_{mABCD} &= e^{(3)}_{mCDAB} \\
l_{mnAB} &= l_{nmAB}
\end{aligned}$$

whilst the condition that $\mathcal{W}$ is a symmetric function with respect to the Lagrange strain, yields the symmetry relations

$$\begin{aligned}
c^{(1)}_{AB} &= c^{(1)}_{BA} \\
c^{(2)}_{ABCD} &= c^{(2)}_{BACD} = c^{(2)}_{ABDC} \\
c^{(3)}_{ABCDEF} &= c^{(3)}_{BACDEF} = c^{(3)}_{ABDCEF} = c^{(3)}_{ABCDFE} \\
e^{(2)}_{mAB} &= e^{(2)}_{mBA} \\
e^{(3)}_{mABCD} &= e^{(3)}_{mBACD} = e^{(3)}_{mABDC} \\
l_{mnAB} &= l_{mnBA}\,.
\end{aligned}$$

These relations can be summarised in the compact form

$$
\begin{aligned}
c^{(1)}_{AB} &= c^{(1)}_{BA}\,, \\
c^{(2)}_{ABCD} &= c^{(2)}_{CDAB} = c^{(2)}_{BACD}\,, \\
c^{(3)}_{ABCDEF} &= c^{(3)}_{CDABEF} = c^{(3)}_{ABEFCD} = c^{(3)}_{BACDEF}\,, \\
\epsilon^{(2)}_{mn} &= \epsilon^{(2)}_{nm}\,, \\
\epsilon^{(3)}_{mnp} &= \epsilon^{(3)}_{nmp} = \epsilon^{(3)}_{mpn}\,, \\
e^{(2)}_{mAB} &= e^{(2)}_{mBA}\,, \\
e^{(3)}_{mABCD} &= e^{(3)}_{mBACD} = e^{(3)}_{mCDAB}\,, \\
l_{mnAB} &= l_{mnBA} = l_{nmAB}\,.
\end{aligned}
\tag{4.2.3}
$$

There appears to be some discrepancy in the literature regarding the symmetry of the third-order dielectric constant, $\epsilon^{(3)}_{mnp}$. Miller's rule [1964] for calculation of the numerical values of this constant relates its value to the electro-optic constant r_{ijk} (which may be directly measured) through

$$
\epsilon^{(3)}_{ijk} = \frac{(\varepsilon_{ii}-1)(\varepsilon_{jj}-1)}{(\varepsilon_i^2-1)(\varepsilon_j^2-1)} n_i^2 n_j^2 r_{ijk}\,,
$$

where ε_i and ε_{ij} represent the material permittivities, n_i the refractive index, and the summation convention is not applied.

This rule is widely quoted in the current literature, see for example Ganguly and Davis (1980) and Nakagawa et al (1973). The electro-optic constant however, possesses the same symmetry as the second-order piezoelectric constant, as expressed in equations $(4.2.3)_6$. Hence Miller's rule implies that the third-order dielectric constant and the second-order piezoelectric constants possess the same symmetry, which is clearly not true from equations (4.2.3). Taking the trigonal class of material symmetry as an example, the second-order piezoelectric constant has four independent values. The third-order dielectric constant, however, possesses higher symmetry and only has three independent values. In conclusion, then, it is clear that Miller's rule is not an exact formula and so two of the four independent values of the third-order dielectric constant obtained through using the rule differ only by the accuracy of the rule itself. Cho and Yamanouchi (1986) evaluate the dielectric constants by direct measurements and hence derive only three independent values.

4.3 CONSTITUTIVE RELATIONS

In this section the series expansion of the electric enthalpy (4.2.1) is used to derive expressions for the Piola-Kirchhoff stress tensor and the electric displacement vector. Full use is made of the symmetries of the various constants stated in the previous section to reduce the constitutive equations to their simplest forms.

Recalling equation (4.1.24) we have

$$\sigma_{Ai} = x_{i,B} \frac{\partial \mathcal{W}}{\partial E_{AB}}.$$

The first three non-zero terms in the expansion of $\mathcal{W}$ are identical to those of the strain energy function of equation (3.1.1) and thus yield identical terms in the expression for the stress tensor. The three dielectric terms are independent of strain and hence do not appear in the expression for the stress tensor. Taking the third-order piezoelectric term as representative of the remaining terms, we have

$$\begin{aligned}
\mathcal{T}_1 &= -x_{i,B} \frac{\partial}{\partial E_{AB}} (\tfrac{1}{2} e^{(3)}_{mCDEF} \mathcal{E}_m E_{CD} E_{EF}) \\
&= -x_{i,B} \left[\tfrac{1}{2} e^{(3)}_{mABEF} \mathcal{E}_m E_{EF} + \tfrac{1}{2} e^{(3)}_{mCDAB} \mathcal{E}_m E_{CD} \right] \\
&= -x_{i,B} \left[e^{(3)}_{mABCD} \mathcal{E}_m E_{CD} \right] \\
&= x_{i,B}\, e^{(3)}_{mABCD}\, \phi_{,m} \left[\tfrac{1}{2} u_{C,D} + \tfrac{1}{2} u_{D,C} + \tfrac{1}{2} u_{E,C} u_{E,D} \right] \\
&= (u_{i,B} + \delta_{iB})\, e^{(3)}_{mABCD}\, \phi_{,m}\, u_{C,D} + \tfrac{1}{2} (u_{i,B} + \delta_{iB})\, e^{(3)}_{mABCD}\, u_{E,C}\, u_{E,D}\, \phi_{,m} \\
&= e^{(3)}_{mAiCD}\, \phi_{,m}\, u_{C,D} + e^{(3)}_{mABCD}\, \phi_{,m}\, u_{C,D}\, u_{i,B} \\
&\quad + \tfrac{1}{2} e^{(3)}_{mAiCD}\, \phi_{,m}\, u_{E,C}\, u_{E,D} + \tfrac{1}{2} e^{(3)}_{mABCD}\, \phi_{,m}\, u_{i,B}\, u_{E,C}\, u_{E,D} \\
&= e^{(3)}_{mAiCD}\, \phi_{,m}\, u_{C,D} + \mathrm{O}(u_{A,B})^3 .
\end{aligned}$$

Following this technique and restricting the expression for the stress tensor to quadratic order terms we obtain

$$\begin{aligned}
\sigma_{Ai} = {} & c^{(1)}_{Ai} + c^{(1)}_{AB}\, u_{i,B} + c^{(2)}_{AiCD}\, u_{C,D} \\
& + \tfrac{1}{2} c^{(2)}_{ABCD}\, u_{i,B}\, u_{C,D} + \tfrac{1}{2} c^{(2)}_{ABDC}\, u_{i,B}\, u_{C,D} \\
& + \tfrac{1}{2} c^{(2)}_{AiCD}\, u_{E,C}\, u_{E,D} + \tfrac{1}{2} c^{(3)}_{AiCDEF}\, u_{C,D}\, u_{E,F} \\
& + \delta_{iD}\, e^{(2)}_{BAC}\, \phi_{,B}\, u_{D,C} + e^{(2)}_{BAi}\, \phi_{,B} \\
& + e^{(3)}_{BAiCD}\, \phi_{,B}\, u_{C,D} - \tfrac{1}{2} l_{CDAi}\, \phi_{,C} \phi_{,D} \\
& + \mathrm{O}\big((u_{A,B})^3\big) .
\end{aligned} \tag{4.3.1}$$

Similarly equations (4.1.23) and (4.2.1) yield the following expression for the electric displacement vector

$$\begin{aligned} \mathrm{D}_A &= \epsilon_A^{(1)} + \epsilon_{AB}^{(2)}\mathcal{E}_B + \tfrac{1}{2}\epsilon_{ABC}^{(3)}\mathcal{E}_B\mathcal{E}_C \\ &\quad + e_{ABC}^{(2)}E_{BC} + \tfrac{1}{2}e_{ABCDE}^{(3)}E_{BC}E_{DE} - l_{ABCD}\mathcal{E}_B E_{CD}\,, \end{aligned} \tag{4.3.2}$$

which, together with equations (2.2.10) and (4.1.13) gives the electric displacement vector in terms of displacement and potential gradients as

$$\begin{aligned} \mathrm{D}_A &= \epsilon_A^{(1)} - \epsilon_{AB}^{(2)}\phi_{,B} + \tfrac{1}{2}\epsilon_{ABC}^{(3)}\phi_{,B}\phi_{,C} + e_{ABC}^{(2)}u_{B,C} + \tfrac{1}{2}e_{ABC}^{(2)}u_{D,B}u_{D,C} \\ &\quad + \tfrac{1}{8}e_{ABCDE}^{(3)}[u_{B,C}u_{D,E} + u_{B,C}u_{E,D} + u_{C,B}u_{D,E} + u_{C,B}u_{E,D}] \\ &\quad - \tfrac{1}{2}l_{ABCD}\phi_{,B}[u_{C,D} + u_{D,C}] + \mathrm{O}(u_{A,B}^2)\,, \end{aligned}$$

or

$$\begin{aligned} \mathrm{D}_A &= \epsilon_A^{(1)} - \epsilon_{AB}^{(2)}\phi_{,B} + \tfrac{1}{2}\epsilon_{ABC}^{(3)}\phi_{,B}\phi_{,C} + e_{ABC}^{(2)}u_{B,C} + \tfrac{1}{2}e_{ABC}^{(2)}u_{D,B}u_{D,C} \\ &\quad + \tfrac{1}{2}e_{ABCDE}^{(3)}u_{B,C}u_{D,E} - l_{ABCD}\phi_{,B}u_{C,D}\,, \end{aligned} \tag{4.3.3}$$

to quadratic order in displacement and potential, using the symmetries (4.2.3).

In summary, the constitutive relations governing a deformed piezoelectric substrate may be expressed to quadratic order as

$$\begin{aligned} \sigma_{ij} &= c_{ij}^{(1)} + c_{ik}^{(1)}u_{j,k} + c_{ijkl}^{(2)}u_{k,l} + e_{kij}^{(2)}\phi_{,k} \\ &\quad + \tfrac{1}{2}\left(c_{ijklmn}^{(3)} + c_{inkl}^{(2)}\delta_{jm} + c_{inlk}^{(2)}\delta_{jm} + c_{ijnl}^{(2)}\delta_{km}\right)u_{k,l}\,u_{m,n} \\ &\quad + \left(e_{kijlm}^{(3)} + e_{kim}^{(2)}\delta_{jl}\right)\phi_{,k}\,u_{l,m} - \tfrac{1}{2}l_{kmij}\,\phi_{,k}\phi_{,m}\,, \end{aligned} \tag{4.3.4}$$

and

$$\begin{aligned} \mathrm{D}_i &= \epsilon_i^{(1)} - \epsilon_{ij}^{(2)}\phi_{,j} + e_{ijk}^{(2)}u_{j,k} + \tfrac{1}{2}\epsilon_{ijk}^{(3)}\phi_{,j}\phi_{,k} \\ &\quad + \tfrac{1}{2}\left(e_{ijklm}^{(3)} + e_{ikm}^{(2)}\delta_{jl}\right)u_{j,k}u_{l,m} - l_{ijkl}\phi_{,j}u_{k,l}\,, \end{aligned} \tag{4.3.5}$$

replacing all subscripts by lower case since all derivatives are with respect to the reference frame.

In Section 3.2 we introduced the non-dimensionalised forms

$$
\begin{aligned}
c'^{(2)}_{ijkl} &= \frac{c_{ijkl}}{c_a} \\
d'^{(3)}_{ijklmn} &= \frac{d_{ijklmn}}{c_a}\,, \\
u'_i &= k_0\, u_i\,, \\
x' &= k_0\, x\,, \\
y' &= k_0\, y\,, \\
z' &= k_0\, z\,, \\
\rho' &= \frac{c^2}{c_a}\,\rho_0\,, \\
t' &= k_0\, c\, t\,.
\end{aligned}
\tag{4.3.6}
$$

Introducing these replacements to equation (4.3.4) we may derive that

$$
\begin{aligned}
\sigma'_{ij} \;=\; & c'^{(1)}_{ij} \;+\; c'^{(1)}_{ik}\, u'_{j,k} \;+\; c'^{(2)}_{ijkl}\, u'_{k,l} + \frac{k_0 e^{(2)}_{kij}}{c_a}\,\phi_{,k} \\
& + \tfrac{1}{2}\left(c'^{(3)}_{ijklmn} + c'^{(2)}_{inkl}\delta_{jm} + c'^{(2)}_{inlk}\delta_{jm} + c'^{(2)}_{ijnl}\delta_{km}\right) u'_{k,l}\, u'_{m,n} \\
& + k_0 \left(\frac{e^{(3)}_{kijlm} + e^{(2)}_{kim}\delta_{jl}}{c_a}\right) \phi_{,k}\, u'_{l,m} \;-\; \tfrac{1}{2}\frac{{k_0}^2}{c_a} l_{kmij}\, \phi_{,k}\phi_{,m}\,.
\end{aligned}
\tag{4.3.7}
$$

Since numerical values of both piezoelectric constants are generally of the same order of magnitude it is clear that they should be non-dimensionalised with respect to some typical value e_a, in a similar way to the elastic coefficients in equation (4.3.6),

$$
\begin{aligned}
e'^{(2)}_{ijk} &= \frac{e^{(2)}_{ijk}}{e_a}\,, \\
e'^{(3)}_{ijklm} &= \frac{e^{(3)}_{ijklm}}{e_a}\,.
\end{aligned}
\tag{4.3.8}
$$

Substitution of the replacements (4.3.8) into equation (4.3.4) reveals that we must take

$$
\phi' = \frac{e_a k_0 \phi}{c_a}\,,
\tag{4.3.9}
$$

and subsequently

$$
l'_{ijkl} = \frac{c_a l_{ijkl}}{e_a^2}\,.
\tag{4.3.10}
$$

Equation (4.3.5) now leads us to the replacements

$$\epsilon_i'^{(1)} = \frac{\epsilon_j^{(1)}}{e_a},$$
$$\epsilon_{ij}'^{(2)} = \frac{c_a \epsilon_{ij}^{(2)}}{e_a^2},$$
$$\epsilon_{ijk}'^{(3)} = \frac{c_a^2 \epsilon_{ijk}^{(3)}}{e_a^3}. \tag{4.3.11}$$

It is noted that the non-dimensionalised forms (4.3.8) to (4.3.11) leave the form of equations (4.3.4) and (4.3.5) unaltered and therefore the dashed notation may be dropped henceforth.

4.4 SIMPLIFICATIONS

In this section the constitutive relations (4.3.4) and (4.3.5) are rewritten in much simpler forms.

For a material in its undeformed state the displacement and potential gradients must be zero. For our model it is also convenient to impose that there is zero stress and electric displacement in the undeformed state. Referring to equations (4.3.4) and (4.3.5), these assumed reference conditions imply

$$c_{ij}^{(1)} = 0\,,$$

and

$$\epsilon_i^{(1)} = 0\,.$$

These additional restrictions allow the expressions for the stress and electric displacement to be written

$$\begin{aligned}\sigma_{ij} \;=\; & c_{ijkl}^{(2)}\, u_{k,l} + e_{kij}^{(2)}\, \phi_{,k} \\ & + \tfrac{1}{2}\left(c_{ijklmn}^{(3)} + c_{inkl}^{(2)}\delta_{jm} + c_{inlk}^{(2)}\delta_{jm} + c_{ijnl}^{(2)}\delta_{km}\right) u_{k,l}\, u_{m,n} \\ & + \left(e_{kijlm}^{(3)} + e_{kim}^{(2)}\delta_{jl}\right) \phi_{,k}\, u_{l,m} \;-\; \tfrac{1}{2} l_{kmij}\, \phi_{,k}\phi_{,m}\,, \end{aligned} \tag{4.4.1}$$

and

$$\begin{aligned}\mathrm{D}_i \;=\; & -\epsilon_{ij}^{(2)}\phi_{,j} + e_{ijk}^{(2)} u_{j,k} + \tfrac{1}{2}\epsilon_{ijk}^{(3)}\phi_{,j}\phi_{,k} \\ & + \tfrac{1}{2}\left(e_{ijklm}^{(3)} + e_{ikm}^{(2)}\delta_{jl}\right) u_{j,k} u_{l,m} \\ & - l_{ijkl}\phi_{,j} u_{k,l}\,. \end{aligned} \tag{4.4.2}$$

Nelson [1978] derived analogous expressions and examined the restricted symmetry of the bracketed terms in equations (4.4.1) and (4.4.2), but did not attempt any simplification. It is now important to recall that in Chapter 3 we defined the quasi-third-order constant by

$$\begin{aligned} d_{ijklmn} \;&=\; \frac{1}{2}\left[\delta_{ik}\, c_{jlmn}^{(2)} + \delta_{im}\, c_{jnlk}^{(2)} + \delta_{km}\, c_{ijln}^{(2)} + c_{ijklmn}^{(3)}\right] \\ &\equiv\; d_{(ij)(kl)(mn)}\,, \end{aligned} \tag{4.4.3}$$

where the brackets denote the restricted symmetry defined in Section 2.1.2.

Nelson [1978] showed that the piezoelectric terms of equations (4.4.1) and (4.4.2) possess similar symmetry. It is therefore advantageous to introduce a quasi-third-order piezoelectric constant through the definition

$$f_{ijklm} = \frac{1}{2}\left[e^{(3)}_{ijklm} + \delta_{jl}\, e^{(2)}_{ikm}\right]$$
$$\equiv f_{i(jk)(lm)}\,. \tag{4.4.4}$$

Substituting the expressions (4.4.3) and (4.4.4) into the constitutive relations (4.4.1) and (4.4.2) we obtain

$$\sigma_{ij} = c^{(2)}_{ijkl}\, u_{k,l} + e^{(2)}_{kij}\, \phi_{,k} + d_{ijklmn}\, u_{k,l}\, u_{m,n}$$
$$+ 2\, f_{ijklm}\, \phi_{,k}\, u_{l,m} - \tfrac{1}{2} l_{kmij}\, \phi_{,k}\phi_{,m}\,, \tag{4.4.5}$$

and

$$\mathrm{D}_i = -\epsilon^{(2)}_{ij}\phi_{,j} + e^{(2)}_{ijk}u_{j,k} + \tfrac{1}{2}\epsilon^{(3)}_{ijk}\phi_{,j}\phi_{,k}$$
$$+ f_{ijklm}\, u_{j,k}u_{l,m} - l_{ijkl}\phi_{,j}u_{k,l}\,. \tag{4.4.6}$$

Taylor and Crampin [1978] studied the linearized form of equations (4.4.5) and (4.4.6) and found an elegant notational simplification resulting in a form that lead to forms for these constitutive relations bearing close resemblance to the elastic constitutive equations of Section 3.1.2.

Consider the linear constitutive equations

$$\sigma_{ij} = c^{(2)}_{ijkl}\, u_{k,l} + e^{(2)}_{kij}\, \phi_{,k} \tag{4.4.7}$$

and

$$\mathrm{D}_i = -\epsilon^{(2)}_{ij}\phi_{,j} + e^{(2)}_{ijk}u_{j,k}\,. \tag{4.4.8}$$

Taylor and Crampin proposed extending the mechanical displacement vector u_i to incorporate the electric scalar potential through the definition

$$\mathrm{u} = (u_1,\, u_2,\, u_3,\, \phi)^T\,. \tag{4.4.9}$$

Substituting the expression (4.4.9) into equations (4.4.7) and (4.4.8)

$$\sigma_{ij} = c^{(2)}_{ijkl}\, u_{k,l} + e^{(2)}_{kij}\, u_{4,k} \tag{4.4.10}$$

and

$$\mathrm{D}_i = e^{(2)}_{ijk}u_{j,k} - \epsilon^{(2)}_{ij}u_{4,j}\,. \tag{4.4.11}$$

It can now be seen that introduction of the definitions

$$
\begin{aligned}
\hat{c}_{ijkl} &= c^{(2)}_{ijkl}\,, \\
\hat{c}_{4jkl} &= \hat{c}_{kl4j} = e^{(2)}_{jkl}\,, \\
\hat{c}_{4j4l} &= -\epsilon^{(2)}_{jl}\,, \\
\hat{c}_{44kl} &= \hat{c}_{444l} = \hat{c}_{4444} = 0\,,
\end{aligned}
\tag{4.4.12}
$$

where all subscripts range over the values 1,2 and 3, allows the constitutive relations (4.4.10) and (4.4.11) to be written in the form

$$
\sigma_{ij} \;=\; \hat{c}_{ijkl}\, u_{k,l} + \hat{c}_{4lij}\, u_{4,l} \tag{4.4.13}
$$

and

$$
\mathrm{D}_j \;=\; \hat{c}_{4jkl} u_{k,l} \;+\; \hat{c}_{4j4l} u_{4,l}\,, \tag{4.4.14}
$$

where all implicit summations range over the values 1,2 and 3.

Taylor and Crampin proposed that the equations (4.4.13) and (4.4.14) may now be further simplified if one allows implicit summations to range over the values 1, 2, 3 and 4, unless otherwise stated, so that (4.4.13) and (4.4.14) reduce to

$$
\sigma_{ij} \;=\; \hat{c}_{ijkl}\, u_{k,l}\,, \qquad i,j = 1,2,3, \tag{4.4.15}
$$

and

$$
\mathrm{D}_j \;=\; \hat{c}_{4jkl} u_{k,l}\,, \qquad j = 1,2,3, \tag{4.4.16}
$$

where use is made of the symmetry of $\hat{c}_{ijkl}$.

It should be noted, however, that the definition of the extended second order elastic–electric constant, analagous to equations (4.4.12), used by Taylor and Crampin assumed the full symmetry of the second-order elastic constant to be preserved in the extended constant. Assuming this to be true, equation (4.4.15) contains the term

$$
\begin{aligned}
\mathcal{T} &= \hat{c}_{ijk4} u_{k,4} \\
&= \hat{c}_{ij4k} u_{k,4} \\
&= \hat{c}_{4kij} u_{k,4} \\
&= e^{(2)}_{kij} u_{k,4}\,,
\end{aligned}
$$

which admits differentiation with respect to the undefined variable x_4.

This problem may be easily overcome by restricting the symmetry of the extended constant $\hat{c}_{ijkl}$. It is noted that the full symmetry of the second-order elastic constant has not been used at any stage in the derivation of equations (4.4.15) and (4.4.16), and therefore it is only necessary to prescribe the minimum symmetry necessary for their derivation. Thus we define the extended electro-elastic constant by

$$\left.\begin{aligned} \hat{c}_{ijkl} &\equiv \hat{c}_{(ij)(kl)} = c^{(2)}_{ijkl} \\ \hat{c}_{4jkl} &\equiv \hat{c}_{(4j)(kl)} = e^{(2)}_{jkl} \\ \hat{c}_{4j4l} &\equiv \hat{c}_{(4j)(4l)} = -\epsilon^{(2)}_{jl} \end{aligned}\right\} \quad (i,j,k,l = 1,2,3)$$
$$\hat{c}_{i4kl} \equiv \hat{c}_{(i4)(kl)} = 0 \qquad (i,k,l = 1,2,3,4)\,. \tag{4.4.17}$$

It is now seen that equation $(4.4.17)_4$ eliminates any derivatives with respect to the undefined parameter x_4.

In view of the success of the above approach it seems sensible to look for a similar simplification that could be applied to the quadratically nonlinear constitutive relations. Replacement of dummy subscripts in equations (4.4.5) and (4.4.6) reveals

$$\begin{aligned} \sigma_{ij} \;=\; & c^{(2)}_{ijkl}\, u_{k,l} + e^{(2)}_{lij}\, \phi_{,l} + d_{ijklmn}\, u_{k,l}\, u_{m,n} \\ & + 2\, f_{jklmn}\, \phi_{,l}\, u_{m,n} - \tfrac{1}{2} l_{lnij}\, \phi_{,l} \phi_{,n}\,, \end{aligned}$$

and

$$\begin{aligned} \mathrm{D}_j \;=\; & -\epsilon^{(2)}_{jl}\, \phi_{,l} + e^{(2)}_{jkl} u_{k,l} + \tfrac{1}{2} \epsilon^{(3)}_{jln} \phi_{,l} \phi_{,n} \\ & + f_{jklmn}\, u_{k,l} u_{m,n} - l_{jlmn} \phi_{,l} u_{m,n}\,, \end{aligned}$$

which, upon introduction of the extended displacement vector defined by equation (4.4.9), can be written as

$$\begin{aligned} \sigma_{ij} \;=\; & c^{(2)}_{ijkl}\, u_{k,l} + e^{(2)}_{lij}\, u_{4,l} + d_{ijklmn}\, u_{k,l}\, u_{m,n} \\ & + 2\, f_{jklmn}\, u_{4,l}\, u_{m,n} - \tfrac{1}{2} l_{lnij}\, u_{4,l} u_{4,n}\,, \end{aligned} \tag{4.4.18}$$

and

$$\begin{aligned} \mathrm{D}_j \;=\; & -\epsilon^{(2)}_{jl} u_{4,l} + e^{(2)}_{jkl} u_{k,l} + \tfrac{1}{2} \epsilon^{(3)}_{jln} u_{4,l} u_{4,n} \\ & + f_{jklmn}\, u_{k,l} u_{m,n} - l_{jlmn} u_{4,l} u_{m,n}\,. \end{aligned} \tag{4.4.19}$$

The similarity of terms in equations (4.4.18) and (4.4.19) indicates the replacements

$$\left.\begin{aligned}
&\hat{d}_{ijklmn} \equiv \hat{d}_{(ij)(kl)(mn)} = d_{ijklmn} \\
&\hat{d}_{4jklmn} \equiv \hat{d}_{(4j)(kl)(mn)} = f_{jklmn} \\
&\hat{d}_{ij4l4n} \equiv \hat{d}_{(ij)(4l)(4n)} = -\tfrac{1}{2} l_{lnij} \\
&\hat{d}_{4j4l4n} \equiv \hat{d}_{(4j)(4l)(4n)} = \tfrac{1}{2}\epsilon^{(3)}_{jln}
\end{aligned}\right\} \quad (i,j,k,l,m,n = 1,2,3) \tag{4.4.20}$$

$$\hat{d}_{i4klmn} \equiv \hat{d}_{(i4)(kl)(mn)} = 0 \quad (i,k,l,m,n = 1,2,3,4)\,,$$

yielding the quadratically nonlinear constitutive relations

$$\sigma_{ij} = \hat{c}_{ijkl} u_{k,l} + \hat{d}_{ijklmn} u_{k,l} u_{m,n}\,, \qquad (i,j = 1,2,3) \tag{4.4.21}$$

and

$$\mathrm{D}_j = \hat{c}_{4jkl} u_{k,l} + \hat{d}_{4jklmn} u_{k,l} u_{m,n}\,, \qquad (j = 1,2,3)\,, \tag{4.4.22}$$

where all implicit summations run from 1 to 4.

The above notation may be verified by expanding the quadratic term in equation (4.4.20)

$$\begin{aligned}
\mathcal{Q} &= \hat{d}_{ijklmn} u_{k,l} u_{m,n} \qquad (i,j = 1,2,3) \\
&= d_{ijklmn} u_{k,l} u_{m,n} + \hat{d}_{ij4lmn} \phi_{,l} u_{m,n} + \hat{d}_{ijkl4n} u_{k,l} \phi_{,n} \\
&\quad + \hat{d}_{ij4l4n} \phi_{,l} \phi_{,n} \qquad (i,j,k,l,m,n = 1,2,3) \\
&= d_{ijklmn} u_{k,l} u_{m,n} + f_{lijmn} \phi_{,l} u_{m,n} + f_{nijkl} u_{k,l} \phi_{,n} \\
&\quad - \tfrac{1}{2} l_{lnij} \phi_{,l} \phi_{,n} \qquad (i,j,k,l,m,n = 1,2,3) \\
&= d_{ijklmn} u_{k,l} u_{m,n} + 2 f_{lijmn} \phi_{,l} u_{m,n} \\
&\quad - \tfrac{1}{2} l_{lnij} \phi_{,l} \phi_{,n} \qquad (i,j,k,l,m,n = 1,2,3)\,.
\end{aligned}$$

4.5 FIELD EQUATIONS

In Section 2.2.6, the equations representing the balance of momentum in a deformed solid were derived in a form independent of the nature of the material. Thus equation (2.2.33) is still valid for a piezoelectric material, and we can write

$$\rho\ddot{u}_i = \sigma_{ji,j} \qquad (i,j = 1,2,3)\,. \tag{4.5.1}$$

In Section 4.1 Maxwell's equations gave rise to the relation, (4.1.3),

$$\frac{\partial D_j}{\partial x_j} = 0\,,$$

which leads, through (4.1.20), to

$$J\frac{\partial \mathrm{D}_A}{\partial X_A} = 0\,,$$

or, in the present notation

$$\mathrm{D}_{j,j} = 0 \qquad (j = 1,2,3)\,. \tag{4.5.2}$$

On substitution of the constitutive relations (4.4.20) and (4.4.21) into the field equations (4.5.1) and (4.5.2) we obtain

$$\rho\ddot{u}_i = \hat{c}_{ijkl}u_{k,lj} + 2\hat{d}_{ijklmn}u_{k,l}u_{m,nj} \qquad (i = 1,2,3) \tag{4.5.3}$$

and

$$0 = \hat{c}_{4jkl}u_{k,lj} + 2\hat{d}_{4jklmn}u_{k,l}u_{m,nj}\,. \tag{4.5.4}$$

If the modified Kronecker delta $\hat{\delta}_{ij}$ is defined by

$$\hat{\delta}_{ij} = \delta_{ij} - \delta_{i4}\delta_{j4}\,,$$

which, in matrix form, can be expressed

$$\left[\hat{\delta}_{ij}\right] = \begin{bmatrix} 1 & 0 & 0 & 0 \\ 0 & 1 & 0 & 0 \\ 0 & 0 & 1 & 0 \\ 0 & 0 & 0 & 0 \end{bmatrix}\,,$$

equations (4.5.3) and (4.5.4) may be combined to give

$$\rho\hat{\delta}_{ij}\ddot{u}_j = \hat{c}_{ijkl}u_{k,lj} + 2\hat{d}_{ijklmn}u_{k,l}u_{m,nj}\,, \tag{4.5.5}$$

where all implicit summations now range over the values 1, 2, 3, and 4.

At this stage it is seen that equation (4.5.5) takes an identical form to the field equations (3.2.5) for the purely elastic case and, therefore, it may be assumed that an analagous method of solution to that of Section 3.3.4 may be used for the piezoelectric case.

4.6 BOUNDARY CONDITIONS

Before solving the governing field equations for the deformation of a piezoelectric substrate it is necessary to state appropriate boundary conditions.

As in Chapter 3 we shall be considering a semi-infinite substrate which, in its reference state, occupies the region $-\infty < x_1 < \infty$, $-\infty < x_2 \leq 0$, $-\infty < x_3 < \infty$, referred to the rectangular cartesian coordinate system (x_1, x_2, x_3).

The boundary condition on the stress for a deformed anisotropic elastic substrate were expressed in Section 3.1.4 as

$$\sigma_{2i} = 0 \qquad \text{on } x_2 = 0\,.$$

This condition is still appropriate for a piezoelectric substrate, giving rise to the stress boundary condition

$$\hat{c}_{i2kl}u_{k,l} + \hat{d}_{i2klmn}u_{k,l}u_{m,n} = 0\,, \qquad (i = 1,2,3) \tag{4.6.1}$$

on $x_2 = 0$.

There are many different electrical boundary conditions which may be imposed on a piezoelectric substrate. These mainly depend upon the electrical circuit to which the substrate is connected. Normally one assumes either $\phi = 0$ on $x_2 = 0$ or $\mathbf{D} \cdot \mathbf{n}$ continuous across $x_2 = 0$, where $\mathbf{n}$ is the unit surface normal. The former condition represents the so-called short- circuit condition whilst the latter represents continuity of the electric displacement vector normal to the material surface.

Under the assumption introduced in Section 4.1 that all free-space electric field effects may be neglected, the second of the conditions mentioned above becomes

$$\mathrm{D}_2 = 0 \qquad \text{on } x_2 = 0\,,$$

which can be rewritten

$$\hat{c}_{42kl}u_{k,l} + \hat{d}_{42klmn}u_{k,l}u_{m,n} = 0 \qquad \text{on } x_2 = 0\,. \tag{4.6.2}$$

For the analysis in this thesis we shall adopt the boundary conditions (4.6.2), but, for the purpose of comparison, numerical results shall be presented in Section 4.8 for both choices of boundary conditions mentioned above.

It is seen that the electric boundary condition (4.6.2) may be combined with the stress boundary condition (4.6.1) to yield

$$\hat{c}_{i2kl}u_{k,l} + \hat{d}_{i2klmn}u_{k,l}u_{m,n} = 0 \qquad \text{on } x_2 = 0\,, \tag{4.6.3}$$

where all implicit summations now range over the values 1 to 4.

This compact form of the boundary conditions governing a piezoelectric substrate is identical to the boundary conditions imposed on the anisotropic purely elastic substrate in Section 3.1.4.

Clearly the assumption that free-space electric field effects may be neglected has been significant in reducing the boundary conditions to the compact form of equation (4.6.3). This assumption will be explored further and justified, with the use of numerical results, in Chapter 5.

4.7 SOLUTION

In this section we investigate solutions to the quadratically nonlinear field equations (4.5.5) subject to the boundary conditions (4.6.3). The analyses of Sections 4.4 to 4.6 have reduced the field equations and boundary conditions governing the deformation of a piezoelectric substrate to forms that are directly analagous to those governing an anisotropic elastic solid. Hence it seems obvious that the method of multiple scales will also be used in this chapter as the method of solution. In view of the detailed discussion of the method presented in Chapter 3 only the salient points of the solution will be given here, with references made to Chapter 3 as appropriate.

We introduce the small parameter ϵ and define the slow variables ξ, η and τ by

$$\begin{aligned} \xi &= \epsilon x\,, \\ \eta &= \epsilon y\,, \\ \tau &= \epsilon t\,, \end{aligned}$$

assuming the displacement u_i to depend upon distance, time and the slow variables ξ, η and τ through the perturbation expansion

$$u_j = \epsilon u_j^{(1)}(x,y,t,\xi,\eta,\tau) + \epsilon^2 u_j^{(2)}(x,y,t,\xi,\eta,\tau) + \ldots . \tag{4.7.1}$$

On substituting this series into the field equations and boundary equations (4.5.5) and (4.6.3) and considering the systems which are first- and second-order in ϵ we obtain

$$\rho\hat{\delta}_{ij}\ddot{u}_j^{(1)} - \hat{c}_{ijkl}\,u_{k,lj}^{(1)} = 0 \tag{4.7.2}$$

subject to

$$\hat{c}_{i2kl}\,u_{k,l}^{(1)} = 0 \tag{4.7.3}$$

on $y = \eta = 0$, and

$$\begin{aligned} \rho\hat{\delta}_{ij}\ddot{u}_j^{(2)} - \hat{c}_{ijkl}\,u_{k,lj}^{(2)} &= (\hat{c}_{i1kl} + \hat{c}_{ilk1})\,u_{k,l\xi}^{(1)} + (\hat{c}_{i2kl} + \hat{c}_{ilk2})\,u_{k,l\eta}^{(1)} \\ &\quad - 2\rho\hat{\delta}_{ij}\,\dot{u}_{j,\tau}^{(1)} + 2\hat{d}_{ijklmn}\,u_{k,l}^{(1)}\,u_{m,nj}^{(1)} \end{aligned} \tag{4.7.4}$$

subject to

$$\hat{c}_{i2kl}\,u_{k,l}^{(2)} = -\hat{c}_{i2k1}\,u_{k,\xi}^{(1)} - \hat{c}_{i2k2}\,u_{k,\eta}^{(1)} - \hat{d}_{i2klmn}\,u_{k,l}^{(1)}\,u_{m,n}^{(1)} \tag{4.7.5}$$

on $y = \eta = 0$.

4.7.1 First-order Solution Consider a plane wave propagating in the x-direction, represented by

$$u_j^{(1)} = A(\xi,\eta,\tau)\, a_j\, \mathrm{e}^{\mathrm{i}sy}\, \mathrm{e}^{\mathrm{i}(x-t)} + \text{c.c.}, \tag{4.7.6}$$

where s is the decay parameter. Substituting this form of solution into the field equations (4.7.2) leads to the matrix equations

$$\hat{\mathrm{L}}_{ik}(s)\, a_k = 0, \tag{4.7.7}$$

where

$$\hat{\mathrm{L}}_{ik}(s) = \hat{c}_{i2k2}\, s^2 + (\hat{c}_{i2k1} + \hat{c}_{i1k2})\, s + \hat{c}_{i1k1} - \rho\, \hat{\delta}_{ik}, \tag{4.7.8}$$

The system (4.7.7) has the consistency condition

$$\left|\hat{\mathrm{L}}_{ik}(s)\right| = 0, \tag{4.7.9}$$

yielding an eighth-order polynomial in s with real coefficients, and this equation will have four roots satisfying the appropriate decay condition as $y \to 0$. These roots are denoted by $s^{(n)}$, n =1, 2, 3 and 4, and the corresponding eigenvector solutions to equation (4.7.7) by $a_j^{(n)}$. We take our first-order solution to be a summation over these four admissible surface modes

$$u_j^{(1)} = \sum_{n=1}^{4} A^{(n)}(\xi,\eta,\tau) a_j^{(n)}\, \mathrm{e}^{\mathrm{i}s^{(n)}y}\, \mathrm{e}^{\mathrm{i}(x-t)} + \text{c.c.}. \tag{4.7.10}$$

The first-order boundary conditions (4.7.3) then yield the matrix equation

$$\sum_{n=1}^{4} \hat{\mathrm{M}}_{in}\, A^{(n)} = 0 \qquad \text{on } y = \eta = 0 \tag{4.7.11}$$

where

$$\hat{\mathrm{M}}_{in} = (\hat{c}_{i2k1} + \hat{c}_{i2k2}\, s^{(n)})\, a_k^{(n)}, \tag{4.7.12}$$

and the consistency condition

$$|\mathrm{M}_{in}| = 0 \tag{4.7.13}$$

determines the wavespeed parameter ρ. In general, ρ cannot be found algebraically so it is found numerically using an iterative process of the type described in Chapter 3.

The method of multiple scales requires the first-order solution to include all harmonics generated through the nonlinearities. Thus we must extend the linear solution (4.7.10) to be a summation over every harmonic:

$$u_j^{(1)} = \sum_{K=1}^{\infty} \sum_{n=1}^{4} A_K^{(n)}(\xi, \eta, \tau)\, a_j^{(n)}\, \mathrm{e}^{\mathrm{i}Ks^{(n)}y}\, \mathrm{e}^{\mathrm{i}K(x-t)} + \text{c.c.}, \tag{4.7.14}$$

whilst the particular solution to

$$\sum_{n=1}^{4} \hat{\mathrm{M}}_{in}\, \beta^{(n)} = 0 \tag{4.7.15}$$

reveals the surface displacement in the form

$$u_j^{(1)}(0) = \sum_{K=1}^{\infty} \sum_{n=1}^{4} \gamma_K(\xi, \tau)\, \beta^{(n)}\, a_j^{(n)}\, \mathrm{e}^{\mathrm{i}K(x-t)} + \text{c.c.}, \tag{4.7.16}$$

where γ_K is the slowly varying surface amplitude.

4.7.2 Second-order System

The next stage in the solution procedure is to substitute the first-order representation (4.7.14) into the second-order field and boundary equations (4.7.4) and (4.7.5) to yield

$$\begin{aligned}
\rho\, \hat{\delta}_{ij}\, \ddot{u}_j^{(2)} - \hat{c}_{ijkl}\, u_{k,lj}^{(2)} = {} & \\
& \left(\sum_{K=1}^{\infty} \sum_{n=1}^{4} \left(\hat{F}_{iK1}^{(n)}(y)\, A_{K,\xi}^{(n)} + \hat{F}_{iK2}^{(n)}(y)\, A_{K,\eta}^{(n)} + \hat{F}_{iK3}^{(n)}(y)\, A_{K,\tau}^{(n)} \right) \mathrm{e}^{\mathrm{i}K(x-t)} \right. \\
& + \sum_{K=1}^{\infty} \sum_{L=1}^{K-1} \sum_{n=1}^{4} \sum_{m=1}^{4} \hat{H}_{iKL}^{(m,n)}(y)\, A_{K-L}^{(n)}\, A_L^{(m)}\, \mathrm{e}^{\mathrm{i}K(x-t)} \\
& + \sum_{K=1}^{\infty} \sum_{L=K+1}^{\infty} \sum_{n=1}^{4} \sum_{m=1}^{4} \hat{G}_{iKL}^{(m,n)}(y)\, \bar{A}_{L-K}^{(n)}\, A_L^{(m)}\, \mathrm{e}^{\mathrm{i}K(x-t)} \\
& \left. + \sum_{K=1}^{\infty} \sum_{n=1}^{4} \sum_{m=1}^{4} \hat{Q}_{iK}^{(m,n)}(y)\, A_K^{(m)}\, \bar{A}_K^{(n)} \right) + \text{c.c.}
\end{aligned} \tag{4.7.17}$$

together with

$$\begin{aligned}
\hat{c}_{i2kl}\, u_{k,l}^{(2)} = {} & \left(\sum_{K=1}^{\infty} \sum_{n=1}^{4} \left(\hat{f}_{i1}^{(n)}\, A_{K,\xi}^{(n)} + \hat{f}_{i2}^{(n)}\, A_{K,\eta}^{(n)} \right) \mathrm{e}^{\mathrm{i}K(x-t)} \right. \\
& + \sum_{K=1}^{\infty} \sum_{L=1}^{K-1} \sum_{n=1}^{4} \sum_{m=1}^{4} \hat{h}_{iKL}^{(m,n)}\, A_{K-L}^{(n)}\, A_L^{(m)}\, \mathrm{e}^{\mathrm{i}K(x-t)} \\
& \left. + \sum_{K=1}^{\infty} \sum_{L=K+1}^{\infty} \sum_{n=1}^{4} \sum_{m=1}^{4} \hat{g}_{iKL}^{(m,n)}\, \bar{A}_{L-K}^{(n)}\, A_L^{(m)}\, \mathrm{e}^{\mathrm{i}K(x-t)} \right.
\end{aligned}$$

$$+ \sum_{K=1}^{\infty} \sum_{n=1}^{4} \sum_{m=1}^{4} \hat{q}_{iK}^{(m,n)} A_K^{(m)} \bar{A}_K^{(n)} \Big) + \text{c.c.}. \tag{4.7.18}$$

on $y = \eta = 0$. The coefficients in equations (4.7.17) and (4.7.18) may be derived through the technique described in Chapter 3 to be

$$\hat{F}_{iKw}^{(n)}(y) = \mathrm{i}K((\hat{c}_{iwj2} + \hat{c}_{i2jw})s^{(n)} + (\hat{c}_{iwj2} + \hat{c}_{i2jw}))\, a_j^{(n)}\, \mathrm{e}^{\mathrm{i}Ks^{(n)}y}, \quad w = 1,2, \tag{4.7.19}_1$$

$$\hat{F}_{iK3}^{(n)}(y) = 2\mathrm{i}K\rho a_i^{(n)}\, \mathrm{e}^{\mathrm{i}Ks^{(n)}y}, \tag{4.7.19}_2$$

$$\hat{H}_{iKL}^{(m,n)}(y) = -2\mathrm{i}L^2(K-L)\, \hat{d}_{ijklmn}\, \delta_l^{(n)}\, \delta_n^{(m)}\, \delta_j^{(m)}\, a_k^{(n)}\, a_m^{(m)}\, \mathrm{e}^{\mathrm{i}[Ls^{(m)} + (K-L)s^{(n)}]y}, \tag{4.7.19}_3$$

$$\hat{G}_{iKL}^{(m,n)}(y) = 2\mathrm{i}\hat{d}_{ijklmn} \Big(L^2(L-K)\, \bar{\delta}_l^{(n)}\, \delta_n^{(m)}\, \delta_j^{(m)}\, \bar{a}_k^{(n)}\, a_m^{(m)} - L(L-K)^2\, \delta_l^{(m)}\, \bar{\delta}_n^{(n)}\, \bar{\delta}_j^{(n)}\, a_k^{(m)}\, \bar{a}_m^{(n)}\Big)\, \mathrm{e}^{\mathrm{i}[Ls^{(m)} - (L-K)\bar{s}^{(n)}]y}, \tag{4.7.19}_4$$

$$\hat{Q}_{iKL}^{(m,n)}(y) = 2\mathrm{i}\hat{d}_{ijklmn}K^3 \Big(\bar{\delta}_l^{(n)}\, \delta_n^{(m)}\, \delta_j^{(m)}\, \bar{a}_k^{(n)}\, a_m^{(m)}\Big) \times \mathrm{e}^{\mathrm{i}K[s^{(m)} - \bar{s}^{(n)}]y}, \tag{4.7.19}_5$$

$$\hat{f}_{jw}^{(n)} = -\hat{c}_{j2kw}\, a_k^{(n)}, \quad w = 1,2, \tag{4.7.19}_6$$

$$\hat{g}_{iKL}^{(m,n)} = -2L(L-K)\, \hat{d}_{i2klmn}\, \bar{\delta}_l^{(n)}\, \delta_n^{(m)}\, \bar{a}_k^{(n)}\, a_m^{(m)}, \tag{4.7.19}_7$$

$$\hat{h}_{iKL}^{(m,n)} = -L(L-K)\, \hat{d}_{i2klmn}\, \delta_l^{(n)}\, \delta_n^{(m)}\, a_k^{(n)}\, a_m^{(m)}, \tag{4.7.19}_8$$

and

$$\hat{q}_{iKL}^{(m,n)}(y) = -K^2\, \hat{d}_{i2klmn}\, \bar{\delta}_l^{(n)}\, \delta_n^{(m)}\, \bar{a}_k^{(n)}\, a_m^{(m)}, \tag{4.7.19}_9$$

noting that all implicit summations run from 1 to 4 and $\delta_i^{(n)}$ is defined through

$$\delta_1^{(n)} = 1, \quad \delta_2^{(n)} = s^{(n)}, \quad \delta_3^{(n)} = 0, \quad \delta_4^{(n)} = 0. \tag{4.7.20}$$

From inspection of the nonlinear field equation (4.7.17) we write the particular second-order solution as

$$u_j^{(2)} = \sum_{K=1}^{\infty}\sum_{n=1}^{4} \hat{b}_{jK}^{(n)}\, \mathrm{e}^{\mathrm{i}Ks^{(n)}y}\mathrm{e}^{\mathrm{i}K(x-t)} + \sum_{K=1}^{\infty}\sum_{m=1}^{4}\sum_{n=1}^{4} \hat{r}_{jK}^{(m,n)}\, \mathrm{e}^{\mathrm{i}KT_{0K}^{(m,n)}y}$$
$$+ \sum_{K=1}^{\infty}\sum_{L=1}^{K-1}\sum_{m=1}^{4}\sum_{n=1}^{4} \hat{R}_{jKL}^{(m,n)}\, \mathrm{e}^{\mathrm{i}KP_{KL}^{(m,n)}y}\mathrm{e}^{\mathrm{i}K(x-t)}$$
$$+ \sum_{K=1}^{\infty}\sum_{L=K+1}^{\infty}\sum_{m=1}^{4}\sum_{n=1}^{4} \hat{S}_{jKL}^{(m,n)}\, \mathrm{e}^{\mathrm{i}KT_{KL}^{(m,n)}y}\mathrm{e}^{\mathrm{i}K(x-t)}, \tag{4.7.21}$$

where

$$P_{KL}^{(m,n)} = \frac{(Ls^{(m)} + (K-L)s^{(n)})}{K} \tag{4.7.22}$$

$$T_{KL}^{(m,n)} = \frac{(Ls^{(m)} - (L-K)\bar{s}^{(n)})}{K}. \tag{4.7.23}$$

Upon substituting the representation (4.7.21) into the second-order field equation (4.7.17) it follows from comparison of coefficients that

$$\hat{R}_{jKL}^{(m,n)} = \frac{1}{K^2}\hat{\mathrm{L}}_{ij}^{-1}(P_{KL}^{(m,n)})\,\hat{H}_{iKL}^{(m,n)}(0)\,A_{K-L}^{(n)}\,A_L^{(m)} \tag{4.7.23}$$

$$\hat{S}_{jKL}^{(m,n)} = \frac{1}{K^2}\hat{\mathrm{L}}_{ij}^{-1}(T_{KL}^{(m,n)})\,\hat{G}_{iKL}^{(m,n)}(0)\,\bar{A}_{L-K}^{(n)}\,A_L^{(m)} \tag{4.7.25}$$

$$\hat{b}_{jK}^{(n)} = \hat{\chi}_K^{(n)}\,a_j^{(n)} + \frac{1}{K^2}\hat{\mathrm{U}}_{ji}^{(n)}\,\hat{W}_{iK}^{(n)} \tag{4.7.26}$$

$$\hat{W}_{iK}^{(n)} = \hat{F}_{iK1}^{(n)}(0)\,A_{K,\xi}^{(n)} + \hat{F}_{iK2}^{(n)}(0)\,A_{K,\eta}^{(n)} + \hat{F}_{iK3}^{(0)}(y)\,A_{K,\tau}^{(n)}$$
$$+ \sum_{L=1}^{K-1}\hat{H}_{iKL}^{(n,n)}(0)\,A_{K-L}^{(n)}\,A_L^{(n)}, \tag{4.7.27}$$

where

$$\hat{\mathrm{U}}_{ij}^{(n)} = \sum_{P=1}^{3}\frac{a_{iP}^{(n)}\,a_{jP}^{(n)}}{\lambda_P^{(n)}\,a_{kP}^{(n)}\,a_{kP}^{(n)}}. \tag{4.7.28}$$

and $a_{kP}^{(n)}$ and $\lambda_p^{(n)}$ are the eigenvectors and non-zero eigenvalues respectively of the matrix $\hat{\mathrm{L}}_{ij}(s^{(n)})$. $\hat{\mathrm{L}}_{ij}^{-1}(s)$ is again taken to be the inverse of $\hat{\mathrm{L}}_{ij}(s)$ wherever $\hat{\mathrm{L}}_{ij}(s)$ is non-singular and zero where singular.

The elimination of secular terms leads to the system of coupled partial differential equations

$$\hat{\Gamma}_K^{(n)}\, A_{K,\xi}^{(n)} + \hat{\Delta}_K^{(n)}\, A_{K,\eta}^{(n)} + \hat{\Theta}_K^{(n)}\, A_{K,\tau}^{(n)} + \sum_{L=1}^{K-1} \hat{\Lambda}_{KL}^{(n)}\, A_{K-L}^{(n)}\, A_L^{(n)} = 0\,, \qquad (4.7.29)$$

where

$$\begin{aligned} \hat{\Gamma}_K^{(n)} &= a_j^{(n)}\, \hat{F}_{jK1}^{(n)}(0) \\ \hat{\Delta}_K^{(n)} &= a_j^{(n)}\, \hat{F}_{jK2}^{(n)}(0) \\ \hat{\Theta}_K^{(n)} &= a_j^{(n)}\, \hat{F}_{jK3}^{(n)}(0) \\ \hat{\Lambda}_{KL}^{(n)} &= a_j^{(n)}\, \hat{H}_{jKL}^{(n,n)}(0)\,. \end{aligned} \qquad (4.7.30)$$

Finally, use of the boundary conditions leads to the coupled system of partial differential equations

$$\hat{N}_K\, \gamma_{K,\xi} + \hat{P}_K\, \gamma_{K,\tau} - \sum_{L=1}^{K-1} \hat{\Pi}_{KL}\, \gamma_{K-L}\, \gamma_L - \sum_{L=K+1}^{\infty} \hat{\Delta}_{KL}\, \bar{\gamma}_{L-K}\, \gamma_L = 0\,, \qquad (4.7.31)$$

where

$$\begin{aligned} \hat{N}_K = \sum_{n=1}^{4} \Bigg\{ & \left(\frac{\lambda_i}{(\mathrm{i}K)} \left(\hat{c}_{i2j_2} s^{(n)} + \hat{c}_{i2j_1} \right) \hat{\mathrm{U}}_{jl}^{(n)}\, \hat{F}_{lK1}^{(n)}(0) + \lambda_i\, \hat{f}_{i1}^{(n)} \right) \\ & - \frac{\hat{\Gamma}_K^{(n)}}{\hat{\Delta}_K^{(n)}} \left(\frac{\lambda_i}{(\mathrm{i}K)} \left(\hat{c}_{i2j_2} s^{(n)} + \hat{c}_{i2j_1} \right) \hat{\mathrm{U}}_{jl}^{(n)}\, \hat{F}_{lK2}^{(n)}(0) + \lambda_i\, \hat{f}_{i2}^{(n)} \right) \Bigg\}\, \beta^{(n)} \end{aligned} \qquad (4.7.32)$$

$$\hat{P}_K = -\sum_{n=1}^{4} \lambda_i\, \frac{\hat{\Theta}_K^{(n)}}{\hat{\Delta}_K^{(n)}} \left\{ \frac{1}{(\mathrm{i}K)} \left(\hat{c}_{i2j_2} s^{(n)} + \hat{c}_{i2j_1} \right) \hat{\mathrm{U}}_{jl}^{(n)}\, \hat{F}_{lK2}^{(n)}(0) + \hat{f}_{i2}^{(n)} \right\} \beta^{(n)} \qquad (4.7.33)$$

$$\begin{aligned} \hat{\Pi}_{KL} = & -\sum_{n=1}^{4} \sum_{m=1}^{4} \left[\frac{\lambda_i}{(\mathrm{i}K)} \left(\hat{c}_{i2j_2} P_{KL}^{(m,n)} + \hat{c}_{i2j_1} \right) \hat{\mathrm{L}}_{jl}^{-1}(P_{KL}^{(m,n)})\, \hat{H}_{lKL}^{(m,n)}(0) \right. \\ & \left. + \lambda_i\, \hat{h}_{iKL}^{(m,n)} \right] \beta^{(m)}\, \beta^{(n)} \\ & + \sum_{n=1}^{4} \left\{ \left[\frac{\lambda_i}{(\mathrm{i}K)} \left(\hat{c}_{i2j_2} s^{(n)} + \hat{c}_{i2j_1} \right) \hat{\mathrm{U}}_{jl}^{(n)}\, \hat{F}_{lK2}^{(n)}(0) + \lambda_i\, \hat{f}_{i2}^{(n)} \right] \frac{\hat{\Lambda}_{KL}^{(n)}}{\hat{\Delta}_K^{(n)}} \right. \\ & \left. - \frac{\lambda_i}{(\mathrm{i}K)} \left(\hat{c}_{i2j_2} s^{(n)} + \hat{c}_{i2j_1} \right) \hat{\mathrm{U}}_{jl}^{(n)}\, \hat{H}_{lKL}^{(m,n)}(0) \right\} \beta^{(n)}\, \beta^{(n)} \end{aligned} \qquad (4.7.34)$$

and

$$\hat{\Delta}_{KL} = -\sum_{n=1}^{4}\sum_{m=1}^{4}\left[\frac{\lambda_i}{(iK)}\left(\hat{c}_{i2j2}T_{KL}^{(m,n)} + \hat{c}_{i2j1}\right)\hat{L}_{jl}^{-1}(T_{KL}^{(m,n)})\,\hat{G}_{lKL}^{(m,n)}(0) + \lambda_i\,\hat{g}_{iKL}^{(m,n)}\right]\beta^{(m)}\,\bar{\beta}^{(n)}\,. \tag{4.7.35}$$

Finally, since $\hat{N}_K = \hat{P}_K$, the coupled amplitude equations simplify to

$$\gamma_{K,\xi} + \gamma_{K,\tau} = \sum_{L=1}^{K-1}\hat{\Pi}'_{KL}\,\gamma_{K-L}\,\gamma_L + \sum_{L=K+1}^{\infty}\hat{\Delta}'_{KL}\,\bar{\gamma}_{L-K}\,\gamma_L \tag{4.7.36}$$

where

$$\begin{aligned}\hat{\Pi}'_{KL} &= \frac{\hat{\Pi}_{KL}}{\hat{N}_K}\\ \hat{\Delta}'_{KL} &= \frac{\hat{\Delta}_{KL}}{\hat{N}_K}.\end{aligned} \tag{4.7.37}$$

4.8 RESULTS AND CONCLUSIONS

The results presented in this section were computed for lithium niobate using the "standard" linear elastic and electro–elastic data of Warner et al [1967]. This data is generally accepted as accurate and is quoted even in the most recent evaluations of the nonlinear constants, see Cho and Yamanouchi [1987]. Unfortunately the same cannot be said to be true for any of the third-order constants, where errors as high as 200% are quoted and particular independent values are given with orders of magnitude differing by as much as 10^2. The two main references for data used in this thesis are Ganguly and Davis [1981] and Cho and Yamanouchi [1987]. The data quoted by Ganguly and Davis is, in part, derived through use of Miller's rule, Miller [1964], as described in Section 4.2, and therefore suffers from some inconsistency in the stated values of the third-order dielectric constant. In this thesis, therefore, the data given by Ganguly and Davis is used for comparative purposes only. The data given by Cho and Yamanouchi, on the other hand, is obtained by direct measurement of strain under various electrical conditions and appears to yield accurate results when used to calculate the efficiency of an acoustic convolver (see Chapter 6). It is Cho and Yamanouchi's data that will be used to calculate most of the results in this thesis.

Unfortunately third-order crystallographic data is only available for the material lithium niobate. Extensive searches, including reference to Landolt–Börnstein [1979] and an international database search (INSPEC), yielded no complete set of electro–elastic constants for any other piezoelectric material of any symmetry class. We are therefore unable to present any results for other materials and all conclusions must be drawn from the single case of lithium niobate.

As in Chapter 3, we must first solve the linear (Rayleigh) wave speed problem. A similar Golden Section search routine may be used in conjunction with a polynomial solving procedure to obtain the value of the parameter ρ. Results for the surface wavespeed obtained after using this procedure are given in Figure 4.8.1 and our search routines may then clearly be validated by comparision with the identical results of Campbell and Jones [1974].

In order to facilitate some discussion it is useful at this stage to repeat the small ξ analysis of Section 3.5, deducing the series solution for $\tilde{\gamma}_K = \gamma_K/a$, where a is the initial amplitude of the fundamental, to be

$$\tilde{\gamma}_K = w_K^{(0)} + w_K^{(1)}\xi_1 + w_K^{(2)}\xi_1^{(2)} + w_K^{(3)}\xi_1^3 + \dots , \tag{4.8.1}$$

where

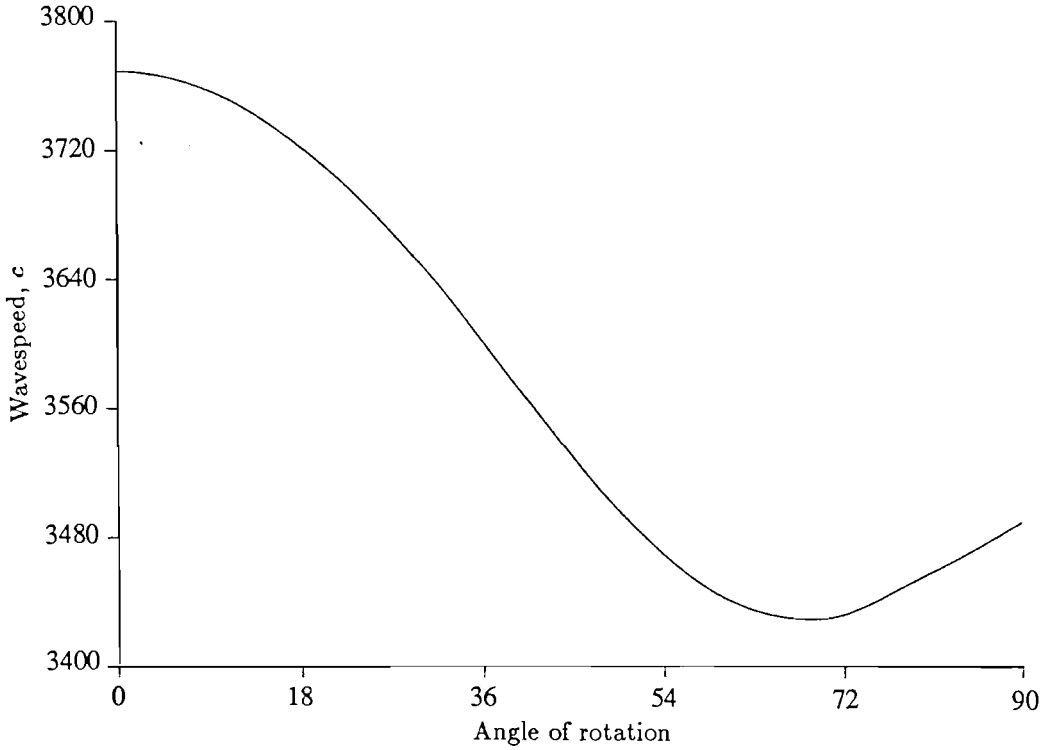

Figure 4.8.1 Surface wavespeed for angles of propagation away from the X-axis on the surface of Y-cut $LiNbO_3$

$$
\begin{aligned}
w_1^{(0)} &= 1 \\
w_1^{(1)} &= 0 \\
w_1^{(2)} &= \hat{\Pi}'_{12}\hat{\Delta}'_{21}/2 \\
w_2^{(0)} &= 0 \\
w_2^{(1)} &= \hat{\Pi}'_{12} \\
w_2^{(2)} &= 0 \\
w_2^{(3)} &= \hat{\Pi}'^{\,2}_{12}\hat{\Delta}'_{21}/3 + \hat{\Pi}'_{12}(\hat{\Pi}'_{13} + \hat{\Pi}'_{23})\hat{\Delta}'_{32}/6 \\
w_3^{(0)} &= 0 \\
w_3^{(1)} &= 0 \\
w_3^{(2)} &= \hat{\Pi}'_{12}(\hat{\Pi}'_{13} + \hat{\Pi}'_{23})/2\,.
\end{aligned}
\tag{4.8.2}
$$

Evaluation of the appropriate eigenvectors for the linear solution together with the third-order constants now enables us to calculate the various coefficients of the coupled amplitude equations and thus compute the finite difference solution to these equations, see equation (3.5.4). Use of this method leads to the results of Figures 4.8.2 to 4.8.12.

The effects of including increasing numbers of harmonics in the finite difference analysis is presented in Figures 4.8.2 to 4.8.5 and these results may be directly compared with Figures 3.5.1 to 3.5.4. It can be seen that both the growth and decay of the surface wave are much slower for piezoelectric materials. This could have been foreseen by the coefficients of the series expansion for γ_K. The coefficients $w_1^{(2)}$ and $w_2^{(1)}$ take the values 0.157 and -0.335 for an unrotated cut of the cubic elastic material magnesium oxide whilst they take the values 0.0079 and 0.089 i for an unrotated cut of the piezoelectric material lithium niobate using the data of Cho and Yamanouchi [1987].

Plots of the amplitudes for rotations away from the principal axis are shown in Figures 4.8.6 to 4.8.8 and these display an increase in the growth and decay factors unlike those of the corresponding purely elastic case. Results are here plotted for $0 \leq \xi \leq 5$ and 10 harmonics are used. This extended range is used to clearly display the growth and decay of the various harmonics. Figures 4.8.9 and 4.8.10 present the amplitude plots for X- and Z-cut lithium niobate. It is noted that the results for these two cuts differ from those for the unrotated or Y-cut crystal, unlike the analogous results for the cubic elastic material. This is easily justified by consideration of the position of the axes of symmetry. In the elastic case these axes are positioned as the diagonal axes of a cube, thus on each of the cuts X, Y and Z, the surface is a plane of mirror symmetry. In the case of the trigonal crystal lithium niobate, however, only the X-cut gives the crystal surface as a plane of mirror symmetry. Figures 4.8.11 and 4.8.12 present the variation of amplitude for rotated X-cuts of lithium niobate.

No surface of a trigonal material possesses a plane of mirror symmetry together with axes of symmetry lying in that surface. Hence, it is not possible to directly compare results for propagation away from the axis of symmetry between the cubically anisotropic elastic material magnesium oxide considered in Chapter 3 and the trigonal piezoelectric material lithium niobate.

The "closed system" nature of the system involving only three harmonics exhibited for the purely elastic material can be clearly seen in Figure 4.8.13, in which the propagation range is taken as $0 \leq \xi \leq 15$. The transfer of energy between harmonics evident in the purely elastic case can be seen through these graphs.

The data from Ganguly and Davis [1981] is used for the plots of Figures 4.8.14 and 4.8.15 and comparison of the calculated values for the coefficient $w_1^{(2)}$, 0.0079 using the Cho and Yamanouchi data and 0.0013 the Ganguly and Davis data respectively, reveals the importance of the third-order constants in determining the harmonic growth.

The variation of the parameters $w_1^{(2)}$, $w_2^{(1)}$ and $w_3^{(2)}$ with angle of propagation away from the X-axis on Y-cut lithium niobate is presented in Figure 4.8.16, whilst Figures 4.8.17 and 4.8.18 present the variation of $w_1^{(2)}$ and $w_2^{(1)}$ respectively for an X-cut of the same material (it should be noted that the dips of these graphs below the ξ-axis are caused by curve estimation errors in the graphical routine used). These show that lithium niobate gives slower amplitude growth and decay for propagation near an axis of symmetry. This apparently contradicts with the results obtained for the purely elastic case considered in Chapter 4 and further supports the case for our proposition that a quantitative measure of the level of anisotropy of any particular crystal cut and orientation is needed.

In Section 4.6 we discused short-circuited boundary conditions, where the potential satisfies the relation

$$\phi = 0 \qquad \text{on } y = \eta = 0\,.$$

Investigation of the propagation of surface waves satisfying this boundary condition changes very little of the analysis of Section 4.7. Replacement of equations (4.7.3) and (4.7.5) by

$$u_4^{(1)} = 0$$

and

$$u_4^{(2)} = 0,$$

respectively, on $y = \eta = 0$, together with the obvious subsequent alterations to the definition of the matrix $\hat{\mathrm{M}}_{in}$ and equation (4.7.18), yields the amplitude variation illustrated in Figures 4.8.19 to 4.8.21. These reveal numerically different results to those for a wave propagating under the free surface boundary conditions, however the underlying pattern of growth and decay relating to the position of the axes of symmetry is still present.

It is clear from the above discussion that the numerical values for the various elastic and electric constants play the leading rôle in the determination of the growth and decay pattern of propagating surface waves. The high errors quoted by Cho and Yamanouchi [1986] lead one to view any conclusions drawn from results obtained using this data with extreme scepticism. Variation of particular constants by 10% has lead to the variations in the growth and decay parameters presented in Table 4.8.1

These variations are in contradiction to the results of Maugin [1985], in which it is stated that the piezoelectric constants e_{ijk} yield the greatest variation in the value of the efficiency of particular acoustic device. The most critical constant in

Constant	Average variation (%) in growth and decay pars., w
$c^{(3)}_{222}$	54.4
$c^{(3)}_{333}$	0
$c^{(3)}_{155}$	1.0
$c^{(3)}_{133}$	0
$c^{(3)}_{123}$	0
$c^{(3)}_{113}$	0
$c^{(3)}_{112}$	12.5
$c^{(3)}_{111}$	10.6
$e^{(3)}_{115}$	0.3
$e^{(3)}_{126}$	7.2
$e^{(3)}_{145}$	0.3
$e^{(3)}_{116}$	0.7
$e^{(3)}_{125}$	3.0

Table 4.8.1 Variation of the small ξ solution coefficients with variation in individual electro-elastic constants

our calculations appears to be the third-order elastic constant $c^{(3)}_{222}$, which varies in value from -4.78 N/m^2 in Nakagawa et al [1973] to -23.3 N/m^2. Results such as these lead to the obvious possibility that surface wave propagation may be used to predict the numerical values of the elastic and electric constants.

Key to Figures

■ Fundamental amplitude, $\tilde{\gamma}_1$.

□ Second harmonic amplitude, $\tilde{\gamma}_2$.

▲ Third harmonic amplitude, $\tilde{\gamma}_3$.

△ Fourth harmonic amplitude, $\tilde{\gamma}_4$ (where shown).

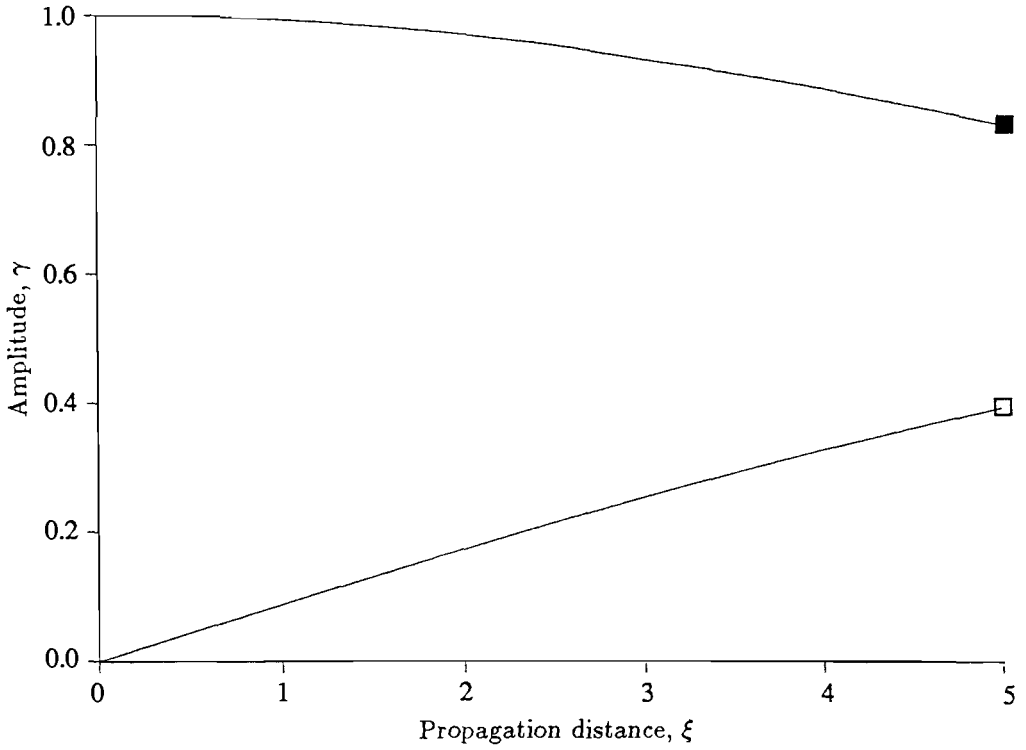

Figure 4.8.2 Growth and decay of the amplitudes $\tilde{\gamma}_K$ with propagation distance ξ_1 for X-propagation on Y-cut $LiNbO_3$, (2 harmonics)

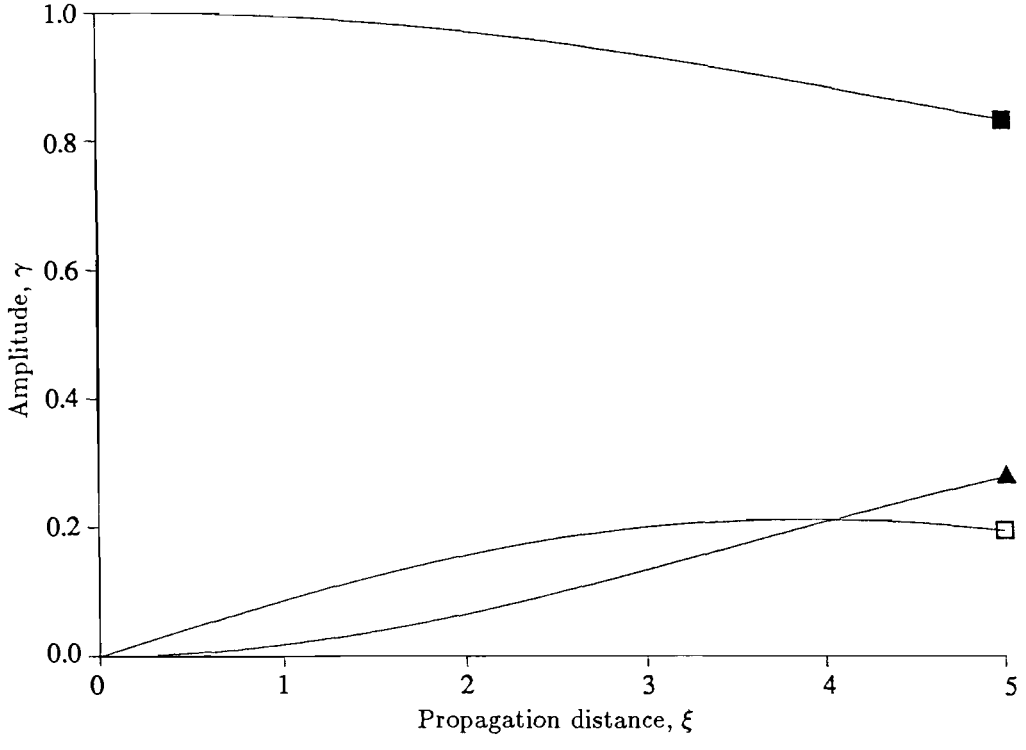

Figure 4.8.3 Growth and decay of the amplitudes $\tilde{\gamma}_K$ with propagation distance ξ_1 for X-propagation on Y-cut $LiNbO_3$, (3 harmonics)

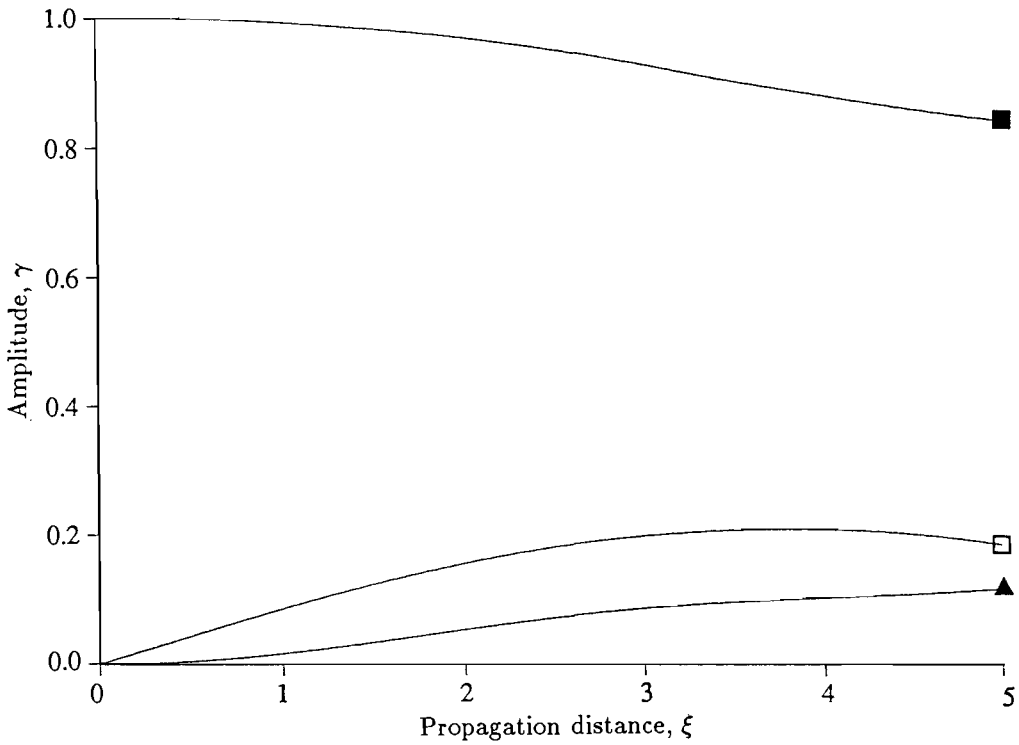

Figure 4.8.4 Growth and decay of the amplitudes $\tilde{\gamma}_K$ with propagation distance ξ_1 for X-propagation on Y-cut $LiNbO_3$, (10 harmonics)

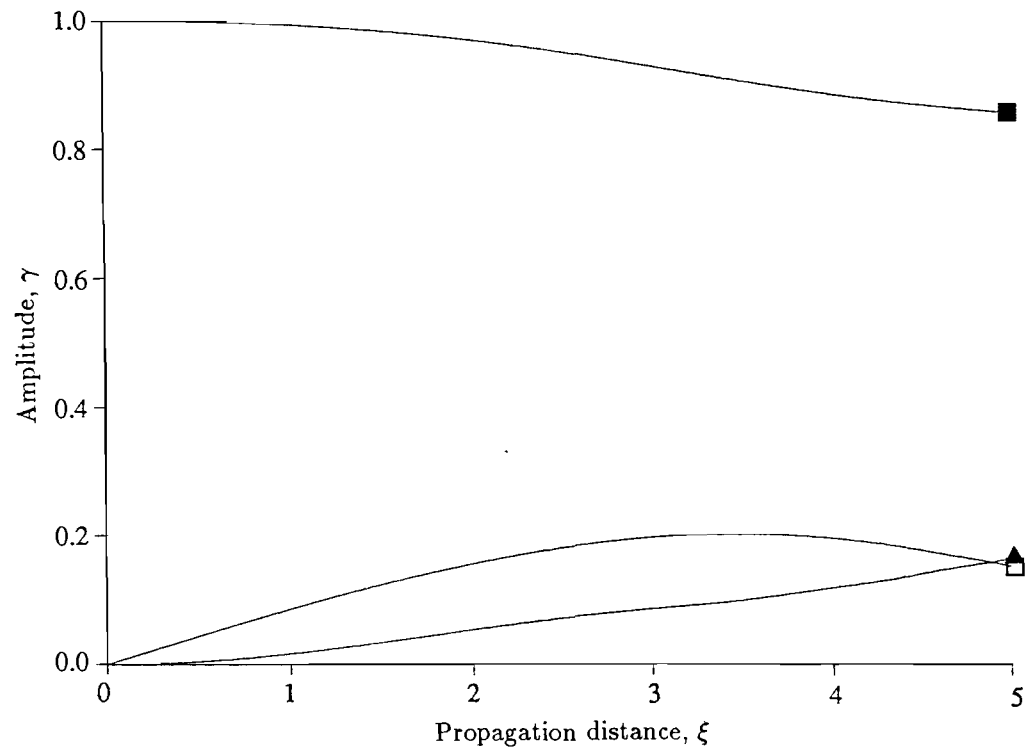

Figure 4.8.5 Growth and decay of the amplitudes $\tilde{\gamma}_K$ with propagation distance ξ_1 for X-propagation on Y-cut $LiNbO_3$, (32 harmonics)

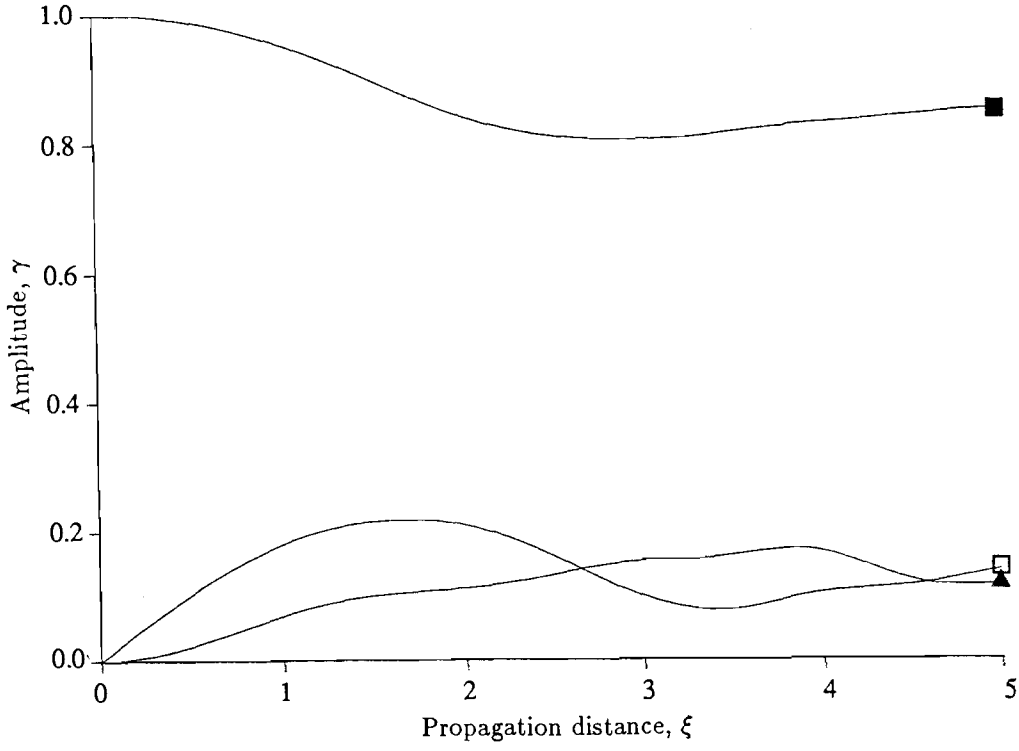

Figure 4.8.6 Growth and decay of the amplitudes $\tilde{\gamma}_K$ with propagation distance ξ_1 for propagation 20° from the X-axis on Y-cut $LiNbO_3$, (10 harmonics)

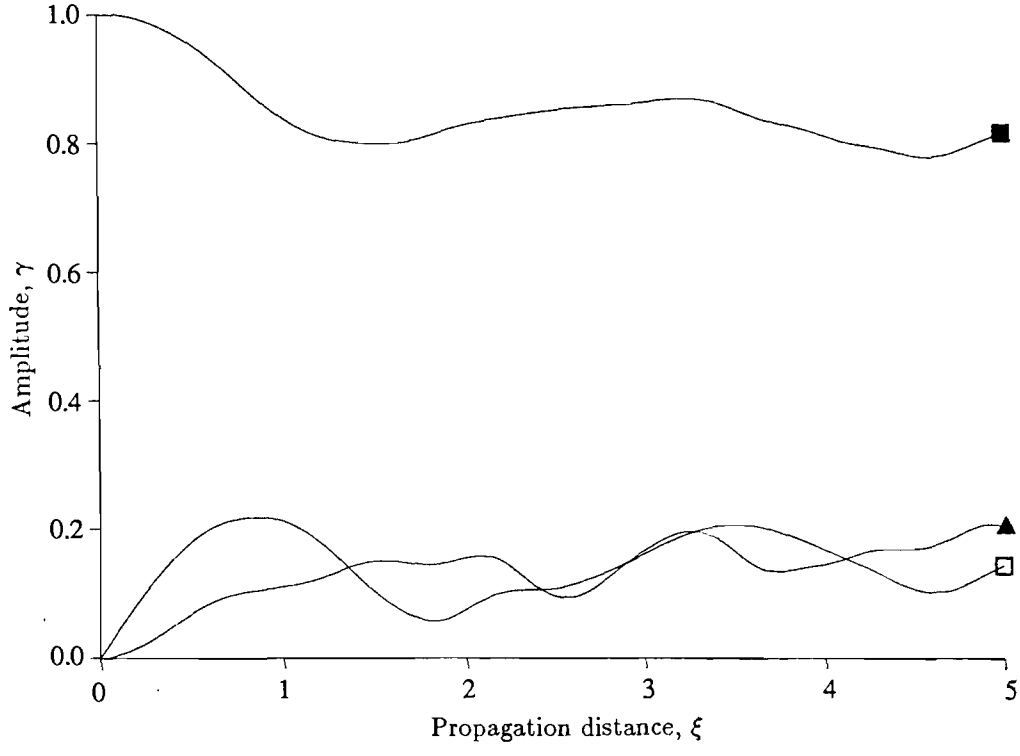

Figure 4.8.7 Growth and decay of the amplitudes $\tilde{\gamma}_K$ with propagation distance ξ_1 for propagation 45° from the X-axis on Y-cut $LiNbO_3$, (10 harmonics)

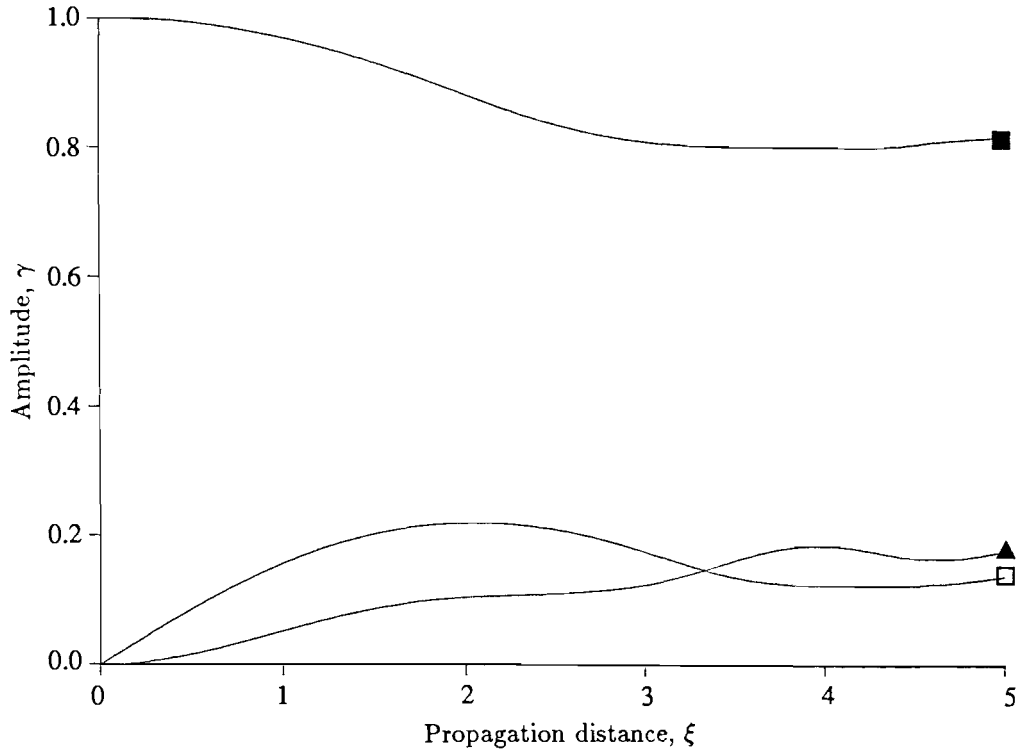

Figure 4.8.8 Growth and decay of the amplitudes $\tilde{\gamma}_K$ with propagation distance ξ_1 for propagation 70° from X-axis on Y-cut $LiNbO_3$, (10 harmonics)

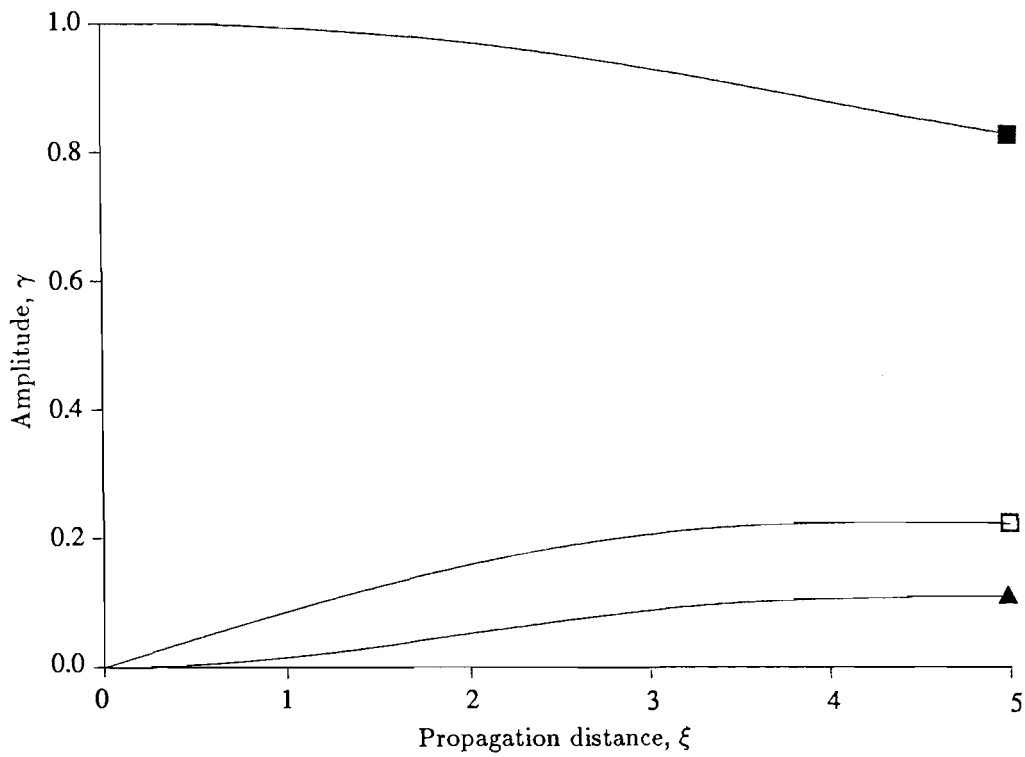

Figure 4.8.9 Growth and decay of the amplitudes $\tilde{\gamma}_K$ with propagation distance ξ_1 for Z-propagation on X-cut $LiNbO_3$, (10 harmonics)

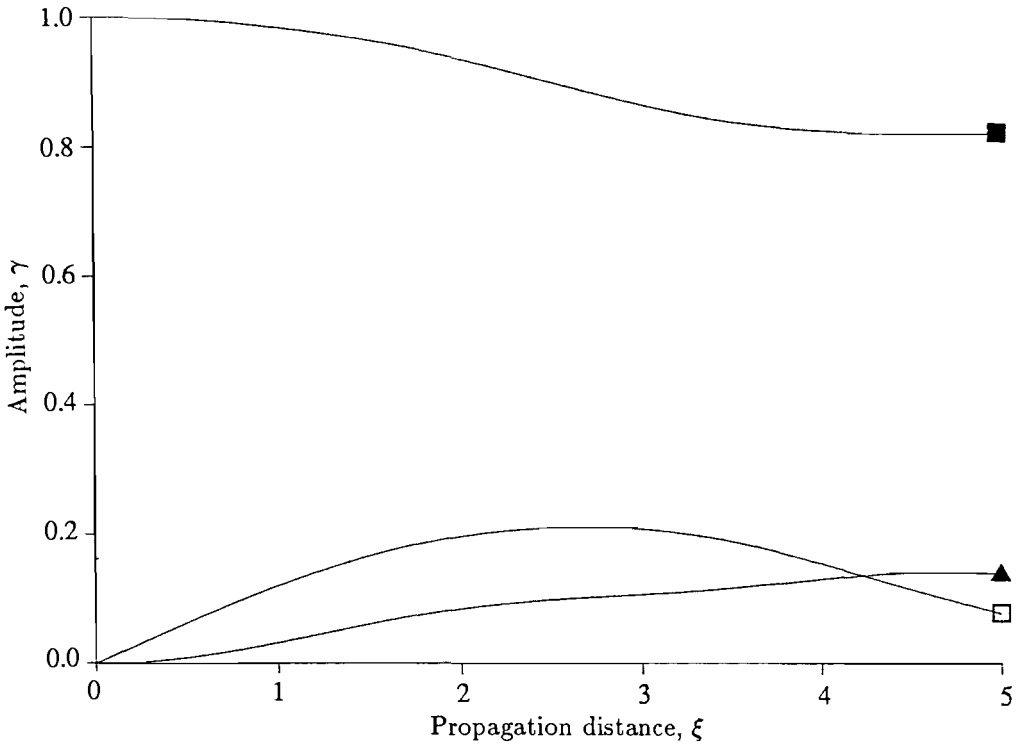

Figure 4.8.10 Growth and decay of the amplitudes $\tilde{\gamma}_K$ with propagation distance ξ_1 for X-propagation on Z-cut $LiNbO_3$, (10 harmonics)

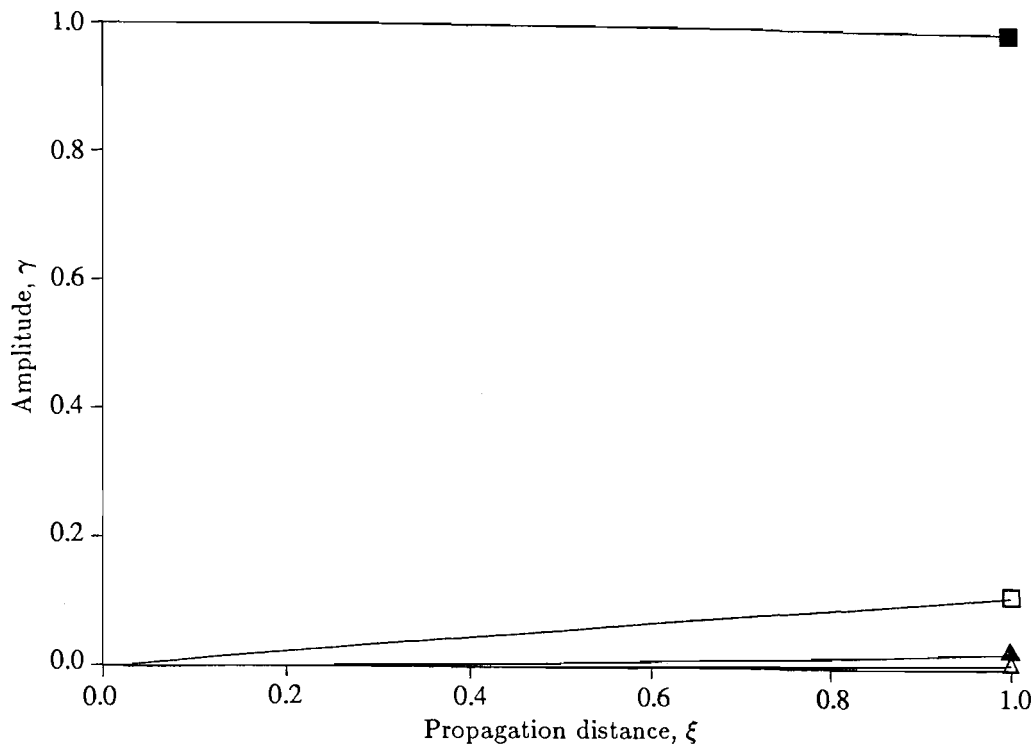

Figure 4.8.11 Growth and decay of the amplitudes $\tilde{\gamma}_K$ with propagation distance ξ_1 for propagation 20° from the Z-axis on X-cut $LiNbO_3$, (10 harmonics)

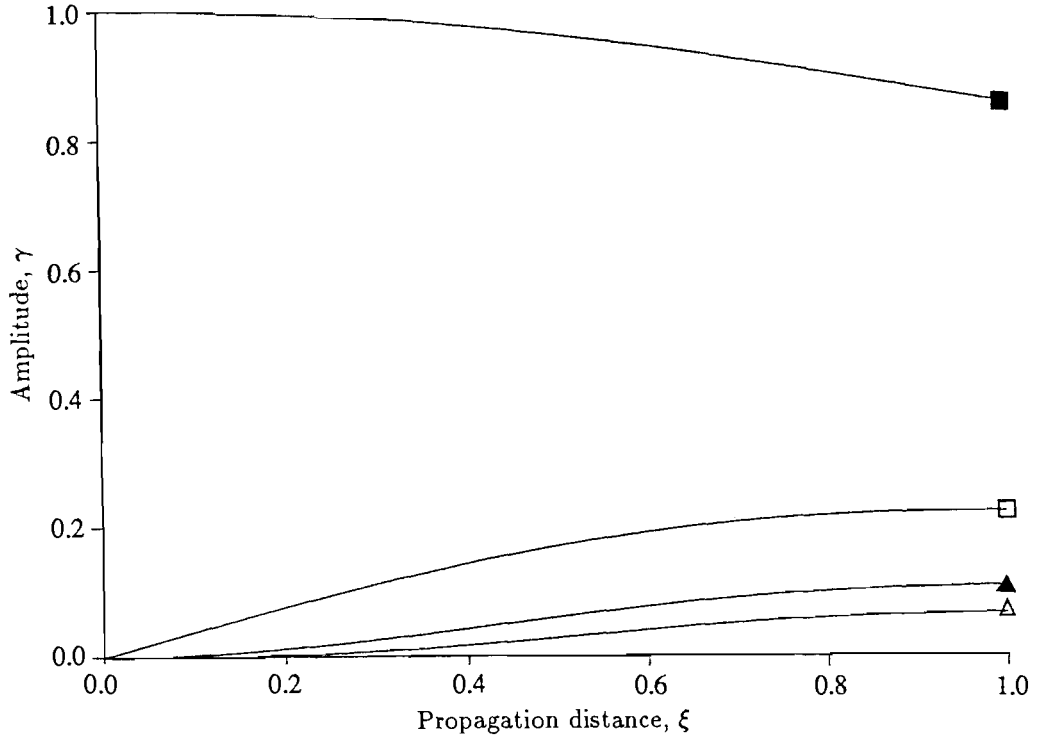

Figure 4.8.12 Growth and decay of the amplitudes $\tilde{\gamma}_K$ with propagation distance ξ_1 for propagation 45° from the Z-axis on X-cut $LiNbO_3$, (10 harmonics)

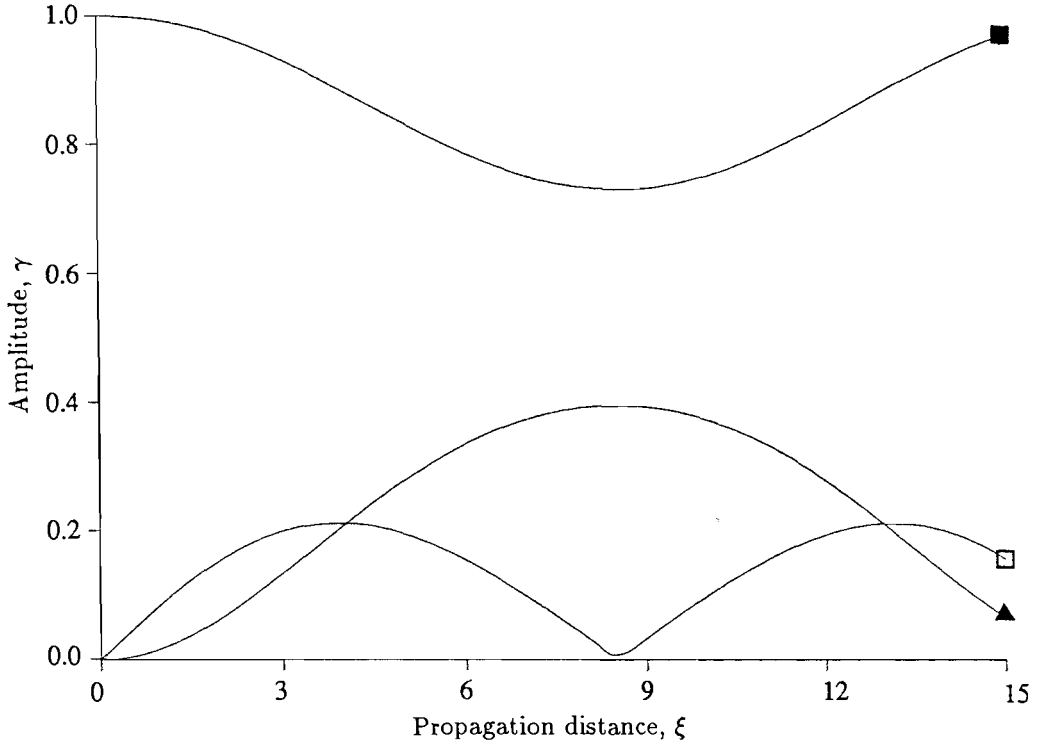

Figure 4.8.13 Growth and decay of the amplitudes $\tilde{\gamma}_K$ with propagation distance ξ_1 for X-propagation on Y-cut $LiNbO_3$, (3 harmonics)

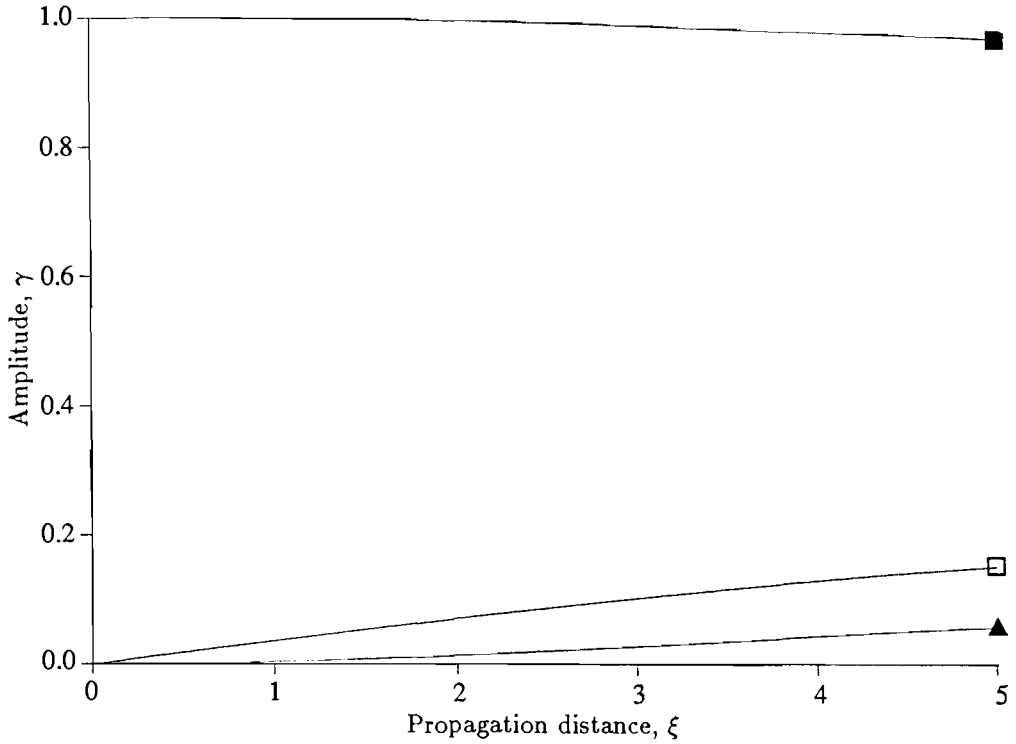

Figure 4.8.14 Growth and decay of the amplitudes $\tilde{\gamma}_K$ with propagation distance ξ_1 for X-propagation on Y-cut $LiNbO_3$, using the data of Ganguly and Davis [1981] (10 harmonics)

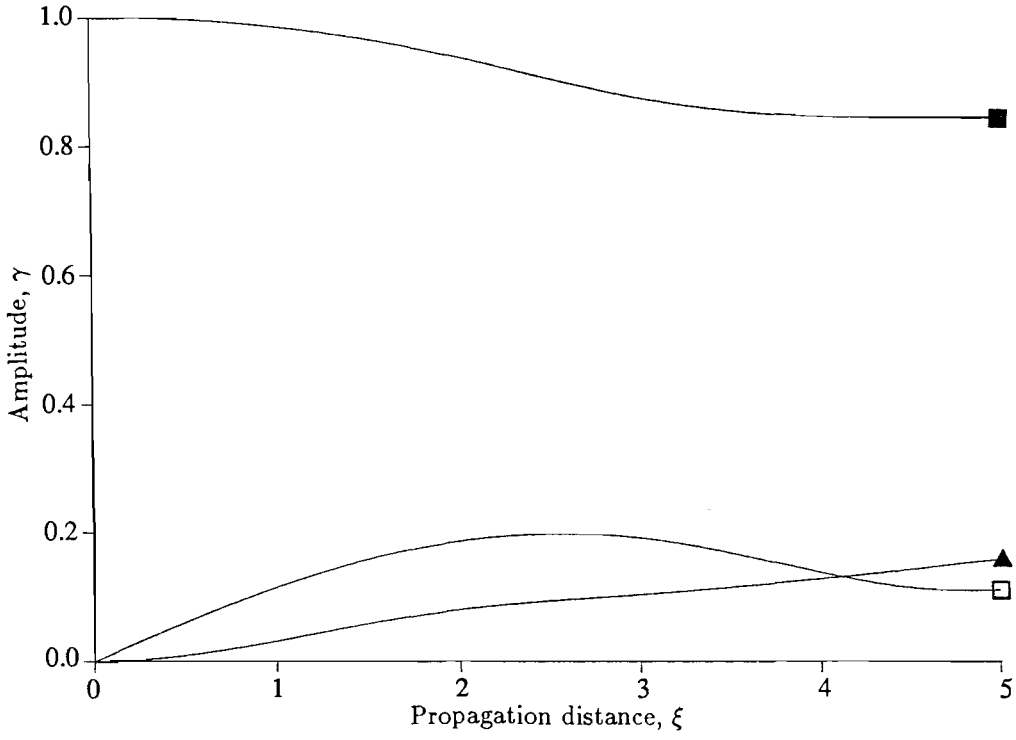

Figure 4.8.15 Growth and decay of the amplitudes $\tilde{\gamma}_K$ with propagation distance ξ_1 for propagation 45° from the X-axis on Y-cut $LiNbO_3$, using the data of Ganguly and Davis [1981] (10 harmonics)

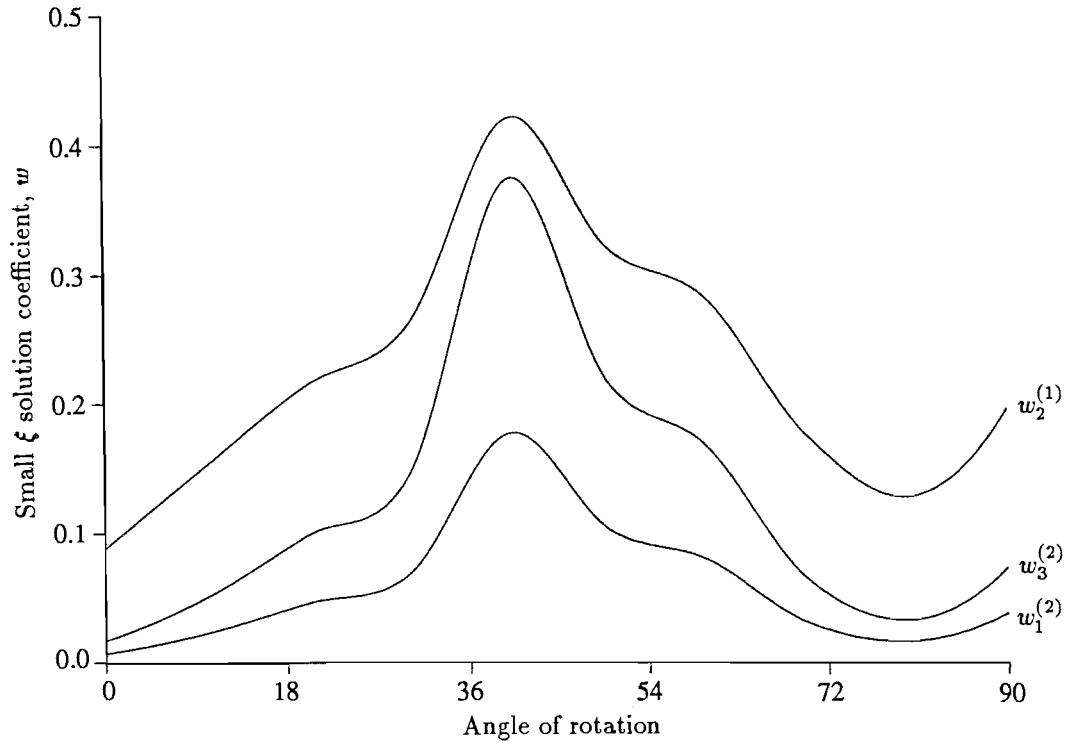

Figure 4.8.16 $w_1^{(2)}$, $w_2^{(1)}$ and $w_3^{(2)}$ for angles of propagation away from the X-axis on Y-cut $LiNbO_3$

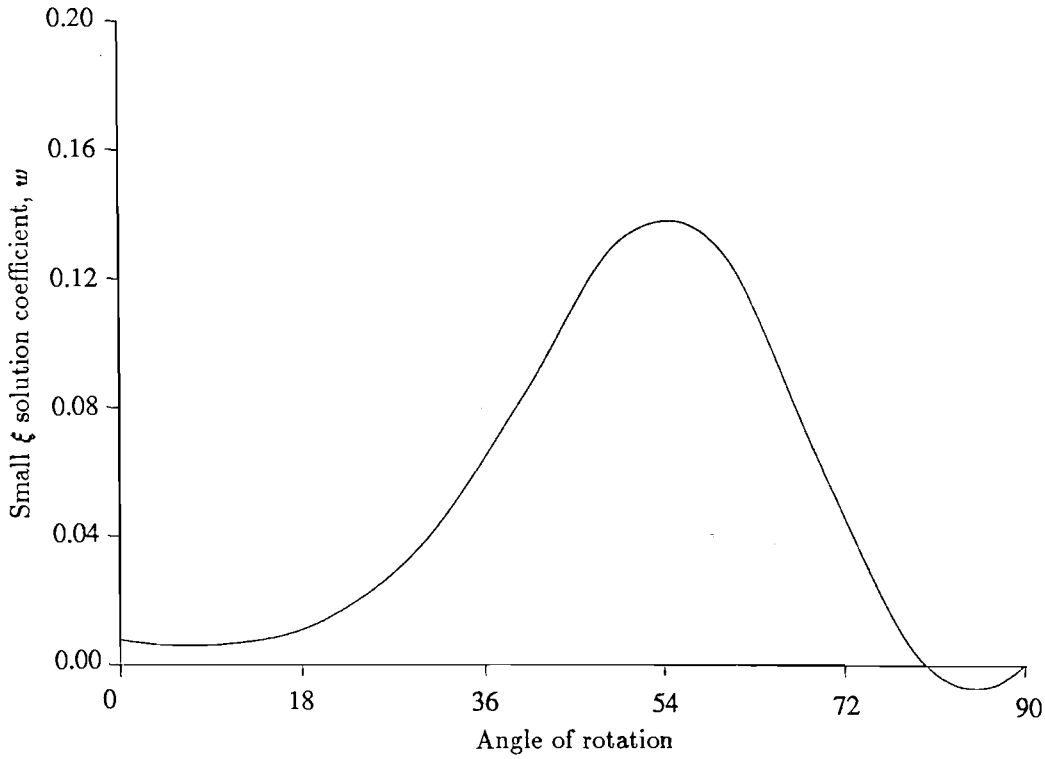

Figure 4.8.17 $w_1^{(2)}$ for angles of propagation away from the Z-axis on X-cut $LiNbO_3$

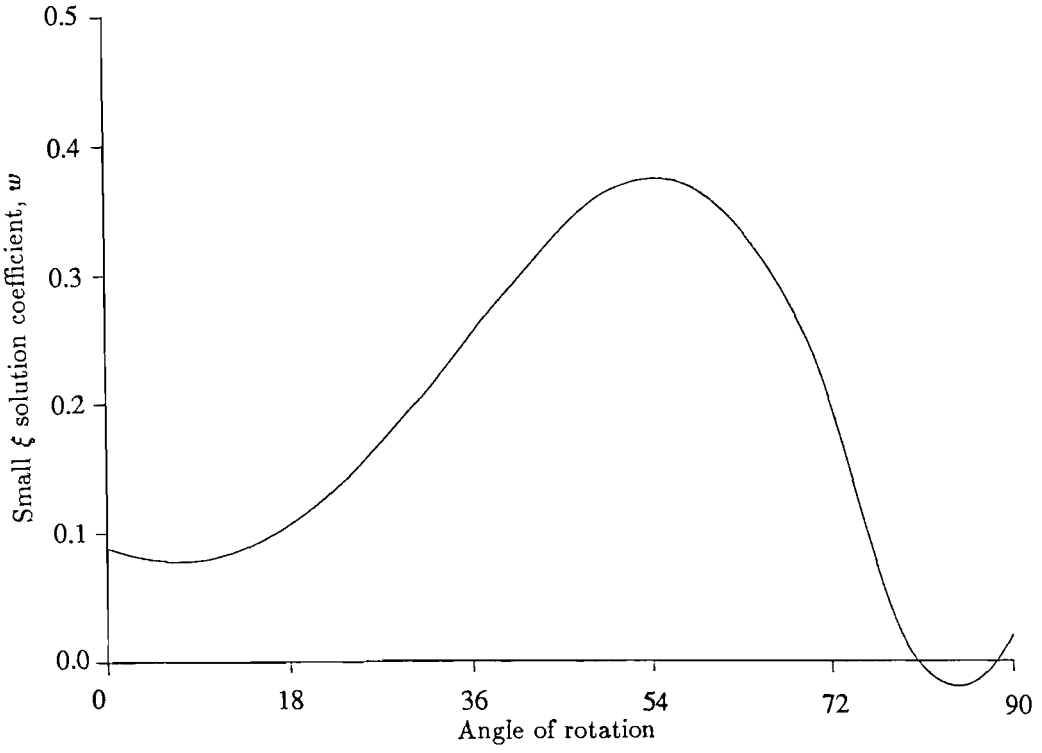

Figure 4.8.18 $w_2^{(1)}$ for angles of propagation away from the Z-axis on X-cut $LiNbO_3$

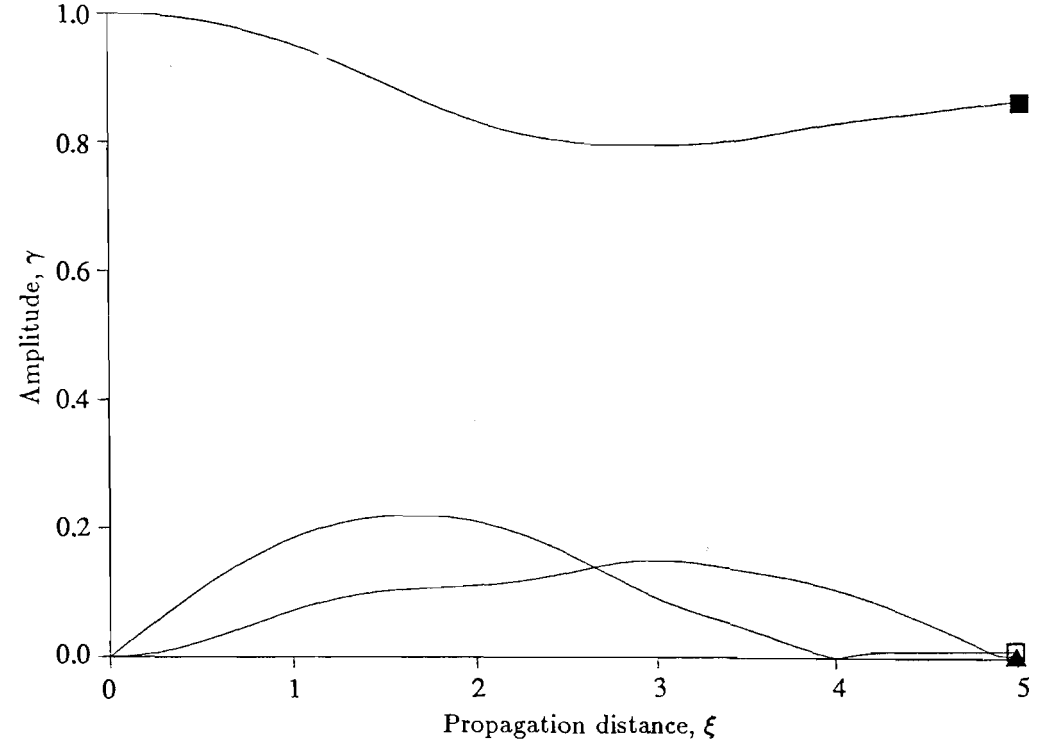

Figure 4.8.19 Growth and decay of the amplitudes $\tilde{\gamma}_K$ with propagation distance ξ_1 for X-propagation on Y-cut $LiNbO_3$, with short-circuited boundary conditions (10 harmonics)

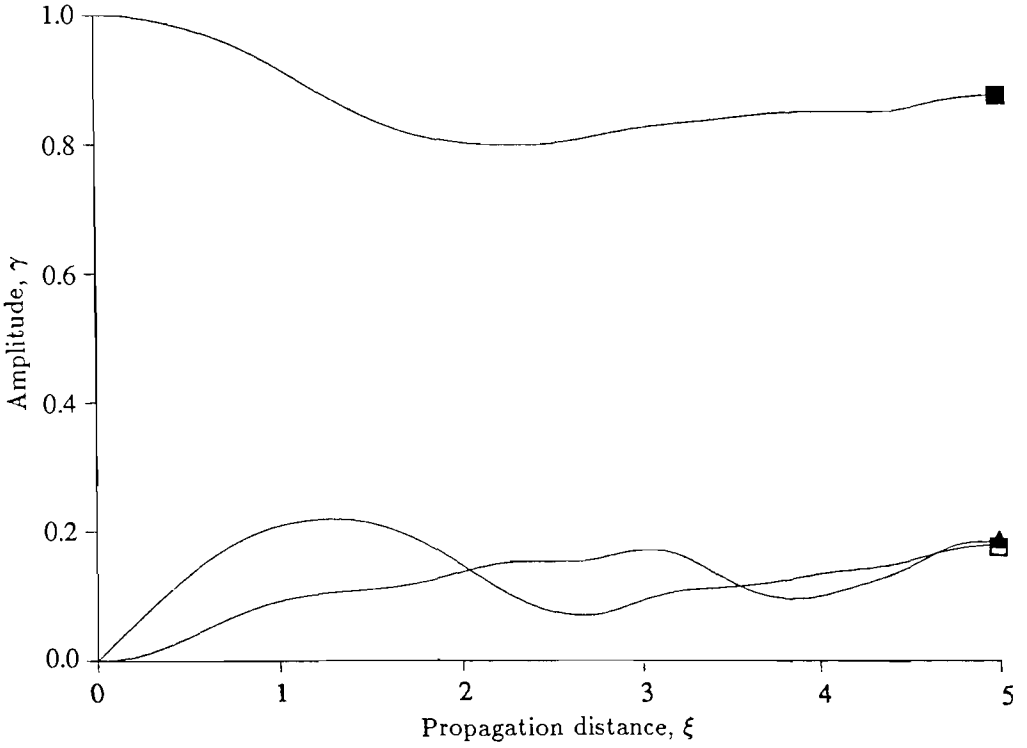

Figure 4.8.20 Growth and decay of the amplitudes $\tilde{\gamma}_K$ with propagation distance ξ_1 for propagation 45° away from the X-axis on Y-cut $LiNbO_3$, with short-circuited boundary conditions (10 harmonics)

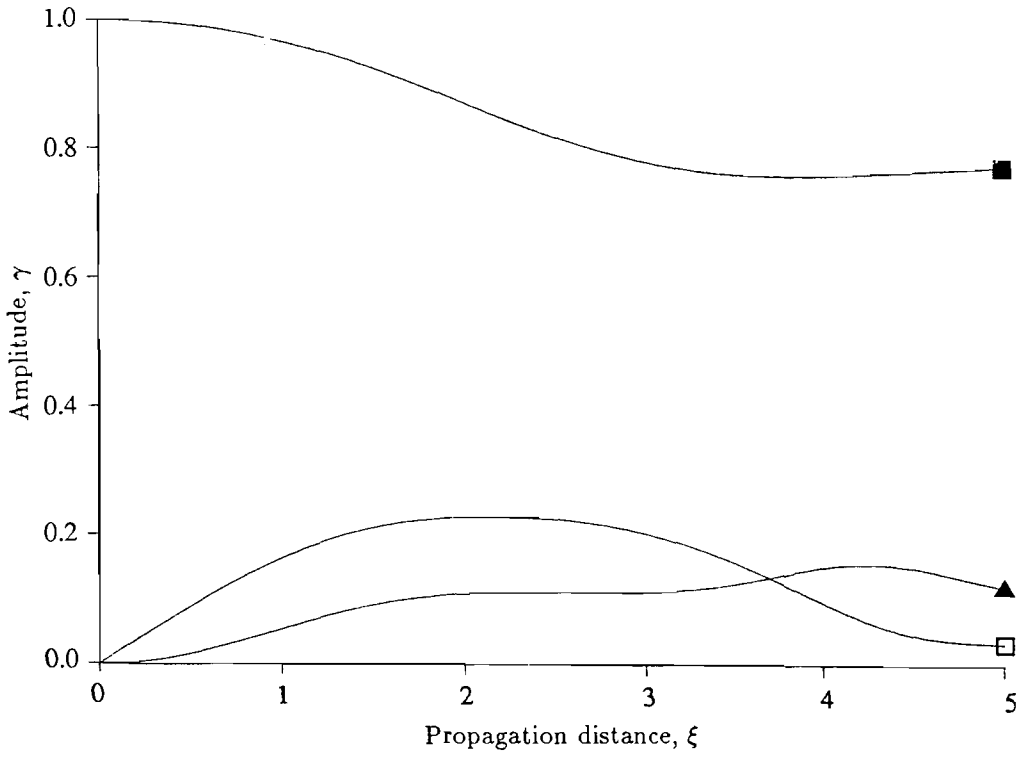

Figure 4.8.21 Growth and decay of the amplitudes $\tilde{\gamma}_K$ with propagation distance ξ_1 for Z-propagation on X-cut $LiNbO_3$, with short-circuited boundary conditions (10 harmonics)

5 The Free Electric Field

In Chapter 4 the constitutive relations for a deformed piezoelectric substrate were derived assuming that all stress and electric displacement effects induced by the free electric field could be neglected. This postulate simplified the piezoelectric constitutive relations (4.5.5) and (4.6.3) and allowed us to neglect any electric field effects in the free space above the material surface, in the configuration used in Chapters 3 and 4. This became significant in Section 4.6 where continuity of the normal stress tensor and electric displacement vector across the material boundary were considered. In this section the validity of the free electric field assumption is examined by consideration of the general boundary conditions.

The same problem was confronted by Tiersten and Baumhauer [1974]. Their solution was to use the reference frame coordinates in the free space above the material boundary, where they are coincident with the spatial coordinates, thus introducing a discontinuity of the reference coordinates between the flat reference frame boundary and the deformed spatial boundary. A Taylor's series expansion was then taken of the reference surface displacements and electric potential in reference coordinates to obtain their respective values on the deformed spatial boundary in reference/spatial coordinates and hence overcome the discontinuity. The main fault of this technique is the implicit assumption that the governing field and constitutive equations may be interpolated into the region above the reference frame boundary.

In this chapter a more rigorous technique is presented, utilising a coordinate transformation in the free-space region to map the deformed spatial boundary onto the reference frame boundary.

For simplicity we revert, temporarily, to the notation of Chapter 2 in order that we may distinguish between the reference and material coordinate systems.

5.1 STRESS AND ELECTRIC DISPLACEMENT

The Maxwell stress induced by the free electric field has been derived in spatial coordinates by Lax and Nelson [1974] as

$$T_{ij}^F = \epsilon_0(\delta_{ik}\delta_{jl} - \tfrac{1}{2}\delta_{ij}\delta_{kl})\phi_{,k}\phi_{,l}\,, \tag{5.1.1}$$

whilst the electric field has already been defined as

$$E_j = -\phi_{,j}\,.$$

The electric polarization of a free electric field is zero and hence, from equation (4.1.2),

$$D_j^F = -\epsilon_0\phi_{,j}\,. \tag{5.1.2}$$

Equations (5.1.1) and (5.1.2) are satisfied both within the material and in the free space above the material. Within the material the total stress and electric displacement are given by

$$T_{ij}^T = T_{ij} + T_{ij}^F \tag{5.1.3}$$

and

$$D_i^T = D_i + D_i^F\,, \tag{5.1.4}$$

whilst in the free space only the free electric field effects are present.

These two differing systems force us to consider the two respective regions separately.

5.1.1 Within the material

In the region $X_2 < 0$ we may define a stress tensor and electric displacement vector induced by a free electric field in reference coordinates. This will allow the total stress tensor and electric displacement vector to be substituted into the field equations (4.5.5) and (4.6.3).

The Piola-Kirchhoff stress tensor and electric displacement vector have been earlier defined in the reference frame through equations (2.2.29) and (4.1.20). It follows directly from these definitions that we may introduce a reference frame Maxwell's stress and electric displacement vector through the relations

$$\sigma_{Ai}^F = J\frac{\partial X_A}{\partial x_j}T_{ji}^F \tag{5.1.5}$$

and

$$\mathrm{D}_A^F = J\frac{\partial X_A}{\partial x_j}D_j^F\,. \tag{5.1.6}$$

Thus, from equations (5.1.3) to (5.1.6), the total stress tensor and total electric displacement vector are given by

$$\begin{aligned}\sigma_{Ai}^T &= J\frac{\partial X_A}{\partial x_j}T_{ji}^T \\ &= \sigma_{Ai} + \sigma_{Ai}^F\end{aligned} \tag{5.1.7}$$

and

$$\begin{aligned}\mathrm{D}_A^T &= J\frac{\partial X_A}{\partial x_j}D_j^T \\ &= \mathrm{D}_A + \mathrm{D}_A^F\,.\end{aligned} \tag{5.1.8}$$

Use of equation (2.2.8) and the Jacobian definition (2.2.3) together with the replacements $u_i \rightarrow \epsilon u_i$, $\phi \rightarrow \epsilon\phi$, $\sigma_{ij} \rightarrow \epsilon\sigma_{ij}$ and $\mathrm{D}_i \rightarrow \epsilon \mathrm{D}_i$ now gives equations (5.1.5) and (5.1.6) in the form

$$\begin{aligned}\sigma_{Ai}^F &= (1+\epsilon u_{B,B}+O(\epsilon^2))(\delta_{Aj}-\epsilon\delta_{Bj}\frac{\partial u_A}{\partial X_B}+O(\epsilon^2))(\epsilon\epsilon_0(\delta_{jk}\delta_{il}-\tfrac{1}{2}\delta_{ij}\delta_{kl})\phi_{,k}\phi_{,l}) \\ &= \epsilon\epsilon_0(\delta_{Ak}\delta_{il}-\tfrac{1}{2}\delta_{Ai}\delta_{kl})\phi_{,k}\phi_{,l}+\mathrm{O}(\epsilon^2)\end{aligned} \tag{5.1.8}$$

and

$$\begin{aligned}\mathrm{D}_A^F &= \big(1+\epsilon u_{B,B}+\mathrm{O}(\epsilon^2)\big)\big(\delta_{Aj}-\epsilon\delta_{Bj}\frac{\partial u_A}{\partial X_B}+\mathrm{O}(\epsilon^2)\big)\big(-\epsilon_0\frac{\partial\phi}{\partial X_D}\big) \\ &\qquad\times\big(\delta_{Dj}-\epsilon\delta_{Cj}\frac{\partial u_D}{\partial X_C}+\mathrm{O}(\epsilon^2)\big) \\ &= -\epsilon_0\phi_{,A}+\epsilon\epsilon_0(\phi_{,D}u_{A,D}+\phi_{,D}u_{D,A}-u_{D,D}\phi_{,A})+\mathrm{O}(\epsilon^2)\,.\end{aligned} \tag{5.1.9}$$

Recalling equations (4.4.5) and (4.4.6), the total Piola-Kirchhoff stress tensor and the electric displacement vector are expressed, using equations (5.1.8) and (5.1.9), as

$$\begin{aligned}\sigma_{Ai}^T &= \overset{(2)}{c}_{AiCD}u_{C,D}+\overset{(2)}{e}_{BAi}\phi_{,B}+\epsilon d_{AiCDEF}u_{C,D}u_{E,F} \\ &\quad+\epsilon f_{AiBCD}u_{C,D}\phi_{,B}-\tfrac{1}{2}\epsilon\, l'_{CDAi}\phi_{,C}\phi_{,D}\end{aligned} \tag{5.1.10}$$

$$\begin{aligned}\mathrm{D}_A^T &= \overset{(2)}{e}_{ABC}u_{B,C}-\epsilon'_{AB}\phi_{,B}+\epsilon f_{ABCDE}u_{B,C}u_{D,E} \\ &\quad+\tfrac{1}{2}\epsilon\,\overset{(3)}{\epsilon}_{ABC}\phi_{,B}\phi_{,C}-\epsilon\, l'_{ABCD}u_{C,D}\phi_{,B}\,,\end{aligned} \tag{5.1.11}$$

where

$$\epsilon'_{AB} = \epsilon_0 \delta_{AB} + \overset{(2)}{\epsilon_{AB}}$$
$$l'_{ABCD} = l_{ABCD} - \epsilon_0(\delta_{AC}\delta_{BD} + \delta_{AD}\delta_{CB} - \delta_{AB}\delta_{CD})\,. \tag{5.1.12}$$

Tiersten [1974] argues that the quadratic free electric field effects, expressed through $(5.1.12)_2$, are indistinguishable from the effects of electrostriction and therefore the numerical values obtained experimentally for the electrostrictive constant must include the free electric field effects. This observation effectively eliminates all the free electric field effects except the linear dielectric effect that appears in equation (5.1.12).

5.1.2 The free space

In the free space above the material boundary the reference coordinates are coincident with the spatial coordinates, since the mechanical displacement is zero (see equation (2.2.4)). This, however, reveals a discontinuity of the reference coordinate system at the material boundary which, in turn, leads to problems when considering the continuity of a quantity referred to the reference frame across this boundary.

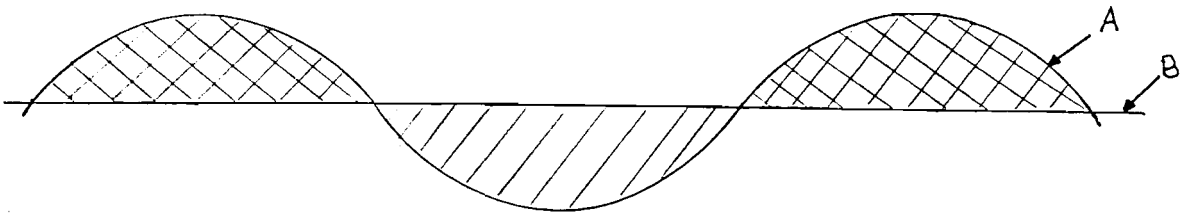

Figure 5.1.1 The free surface in reference and spatial coordinates

This discontinuity may be explained by consideration of Figure 5.1.1. Two boundaries, A and B, are represented in this figure: boundary A is the true material surface, which may be represented by $X_2 = 0$ in the reference coordinates valid within the material; boundary B represents the plane $x_2 = 0$ in spatial coordinates.

The boundaries A and B may also be referred to the coordinate systems valid in the free space above the material boundary. In free space coordinates, the planes $X_2 = 0$ and $x_2 = 0$ are coincident and represented by the boundary B. The boundary A may only be expressed in terms of the unknown surface displacement vector, $u_j(X_1, 0, t)$.

It is known that the scalar electric potential satisfies Laplace's equation in the free space above the material, referred to spatial coordinates. Thus

$$\tilde{\phi}_{jj} = 0\,. \tag{5.1.13}$$

The scalar potential must also be continuous across the material boundary, thus

$$\tilde{\phi} = \phi\,, \qquad \text{on } x_i = X_i + u_i(X_1, 0, t)\,. \tag{5.1.14}$$

Equation (5.1.13) is only valid in the free space above the material boundary.

Tiersten and Baumhauer [1974] take equation (5.1.13) to be valid down to the reference boundary B, or $X_2 = 0$, a region including the two hatched regions of Figure 5.1.1. A Taylor's expansion of $\tilde{\phi}$ in the unknown mechanical displacement vector is then taken to give the value of $\tilde{\phi}$ on the true material boundary A. Thus the governing equation for the free space scalar electric potential (5.1.13) is taken to be valid in regions in which it clearly does not hold. This could cause problems if discontinuities were present.

A more rigorous approach would be to introduce a transformation of the spatial coordinates in the free space to eliminate the discontinuity at the true material boundary. We thus define the free space reference coordinates through the relation

$$\tilde{X}_\alpha = \delta_{\alpha i} x_i - \epsilon \delta_{\alpha A} u_A(X_1, 0, t)\,, \tag{5.1.15}$$

leading to the representation

$$\tilde{X}_2 = 0$$

for the material boundary A.

Making use of the coordinate transformation (5.1.15), the governing equation (5.1.13) is valid up to the *known* boundary $\tilde{X}_2 = 0$.

It is worth noting at this point that the free space reference coordinates (5.1.15) are coincident with the reference coordinates on the material boundary and thus choice of the free space reference coordinates for the region $\tilde{X}_2 > 0$ and reference coordinates for the region $X_2 < 0$ gives a continuous coordinate system.

From equation (5.1.15)

$$\frac{\partial \tilde{X}_\alpha}{\partial x_i} = \delta_{\alpha i} - \epsilon \delta_{\alpha A} \frac{\partial \tilde{u}_A}{\partial x_i},$$

where

$$\tilde{u}_A(X_1, t) = u_A(X_1, 0, t).$$

Use of equations (2.2.8) now yields

$$\frac{\partial \tilde{X}_\alpha}{\partial x_i} = \delta_{\alpha i} - \epsilon \delta_{\alpha A} \tilde{u}_{A,B}[\delta_{iB} - \epsilon \delta_{iC} \tilde{u}_{B,C} + O(\epsilon^2)],$$

and hence

$$\frac{\partial \tilde{X}_\alpha}{\partial x_i} = \delta_{\alpha i} - \epsilon \delta_{\alpha A} \delta_{iB} \tilde{u}_{A,B} + O(\epsilon^2). \tag{5.1.16}$$

From equation (5.1.16) it is seen that

$$\phi_{,j} = (\delta_{\alpha j} - \epsilon \delta_{\alpha A} \delta_{jB} \tilde{u}_{A,B} + O(\epsilon^2)) \phi_{,\alpha}, \tag{5.1.17}$$

where greek subscripts denote differentiation with respect to the free space reference coordinates.

Differentiating equation (5.1.17) with respect to x_i and using equations (5.1.16) and (2.2.8) now yields

$$\begin{aligned} \phi_{,ij} = {} & \delta_{\alpha j} \phi_{,\alpha\beta} (\delta_{\beta i} - \epsilon \delta_{\beta A} \delta_{iB} \tilde{u}_{A,B}) - \epsilon \delta_{\alpha A} \delta_{jB} \delta_{\beta i} \tilde{u}_{A,B} \phi_{,\alpha\beta} \\ & - \epsilon \delta_{\alpha A} \delta_{jB} \delta_{iC} \tilde{u}_{A,BC} \phi_{,\alpha} + O(\epsilon^2), \end{aligned}$$

and hence

$$\phi_{,jj} = \phi_{,\alpha\alpha} - 2\epsilon \delta_{\alpha A} \delta_{\beta B} \tilde{u}_{A,B} \phi_{,\alpha\beta} - \epsilon \delta_{\alpha A} \tilde{u}_{A,BB} \phi_{,\alpha} + O(\epsilon^2). \tag{5.1.18}$$

From equation (5.1.18) it is seen that the field equation (5.1.13) in free space reference coordinates becomes

$$\tilde{\phi}_{,\alpha\alpha} = 2\epsilon\delta_{\alpha A}\delta_{\beta B}\tilde{u}_{A,B}\tilde{\phi}_{,\alpha\beta} + \epsilon\delta_{\alpha A}\tilde{u}_{A,BB}\tilde{\phi}_{,\alpha}\,, \tag{5.1.19}$$

where terms of quadratic order in ϵ and above are neglected from here on.

Noting that $\tilde{u}_A$ depends only upon X_1, equation (5.1.19) may be rewritten as

$$\tilde{\phi}_{,\alpha\alpha} = 2\epsilon\delta_{\alpha A}\tilde{u}_{A,1}\tilde{\phi}_{,\alpha 1} + \epsilon\delta_{\alpha A}\tilde{u}_{A,11}\tilde{\phi}_{,\alpha}\,. \tag{5.1.20}$$

Equation (5.1.20) is valid in the free space $\tilde{X}_2 > 0$ up to the boundary $\tilde{X}_2 = 0$ and is subject to the continuity boundary condition (5.1.14) on $\tilde{X}_2 = X_2 = 0$. Since the reference coordinate systems are coincident on the material boundary, the continuity condition for the scalar electric potential may simply be written as

$$\tilde{\phi} = \phi\,, \qquad \text{on } \tilde{X}_2 = X_2 = 0\,, \tag{5.1.21}$$

with the quantities referred to their respective coordinate systems.

The situation is not so simple for consideration of the continuity of a vector quantity across the material boundary, where the two surface normals are not necessarily parallel.

Referring to equation (2.2.27) it may easily be seen that

$$n_i\, d\mathcal{S} = \tilde{J}\frac{\partial \tilde{X}_\alpha}{\partial x_i}\tilde{N}_\alpha d\tilde{\mathcal{S}}\,, \tag{5.1.22}$$

where n_i and $d\mathcal{S}$ are the surface normal and surface element respectively in spatial coordinates, and $\tilde{N}_\alpha$ and $d\tilde{\mathcal{S}}$ are the equivalent quantities in free space reference coordinates. The Jacobian $\tilde{J}$ is defined by

$$\tilde{J} = \left|\frac{\partial x_i}{\partial \tilde{X}_\alpha}\right|\,.$$

Premultiplying equation (5.1.22) by some vector quantity P_i, defined in the spatial frame, we have

$$\begin{aligned} P_i n_i\, d\mathcal{S} &= \tilde{J}\frac{\partial \tilde{X}_\alpha}{\partial x_i}P_i\tilde{N}_\alpha\, d\tilde{\mathcal{S}} \\ &= \tilde{P}_\alpha\tilde{N}_\alpha\, d\tilde{\mathcal{S}}\,, \end{aligned} \tag{5.1.23}$$

where $\tilde{P}_\alpha = \tilde{J}\frac{\partial \tilde{X}_\alpha}{\partial x_i}P_i$ is the vector P_i referred to the free space reference coordinates.

Thus the stress tensor and electric displacement vector referred to the free space reference frame may be represented by

$$\tilde{\sigma}^F_{\alpha i} = \tilde{J}\frac{\partial \tilde{X}_\alpha}{\partial x_j}T^F_{ij} \tag{5.1.24}$$

$$\tilde{\mathrm{D}}^F_\alpha = \tilde{J}\frac{\partial \tilde{X}_\alpha}{\partial x_j}D^F_j\,, \tag{5.1.25}$$

where T^F_{ij} and D^F_j are defined through equations (5.1.1) and (5.1.2) respectively.

It is clearly seen from equation (5.1.23) that any vector flux normal to the material surface in spatial coordinates is equal to the normal vector flux to the same surface element referred to the free space reference frame. Since it is known that the material boundary is the same in both free space reference coordinates and reference coordinates, we may choose the two reference frames in their appropriate half spaces to give continuity of normal flux across the boundary.

Using equations (5.1.24) and (5.1.25) together with (5.1.1) and (5.1.2), the Maxwell's stress tensor and electric displacement vector of a free electric field in free space reference coordinates may be represented by

$$\tilde{\sigma}^F_{\alpha i} = \epsilon\epsilon_0\delta_{\alpha j}(\delta_{jk}\delta_{il} - \tfrac{1}{2}\delta_{ij}\delta_{kl})\delta_{k\beta}\delta_{l\gamma}\tilde{\phi}_{,\beta}\tilde{\phi}_{,\gamma} + \mathrm{O}(\epsilon^2)$$

and

$$\tilde{\mathrm{D}}^F_\alpha = -\epsilon_0(1+\epsilon\tilde{u}_{\beta,\beta})(\delta_{\alpha j} - \epsilon\delta_{\beta j}\tilde{u}_{\alpha,\beta})(\delta_{j\gamma} - \epsilon\delta_{j\epsilon}\tilde{u}_{\gamma,\epsilon})\tilde{\phi}_{,\gamma} + \mathrm{O}(\epsilon^2)\,,$$

which simplify to give

$$\tilde{\sigma}^F_{\alpha i} = \epsilon\epsilon_0(\delta_{i\beta}\tilde{\phi}_{,\alpha}\tilde{\phi}_{,\beta} - \tfrac{1}{2}\delta_{\alpha i}\tilde{\phi}_{,\beta}\tilde{\phi}_{,\beta}) + \mathrm{O}(\epsilon^2) \tag{5.1.26}$$

and

$$\tilde{\mathrm{D}}^F_\alpha = -\epsilon_0\tilde{\phi}_{,\alpha} + \epsilon\epsilon_0(\tilde{\phi}_{,\beta}\tilde{u}_{\alpha,\beta} + \tilde{\phi}_{,\beta}\tilde{u}_{\beta,\alpha} - \tilde{\phi}_{,\alpha}\tilde{u}_{\beta,\beta}) + \mathrm{O}(\epsilon^2)\,, \tag{5.1.27}$$

for $\tilde{X}_2 > 0$.

5.2 SUMMARY AND SIMPLIFICATIONS

A fifth field equation valid in the half space above the material surface has been introduced in this chapter and we have extended the concept of continuity across the material boundary. It is now useful, therefore, at this stage to summarise the equations and to simplify them where appropriate.

1) Within the material we have the constitutive relations

$$\sigma^T_{Ai} = c_{AiCD}u_{C,D} + e_{BAi}\phi_{,B} + \epsilon\, d_{AiCDEF}u_{C,D}u_{E,F} + 2\epsilon f_{BAiCD}u_{C,D}\phi_{,B} - \tfrac{1}{2}\epsilon\, l_{CDAi}\phi_{,C}\phi_{,D} \tag{5.2.1}$$

and

$$\mathrm{D}^T_A = e_{ABC}u_{B,C} - \epsilon'_{AB}\phi_{,B} + \epsilon f_{ABCDE}u_{B,C}u_{D,E} + \tfrac{1}{2}\epsilon\,\epsilon^{(3)}_{ABC}\phi_{,B}\phi_{,C} - \epsilon\, l_{ABCD}u_{C,D}\phi_{,B}\,, \tag{5.2.2}$$

satisfying the balance relations

$$\sigma^T_{Ai,A} = \rho\ddot{u}_i \tag{5.2.3}$$

$$\mathrm{D}^T_{A,A} = 0 \tag{5.2.4}$$

These equations, together with the replacements $u_j \rightarrow \epsilon u_j$ and $\phi \rightarrow \epsilon\phi$, yield the field equations

$$\rho\ddot{u}_i - c_{AiCD}u_{C,DA} - e_{BAi}\phi_{,BA} = \epsilon[2d_{AiCDEF}u_{C,D}u_{E,FA} - l_{CDAi}\phi_{,C}\phi_{,DA} + 2f_{BAiCD}(u_{C,D}\phi_{,BA} + u_{C,DA}\phi_{,B})]\,, \tag{5.2.5}$$

and

$$-e_{ABC}u_{B,CA} + \epsilon'_{AB}\phi_{,BA} = \epsilon[2f_{ABCDE}u_{B,C}u_{D,EA} + \epsilon^{(3)}_{ABC}\phi_{,B}\phi_{,CA} - l_{ABCD}(u_{C,DA}\phi_{,B} + u_{C,D}\phi_{,BA})]\,. \tag{5.2.6}$$

2) In the free space we have the constitutive relations

$$\tilde{\sigma}^F_{\alpha i} = \epsilon\epsilon_0(\delta_{i\beta}\tilde{\phi}_{,\alpha}\tilde{\phi}_{,\beta} - \tfrac{1}{2}\delta_{\alpha i}\tilde{\phi}_{,\beta}\tilde{\phi}_{,\beta}) \tag{5.2.7}$$

and

$$\tilde{\mathrm{D}}^F_\alpha = -\epsilon_0\tilde{\phi}_{,\alpha} + \epsilon\epsilon_0(\tilde{\phi}_{,\beta}\tilde{u}_{\alpha,\beta} + \tilde{\phi}_{,\beta}\tilde{u}_{\beta,\alpha} - \tilde{\phi}_{,\alpha}\tilde{u}_{\beta,\beta})\,, \tag{5.2.8}$$

where the free electric field scalar potential $\tilde{\phi}$ satisfies the field equation

$$\tilde{\phi}_{,\alpha\alpha} = \epsilon(2\tilde{u}_{\alpha,1}\tilde{\phi}_{,\alpha 1} + \tilde{u}_{\alpha,11}\tilde{\phi}_{,\alpha}) \tag{5.2.9}$$

referred to free space reference coordinates.

3) On the material boundary $X_2 = \tilde{X}_2 = 0$ we have the continuity conditions

$$\begin{aligned} \sigma_{i2} &= \tilde{\sigma}_{i2} \\ \mathrm{D}_2 &= \tilde{\mathrm{D}}_2 \\ \phi &= \tilde{\phi}\,, \end{aligned} \tag{5.2.10}$$

whilst the displacement and potential must also satisfy the decay conditions

$$\begin{aligned} u_i &\to 0 \qquad \text{as } X_2 \to -\infty\,, \\ \phi &\to 0 \qquad \text{as } X_2 \to -\infty\,, \\ \tilde{\phi} &\to 0 \qquad \text{as } \tilde{X}_2 \to \infty\,. \end{aligned} \tag{5.2.11}$$

Referring to Section 4.4 it is easily seen that equations (5.2.5) and (5.2.6) can again be simplified by contracting the notation, in an analogous way to before except that now we take account of the primed dielectric constant.

Denoting these extended constants by $\hat{c}'_{ijkl}$ and $\hat{d}_{ijklmn}$, $(i,j,k,l,m,n = 1,\ldots,4)$, equations (5.2.5) and (5.2.6) may be written in the compact form

$$\hat{\delta}_{ij}\rho\ddot{u}_j - \hat{c}'_{ijkl}u_{k,li} = 2\epsilon\hat{d}_{ijklmn}u_{k,l}u_{m,nj}\,, \tag{5.2.12}$$

where $\hat{\delta}_{ij}$ is the modified Kronecker delta.

Equation (5.2.9) can be written

$$\tilde{\phi}_{,jj} = \epsilon(2\tilde{u}_{j,1}\tilde{\phi}_{,j1} + \tilde{u}_{j,11}\tilde{\phi}_{,j}) \qquad \text{for } j = 1,2\,, \tag{5.2.13}$$

whilst the continuity conditions (5.2.10) become

$$\begin{aligned} \hat{c}'_{i2kl}u_{k,l} + \epsilon\hat{d}_{i2klmn}u_{k,l}u_{m,n} = \epsilon\epsilon_0\hat{\delta}_{ij}(\tilde{\phi}_{,j}\tilde{\phi}_{,2} - \tfrac{1}{2}\delta_{j2}\tilde{\phi}_{,k}\tilde{\phi}_{,k}) \\ + \epsilon\epsilon_0\delta_{i4}(\tilde{\phi}_{,1}\tilde{u}_{2,1} - \tilde{u}_{1,1}\tilde{\phi}_{,2}) - \epsilon_0\delta_{i4}\tilde{\phi}_{,2}\,. \end{aligned} \tag{5.2.14}$$

and

$$\phi = \tilde{\phi} \tag{5.2.15}$$

on $X_2 = \tilde{X}_2 = 0$, for $i,j,k,l,m,n = 1,\ 2,\ 3,\ 4$.

5.3 SOLUTION

In this section the method of multiple scales outlined in earlier chapters is used to solve the nonlinear field equations (5.2.12) and (5.2.13) subject to the boundary conditions (5.2.14) and (5.2.15). Coupled amplitude equations are derived and numerical solutions are obtained which may be directly compared to the numerical results of Chapter 4 for validation of the assumption (4.1.18).

It is seen that the field equation (5.2.12) is identical in form to the earlier field equations (3.2.5) and (4.5.5), whilst the boundary continuity conditions (5.2.14) are of an essentially similar form to conditions (3.2.6) and (4.6.3). We therefore may proceed, as in earlier chapters by introducing the small parameter ϵ and defining the slow variables ξ, η and τ by

$$\begin{aligned} \xi &= \epsilon x\,, \\ \eta &= \epsilon y\,, \\ \tau &= \epsilon t\,, \end{aligned}$$

where we use x, y, z synonymously with x_1, x_2, x_3.

We allow the displacement u_i and potential $\tilde{\phi}$ to depend upon distance, time and the slow variables ξ, η and τ, through the perturbation expansions

$$\begin{aligned} u_j &= u_j^{(1)}(x,y,t,\xi,\eta,\tau) + \epsilon\, u_j^{(2)}(x,y,t,\xi,\eta,\tau) + \dots\,, \qquad j = 1 \dots 4\,, \\ \tilde{\phi} &= \tilde{\phi}^{(1)}(x,y,t,\xi,\eta,\tau) + \epsilon\, \tilde{\phi}^{(2)}(x,y,t,\xi,\eta,\tau) + \dots \end{aligned} \tag{5.3.1}$$

Substituting the representations (5.3.1) into the field and boundary equations (5.2.12) to (5.2.15) we obtain the two systems at first- and second-order in ϵ.

5.3.1 First-order

At zero-order in ϵ the field and boundary equations (5.2.12) to (5.2.15) yield

$$\hat{\delta}_{ij}\rho\, \ddot{u}_j^{(1)} - \hat{c}'_{ijkl}\, u_{k,lj}^{(1)} = 0 \qquad (i = 1, \dots, 4) \tag{5.3.2}$$

and

$$\tilde{\phi}_{,jj}^{(1)} = 0\,, \qquad (i = 1,\, 2) \tag{5.3.3}$$

which must be solved subject to the boundary continuity conditions

$$\hat{c}'_{i2kl}\, u_{k,l}^{(1)} + \epsilon_0 \delta_{i4} \tilde{\phi}_{,2}^{(1)} = 0 \qquad (i = 1, \dots, 4) \tag{5.3.4}$$

and

$$\phi^{(1)} = \tilde{\phi}^{(1)}, \tag{5.3.5}$$

on $y = \eta = 0$.

Here we have five field equations and boundary conditions in five unknowns. Comparing these field equations with the field equations (4.7.2), we may assume a solution of the form

$$u_j^{(1)} = \sum_{n=1}^{4} A^{(n)}(\xi, \eta, \tau)\, a_j^{(n)}\, \mathrm{e}^{\mathrm{i}s^{(n)}y}\, \mathrm{e}^{\mathrm{i}(x-t)} + \text{c.c.} \tag{5.3.6}$$

where

$$\hat{\mathrm{L}}'_{ik}(s^{(n)})\, a_k^{(n)} = 0, \tag{5.3.7}$$

which requires

$$\left|\hat{\mathrm{L}}'_{ik}(s)\right| = 0,$$

and where

$$\hat{\mathrm{L}}'_{ik}(s) = \hat{c}'_{i2k2}\, s^2 + (\hat{c}'_{i2k1} + \hat{c}'_{i1k2})\, s + \hat{c}'_{i1k1} - \rho\, \hat{\delta}_{ik}\,.$$

More details were written down in Chapter 3.

A solution to the field equation (5.3.3) satisfying the necessary decay condition $(5.2.11)_3$ and continuity condition (5.2.10) can now be seen, from the representation (5.3.6), to take the form

$$\tilde{\phi}^{(1)} = \sum_{n=1}^{4} A^{(n)}(\xi, \eta, \tau)\, a_4^{(n)}\, \mathrm{e}^{-y}\, \mathrm{e}^{\mathrm{i}(x-t)} + \text{c.c.} \tag{5.3.8}$$

The first-order boundary conditions (5.3.4), together with the representations (5.3.6), (5.3.7) and (5.3.8), now yield the matrix equation

$$\sum_{n=1}^{3} \hat{\mathrm{M}}'_{in}\, A^{(n)} = 0 \qquad \text{on } y = \eta = 0 \tag{5.3.9}$$

where

$$\begin{aligned} \hat{\mathrm{M}}'_{in} &= (\hat{c}'_{i2k1} + \hat{c}'_{i2k2}\, s^{(n)})\, a_k^{(n)} + \mathrm{i}\epsilon_0 \delta_{i4} a_4^{(n)} \\ &= \hat{\mathrm{N}}'_{ik}(s^{(n)}) a_k^{(n)}, \end{aligned} \tag{5.3.10}$$

Equation (5.3.9) has the particular solution

$$\sum_{n=1}^{4} \hat{\mathrm{M}}'_{in}\, \beta^{(n)} = 0 \tag{5.3.11}$$

leading to the replacement

$$A^{(n)} = \beta^{(n)}\gamma \qquad \text{on } y = \eta = 0\,. \tag{5.3.12}$$

A nontrivial solution to equation (5.3.11) is ensured through the determinental condition

$$\left|\hat{\mathrm{M}}'_{in}\right| = 0\,, \tag{5.3.13}$$

which determines the linear wavespeed parameter ρ.

We now express the first-order solution as a summation over all harmonics:

$$u_j^{(1)} = \sum_{K=1}^{\infty}\sum_{n=1}^{4} A_K^{(n)}(\xi,\eta,\tau)\, a_j^{(n)}\, \mathrm{e}^{\mathrm{i}Ks^{(n)}y}\, \mathrm{e}^{\mathrm{i}K(x-t)} + \text{c.c. for } j = 1,\,2,\,3,\,4\,, \tag{5.3.14}$$

$$\tilde{\phi}^{(1)} = \sum_{K=1}^{\infty}\sum_{n=1}^{4} A_K^{(n)}(\xi,\eta,\tau)\, a_4^{(n)}\, \mathrm{e}^{-Ky}\, \mathrm{e}^{\mathrm{i}K(x-t)} + \text{c.c.} \tag{5.3.15}$$

,

with the surface displacement and potential defined by

$$u_j^{(1)}(0) = \sum_{K=1}^{\infty}\sum_{n=1}^{4} \gamma_K(\xi,\tau)\, \beta^{(n)}\, a_j^{(n)}\, \mathrm{e}^{\mathrm{i}K(x-t)} + \text{c.c.}\,, \tag{5.3.16}$$

on $y = \eta = 0$, where γ_K is the slowly varying surface amplitude.

5.3.2 Second-order System

On substituting the expansions (5.3.1) into the equations (5.2.12) to (5.2.15) and comparing the terms of first-order in ϵ, we obtain

$$\begin{aligned}\rho\,\hat{\delta}_{ij}\ddot{u}_j^{(2)} - \hat{c}'_{ijkl}\,u_{k,lj}^{(2)} &= (\hat{c}'_{i1kl} + \hat{c}'_{ilk1})\,u_{k,l\xi}^{(1)} \\ &\quad + (\hat{c}'_{i2kl} + \hat{c}'_{ilk2})\,u_{k,l\eta}^{(1)} - 2\rho\,\hat{\delta}_{ij}\dot{u}_{j,\tau}^{(1)} \\ &\quad + 2\hat{d}_{ijklmn}\,u_{k,l}^{(1)}\,u_{m,nj}^{(1)}\end{aligned} \tag{5.3.17}$$

and

$$\tilde{\phi}_{,jj}^{(2)} = 2\tilde{u}_{j,1}^{(1)}\tilde{\phi}_{,j1}^{(1)} + \tilde{u}_{j,11}^{(1)}\tilde{\phi}_{,j}^{(1)} \qquad \text{for } j = 1,2\,, \tag{5.3.18}$$

with the corresponding boundary conditions given by

$$\hat{c}'_{i2kl}\,u^{(2)}_{k,l} + \epsilon_0\delta_{i4}\tilde{\phi}^{(2)}_{,2} = -\hat{c}'_{i2k1}\,u^{(1)}_{k,\xi} - \hat{c}'_{i2k2}\,u^{(1)}_{k,\eta} - \epsilon_0\delta_{i4}\tilde{\phi}^{(1)}_{,\eta} - \hat{d}_{i2klmn}\,u^{(1)}_{k,l}\,u^{(1)}_{m,n} + \epsilon_0\hat{\delta}_{ij}\left(\tilde{\phi}^{(1)}_{,j}\tilde{\phi}^{(1)}_{,2} - \tfrac{1}{2}\hat{\delta}_{j2}\tilde{\phi}^{(1)}_{,k}\tilde{\phi}^{(1)}_{,k}\right) + \epsilon_0\delta_{i4}\left(\tilde{\phi}^{(1)}_{,1}\tilde{u}^{(1)}_{2,1} - \tilde{u}^{(1)}_{1,1}\tilde{\phi}^{(1)}_{,2}\right), \tag{5.3.19}$$

and

$$\phi^{(2)} = \tilde{\phi}^{(2)}, \tag{5.3.20}$$

on $y = \eta = 0$.

In equations (5.3.17) to (5.3.20) we take

$$\tilde{u}^{(1)}_j = \sum_{K=1}^{\infty}\sum_{n=1}^{4} A^{(n)}_K(\xi,\tau)\,a^{(n)}_j\,\mathrm{e}^{\mathrm{i}K(x-t)} + \text{c.c.},\ j = 1,2 \tag{5.3.21}$$

Substituting the linear representations (5.3.14) and (5.3.15) into the second-order field equations (5.3.17) and (5.3.18) yields

$$\begin{aligned}\rho\,\hat{\delta}_{ij}\,\ddot{u}^{(2)}_j - \hat{c}'_{ijkl}\,u^{(2)}_{k,lj} = {} & \left(\sum_{K=1}^{\infty}\sum_{n=1}^{4}\left(\hat{F}'^{(n)}_{iK1}(y)\,A^{(n)}_{K,\xi} + \hat{F}'^{(n)}_{iK2}(y)\,A^{(n)}_{K,\eta} + \hat{F}'^{(n)}_{iK3}(y)\,A^{(n)}_{K,\tau}\right)\mathrm{e}^{\mathrm{i}K(x-t)}\right. \\ & + \sum_{K=1}^{\infty}\sum_{L=1}^{K-1}\sum_{n=1}^{4}\sum_{m=1}^{4}\hat{H}^{(m,n)}_{iKL}(y)\,A^{(n)}_{K-L}\,A^{(m)}_{L}\,\mathrm{e}^{\mathrm{i}K(x-t)} \\ & + \sum_{K=1}^{\infty}\sum_{L=K+1}^{\infty}\sum_{n=1}^{4}\sum_{m=1}^{4}\hat{G}^{(m,n)}_{iKL}(y)\,\bar{A}^{(n)}_{L-K}\,A^{(m)}_{L}\,\mathrm{e}^{\mathrm{i}K(x-t)} \\ & \left. + \sum_{K=1}^{\infty}\sum_{n=1}^{4}\sum_{m=1}^{4}\hat{Q}^{(m,n)}_{iK}(y)\,A^{(m)}_{K}\,\bar{A}^{(n)}_{K}\right) + \text{c.c.}\end{aligned} \tag{5.3.22}$$

and

$$\begin{aligned}\tilde{\phi}^{(2)}_{,jj} = {} & \sum_{K=1}^{\infty}\sum_{n=1}^{4}\sum_{m=1}^{4}\left(\sum_{L=1}^{K-1}\zeta^{1(m,n)}_{KL}(y)\,A^{(n)}_{K-L}\,A^{(m)}_{L} + \right. \\ & \left.\sum_{L=K+1}^{\infty}\left(\zeta^{21(m,n)}_{KL}(y) + \zeta^{22(m,n)}_{KL}(y)\right)\bar{A}^{(n)}_{L-K}\,A^{(m)}_{L}\right)\mathrm{e}^{\mathrm{i}K(x-t)} \\ & + \sum_{K=1}^{\infty}\sum_{n=1}^{4}\sum_{m=1}^{4}\zeta^{3(m,n)}_{K}(y)\,A^{(m)}_{K}\,\bar{A}^{(n)}_{K} + \text{c.c., for } j = 1,2\end{aligned} \tag{5.3.23}$$

where the coefficients are identical to those defined in Chapter 4 except for the change to primed constants, and

$$
\begin{aligned}
\zeta_{KL}^{1(m,n)}(y) &= L(K^2 - L^2)a_4^{(m)}(a_2^{(n)} - \mathrm{i}a_1^{(n)})\mathrm{e}^{-Ly}\,, \\
\zeta_{KL}^{21(m,n)}(y) &= L(L^2 - K^2)a_4^{(m)}(\mathrm{i}\bar{a}_1^{(n)} - \bar{a}_2^{(n)})\mathrm{e}^{-Ly}\,, \\
\zeta_{KL}^{22(m,n)}(y) &= L(L-K)(2K-L)\bar{a}_4^{(n)}(\mathrm{i}a_1^{(m)} + a_2^{(m)})\,\mathrm{e}^{-(L-K)y} \\
\zeta_{KL}^{3(m,n)}(y) &= -K^3\left[\bar{a}_4^{(n)}(\mathrm{i}a_1^{(m)} + a_2^{(m)})\right]\mathrm{e}^{-Ky}\,.
\end{aligned}
$$

In a similar way the boundary conditions (5.3.19) and (5.3.20) may be written as

$$
\begin{aligned}
\hat{c}'_{i2kl}\,u_{k,l}^{(2)} + \epsilon_0\delta_{i4}\tilde{\phi}_{,2}^{(2)} = &\left(\sum_{K=1}^{\infty}\sum_{n=1}^{4}\left(\hat{f}_{i1}^{(n)}\,A_{K,\xi}^{(n)} + \hat{f}_{i2}^{(n)}\,A_{K,\eta}^{(n)}\right)\mathrm{e}^{\mathrm{i}K(x-t)}\right. \\
&+ \sum_{K=1}^{\infty}\sum_{L=1}^{K-1}\sum_{n=1}^{4}\sum_{m=1}^{4}\hat{h}'^{(m,n)}_{iKL}\,A_{K-L}^{(n)}\,A_L^{(m)}\,\mathrm{e}^{\mathrm{i}K(x-t)} \\
&+ \sum_{K=1}^{\infty}\sum_{L=K+1}^{\infty}\sum_{n=1}^{4}\sum_{m=1}^{4}\hat{g}'^{(m,n)}_{iKL}\,\bar{A}_{L-K}^{(n)}\,A_L^{(m)}\,\mathrm{e}^{\mathrm{i}K(x-t)} \\
&\left.+ \sum_{K=1}^{\infty}\sum_{n=1}^{4}\sum_{m=1}^{4}\hat{q}'^{(m,n)}_{iK}\,A_K^{(m)}\,\bar{A}_K^{(n)}\right) + \text{c.c.}\,, \qquad (5.3.24)
\end{aligned}
$$

on $y = \eta = 0$.

Here it is noted that the linear coefficients, $\hat{f}_{i1}^{(n)}$ and $\hat{f}_{i2}^{(n)}$, are unprimed and have been defined in Chapter 4. This is due to the term $-\epsilon_0\delta_{i4}\tilde{\phi}_{,\eta}^{(1)}$ which, since $\phi^{(1)} = \tilde{\phi}^{(1)}$ on $y = \eta = 0$, cancels out the linear free electric field effects within the material, assuming continuity of the slow dependence and slow derivative of the amplitude across the material surface.

The quadratic order coefficients are defined by

$$
\begin{aligned}
\hat{h}'^{(m,n)}_{iKL} &= \hat{h}^{(m,n)}_{iKL} + h^{F(m,n)}_{iKL} \\
\hat{g}'^{(m,n)}_{iKL} &= \hat{g}^{(m,n)}_{iKL} + g^{F(m,n)}_{iKL} \\
\hat{q}'^{(m,n)}_{iK} &= \hat{q}^{(m,n)}_{iK} + q^{F(m,n)}_{iK}\,,
\end{aligned} \qquad (5.3.25)
$$

where

$$
\begin{aligned}
h^{F(m,n)}_{iKL} &= \epsilon_0 L(K-L)\left[(\hat{\delta}_{i2} - \mathrm{i}\hat{\delta}_{i1})a_4^{(m)}a_4^{(n)} - \delta_{i4}(a_4^{(m)}a_2^{(n)} - \mathrm{i}a_4^{(m)}a_1^{(n)})\right] \\
g^{F(m,n)}_{iKL} &= \epsilon_0 L(L-K)\left[\delta_{i4}(a_4^{(m)}\bar{a}_2^{(n)} + \bar{a}_4^{(n)}a_2^{(m)} - \mathrm{i}a_4^{(m)}\bar{a}_1^{(n)} + \mathrm{i}\bar{a}_4^{(n)}a_1^{(m)})\right] \\
q^{F(m,n)}_{iK} &= \epsilon_0 K^2\left[\delta_{i4}(a_4^{(m)}\bar{a}_2^{(n)} - \mathrm{i}a_4^{(m)}\bar{a}_1^{(n)})\right]
\end{aligned} \qquad (5.3.26)
$$

Now we have expressed equation (5.3.22) in an identical form to the second-order field equations (4.7.17), it follows that a solution exists in the form

$$
\begin{aligned}
u_j^{(2)} = & \sum_{K=1}^{\infty}\sum_{n=1}^{4} \hat{b}_{jK}^{(n)} \mathrm{e}^{\mathrm{i}Ks^{(n)}y} \mathrm{e}^{\mathrm{i}K(x-t)} + \sum_{K=1}^{\infty}\sum_{m=1}^{4}\sum_{n=1}^{4} \hat{r}_{jK}^{(m,n)} \mathrm{e}^{\mathrm{i}KT_{0K}^{(m,n)}y} \\
& + \sum_{K=1}^{\infty}\sum_{L=1}^{K-1}\sum_{m=1}^{4}\sum_{\substack{n=1 \\ n\neq m}}^{4} \hat{R}_{jKL}^{(m,n)} \mathrm{e}^{\mathrm{i}KP_{KL}^{(m,n)}y} \mathrm{e}^{\mathrm{i}K(x-t)} \\
& + \sum_{K=1}^{\infty}\sum_{L=K+1}^{\infty}\sum_{m=1}^{4}\sum_{n=1}^{4} \hat{S}_{jKL}^{(m,n)} \mathrm{e}^{\mathrm{i}KT_{KL}^{(m,n)}y} \mathrm{e}^{\mathrm{i}K(x-t)}, \qquad (5.3.27)
\end{aligned}
$$

where

$$
\begin{aligned}
P_{KL}^{(m,n)} &= \left(Ls^{(m)} + (K-L)s^{(n)}\right)/K \\
T_{KL}^{(m,n)} &= \left(Ls^{(m)} - (L-K)\bar{s}^{(n)}\right)/K . \\
\hat{R}_{jKL}^{(m,n)} &= \frac{1}{K^2}\hat{\mathrm{L}}_{ij}^{\prime\,-1}(P_{KL}^{(m,n)})\,\hat{H}_{iKL}^{(m,n)}(0)\,A_{K-L}^{(n)}\,A_L^{(m)} \qquad (5.3.28) \\
\hat{S}_{jKL}^{(m,n)} &= \frac{1}{K^2}\hat{\mathrm{L}}_{ij}^{\prime\,-1}(T_{KL}^{(m,n)})\,\hat{G}_{iKL}^{(m,n)}(0)\,\bar{A}_{L-K}^{(n)}\,A_L^{(m)},
\end{aligned}
$$

and $\hat{\mathrm{L}}_{ji}^{\prime\,-1}(s)$ is defined as the inverse of the non-singular matrix $\hat{\mathrm{L}}_{ij}^{\prime}(s)$, and zero wherever $\hat{\mathrm{L}}_{ij}^{\prime}(s)$ is singular.

Inspection of the right hand side of equation (5.3.23) leads us to the following form for the free space scalar electric potential

$$
\begin{aligned}
\tilde{\phi}^{(2)} = & \sum_{K=1}^{\infty}\sum_{n=1}^{4}\Bigg[\tilde{b}_{4K}^{(n)}\,\mathrm{e}^{-Ky} + \sum_{L=1}^{K-1}\sum_{m=1}^{4}\tilde{R}_{4KL}^{(m,n)}\,\mathrm{e}^{-Ly} \\
& + \sum_{L=K+1}^{\infty}\sum_{m=1}^{4}\left\{\tilde{S}_{4KL}^{1(m,n)}\,\mathrm{e}^{-Ly} + \tilde{S}_{4KL}^{2(m,n)}\,\mathrm{e}^{-(L-K)y}\right\}\Bigg]\mathrm{e}^{\mathrm{i}K(x-t)} \\
& + \sum_{K=1}^{\infty}\sum_{m=1}^{4}\sum_{n=1}^{4}\tilde{r}_{jK}^{(m,n)}\,\mathrm{e}^{-Ky}, \qquad (5.3.29)
\end{aligned}
$$

and substitution of this representation into equations (5.3.23) yields coefficients of the form

$$\begin{aligned}
\tilde{R}^{(m,n)}_{4KL} &= \frac{1}{L^2-K^2}\,\zeta^{1(m,n)}_{KL}(0)\,A^{(n)}_{K-L}\,A^{(m)}_{L} \\
\tilde{S}^{1(m,n)}_{4KL} &= \frac{1}{L^2-K^2}\,\zeta^{21(m,n)}_{KL}(0)\,\bar{A}^{(n)}_{L-K}\,A^{(m)}_{L} \\
\tilde{S}^{2(m,n)}_{4KL} &= \frac{1}{L(L-2K)}\,\zeta^{22(m,n)}_{KL}(0)\,\bar{A}^{(n)}_{L-K}\,A^{(m)}_{L}\,, \quad L \neq 2K\,.
\end{aligned} \tag{5.3.30}$$

Following the techniques of Chapters 3 and 4, secular terms may be eliminated from the representation (5.3.27) by imposing the consistency condition that must be satisfied by the right hand sides of equations (5.3.22). This condition may be expressed as the system of coupled partial differential equations

$$\hat{\Gamma}'^{(n)}_{K}\,A^{(n)}_{K,\xi} + \hat{\Delta}'^{(n)}_{K}\,A^{(n)}_{K,\eta} + \hat{\Theta}'^{(n)}_{K}\,A^{(n)}_{K,\tau} + \sum_{L=1}^{K-1}\hat{\Lambda}^{(n)}_{KL}\,A^{(n)}_{K-L}\,A^{(n)}_{L} = 0\,, \tag{5.3.31}$$

where the coefficients are defined in Chapter 4 but we must now take account of the primed second-order electro–elastic constant.

As before, introducing the partial inverse of the singular matrix $\hat{\mathrm{L}}'_{ij}(s^{(n)})$ restricted to the subspace orthogonal to the eigenvector $a^{(n)}_{j}$

$$\hat{\mathrm{U}}'^{(n)}_{ij} = \sum_{P=1}^{3}\frac{a^{(n)}_{iP}\,a^{(n)}_{jP}}{\lambda^{(n)}_{P}\,a^{(n)}_{kP}\,a^{(n)}_{kP}}\,, \tag{5.3.32}$$

where $a^{(n)}_{jP}$ are the eigenvectors of $\hat{\mathrm{L}}'_{ij}(s^{(n)})$ corresponding to non-zero eigenvalues, $\lambda^{(n)}_{P}$, we may obtain the representation

$$\hat{b}^{(n)}_{jK} = \hat{\chi}^{(n)}_{K}\,a^{(n)}_{j} + \frac{1}{K^2}\,\hat{\mathrm{U}}'^{(n)}_{ji}\,\hat{W}'^{(n)}_{iK}\,, \tag{5.3.33}$$

where

$$\begin{aligned}
\hat{W}'^{(n)}_{iK} = {} & \hat{F}'^{(n)}_{iK1}(0)\,A^{(n)}_{K,\xi} + \hat{F}'^{(n)}_{iK2}(0)\,A^{(n)}_{K,\eta} + \hat{F}'^{(n)}_{iK3}(0)\,A^{(n)}_{K,\tau} \\
& + \sum_{L=1}^{K-1}\hat{H}^{(n,n)}_{iKL}(0)\,A^{(n)}_{K-L}\,A^{(n)}_{L}\,.
\end{aligned} \tag{5.3.34}$$

Consideration of the boundary continuity condition (5.3.20) further yields

$$\begin{aligned}
\tilde{b}^{(n)}_{4k} = \hat{b}^{(n)}_{4k} & + \sum_{L=1}^{K-1}\sum_{m=1}^{4}\left[\hat{R}^{(m,n)}_{4KL} - \tilde{R}^{(m,n)}_{4KL}\right] \\
& + \sum_{L=K+1}^{\infty}\sum_{m=1}^{4}\left[\hat{S}^{(m,n)}_{4KL} - \tilde{S}^{1(m,n)}_{4KL} - \tilde{S}^{2(m,n)}_{4KL}\right]\,.
\end{aligned} \tag{5.3.35}$$

Now the boundary condition represented by equation (5.3.19) is of the same form as equation (4.7.18) except for the second-order term $\mathcal{T} = \epsilon_0 \delta_{i4} \tilde{\phi}^{(2)}_{,2}$ on $y = \eta = 0$. Using equations (5.3.29), (5.3.30) and (5.3.35) this term may be given by

$$\begin{aligned}\mathcal{T} &= \epsilon_0 \delta_{i4} \sum_{K=1}^{\infty} \sum_{n=1}^{4} \Bigg[-K \tilde{b}^{(n)}_{4K} + \sum_{L=1}^{K-1} \sum_{m=1}^{4} -L \tilde{R}^{(m,n)}_{4KL} \\ &\quad + \sum_{L=K+1}^{\infty} \sum_{m=1}^{4} \left\{ -L \tilde{S}^{1(m,n)}_{4KL} + (K-L) \tilde{S}^{2(m,n)}_{4KL} \right\} \Bigg] \\ &= \epsilon_0 \delta_{i4} \sum_{K=1}^{\infty} \sum_{n=1}^{4} \left[-K \hat{b}^{(n)}_{4K} \right] + \mathcal{N}_i \,, \end{aligned} \tag{5.3.36}$$

where

$$\begin{aligned}\mathcal{N}_i = \epsilon_0 \delta_{i4} \sum_{K=1}^{\infty} \sum_{n=1}^{4} \Bigg[& \sum_{L=1}^{K-1} \sum_{m=1}^{4} \left\{ -K \hat{R}^{(m,n)}_{4KL} + (K-L) \tilde{R}^{(m,n)}_{4KL} \right\} \\ & + \sum_{L=K+1}^{\infty} \sum_{m=1}^{4} \left\{ -K \hat{S}^{(m,n)}_{4KL} + (K-L) \tilde{S}^{1(m,n)}_{4KL} + (2K-L) \tilde{S}^{2(m,n)}_{4KL} \right\} \Bigg] \,. \end{aligned} \tag{5.3.37}$$

Thus, finally, use of the boundary conditions (5.3.19) leads to the singular matrix equations

$$\begin{aligned}(\mathrm{i}K) \sum_{n=1}^{4} \hat{\mathrm{M}}'_{in} \chi^{(n)}_K &= \sum_{n=1}^{4} \frac{1}{(\mathrm{i}K)} \hat{N}'_{ij}(s^{(n)}) \hat{\mathrm{U}}'^{(n)}_{jl} \hat{W}'^{(n)}_{lK} - \mathcal{N}_i \\ &+ \sum_{n=1}^{4} \sum_{m=1}^{4} \Bigg[\sum_{L=1}^{K-1} \frac{1}{(\mathrm{i}K)} \left(\hat{c}'_{i2j2} P^{(m,n)}_{KL} + \hat{c}'_{i2j1} \right) \hat{\mathrm{L}}'^{-1}_{jl}(P^{(m,n)}_{KL}) \hat{H}^{(m,n)}_{lKL}(0) A^{(n)}_{K-L} A^{(m)}_L \\ &\quad + \sum_{L=K+1}^{\infty} \frac{1}{(\mathrm{i}K)} \left(\hat{c}'_{i2j2} T^{(m,n)}_{KL} + \hat{c}'_{i2j1} \right) \mathrm{L}'^{-1}_{jl}(T^{(m,n)}_{KL}) \hat{G}'^{(m,n)}_{lKL}(0) \bar{A}^{(n)}_{L-K} A^{(m)}_L \Bigg] \\ &+ \sum_{n=1}^{4} \Bigg[\hat{f}^{(n)}_{i1} A^{(n)}_{K,\xi} + \hat{f}^{(n)}_{i2} A^{(n)}_{K,\eta} + \sum_{m=1}^{4} \sum_{L=1}^{K-1} \hat{h}'^{(m,n)}_{iKL} A^{(n)}_{K-L} A^{(m)}_L \\ &\quad + \sum_{m=1}^{4} \sum_{L=K+1}^{\infty} \hat{g}'^{(m,n)}_{iKL} \bar{A}^{(n)}_{L-K} A^{(m)}_L \Bigg] \,, \end{aligned} \tag{5.3.38}$$

on $y = \eta = 0$.

Use of the secularity condition (5.3.31) and equations (5.3.38) now yields the infinite system of coupled amplitude equations

$$\hat{N}'_K \gamma_{K,\xi} + \hat{P}'_K \gamma_{K,\tau} - \sum_{L=1}^{K-1} \hat{\Pi}'_{KL} \gamma_{K-L} \gamma_L - \sum_{L=K+1}^{\infty} \hat{\Delta}'_{KL} \bar{\gamma}_{L-K} \gamma_L = 0 \,, \tag{5.3.39}$$

where

$$\hat{N}'_K = \sum_{n=1}^{4} \left\{ \left(\frac{\lambda_i}{(iK)} \hat{N}'_{ij}(s^{(n)}) \hat{U}'^{(n)}_{jl} \hat{F}'^{(n)}_{lK1}(0) + \lambda_i \hat{f}^{(n)}_{i1} \right) - \frac{\hat{\Gamma}'^{(n)}_K}{\hat{\Delta}'^{(n)}_K} \left(\frac{\lambda_i}{(iK)} \hat{N}'_{ij}(s^{(n)}) \hat{U}'^{(n)}_{jl} \hat{F}'^{(n)}_{lK2}(0) + \lambda_i \hat{f}^{(n)}_{i2} \right) \right\} \beta^{(n)} \quad (5.3.40)$$

$$\hat{P}'_K = - \sum_{n=1}^{4} \left\{ \frac{\lambda_i}{(iK)} \hat{N}'_{ij}(s^{(n)}) \hat{U}'^{(n)}_{jl} \hat{F}'^{(n)}_{lK2}(0) + \lambda_i \hat{f}^{(n)}_{i2} \right\} \frac{\hat{\Theta}'^{(n)}_K}{\hat{\Delta}'^{(n)}_K} \beta^{(n)} \quad (5.3.41)$$

$$\begin{aligned} \hat{\Pi}'_{KL} = & - \sum_{n=1}^{4} \sum_{m=1}^{4} \left[\frac{\lambda_i}{(iK)} \hat{N}'_{ij}(P^{(m,n)}_{KL}) \hat{L}'^{-1}_{jl}(P^{(m,n)}_{KL}) \hat{H}'^{(m,n)}_{lKL}(0) \right. \\ & \left. + \frac{1}{K+L} \epsilon_0 \lambda_4 \zeta^{1(m,n)}_{KL}(0) + \lambda_i \hat{h}'^{(m,n)}_{iKL} \right] \beta^{(m)} \beta^{(n)} \\ & + \sum_{n=1}^{4} \left\{ \left[\frac{\lambda_i}{(iK)} \hat{N}'_{ij}(s^{(n)}) \hat{U}'^{(n)}_{jl} \hat{F}'^{(n)}_{lK2}(0) + \lambda_i \hat{f}^{(n)}_{i2} \right] \frac{\hat{\Lambda}'^{(n)}_{KL}}{\hat{\Delta}'^{(n)}_K} \right. \\ & \left. - \frac{\lambda_i}{(iK)} \hat{N}'_{ij}(s^{(n)}) \hat{U}'^{(n)}_{jl} \hat{H}'^{(n,n)}_{lKL}(0) \right\} \beta^{(n)} \beta^{(n)} \end{aligned} \quad (5.3.42)$$

and

$$\begin{aligned} \hat{\Delta}'_{KL} = & - \sum_{n=1}^{4} \sum_{m=1}^{4} \left[\frac{\lambda_i}{(iK)} \hat{N}'_{ij}(T^{(m,n)}_{KL}) \hat{L}'^{-1}_{jl}(T^{(m,n)}_{KL}) \hat{G}'^{(m,n)}_{lKL}(0) + \lambda_i \hat{g}'^{(m,n)}_{iKL} \right. \\ & \left. + \lambda_4 \left(\frac{1}{K+L} \zeta^{21(m,n)}_{KL}(0) + \frac{1}{L} \zeta^{22(m,n)}_{KL}(0) \right) \right] \beta^{(m)} \bar{\beta}^{(n)} . \end{aligned} \quad (5.3.43)$$

Finally, since $\hat{N}'_K = \hat{P}'_K$, these coupled amplitude equations simplify to

$$\gamma_{K,\xi} + \gamma_{K,\tau} = \sum_{L=1}^{K-1} \hat{\Pi}''_{KL} \gamma_{K-L} \gamma_L + \sum_{L=K+1}^{\infty} \hat{\Delta}''_{KL} \bar{\gamma}_{L-K} \gamma_L , \quad (5.3.44)$$

where

$$\hat{\Pi}''_{KL} = \frac{\hat{\Pi}'_{KL}}{\hat{N}'_K}$$

$$\hat{\Delta}''_{KL} = \frac{\hat{\Delta}'_{KL}}{\hat{N}'_K} .$$

5.4 RESULTS AND CONCLUSIONS

As in previous chapters, we must first solve the linear (Rayleigh) wave speed problem. Using the search routines of Chapters 3 and 4 we obtain the results given in Figure 5.4.1 again using the data of Warner et al [1967] for the material lithium niobate. Comparison with Figure 4.8.1 reveals very small percentage changes in the linear wave speed.

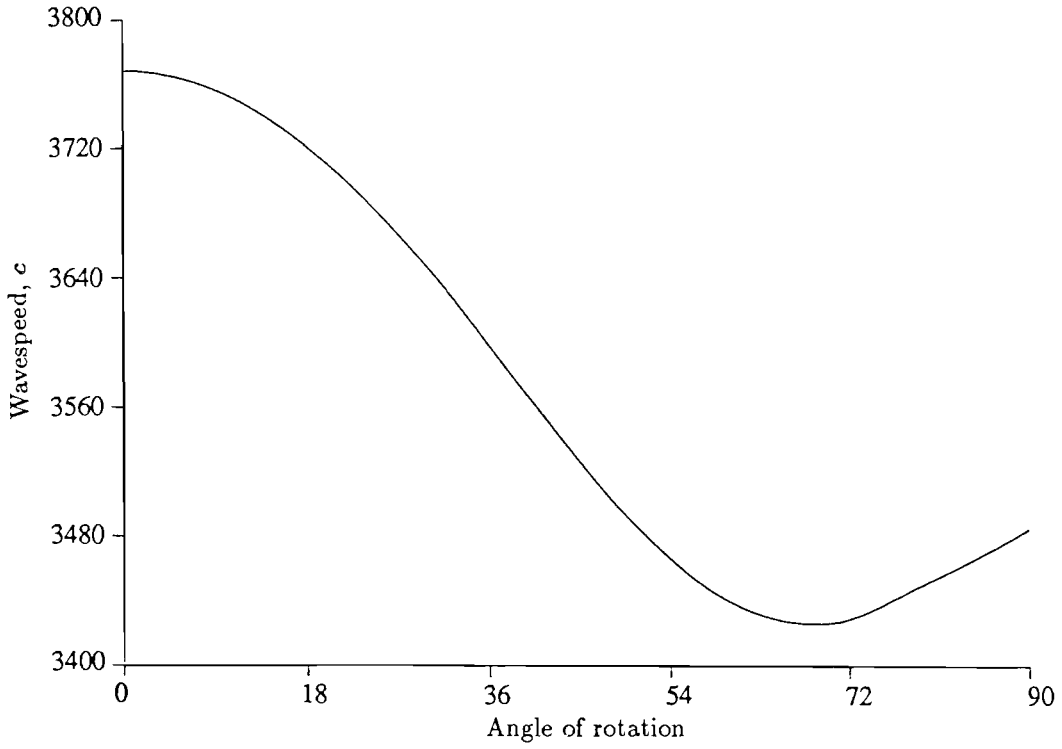

Figure 5.4.1 Variation of wavespeed with angle of propagation away from the X-axis on Y-cut lithium niobate

Evaluating the appropriate eigenvectors for the linear solution we may now calculate the various coefficients of the coupled amplitude equations (5.3.44) and compute the finite difference solution to these equations.

Returning to the small ξ analysis of earlier chapters we may make direct comparison between the corresponding harmonic growth and decay parameters. For the simplest case of an unrotated (Y-)cut of lithium niobate we obtain $w_1^{(2)}$ and $w_2^{(1)}$ as 0.0079 and 0.089 i respectively when following the simplified method of Chapter 4. Upon introduction of the free-space electric field effects in Chapter 5 these parameters become 0.0081 and 0.0898 i respectively, indicating a very small percentage change.

Figures, 5.4.2 to 5.4.4, duplicate cases studied in Chapter 4, except for the inclusion here of the free-space electric field effects, and it is easily seen that the results further indicate that the inclusion of the free-space electric field produce only a fraction of a percentage difference in the growth and decay parameters. This may be compared to the very high percentage change indicated in Chapter 4 induced by slight changes in the material constants, which in turn are subject to high statistical errors. It is therefore felt that the assumption introduced in Chapter 4 that the free-space electric field can be neglected has been justified, since it greatly simplifies the solution and yields results that differ very little from the "true" solution.

Key to Figures

- ■ Fundamental amplitude, $\tilde{\gamma}_1$.
- □ Second harmonic amplitude, $\tilde{\gamma}_2$.
- ▲ Third harmonic amplitude, $\tilde{\gamma}_3$.
- △ Fourth harmonic amplitude, $\tilde{\gamma}_4$ (where shown).

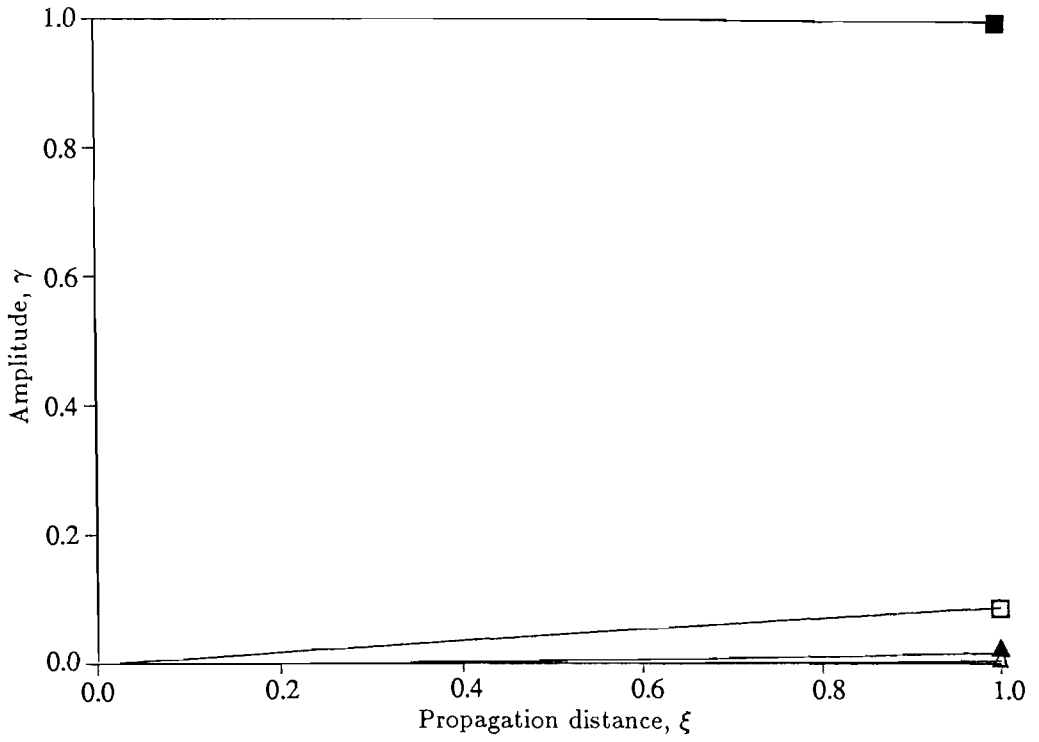

Figure 5.4.2 Growth and decay of the amplitudes $\tilde{\gamma}_K$ with propagation distance ξ_1 for X-propagation on Y-cut $LiNbO_3$, (10 harmonics)

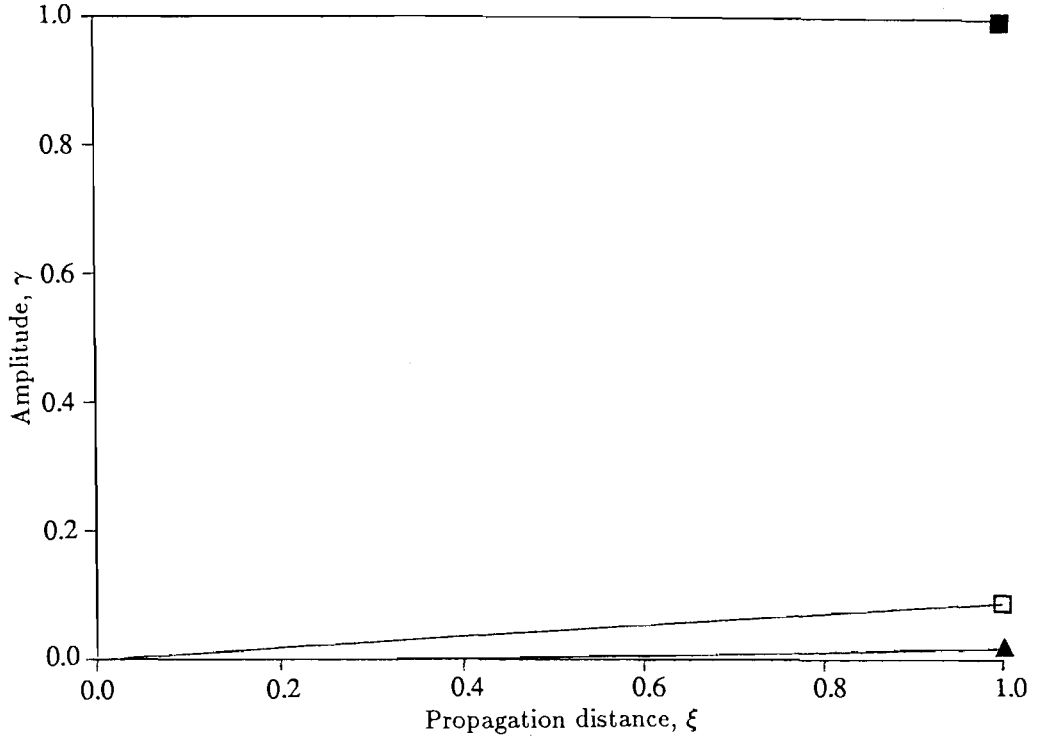

Figure 5.4.3 Growth and decay of the amplitudes $\tilde{\gamma}_K$ with propagation distance ξ_1 for X-propagation on Y-cut $LiNbO_3$, (3 harmonics)

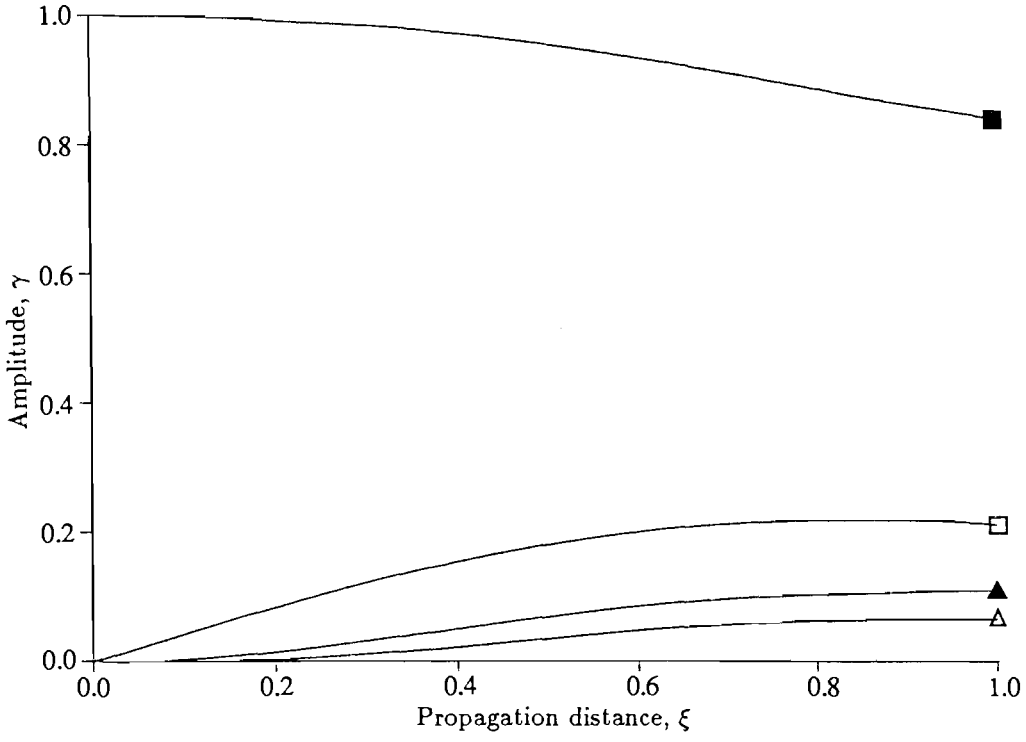

Figure 5.4.4 Growth and decay of the amplitudes $\tilde{\gamma}_K$ with propagation distance ξ_1 for propagation 40° from the X-axis on Y-cut $LiNbO_3$, (10 harmonics)

6 Acoustic Convolvers

The abstract problems of the propagation of a single wave on a semi-infinite elastic and piezoelectric substrate have been considered in the previous chapters. The motivation for such an analysis was the growing interest in nonlinear acoustic wave devices such as convolvers which, in general, operate through the nonlinear interaction of two waves. Acoustic devices are of interest to experimentalists since the nonlinear harmonic generation allows parametric amplification of a particular frequency through its higher harmonics.

Such devices have developed rapidly since the early investigations of harmonic generation and coupling, see Lean and Tseng [1970] and Thompson and Quate [1971]. Lean and Tseng [1970] used optical probing to study the generation of harmonics from a single frequency input to the surface of the crystal substrate using a surface transducer. An elementary theoretical justification of their results was also given and used to correct previous estimates of the various nonlinear electro-elastic constants. Thompson and Quate [1971], meanwhile, investigated the coupling of two oppositely propagating waves on a lithium niobate substrate. They observed that the output signal consisted of a standing wave at twice the input frequency and represented the convolution of the two input signals. Both investigations considered the propagation of a general plane wave in the material and observed the dominant effects of bulk wave generation. The application of surface waves in such devices was first recognised by Luukkala and Kino [1971] who observed the convolution and time-inversion of input surface wave signals in lithium niobate. The importance of surface wave generation in acoustic devices has become increasingly recognised since the energy of the surface wave is concentrated in a thin layer near the substrate surface, thus low acoustic powers produce a power density sufficiently high for nonlinear effects to be easily observed.

An acoustic convolver is generally used as a real-time signal processing device to generate the convolution of two envelope functions. The functions, represented by electric spectra, are used to generate, through surface transducers, two oppositely

propagating surface waves. The nonlinear interaction of the surface waves generates the convolution signal observed by Thompson and Quate [1971] and Luukkala and Kino [1971].

The efficiency of a convolver is easily defined to be the ratio of power output to power input. It is convenient, for the purposes of standardisation, to restrict the measurement of convolver efficiency to one single input frequency rather than a spectrum of frequencies. When input to both surface transducers, this single frequency will generate a convolution signal at twice the input frequency. This convolution signal may be directly measured as the surface potential at twice the input frequency, ω, and the efficiency can therefore be defined through

$$M = \frac{\phi_{2\omega}^{rms}(0)}{(P_1 P_2)^{1/2}},$$

where $\phi_{2\omega}^{rms}(0)$ is the root mean square surface potential at twice the input frequency, and P_i is the power input to each wave per unit width. This measure is commonly known as the Figure of Merit for the convolver. It is clear that, since the Figure of Merit relies upon the strength of the surface potential generated at the particular frequency, it will largely depend upon the substrate's electro-elastic coupling.

The interest in surface acoustic wave convolvers developed rapidly because of the high electro-elastic coupling, and thus high figure of merit, attainable and Lim, Kraut and Thompson [1972] experimented with various classes of crystal symmetry in order to obtain the most efficient substrate and orientation for such devices. Their results show that the material PZT-8 produces the largest value for the Figure of Merit but, unfortunately, this material has proved to be both expensive and unreliable to produce in large quantities.

An overview of acoustic device development and their possible uses may be found in the review articles by Morgan [1973, 1974] and his more recent book, Morgan [1985], in which the various experimental configurations are discussed together with brief theoretical justifications. The merits of the various forms of substrate, such as piezoelectric, elastic and semiconductor crystals, are also discussed.

The early convolvers consisted simply of two piezoelectric transducers arranged on the surface of a rectangular slab of substrate, see Figure 6.1, with a third transducer placed on the surface, between the two input transducers, to measure the output signal. Transducer development had already led to the introduction of the interdigitated input transducers illustrated in Figure 6.1. Theoretical studies

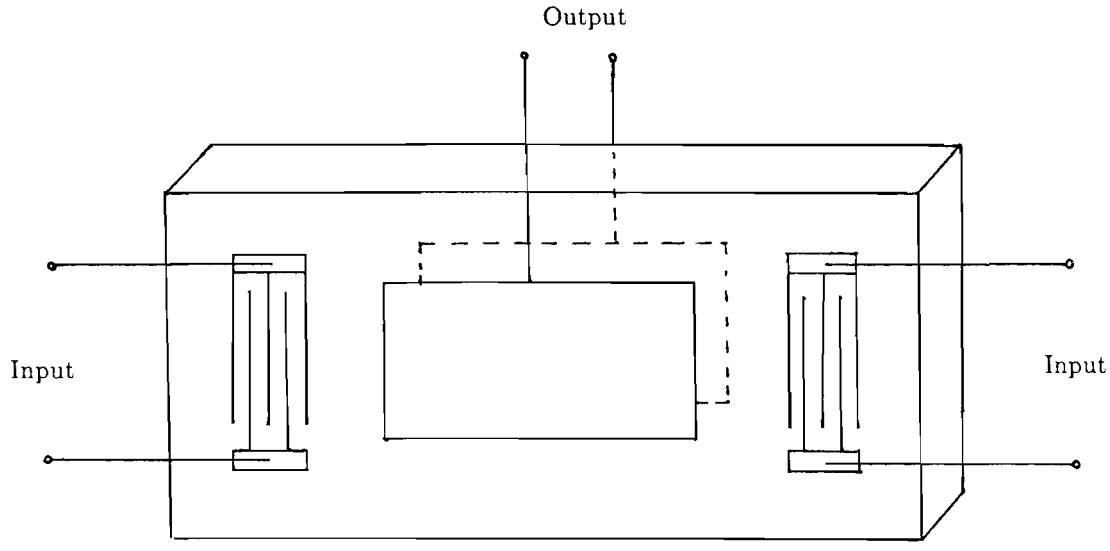

Figure 6.1 The configuration of a simple degenerate convolver

of the problem of surface wave excitation can be found in Yashiro and Goto [1978] and Bechtel and Bogy [1984].

One of the first developments was the waveguide studied by Shtykov, Mason and Motz [1975], designed to "channel" the wave power along the output transducer. An analysis of convolvers with waveguides was later given by Planat et al [1985] who used a finite element analysis to obtain the surface potential and thus calculate the figure of merit, or efficiency, of the convolver.

The output of most convolvers in current usage relies upon the transverse–vertical polarisation field of the convolver, that is the potential developed between the surface and base of the substrate, see Figure 6.1. Recently, convolvers have been developed which utilise the transverse–horizontal polarisation by placing two parallel output transducers on the surface of the substrate, Monks, Paige and Woods [1983] and Cho and Yamanouchi [1987]. The configuration of the transverse–horizontal convolver is given in Figure 6.2, and it should be noted their orientation allows the devices to be made much smaller.

The latest developments in surface acoustic wave convolver design may be found in the paper by Grassl et al [1988] and include beam compressors for wave guiding and chirp transducers which focus the wave onto the waveguide, see Figure 6.3. Such innovations make the problem of acurately modelling a real convolver much

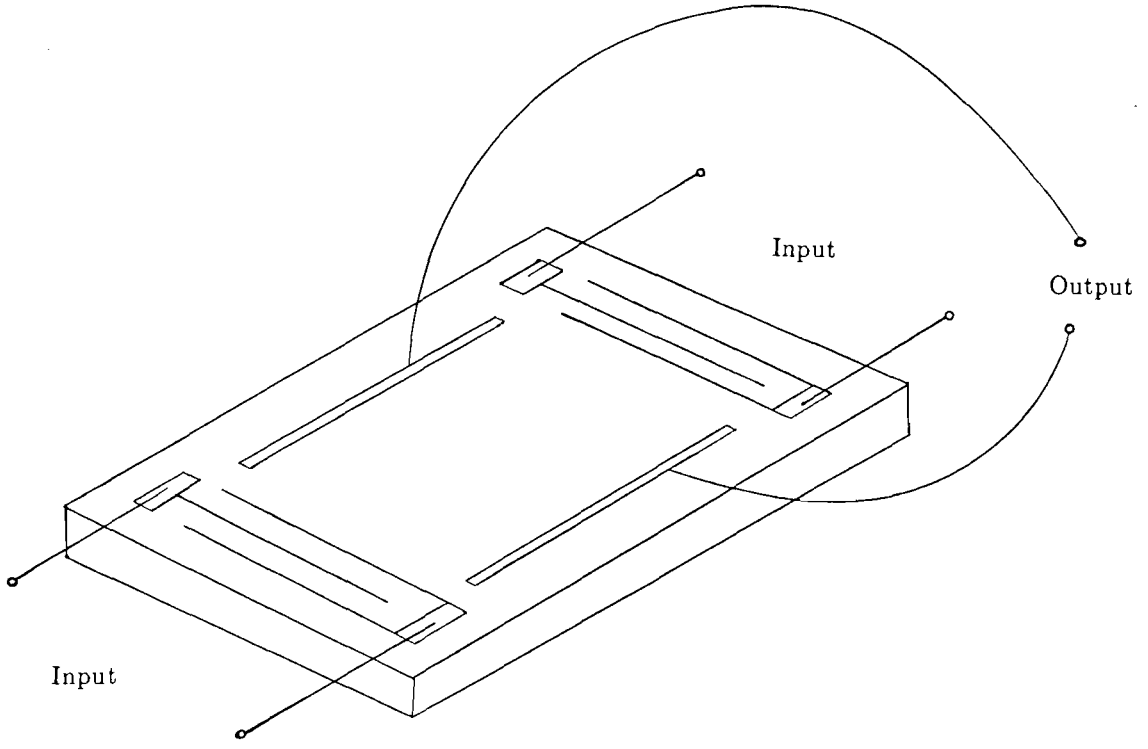

Figure 6.2 The transverse–horizontal convolver

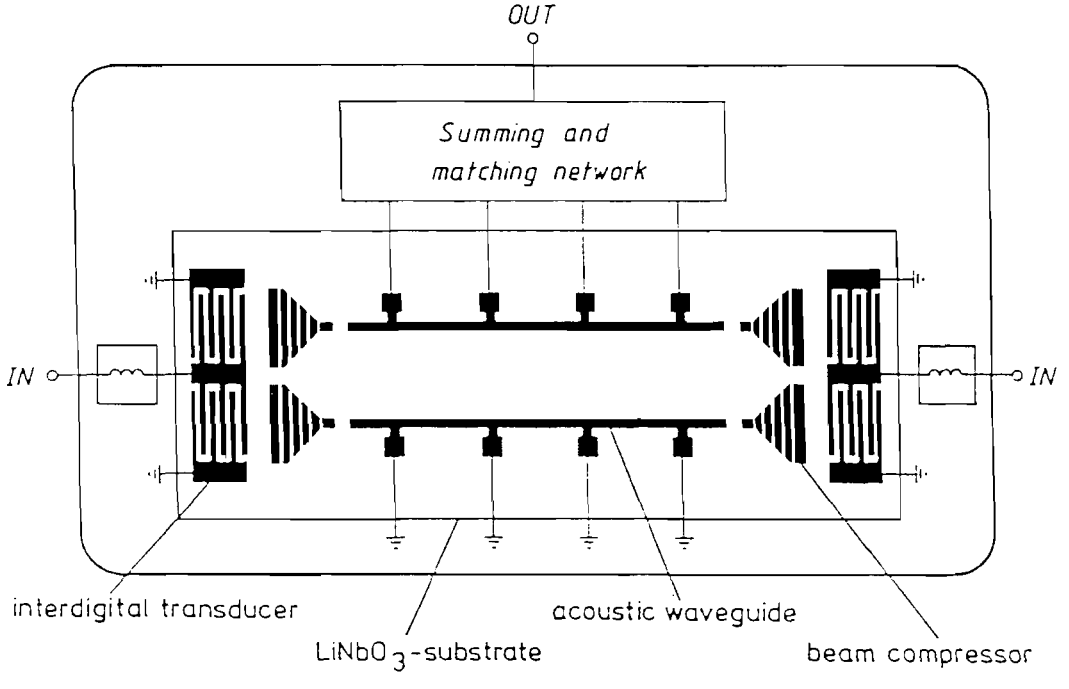

Figure 6.3 The configuration of a convolver surface, including beam compressors, waveguides and mathching parallel networks

harder. Although techniques such as the finite element method employed by Planat et al [1985] lead to useful results for particular configurations of the device under

consideration, little constructive advice regarding design can be gained from such studies.

It was decided for this thesis that the problem should be reduced to its simplest form and so in this chapter we present a study of the interaction of two oppositely propagating surface waves on a piezoelectric substrate, without considering the rôle played by transducer design and waveguides.

6.1 IDEALISED CONVOLVER

In view of the discussion above we consider in this section an idealised convolver, and set out the governing field equations and boundary conditions.

To avoid boundary reflections and the problems of imposing boundary conditions at the edges of the crystal slab, the convolver base is assumed to be a semi-infinite piezoelectric substrate occupying the half-space $-\infty < x_1 < \infty$, $-\infty < x_2 < 0$, $-\infty < x_3 < \infty$ in its reference configuration, referred to the rectangular cartesian coordinate system (x_1, x_2, x_3). The wave is assumed to propagate on the surface of the convolver in a direction parallel to the x_1-axis.

Since the problem of how the surface wave is excited would warrant an entire thesis, the transducers are replaced by two signalling conditions at $x_1 = 0$ and $x_1 = d$ on the surface $x_2 = 0$ and it is assumed that the generation of each wave is not affected by the propagation of the opposite wave. The interaction of the two oppositely propagating waves is detected by an infinitesimally thin transducer of width W, which is assumed not to affect the surface displacement and leads to the condition that the substrate surface must be stress free.

In a real convolver the base of the piezoelectric slab would be connected to the output transducer via some external circuit. This external circuit may then be in one of a number of electrical states of which the two of most interest are: open circuit (i.e. no current flowing) and short circuit (i.e. connected to ground and hence at zero electric potential).

Since we shall be considering the semi-infinite piezoelectric substrate of the idealised convolver, boundary conditions on the "base" of the convolver must be considered to be limiting conditions imposed as $x_2 \to -\infty$. For both of the external circuit states considered the convolver "base" may be assumed to be ground, that is with zero potential. It follows from this assumption that $\phi \to 0$ as $x_2 \to -\infty$. For the short-circuit condition we have that $\phi = 0$ on $x_2 = 0$, whilst, for the open circuit condition, the open circuit voltage may be assumed to be the surface potential subject to certain boundary conditions arising from the definition of the current flowing through the external circuit.

6.2 SURFACE POTENTIAL

We wish to calculate the voltage across the open circuit external to the substrate at twice the input frequency. As described earlier, in the idealised convolver this voltage is equivalent to the potential on the surface of the substrate at that particular frequency subject to certain boundary conditions.

In this section we shall derive the surface potential of the piezoelectric substrate from the momentum balance equations, solved subject to the approporiate boundary conditions. Only those interaction terms at twice the input frequency need to be considered, generic notation shall be used to denote the remaining terms.

6.2.1 Field and Boundary Equations

As in Chapter 4, the mechanical displacement and electric potential of a deformed piezoelectric substrate may be shown to satisfy the momentum balance equations

$$\rho\hat{\delta}_{ij}\ddot{u}_j - \hat{c}_{ijkl}u_{k,lj} = 2\hat{d}_{ijklmn}u_{k,l}u_{m,nj}\,, \tag{6.2.1}$$

for $y \leq 0$, where the subscripts take the values 1 to 4 and (x, y, z) are used synonymously with (x_1, x_2, x_3).

For a stress free surface $y = 0$, we require that

$$\hat{c}_{i2kl}u_{k,l} + \hat{d}_{i2klmn}u_{k,l}u_{m,n} = 0 \text{ on } y = 0\,, \tag{6.2.2}$$

for $i = 1, 2, 3$. In this chapter, in a similar way to Chapter 4, we neglect the effects of the free electric field. In view of Chapter 5 this simplification is expected only to change the results by very small amounts.

The fourth boundary condition is obtained from the "state" of the external electric circuit, and to specify it we need to describe the current flowing through this circuit in terms of the surface potential.

The current flowing across a surface may be found to be, Auld [1973],

$$I = \int_{\mathcal{S}} \mathbf{D}\cdot\mathbf{n}\,\mathrm{d}\mathcal{S}\,, \tag{6.2.3}$$

where $\mathbf{n}$ is the unit surface normal.

It therefore follows that the current flowing across the boundary of the piezoelectric substrate, and hence into the output transducer and through the external circuit, is given by

$$I^0 = \int_0^d \int_{-W/2}^{W/2} \mathrm{D}_2 \, \mathrm{d}z \, \mathrm{d}x \qquad \text{on } y = 0$$
$$= \int_0^d \int_{-W/2}^{W/2} [\hat{c}_{42kl} u_{k,l} + \hat{d}_{42klmn} u_{k,l} u_{m,n}] \, \mathrm{d}z \, \mathrm{d}x \qquad \text{on} \quad y = 0 . \qquad (6.2.4)$$

Two electrical boundary conditions are now possible. Either the external circuit is open, when we require

$$I^0 = 0 \qquad \text{on} \quad y = 0 , \qquad (6.2.5)$$

or, if the external circuit is shorted, the potential satisfies

$$u_4 = 0 \qquad \text{on} \quad y = 0 . \qquad (6.2.6)$$

Finally, since there must be no potential difference between any two points on the conducting transducer, there can be no tangential component of the electric field vector on the substrate surface. Thus it is necessary that

$$\mathbf{E} \times \mathbf{n} = 0 \qquad \text{on} \quad y = 0 ,$$

or, under the present configuration of axes,

$$E_1 = 0 \text{ and } E_3 = 0 \qquad \text{on} \quad y = 0 . \qquad (6.2.7)$$

Now $E_j = -\phi_{,j}$ and therefore equation (6.2.7) is equivalent to

$$\phi_{,1} = 0 \text{ and } \phi_{,3} = 0 , \qquad \text{on } y = 0 . \qquad (6.2.8)$$

In view of the above discussion we now have a system of four governing equations in four variables but five boundary conditions must be satisfied. We shall be considering plane surface waves propagating in the x direction and may thus take the displacement vector $\mathbf{u}$ to be independent of z. The boundary conditions (6.2.5) and (6.2.8) then simplify to

$$\int_0^d [\hat{c}_{42kl} u_{k,l} + \hat{d}_{42klmn} u_{k,l} u_{m,n}] \, \mathrm{d}x = 0 , \qquad (6.2.9)$$

and

$$u_{4,x} = 0 . \qquad (6.2.10)$$

It shall be shown later that one of the boundary conditions may be identically satisfied at each of linear order and quadratically nonlinear order, and hence the problem is not, in practice, overspecified.

The system of equations considered here is sufficiently similar to that satisfied by the single piezoelectric wave considered in Chapter 4 for us to adopt the same method of solution, multiple scales. As in Chapter 4 this technique yields a system of coupled partial differential equations in the surface amplitude which may be solved by numerical techniques. The surface potential may then be evaluated and used to calculate the open circuit voltage.

6.2.2 Slow Scales

The method of multiple scales is here applied to the field equations (6.2.1) subject to the boundary conditions (6.2.2), (6.2.9) and (6.2.10). Slow variables are introduced and a perturbation expansion of the displacement vector is used to derive field equations and boundary conditions at the various orders of approximation.

Recalling the perturbation expansion of Chapter 4 (equation (4.7.1)),

$$u_j = \epsilon u_j^{(1)}(x,y,t,\xi,\eta,\tau) + \epsilon^2 u_j^{(2)}(x,y,t,\xi,\eta,\tau) + \ldots \tag{6.2.11}$$

where ϵ is some small parameter related to the wavelength of the input waves, and the slow variables ξ, η and τ, defined through

$$\begin{aligned} \xi &= \epsilon x\,, \\ \eta &= \epsilon y\,, \\ \tau &= \epsilon z\,, \end{aligned}$$

equations (6.2.2), (6.2.9) and (6.2.10) may be written as separate systems of equations at the various orders of ϵ.

At first-order we have

$$\hat{\delta}_{ij}\ddot{u}_j^{(1)} - \hat{c}_{ijkl}\,u_{k,lj}^{(1)} = 0\,, \tag{6.2.12}$$

with the boundary conditions

$$\hat{c}_{i2kl}\,u_{k,l}^{(1)} = 0\,, \qquad i = 1,2,3\,, \tag{6.2.13}$$

$$\int_0^d [\hat{c}_{42kl}\,u_{k,l}^{(1)}]\,dx = 0\,, \tag{6.2.14}$$

$$u_{4,x}^{(1)} = 0\,, \tag{6.2.15}$$

on $y = \eta = 0$, whilst at second-order we have

$$\rho\,\hat{\delta}_{ij}\ddot{u}_j^{(2)} - \hat{c}_{ijkl}\,u_{k,lj}^{(2)} = (\hat{c}_{i1kl} + \hat{c}_{ilk1})\,u_{k,l\xi}^{(1)} + (\hat{c}_{i2kl} + \hat{c}_{ilk2})\,u_{k,l\eta}^{(1)} - 2\rho\hat{\delta}_{ij}\,\dot{u}_{j,\tau}^{(1)} + \hat{d}_{ijklmn}\,u_{k,l}^{(1)}\,u_{m,nj}^{(1)}\,, \tag{6.2.16}$$

the solution of which must satisfy the boundary conditions

$$\hat{c}_{i2kl}\,u_{k,l}^{(2)} = -\hat{c}_{i2k1}\,u_{k,\xi}^{(1)} - \hat{c}_{i2k2}\,u_{k,\eta}^{(1)} - \hat{d}_{i2klmn}\,u_{k,l}^{(1)}\,u_{m,n}^{(1)}\,, \tag{6.2.17}$$

$$0 = \int_0^d [\hat{c}_{42kl}\,u_{k,l}^{(2)} + \hat{c}_{42k1}\,u_{k,\xi}^{(1)} + \hat{c}_{42k2}\,u_{k,\eta}^{(1)} + \hat{d}_{42klmn}u_{k,l}^{(1)}u_{m,n}^{(1)}]\,dx\,, \tag{6.2.18}$$

$$u_{4,x}^{(2)} = -u_{4,\xi}^{(1)}\,, \tag{6.2.19}$$

on $y = \eta = 0$.

The boundary conditions (6.2.18) are those satisfied by an open circuit.

6.2.3 First-order solution

A solution to equations (6.2.14) and (6.2.12) subject to the boundary conditions (6.2.13) to (6.2.15) in the form of two plane surface waves, propagating parallel to the x-axis in opposite directions from $x = 0$ and $x = d$, may be represented by

$$u_j^{(1)} = A_j(y,\xi,\eta,\tau)\mathrm{e}^{\mathrm{i}K(x-t)} + B_j(y,\xi,\eta,\tau)\mathrm{e}^{\mathrm{i}K(x+t-d)} + \text{c.c.}\,. \tag{6.2.20}$$

Proceeding as in earlier chapters, it may easily be shown that the amplitudes in (6.2.20) can be expressed

$$A_j = \sum_{n=1}^{4} A_K^{(n)}(\xi,\eta,\tau)\,a_j^{(n)}\mathrm{e}^{\mathrm{i}Ks^{(n)}y}\,, \tag{6.2.21}$$

$$B_j = \sum_{n=1}^{4} B_K^{(n)}(\xi,\eta,\tau)\,a_j^{(n)}\mathrm{e}^{\mathrm{i}Ks^{(n)}y}\,, \tag{6.2.22}$$

where

$$\hat{\mathrm{L}}_{ij}(s^{(n)})\,a_j^{(n)} = 0\,, \tag{6.2.23}$$

and

$$\left|\hat{\mathrm{L}}_{ij}(s^{(n)})\right| = 0\,. \tag{6.2.24}$$

It should be noted here that $\hat{\mathrm{L}}_{ij}(s)$ has been defined by equation (4.7.8) and K represents the wavenumber.

The representation (6.2.20) may therefore be expressed

$$u_j^{(1)} = \sum_{K=1}^{\infty}\sum_{n=1}^{4}\left(A_K^{(n)}(\xi,\eta,\tau)\,\mathrm{e}^{\mathrm{i}K(x-t)} + B_K^{(n)}(\xi,\eta,\tau)\,\mathrm{e}^{\mathrm{i}K(x+t-d)}\right) a_j^{(n)}\,\mathrm{e}^{\mathrm{i}Ks^{(n)}y} + \text{c.c.}, \qquad (6.2.25)$$

where the summation is over the four admissible surface modes and all harmonics generated by the material nonlinearities.

The representation (6.2.25) may then be substituted into the boundary conditions (6.2.13) to (6.2.15). From (6.2.3) we obtain the matrix equation

$$\sum_{n=1}^{4} \hat{\mathrm{M}}_{in}\, A_K^{(n)} = 0 \quad i = 1,2,3, \qquad (6.2.26)$$

where $\hat{\mathrm{M}}_{in}$ is as defined in Chapter 4 but here there is a restriction on the subscript i.

From (6.2.15) we have

$$\sum_{n=1}^{4} A_K^{(n)} a_4^{(n)} = 0,$$

which may be combined with equation (6.2.26) to give

$$\sum_{n=1}^{4} \hat{\mathrm{M}}'_{in}\, A_K^{(n)} = 0 \quad i = 1,2,3 \text{ and } 4, \qquad (6.2.27)$$

where

$$\begin{aligned} \hat{\mathrm{M}}'_{in} &= \hat{\mathrm{M}}_{in} \quad i = 1,2,3, \\ &= a_4^{(n)} \quad i = 4. \end{aligned}$$

The condition (6.2.14) requires the evaluation of an integral with respect to the propagation distance x, between the limits $x = 0$ and $x = d$, which may be reduced to

$$\mathrm{i}K(\hat{c}_{42k1} + \hat{c}_{42k2}s^{(n)})a_k^{(n)}\left[A_K^{(n)}\mathrm{e}^{-\mathrm{i}Kt} + B_K^{(n)}\mathrm{e}^{\mathrm{i}K(t-d)}\right]\left(\mathrm{e}^{\mathrm{i}Kd} - 1\right) = 0.$$

This condition may always be satisfied with careful choice of the range of integration (that is the length of the convolver). Therefore this condition gives us no further information about the representation (6.2.25).

This leads to a crucial point in the derivation of the output voltage of the convolver. The output voltage will be calculated as the integral of the surface potential along

the length of the output transducer. Thus any surface potential term possessing exponential x dependence will lead to an integral of the above form and thus zero output voltage. We shall therefore only be interested in x-independent surface potential forms.

Now a non-trivial solution to equation (6.2.27) is ensured by satisfying the determinental condition

$$\left|\hat{\mathrm{M}}'_{in}\right| = 0\,, \tag{6.2.28}$$

which determines the surface (Rayleigh) wavespeed through the values obtained for the parameter ρ.

The particular solution, $\beta^{(n)}$, to equation (6.2.27) such that

$$\sum_{n=1}^{4} \hat{\mathrm{M}}'_{in}\beta^{(n)} = 0\,, \tag{6.2.29}$$

leads to the surface displacement

$$u_j^{(1)}(0) = \sum_{K=1}^{\infty}\sum_{n=1}^{4}\left(\gamma_K\beta^{(n)}\,a_j^{(n)}\,\mathrm{e}^{\mathrm{i}K(x-t)} + \theta_K\beta^{(n)}\,a_j^{(n)}\,\mathrm{e}^{\mathrm{i}K(x+t-d)}\right) + \text{c.c.}\,, \tag{6.2.30}$$

where γ_K and θ_K are the surface amplitudes.

In earlier chapters the linear, or first-order, solution has contained all frequencies generated by the nonlinearity. It is clear that in the case of two waves travelling in opposite directions the nonlinearities will generate terms of the type

$$u_j = f_j(y)\mathrm{e}^{\mathrm{i}(kx \pm lt)}\,,$$

where $k \neq l$. It is seen that such terms have not been included in the linear representation (6.2.25). This is because the interaction terms do not satisfy the "phase matching" condition (Kalyanasundaram [1983]).

The phase matching condition requires that all linear solutions travel in the same phase, or at the same speed. Thus, taking the fundamental waves to have $x - t$ dependence of the type

$$\mathrm{e}^{\mathrm{i}(x \pm t)}\,,$$

the linear solution may only contain terms of the form

$$u_j = f_j(y)\mathrm{e}^{\mathrm{i}k(x \pm t)}\,,$$

which can clearly only be satisfied by the harmonics of the separate input waves.

6.2.4 Second-order system

Upon substitution of the linear representation (6.2.25) into equations (6.2.16), we obtain the system

$$
\begin{aligned}
\rho\,\hat{\delta}_{ij}\,\ddot{u}_j^{(2)} - \hat{c}_{ijkl}\,u_{k,lj}^{(2)} = \\
&\sum_{K=1}^{\infty}\sum_{n=1}^{4}\Big[\Big(\hat{F}_{iK1}^{(n)}(y)\,A_{K,\xi}^{(n)} + \hat{F}_{iK2}^{(n)}(y)\,A_{K,\eta}^{(n)} + \hat{F}_{iK3}^{(n)}(y)\,A_{K,\tau}^{(n)}\Big) \\
&+ \sum_{L=1}^{K-1}\sum_{m=1}^{4}\hat{H}_{iKL}^{(m,n)}(y)\,A_{K-L}^{(n)}\,A_L^{(m)} + \sum_{L=K+1}^{\infty}\sum_{m=1}^{4}\hat{G}_{iKL}^{(m,n)}(y)\,\bar{A}_{L-K}^{(n)}\,A_L^{(m)}\Big]\,\mathrm{e}^{\mathrm{i}K(x-t)} \\
&+ \sum_{K=1}^{\infty}\sum_{n=1}^{4}\Big[\Big(\hat{F}_{iK1}^{(n)}(y)\,B_{K,\xi}^{(n)} + \hat{F}_{iK2}^{(n)}(y)\,B_{K,\eta}^{(n)} + \hat{F}_{iK3}^{(n)}(y)\,B_{K,\tau}^{(n)}\Big) \\
&+ \sum_{L=1}^{K-1}\sum_{m=1}^{4}\hat{H}_{iKL}^{(m,n)}(y)\,B_{K-L}^{(n)}\,B_L^{(m)} + \sum_{L=K+1}^{\infty}\sum_{m=1}^{4}\hat{G}_{iKL}^{(m,n)}(y)\,\bar{B}_{L-K}^{(n)}\,B_L^{(m)}\Big]\,\mathrm{e}^{\mathrm{i}K(x+t-d)} \\
&+ \sum_{K=1}^{\infty}\sum_{n=1}^{4}\sum_{m=1}^{4}\hat{Q}_{iK}^{(m,n)}(y)\,(B_K^{(m)}\,\bar{B}_K^{(n)} + A_K^{(m)}\,\bar{A}_K^{(n)}) \\
&+ \sum_{m=1}^{4}\sum_{n=1}^{4}N_i^{(m,n)}(y)\mathrm{e}^{\mathrm{i}(2t-d)} + \sum_{K=1}^{\infty}\sum_{\substack{L=-\infty\\K\neq L}}^{\infty}\sum_{m=1}^{4}\sum_{n=1}^{4}N_{iKL}^{(m,n)}(y)\mathrm{e}^{\mathrm{i}(Kx+Lt-\frac{1}{2}(K+L)d)} \\
&+ \text{c.c.}\,, \qquad (6.2.31)
\end{aligned}
$$

together with the boundary conditions, from (6.2.17),

$$
\begin{aligned}
\hat{c}_{i2kl}\,u_{k,l}^{(2)} = &\sum_{K=1}^{\infty}\sum_{n=1}^{4}\Big[\Big(\hat{f}_{i1}^{(n)}\,A_{K,\xi}^{(n)} + \hat{f}_{i2}^{(n)}\,A_{K,\eta}^{(n)}\Big) \\
&+ \sum_{L=1}^{K-1}\sum_{m=1}^{4}\hat{h}_{iKL}^{(m,n)}\,A_{K-L}^{(n)}\,A_L^{(m)} + \sum_{L=K+1}^{\infty}\sum_{m=1}^{4}\hat{g}_{iKL}^{(m,n)}\,\bar{A}_{L-K}^{(n)}\,A_L^{(m)}\Big]\,\mathrm{e}^{\mathrm{i}K(x-t)} \\
&+ \sum_{K=1}^{\infty}\sum_{n=1}^{4}\Big[\Big(\hat{f}_{i1}^{(n)}\,B_{K,\xi}^{(n)} + \hat{f}_{i2}^{(n)}\,B_{K,\eta}^{(n)}\Big) \\
&+ \sum_{L=1}^{K-1}\sum_{m=1}^{4}\hat{h}_{iKL}^{(m,n)}\,B_{K-L}^{(n)}\,B_L^{(m)} + \sum_{L=K+1}^{\infty}\sum_{m=1}^{4}\hat{g}_{iKL}^{(m,n)}\,\bar{B}_{L-K}^{(n)}\,B_L^{(m)}\Big]\,\mathrm{e}^{\mathrm{i}K(x+t-d)} \\
&+ \sum_{K=1}^{\infty}\sum_{n=1}^{4}\sum_{m=1}^{4}\hat{q}_{iK}^{(m,n)}\,(A_K^{(m)}\,\bar{A}_K^{(n)} + B_K^{(m)}\,\bar{B}_K^{(n)})
\end{aligned}
$$

$$+\sum_{m=1}^{4}\sum_{n=1}^{4} n_i^{(m,n)} e^{i(2t-d)} + \sum_{K=1}^{\infty}\sum_{\substack{L=-\infty \\ K\neq L}}^{\infty}\sum_{m=1}^{4}\sum_{n=1}^{4} n_{iKL}^{(m,n)} e^{i(Kx+Lt-\frac{1}{2}(K+L)d)}$$

$$+ \text{c.c.} \tag{6.2.32}$$

for $i = 1, 2, 3$, which must be satisfied on $y = \eta = 0$. The remaining boundary conditions (6.2.18) and (6.2.19) shall be separately considered later in this section.

Here the coefficients $\hat{F}_{iK1}^{(n)}(y)$, $\hat{G}_{iKL}^{(m,n)}(y)$, $\hat{H}_{iKL}^{(m,n)}(y)$,$\hat{f}_{iK}^{(n)}$, $\hat{g}_{iKL}^{(m,n)}$ and $\hat{h}_{iKL}^{(m,n)}$ are as defined in Chapter 4. The remaining nonlinear terms are separated to indicate those terms independent of x and of frequency 2ω, where ω is the fundamental frequency. The coefficients of these terms may be deduced to be

$$n_i^{(m,n)} = 2\hat{d}_{i2klmn} B_1^{(m)} \bar{A}_1^{(n)} \beta_k^{(m)} \bar{\beta}_m^{(n)} \delta_l^{(m)} \bar{\delta}_n^{(n)}, \tag{6.2.33}$$

and

$$N_i^{(m,n)}(y) = 2i\hat{d}_{ijklmn} B_1^{(m)} \bar{A}_1^{(n)} [\beta_k^{(m)} \bar{\beta}_m^{(n)} \delta_l^{(m)} \bar{\delta}_n^{(n)} \bar{\delta}_j^{(n)} - \beta_m^{(m)} \bar{\beta}_k^{(n)} \delta_n^{(m)} \delta_j^{(m)} \bar{\delta}_l^{(n)}] e^{i(s^{(m)} - \bar{s}^{(n)})y}, \tag{6.2.34}$$

where

$$\delta_1^{(n)} = 1, \quad \delta_2^{(n)} = s^{(n)}, \quad \delta_3^{(n)} = \delta_4^{(n)} = 0.$$

It is recalled from the linear solution that the boundary condition (6.2.14), and subsequently (6.2.18), require integration along the length of the convolver. Any term possessing exponential x-dependence may be shown to identically satisfy the boundary condition (6.2.18) and thus may be neglected in the derivation of the surface potential. The nonlinear interaction terms at frequencies other than 2ω (and those at frequency 2ω arising from interaction between harmonics) will therefore not be required explicitly in this thesis, since they will possess exponential x dependence, and hence nothing is gained by stating here the explicit form of their coefficients. It is noted that the harmonics of the two propagating input waves (represented by the first two terms on the right-hand sides of each of equations (6.2.31) and (6.2.32)) also possess exponential x-dependence. However these terms will not be used in the calculation of the output and may be included to predict the growth and decay of the linear amplitudes $A_K^{(n)}$ and $B_K^{(n)}$.

It is clear that the equations (6.2.31) and (6.2.32) may, without loss of generality, be separated into three distinct systems. The first two systems represent the two "input waves"

$$\rho\,\hat{\delta}_{ij}\,\ddot{u}_j^{(2)} - \hat{c}_{ijkl}\,u_{k,lj}^{(2)} =$$

$$\sum_{K=1}^{\infty}\sum_{n=1}^{4}\Big[\Big(\hat{F}_{iK1}^{(n)}(y)\,A_{K,\xi}^{(n)} + \hat{F}_{iK2}^{(n)}(y)\,A_{K,\eta}^{(n)} + \hat{F}_{iK3}^{(n)}(y)\,A_{K,\tau}^{(n)}\Big)$$

$$+ \sum_{L=1}^{K-1}\sum_{m=1}^{4}\hat{H}_{iKL}^{(m,n)}(y)\,A_{K-L}^{(n)}\,A_L^{(m)} + \sum_{L=K+1}^{\infty}\sum_{m=1}^{4}\hat{G}_{iKL}^{(m,n)}(y)\,\bar{A}_{L-K}^{(n)}\,A_L^{(m)}\Big]\,\mathrm{e}^{\mathrm{i}K(x-t)}$$

$$+ \sum_{K=1}^{\infty}\sum_{n=1}^{4}\sum_{m=1}^{4}\hat{Q}_{iK}^{(m,n)}(y)\,A_K^{(m)}\,\bar{A}_K^{(n)} + \text{c.c.}\,, \tag{6.2.35}$$

and

$$\rho\,\hat{\delta}_{ij}\,\ddot{u}_j^{(2)} - \hat{c}_{ijkl}\,u_{k,lj}^{(2)} =$$

$$\sum_{K=1}^{\infty}\sum_{n=1}^{4}\Big[\Big(\hat{F}_{iK1}^{(n)}(y)\,B_{K,\xi}^{(n)} + \hat{F}_{iK2}^{(n)}(y)\,B_{K,\eta}^{(n)} + \hat{F}_{iK3}^{(n)}(y)\,B_{K,\tau}^{(n)}\Big)$$

$$+ \sum_{L=1}^{K-1}\sum_{m=1}^{4}\hat{H}_{iKL}^{(m,n)}(y)\,B_{K-L}^{(n)}\,B_L^{(m)} + \sum_{L=K+1}^{\infty}\sum_{m=1}^{4}\hat{G}_{iKL}^{(m,n)}(y)\,\bar{B}_{L-K}^{(n)}\,B_L^{(m)}\Big]\,\mathrm{e}^{\mathrm{i}K(x+t-d)}$$

$$+ \sum_{K=1}^{\infty}\sum_{n=1}^{4}\sum_{m=1}^{4}\hat{Q}_{iK}^{(m,n)}(y)\,B_K^{(m)}\,\bar{B}_K^{(n)} + \text{c.c.}\,, \tag{6.2.36}$$

together with the boundary conditions

$$\hat{c}_{i2kl}\,u_{k,l}^{(2)} = \sum_{K=1}^{\infty}\sum_{n=1}^{4}\Big[\Big(\hat{f}_{i1}^{(n)}\,A_{K,\xi}^{(n)} + \hat{f}_{i2}^{(n)}\,A_{K,\eta}^{(n)}\Big)$$

$$+ \sum_{L=1}^{K-1}\sum_{m=1}^{4}\hat{h}_{iKL}^{(m,n)}\,A_{K-L}^{(n)}\,A_L^{(m)} + \sum_{L=K+1}^{\infty}\sum_{m=1}^{4}\hat{g}_{iKL}^{(m,n)}\,\bar{A}_{L-K}^{(n)}\,A_L^{(m)}\Big]\,\mathrm{e}^{\mathrm{i}K(x-t)}$$

$$+ \sum_{K=1}^{\infty}\sum_{n=1}^{4}\sum_{m=1}^{4}\hat{q}_{iK}^{(m,n)}\,A_K^{(m)}\,\bar{A}_K^{(n)} + \text{c.c.}\,, \tag{6.2.37}$$

and

$$\hat{c}_{i2kl}\,u_{k,l}^{(2)} = \sum_{K=1}^{\infty}\sum_{n=1}^{4}\Big[\Big(\hat{f}_{i1}^{(n)}\,B_{K,\xi}^{(n)} + \hat{f}_{i2}^{(n)}\,B_{K,\eta}^{(n)}\Big)$$

$$+ \sum_{L=1}^{K-1}\sum_{m=1}^{4}\hat{h}_{iKL}^{(m,n)}\,B_{K-L}^{(n)}\,B_L^{(m)} + \sum_{L=K+1}^{\infty}\sum_{m=1}^{4}\hat{g}_{iKL}^{(m,n)}\,\bar{B}_{L-K}^{(n)}\,B_L^{(m)}\Big]\,\mathrm{e}^{\mathrm{i}K(x+t-d)}$$

$$+ \sum_{K=1}^{\infty}\sum_{n=1}^{4}\sum_{m=1}^{4}\hat{q}_{iK}^{(m,n)}\,B_K^{(m)}\,\bar{B}_K^{(n)} + \text{c.c.}\,, \tag{6.2.38}$$

on $y = \eta = 0$.

The boundary condition (6.2.18) may be considered redundant as a result of the earlier x-dependence discussion, whilst (6.2.19) reveals the relations $u^{(2)}_{4,1} = -\sum_{K=1}^{\infty}\sum_{n=1}^{4} A^{(n)}_{K,\xi} e^{iK(x-t)}$, and $u^{(2)}_{4,1} = -\sum_{K=1}^{\infty}\sum_{n=1}^{4} B^{(n)}_{K,\xi} e^{iK(x-t)}$, which may be simply be incorporated into equations (6.2.37) and (6.2.38).

The third system represents the interaction frequencies

$$\rho\,\hat{\delta}_{ij}\,\ddot{u}^{(2)}_{j} - \hat{c}_{ijkl}\,u^{(2)}_{k,lj} = \sum_{m=1}^{4}\sum_{n=1}^{4} N^{(m,n)}_{i}(y) e^{i(2t-d)} + \text{c.c.}, \tag{6.2.39}$$

together with the boundary conditions

$$\hat{c}_{i2kl}\,u^{(2)}_{k,l} = \sum_{m=1}^{4}\sum_{n=1}^{4} n^{(m,n)}_{i}\, e^{i(2t-d)} + \text{c.c.}, \quad (i = 1, 2, 3, 4) \tag{6.2.40}$$

on $y = \eta = 0$. The inclusion of the fourth equation in the system (6.2.40) arisies from the fact that the interaction terms of interest are independent of x and thus the boundary condition (6.2.18) yields a constant multiple of the integrand. The condition (6.2.19) is identically satisfied by the interaction terms.

6.2.5 Second-order solution

Equations (6.2.35) to (6.2.38) are identical to equations (4.7.17) and (4.7.18) and thus, following closely the method of solution of Chapter 4, eliminating secular terms and obtaining consistency conditions for the boundary conditions, we may clearly deduce that the two slowly varying surface amplitudes satisfy the coupled equations

$$\gamma_{K,\xi} + \gamma_{K,\tau} = \sum_{L=1}^{K-1} \hat{\Pi}''_{KL}\,\gamma_{K-L}\,\gamma_{L} + \sum_{L=K+1}^{\infty} \hat{\Delta}''_{KL}\,\bar{\gamma}_{L-K}\,\gamma_{L}, \tag{6.2.41}$$

and

$$\theta_{K,\xi} - \theta_{K,\tau} = \sum_{L=1}^{K-1} \hat{\Pi}''_{KL}\,\theta_{K-L}\,\theta_{L} + \sum_{L=K+1}^{\infty} \hat{\Delta}''_{KL}\,\bar{\theta}_{L-K}\,\theta_{L}, \tag{6.2.42}$$

where the double dashed coefficients incorporate the simplified fourth boundary conditions arising from (6.2.19).

For the interaction system (6.2.39) and (6.2.40) we shall be interested in a solution of the form

$$u^{(2)}_{j} = U_{j}(y) e^{i(2t-d)}, \tag{6.2.43}$$

obtained from inspection of the nonlinear term of equation (6.2.39).

Substituting the representation (6.2.43) into the field equations (6.2.40) yields the equation

$$\hat{c}_{i2k2}U_{k,yy} + 4\rho\hat{\delta}_{ik}U_k = -N_i^{(m,n)} . \tag{6.2.44}$$

We firstly determine the complementary function to the above which is the solution to the homogeneous form of equation (6.2.44),

$$\hat{c}_{i2k2}U_{k,yy} + 4\rho\hat{\delta}_{ik}U_k = 0 . \tag{6.2.45}$$

The surface waveform

$$U_j = a_j e^{iqy} \tag{6.2.46}$$

is suggested and, upon substitution into equation (6.2.45), we obtain the matrix equation

$$\tilde{\mathrm{M}}_{ik}(q)a_k = 0 , \tag{6.2.47}$$

where

$$\tilde{\mathrm{M}}_{ik}(q) = -\hat{c}_{i2k2}q^2 + 4\rho\hat{\delta}_{ik} .$$

For a nontrivial solution (6.2.47) we require that $\det[\tilde{\mathrm{M}}_{ik}(q)] = 0$, yielding a polynomial in q of order eight. This system, however, admits the solution $q = 0$, $\mathbf{a}^T = (0, 0, 0, 1)$, i.e. a potential that does not attenuate as the depth increases. It is possible to reduce the matrix equations (6.2.47) to a system of three equations on using the rearrangement of the fourth row

$$\hat{c}_{4212}a_1 + \hat{c}_{4222}a_2 + \hat{c}_{4232}a_3 + \hat{c}_{4242}a_4 = 0 ,$$

which implies

$$\begin{aligned} a_4 &= -(\hat{c}_{4212}a_1 + \hat{c}_{4222}a_2 + \hat{c}_{4232}a_3)/\hat{c}_{4242} \\ &= -\frac{\hat{c}_{42k2}a_k}{\hat{c}_{4242}} \qquad (k = 1, 2, 3) . \end{aligned} \tag{6.2.48}$$

Substitution of (6.2.48) into the first three rows then yields the matrix equation

$$\check{\mathrm{M}}_{ik}(q)a_k = 0 \qquad \text{for} \quad i, k = 1, 2, 3 , \tag{6.2.49}$$

where

$$\check{\mathrm{M}}_{ik}(q) = -\hat{c}_{i2k2}q^2 + \frac{\hat{c}_{i242}\hat{c}_{42k2}}{\hat{c}_{4242}}q^2 + 4\rho\delta_{ik} ,$$

for i, $k = 1, 2, 3$.

Applying our earlier determinental condition to this matrix equation yields a cubic polynomial in q^2 which, for real crystallographic data, is assumed to possess positive real roots. Taking the three negative roots for q, namely $q^{(r)}$ for $r = 1, 2, 3$, we have three bulk wave modes which must be absorbed at the base of the convolver. This corresponds with results obtained experimentally and discussed by Morgan [1974].

Hence it follows that

$$\begin{aligned} U_j &= \sum_{r=1}^{3} h^{(n)} a_j^{(r)} e^{iq^{(r)}y}, \qquad \text{for } j = 1, 2, 3, 4, \\ a_4 &= -\frac{\hat{c}_{42k2}}{\hat{c}_{4242}} a_k^{(r)}, \text{ for } k = 1, 2, 3, \end{aligned} \tag{6.2.50}$$

where $h^{(r)}$ depends upon the slow variables and U_4 is obtained by integration of the fourth row of the matrix equation (6.2.45). In order to satisfy the amplitude decay condition it may be shown that the constants of integration are zero.

Returning to the inhomogeneous field equations (6.2.44), the particular solution must take the form

$$U_j = \sum_{m=1}^{4} \sum_{n=1}^{4} \sigma_j^{(m,n)} e^{i(s^{(m)} - \bar{s}^{(n)})y}, \tag{6.2.51}$$

in view of the form of $N_i^{(m,n)}$.

Upon substitution into equation (6.2.44) we obtain the matrix equation

$$\tilde{M}_{ik}(s^{(m)} - \bar{s}^{(n)}) \sigma_k^{(m,n)} = -N_i^{(m,n)}. \tag{6.2.52}$$

Now $\tilde{M}_{ik}(s^{(m)} - \bar{s}^{(n)})$ will, in general, be non-singular and may therefore be inverted to give

$$\sigma_i^{(m,n)} = -\tilde{M}_{ik}^{-1}(s^{(m)} - \bar{s}^{(n)}) N_k^{(m,n)}. \tag{6.2.53}$$

Thus the complete solution to the field equations (6.2.37) is

$$U_j = \sum_{r=1}^{3} h^{(r)} a_j^{(r)} e^{iq^{(r)}y} + \sum_{m=1}^{4} \sum_{n=1}^{4} \sigma_j^{(m,n)} e^{i(s^{(m)} - \bar{s}^{(n)})y}, \tag{6.2.54}$$

where $h^{(r)}$ must be determined from the boundary conditions (6.2.40). On substituting the representation (6.2.54) into the boundary conditions (6.2.40) we obtain the system

$$\mathrm{i}\sum_{r=1}^{3}[\hat{c}_{i2k2}a_k^{(r)}q^{(r)}]h^{(r)} = -\mathrm{i}\sum_{m=1}^{4}\sum_{n=1}^{4}[\hat{c}_{i2j2}\sigma_j^{(m,n)}(s^{(m)} - \bar{s}^{(n)})] - \sum_{m=1}^{4}\sum_{n=1}^{4} n_i^{(m,n)}, \quad (6.2.55)$$

which admits the solution

$$h^{(r)} = -\Xi_{ri}^{-1}\sum_{m=1}^{4}\sum_{n=1}^{4}\left[\hat{c}_{i2j2}\sigma_j^{(m,n)}(s^{(m)} - \bar{s}^{(n)}) - \mathrm{i}\, n_i^{(m,n)}\right], \quad (6.2.56)$$

where Ξ_{ri}^{-1} is the inverse of the non-singular matrix Ξ_{ir}, defined through

$$\Xi_{ir} = \hat{c}_{i2k2}a_k^{(r)}q^{(r)}. \quad (6.2.57)$$

The surface potential at frequency 2ω may now be expressed as

$$\phi_{2\omega}(0) = \left(\sum_{r=1}^{3} h^{(r)}a_4^{(r)} + \sum_{m=1}^{4}\sum_{n=1}^{4}\sigma_4^{(m,n)}\right)\mathrm{e}^{\mathrm{i}(2t-d)}. \quad (6.2.58)$$

6.3 POWER VECTOR

Having defined the surface potential we now wish to express the power of a surface wave in terms of its surface displacement derived in the previous section. The linear displacement vector is given by the representation

$$u_j^{(1)} = \sum_{K=1}^{\infty} \sum_{n=1}^{4} A_K^{(n)}(\xi, \eta, \tau)\, a_j^{(n)}\, \mathrm{e}^{\mathrm{i}Ks^{(n)}y}\, \mathrm{e}^{\mathrm{i}K(x-t)} + \text{c.c.}. \tag{6.3.1}$$

The definition of the power vector for a propagating piezoelectric wave in terms of the displacement vector is given in a number of standard references, see for example Auld [1973], as

$$P_j = -\frac{1}{2}\Re\left[\int_{-W/2}^{W/2}\int_{-\infty}^{0}\left\{\overline{\frac{\partial u_j^{(1)}}{\partial t}}\sigma_{jk} - \phi^{(1)}\frac{\partial \bar{\mathrm{D}}_j}{\partial t}\right\}\mathrm{d}y\,\mathrm{d}z\right], \tag{6.3.2}$$

where $\Re$ denotes the real part of a complex function.

In the linear approximation, we have the constitutive relations, see (4.4.21) and (4.4.22),

$$\begin{aligned} \sigma_{ij} &= \hat{c}_{ijkl}u_{k,l}^{(1)}, \qquad \text{for} \quad i,j = 1,\,2,\,3,\;\; k,l = 1,\,2,\,3,\,4\,, \\ D_j &= \hat{c}_{4jkl}u_{k,l}^{(1)}, \qquad \text{for} \quad j = 1,\,2,\,3,\;\; k,l = 1,\,2,\,3,\,4\,. \end{aligned} \tag{6.3.3}$$

Substituting expressions (6.3.3) into the power vector representation (6.3.2), and using (6.3.1), we obtain

$$\begin{aligned} P_j = -\frac{1}{2}\Re\Bigg[\int_{-W/2}^{W/2}\int_{-\infty}^{0}\Bigg\{\sum_{K=1}^{\infty}\sum_{m=1}^{4}(\ \mathrm{i}K)\bar{A}_K^{(m)}\bar{a}_i^{(m)}\mathrm{e}^{-\mathrm{i}K\bar{s}^{(m)}y}\mathrm{e}^{-\mathrm{i}K(x-t)}\Bigg\} \\ \times\Bigg\{\sum_{L=1}^{\infty}\sum_{n=1}^{4}(\mathrm{i}L\hat{c}_{ijk1} + \mathrm{i}Ls^{(n)}\hat{c}_{ijk2})A_L^{(n)}a_k^{(n)}\mathrm{e}^{\mathrm{i}Ls^{(n)}y}\mathrm{e}^{\mathrm{i}L(x-t)}\Bigg\} \\ -\Bigg\{\sum_{K=1}^{\infty}\sum_{m=1}^{4}A_K^{(m)}a_4^{(m)}\mathrm{e}^{\mathrm{i}Ks^{(m)}y}\mathrm{e}^{\mathrm{i}K(x-t)}\Bigg\} \\ \times\Bigg\{\sum_{L=1}^{\infty}\sum_{n=1}^{4}(-\mathrm{i}L\hat{c}_{4jk1} - \mathrm{i}L\bar{s}^{(n)}\hat{c}_{4jk2})(\mathrm{i}L)\bar{A}_L^{(n)}\bar{a}_k^{(n)}\mathrm{e}^{-\mathrm{i}L\bar{s}^{(n)}y}\mathrm{e}^{-\mathrm{i}L(x-t)}\Bigg\}\,\mathrm{d}y\,\mathrm{d}z\Bigg], \end{aligned} \tag{6.3.4}$$

for $i,j = 1,\,2,\,3$.

Now the product of two summations may be reduced to a double summation, as in Chapter 3, yielding from the representation (6.3.4)

$$P_j = -\frac{1}{2}\Re\Bigg[\int_{-W/2}^{W/2}\int_{-\infty}^{0}\sum_{K=1}^{\infty}\sum_{m=1}^{4}\sum_{L=1}^{\infty}\sum_{n=1}^{4}\Big[(\ \mathrm{i}K)\bar{A}_K^{(m)}A_L^{(n)}\bar{a}_i^{(m)}a_k^{(n)}\mathrm{e}^{\ \mathrm{i}(Ls^{(n)}-K\bar{s}^{(m)})y} \times \mathrm{e}^{\mathrm{i}(L-K)\phi}(\mathrm{i}L\hat{c}_{ijk1}+\mathrm{i}Ls^{(n)}\hat{c}_{ijk2}) - (\mathrm{i}L)A_K^{(m)}\bar{A}_L^{(n)}a_4^{(m)}\bar{a}_k^{(n)}\mathrm{e}^{\mathrm{i}(Ks^{(m)}-L\bar{s}^{(n)})y}\mathrm{e}^{\mathrm{i}(K-L)\phi}(-\mathrm{i}L\hat{c}_{4jk1}-\ \mathrm{i}L\bar{s}^{(n)}\hat{c}_{4jk2})\Big]\,\mathrm{d}y\,\mathrm{d}z\Bigg]. \tag{6.3.5}$$

We shall now simplify the previous representation by only considering those terms deriving from the fundamental frequency of the input wave. This is possible since we shall later restrict our attention to the initial signalling condition in which the higher harmonics have zero amplitude. With this approach we obtain

$$P_j = -\frac{1}{2}\Re\Bigg[\int_{-W/2}^{W/2}\int_{-\infty}^{0}\sum_{m=1}^{4}\sum_{n=1}^{4}\Big[\ \mathrm{i}\bar{A}_1^{(m)}A_1^{(n)}\bar{a}_i^{(m)}a_k^{(n)}\mathrm{e}^{\ \mathrm{i}(s^{(n)}-\bar{s}^{(m)})y}(\mathrm{i}\hat{c}_{ijk1}+\mathrm{i}s^{(n)}\hat{c}_{ijk2}) - A_1^{(m)}\bar{A}_1^{(n)}a_4^{(m)}\bar{a}_k^{(n)}\mathrm{e}^{\mathrm{i}(s^{(m)}-\bar{s}^{(n)})y}\mathrm{i}(-\mathrm{i}\hat{c}_{4jk1}-\mathrm{i}\bar{s}^{(n)}\hat{c}_{4jk2})\Big]\,\mathrm{d}y\,\mathrm{d}z\Bigg],$$

or

$$P_j = -\frac{1}{2}\Re\Bigg[\int_{-W/2}^{W/2}\int_{-\infty}^{0}\sum_{m=1}^{4}\sum_{n=1}^{4}\Big[A_1^{(m)}\bar{A}_1^{(n)}\Big(\bar{a}_i^{(n)}a_k^{(m)}(\hat{c}_{ijk1}-s^{(m)}\hat{c}_{ijk2}) - a_4^{(m)}\bar{a}_k^{(n)}(\hat{c}_{4jk1}+\bar{s}^{(n)}\hat{c}_{4jk2})\Big)\mathrm{e}^{\mathrm{i}(s^{(m)}-\bar{s}^{(n)})y}\Big]\,\mathrm{d}y\,\mathrm{d}z\Bigg], \tag{6.3.6}$$

and, performing the integrations,

$$\frac{P_j}{W} = \frac{1}{2}\Re\left[\sum_{m=1}^{4}\sum_{n=1}^{4}\frac{\mathrm{i}\left[A_1^{(m)}\bar{A}_1^{(n)}\left(\bar{a}_i^{(n)}a_k^{(m)}(\hat{c}_{ijk1}-s^{(m)}\hat{c}_{ijk2}) - a_4^{(m)}\bar{a}_k^{(n)}(\hat{c}_{4jk1}+\bar{s}^{(n)}\hat{c}_{4jk2})\right)\right]}{(s^{(m)}-\bar{s}^{(n)})}\right]. \tag{6.3.7}$$

In this section we are concerned with the power input to the wave. Thus we may take $A_1^{(n)} = \gamma_1\beta^{(n)}$, where γ_1 is the initial amplitude of the wave, yielding the power vector per unit width $\tilde{P}_j$ as

$$\tilde{P}_j = \frac{1}{2}\Re\left[\sum_{m=1}^{4}\sum_{n=1}^{4}\frac{\mathrm{i}\left[\gamma_1^2\beta^{(m)}\bar{\beta}^{(n)}\left(\bar{a}_i^{(n)}a_k^{(m)}(\hat{c}_{ijk1}-s^{(m)}\hat{c}_{ijk2}) - a_4^{(m)}\bar{a}_k^{(n)}(\hat{c}_{4jk1}+\bar{s}^{(n)}\hat{c}_{4jk2})\right)\right]}{(s^{(m)}-\bar{s}^{(n)})}\right]. \tag{6.3.8}$$

The power input to the wave is defined to be $|\tilde{\mathbf{P}}|$.

6.4 FIGURE OF MERIT

The figure of merit, as described earlier in this chapter, is the accepted measure of the efficiency of a convolver. The measurement is based on what is commonly called a degenerate convolver, that is a convolver in which both input signals are the same single frequency and the output is only measured at twice this input frequency. The figure of merit may then be defined mathematically, Lim et al [1974], as

$$M = \frac{\phi_{2\omega}^{rms}(0)}{\left(\tilde{P}^{(1)}\tilde{P}^{(2)}\right)^{1/2}}, \tag{6.4.1}$$

where $\tilde{P}^{(1)}$ and $\tilde{P}^{(2)}$ are the power per unit width input to each of the transducers respectively, and $\phi_{2\omega}^{rms}$ is the root mean square open circuit voltage of the convolver.

Using the results (6.2.58), (6.3.8) and (6.4.1), we have that

$$M = \frac{\frac{1}{\sqrt{2}}\left(\sum_{r=1}^{3} h^{(r)} a_4^{(r)} + \sum_{m=1}^{4}\sum_{n=1}^{4} \sigma_4^{(m,n)}\right)}{\left((\tilde{P}_1)^2 + (\tilde{P}_2)^2\right)^{1/2}} \tag{6.4.2}$$

where

$$\tilde{P}_i = \frac{1}{2}\Im\left[\sum_{m=1}^{4}\sum_{n=1}^{4} \frac{\left[\gamma_1^2 \beta^{(m)} \bar{\beta}^{(n)} \left(\bar{a}_i^{(n)} a_k^{(m)} (\hat{c}_{ijk1} + s^{(m)} \hat{c}_{ijk2}) + a_4^{(m)} \bar{a}_k^{(n)} (\hat{c}_{4jk1} + \bar{s}^{(n)} \hat{c}_{4jk2})\right)\right]}{(s^{(m)} - \bar{s}^{(n)})}\right].$$

Before evaluating the figure of merit for a particular material and orientation we must make a realistic estimate of the surface amplitude in order to define the small parameter ϵ. From information supplied in a personal communication from Dr H. Grassl, we can assume that the wavelength used in a convolver is typically of the order 10^{-5}m, whilst, from power loss measurements, the initial amplitude is of the order 10^{-7}m and the wavenumber 10^{5}m^{-1}. Using the definition of the slow parameter given by Kalyanasundaram [1983], the estimate of ϵ now becomes

$$\begin{aligned} \epsilon &= k_0 |\mathbf{u}| \\ &= 10^{-2}, \end{aligned} \tag{6.4.3}$$

where here $\mathbf{u}$ represents the actual (dimensional) surface displacement.

Thus, for an actual convolver of length 3×10^{-2}m, we only require to consider propagation up to a non-dimensional distance of $\xi_1 = \epsilon a x \approx 10^{-6}$. This distance is so short that the decay of the fundamental and growth of the higher harmonics

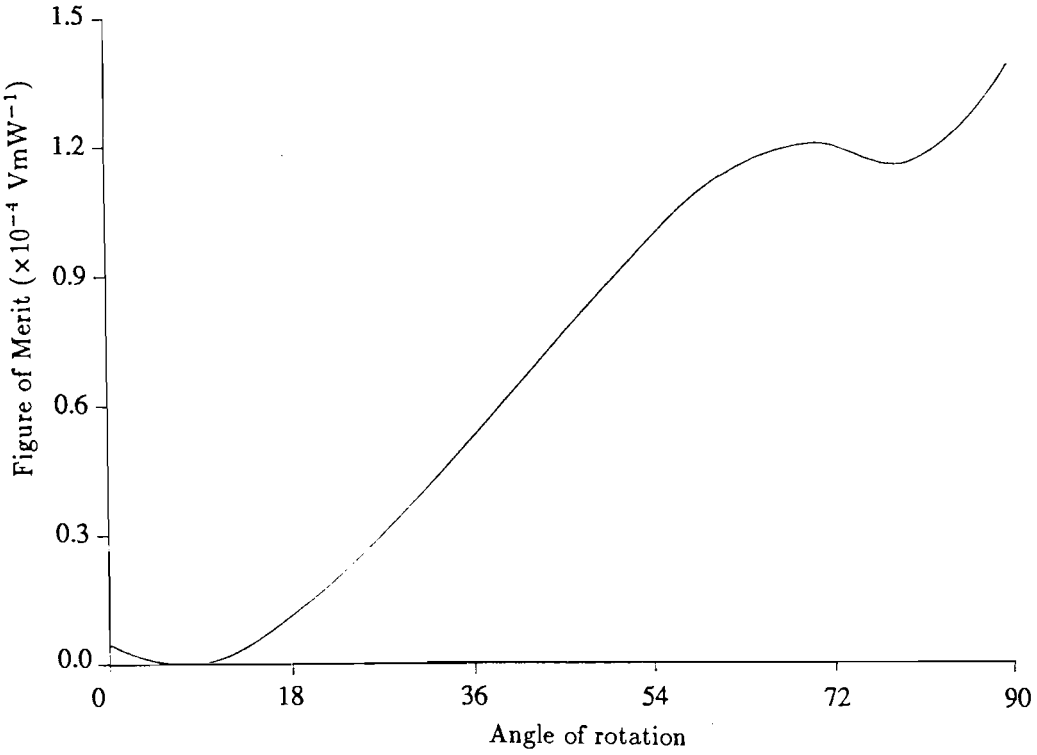

Figure 6.4.1 Figure of Merit for a degenerate convolver using the data of Cho and Yamanouchi [1987]

will be unnoticed. We can therefore, to a good approximation, use the simplest form of amplitude relation namely $\gamma_1 = 1$.

Using the numerical routines written for the analyses of earlier chapters, the Figure of Merit may now be evaluated for any material substrate in any orientation. Figures 6.4.1 and 6.4.2 present results obtained using this technique, for the data given in both Cho and Yamanouchi [1987] and Ganguly and Davis [1980]. Since the advantages of the method of multiple scales in predicting the growth of higher harmonic terms has been eliminated through the boundary conditions, the final analysis of this chapter is identical to that of Ganguly and Davis and thus no further information may be obtained from this study.

Cho and Yamanouchi present results for this specific case but do not discuss the apparent inconsistencies between the results they obtained using the data of Ganguly and Davis and the results of Ganguly and Davis themselves. The numerical value of the Figure of Merit for propagation along the Z-axis of Y-cut lithium niobate attained by Cho and Yamanouchi appears to be approximately half that of Ganguly and Davis. Since our results appear to duplicate those of Cho and

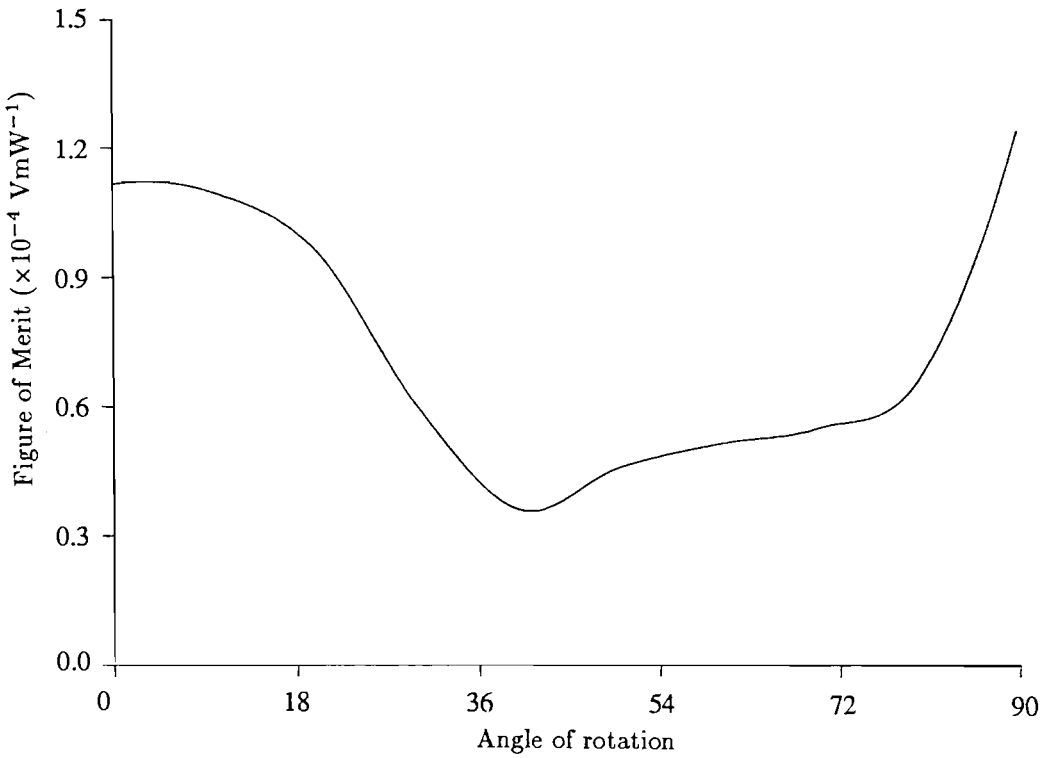

Figure 6.4.2 Figure of Merit for a degenerate convolver using the data of Ganguly and Davis [1981]

Yamanouchi, it must be assumed that a numerical error is present in the results of Ganguly and Davis.

Private communications with Dr H. Grassl have also recently revealed that most convolver designers treat such devices as essentially linear with a nonlinear "correction factor" and only nonlinear theories incorporating models of the complicated transducer configurations and waveguide networks described in the introduction to this chapter would be likely to influence their choice of design. Such extensions would be very difficult to include and are not pursued further in this thesis. The work in this chapter is not therefore of direct use to experimentalists, but sets out a general approach for calculating the Figure of Merit and, by agreeing with the results of Cho and Yamanouchi, our results support the accuracy of our numerical routines.

7 Co-Directional Waves

The development of filtering devices has progressed concurrently with that of general surface acoustic wave devices outlined in the previous chapter. A detailed literature study of the history of filter design will not be presented here since it would be predominantly experimental results pertaining to particular operational and design advances which shall be neglected in our idealised model. The interested reader is referred to the book of Mathews [1977] which presents a collection of theoretical and experimental papers. It is useful, however to outline briefly the function of an acoustic filtering device.

The process of filtering in electronics requires that certain frequencies be removed from a spectrum of input frequencies. This may be easily achieved by the nonlinear interaction of acoustic waves propagating in the same direction, in which two waves of different frequencies interact to produce sum and difference frequencies. Careful arrangement of frequency ranges and position of excitation can result in certain frequencies being effectively "cancelled out", thus achieving the required filtering effect.

Private communication with Dr Grassl of Siemens Research revealed that one specific problem of nonlinear acoustic filtering could be of possible interest, namely that of noise, or distortion, in the external circuit caused by spurious interactions.

Nonlinear harmonic generation causes terms of the frequencies

$$(\pm K f_1 \pm L f_2)$$

to be generated, where f_1 and f_2 are two particular input frequencies and K and L are positive integers.

If $K = L = 1$, then such interactions will most commonly lie outside the output response range of the filter which will most commonly be less than one octave

(Jacobi [1986]). Such interaction waves can, however, lead to the elimination of certain frequencies and it may be required that they be maximised.

If $K + L = 3$, the nonlinear interaction can be of the type

$$2f_1 - f_2 ,$$

which, if f_2 is sufficiently close to f_1, will be close to both f_1 and f_2 in the output spectrum. This may lead to unwanted "noise" in the external circuit to the convolver and must therefore be minimised.

This effect is known as intermodulation distortion (IMD), with $K + L = 2$ termed second-order IMD, and $K + L = 3$ third-order. At present the order of magnitude of these IMD effects may be calculated by an *ad hoc* method derived from power considerations and resulting in logarithmic scale plots of input against output power from which "intercept points", determining the strength of the distortion, are read.

Kalyanasundaram [1982] studied a very similar problem in nonlinear isotropic elasticity by the multiple scales technique developed for single propagating surface waves, Kalyanasundaram [1981]. This paper necessarily possesed the limitations of Kalyanasundaram's earlier work, as discussed by Lardner [1983], namely the omission of a secularity condition with respect to the depth component. The simplest problem of second-order IMD effect were considered together with second harmonic generation. This procedure will be adapted for use in this chapter and extended to include third-order effects.

The simplifications of Chapter 4 will be utilised to present a method of solution applicable to both anisotropic elastic and piezoelectric substrates. Results will be presented for the two sample materials, magnesium oxide and lithium niobate, considered in earlier chapters.

7.1 THE PROBLEM

Again we consider a piezoelectric substrate which in its natural reference state occupies the semi-infinite region $x_2 < 0$, relative to a reference system of rectangular Cartesian coordinates x_1, x_2, x_3. As in Chapter 4 we adopt the assumption that all free-space stress and electric field effects may be realistically neglected because of the small relative magnitude of the material permittivity.

The field equations governing the deformation of the material can then be written as

$$\rho\,\ddot{u}_i = \sigma_{ij,j}\,, \tag{7.1.1}$$

$$\mathrm{D}_{j,j} = 0\,, \tag{7.1.2}$$

cf. equations (4.5.1) and (4.5.2).

Assuming that the interface between the solid and free space ($x_2 = 0$, $-\infty < x_1 < \infty$, $-\infty < x_3 < \infty$) remains stress free and that the electric displacement vector is continuous across this interface (neglecting free-space electric field effects as in Chapter 4), we impose the boundary conditions

$$\sigma_{i2} = 0 \text{ on } x_2 = 0\,, \tag{7.1.3}$$

and

$$\mathrm{D}_2 = 0 \text{ on } x_2 = 0\,. \tag{7.1.4}$$

Adopting the contracted notation introduced through equations (4.4.17) and (4.4.20), the field equations and boundary conditions may be written compactly as

$$\hat{c}_{ijkl}u_{k,lj} - \rho\hat{\delta}_{ij}\ddot{u}_j = -2\epsilon\hat{d}_{ijklmn}u_{k,l}u_{m,nj}\,, \tag{7.1.5}$$

with

$$\hat{c}_{i2kl}u_{k,l} = -\epsilon\hat{d}_{i2klmn}u_{k,l}u_{m,n} \text{ on } x_2 = 0\,, \tag{7.1.6}$$

where $\hat{\delta}_{ij}$ denotes the modified Kronecker delta and repeated subscripts are allowed to range over the values 1 to 4. The small parameter ϵ is introduced through the replacements $u_j \to \epsilon u_j$, $\phi \to \epsilon\phi$, $\sigma_{ij} \to \epsilon\sigma_{ij}$ and $\mathrm{D}_j \to \epsilon\mathrm{D}_j$ to trace the various orders of magnitude.

7.2 SOLUTION

Utilising the small positive scaling parameter, ϵ, we define the slow variables $\xi = \epsilon x$, $\eta = \epsilon y$ and $\tau = \epsilon t$, and seek a perturbation solution in the form

$$u_j(x,y,t,\xi,\eta,\tau) = u_j^{(1)}(x,y,t,\xi,\eta,\tau) + \epsilon u_j^{(2)}(x,y,t,\xi,\eta,\tau) + \dots \,. \tag{7.2.1}$$

When equations (7.2.1) are substituted into equations (7.1.5) and (7.1.6) and coefficients of ϵ are compared we obtain the first- and second-order systems of equations

$$\hat{c}_{ijkl}u_{k,lj}^{(1)} - \rho\hat{\delta}_{ij}\ddot{u}_j^{(1)} = 0\,, \tag{7.2.2}$$

$$\begin{aligned}\hat{c}_{ijkl}u_{k,lj}^{(2)} - \rho\hat{\delta}_{ij}\ddot{u}_j^{(2)} &= -2\hat{d}_{ijklmn}u_{k,l}^{(1)}u_{m,nj}^{(1)} - \hat{c}_{i1kl}u_{k,l\xi}^{(1)} - \hat{c}_{ijk1}u_{k,j\xi}^{(1)} \\ &\quad - \hat{c}_{i2kl}u_{k,l\eta}^{(1)} - \hat{c}_{ijk2}u_{k,j\eta}^{(1)} + 2\rho\hat{\delta}_{ij}u_{j,t\tau}^{(1)}\,,\end{aligned} \tag{7.2.3}$$

with the corresponding boundary conditions on $y = \eta = 0$ being

$$\hat{c}_{i2kl}u_{k,l}^{(1)} = 0\,, \tag{7.2.4}$$

$$\hat{c}_{i2kl}u_{k,l}^{(2)} = -\hat{d}_{i2klmn}u_{k,l}^{(1)}u_{m,n}^{(1)} - \hat{c}_{i2k1}u_{k,\xi}^{(1)} - \hat{c}_{i2k2}u_{k,\eta}^{(1)}\,. \tag{7.2.5}$$

7.2.1 First-Order Solution

It can be deduced from earlier chapters that equation (7.2.2) has the particular Rayleigh wave solution

$$u_j^{(1)} = \sum_{n=1}^{4} a_j^{(n)} e^{is^{(n)}y} e^{i\psi}\,, \tag{7.2.6}$$

where

$$\begin{aligned}&\psi = x - t\,,\\ &\hat{L}_{jk}(s^{(n)})a_k^{(n)} = 0\,,\end{aligned} \tag{7.2.7}$$

with

$$\hat{L}_{jk}(s) = \hat{c}_{j2k2}s^2 + (\hat{c}_{j2k1} + \hat{c}_{j1k2})s + \hat{c}_{j1k1} - \rho\hat{\delta}_{jk}\,.$$

and the non-dimensionalisation of Chapter 4 is assumed.

Non-zero solutions to (7.2.7) exist only when

$$\left|\hat{L}_{jk}(s^{(n)})\right| = 0\,, \tag{7.2.8}$$

In order to study the nonlinear mode coupling of two co-directional surface acoustic waves by the method of multiple scales we consider a first-order solution which

includes all the harmonics and all the combination frequencies of the two waves introduced through the nonlinearities. Thus our linear solution has the form

$$u_j^{(1)} = \sum_{K>0}\sum_{n=1}^{4}\left[A_K^{(n)}a_j^{(n)}\mathrm{e}^{\mathrm{i}Ks^{(n)}y}\mathrm{e}^{\mathrm{i}K\psi} + B_K^{(n)}a_j^{(n)}\mathrm{e}^{\mathrm{i}Krs^{(n)}y}\mathrm{e}^{\mathrm{i}Kr\psi}\right]$$
$$+ \sum_{K,L>0}\sum_{n=1}^{4} C_{KL}^{(n)}a_j^{(n)}\mathrm{e}^{\mathrm{i}(K+Lr)s^{(n)}y}\mathrm{e}^{\mathrm{i}(K+Lr)\psi}$$
$$+ \sum_{\substack{K,L>0\\K\neq Lr}}\sum_{n=1}^{4} D_{KL}^{(n)}a_j^{(n)}\mathrm{e}^{\mathrm{i}|K-Lr|s^{(n)}y}\mathrm{e}^{\mathrm{i}|K-Lr|\psi} \quad + \quad \text{c.c.}, \qquad (7.2.9)$$

where $r = K_2/K_1$ $(K_2 < K_1)$, the ratio of the wavenumbers of the two interacting waves.

Here, unlike the earlier case of two oppositely propagating waves discussed in Chapter 6, combination frequencies are included in the linear expansion since any nonzero multiple of both the wavenumber and decay parameter will satisfy the dispersion relation and hence all interactions will satisfy the "phase matching" condition.

The complex amplitudes, $A_K^{(n)}$ and $B_K^{(n)}$ (of the harmonic terms) and $C_{KL}^{(n)}$ and $D_{KL}^{(n)}$ (of the combination frequency terms) are taken here to be functions of the slow variables ξ, η and τ alone, to allow for slow modulation of the amplitudes with respect to space and time.

Motivated by the approximations adopted by Kalyanasundaram [1981,1983], attention is restricted to the truncated system involving only $A_K^{(n)}$, $B_K^{(n)}$, $K = 1, 2$, and $C_{KL}^{(n)}$, $D_{KL}^{(n)}$, $K = L = 1$, thus considering only second-order IMD terms. At this stage, for notational simplicity it is convenient to define

$$q_1 = 1\,, \quad q_2 = r\,, \quad q_3 = 2\,, \quad q_4 = 2r\,, \quad q_5 = 1+r\,, \quad q_6 = 1-r\,, \qquad (7.2.10)$$

and

$$\alpha_1^{(n)} = A_1^{(n)}\,, \quad \alpha_2^{(n)} = B_1^{(n)}\,, \quad \alpha_3^{(n)} = A_2^{(n)}\,,$$
$$\alpha_4^{(n)} = B_2^{(n)}\,, \quad \alpha_5^{(n)} = C_{11}^{(n)}\,, \quad \alpha_6^{(n)} = D_{11}^{(n)}\,, \qquad (7.2.11)$$

so that the truncated first-order solution can now be neatly represented by

$$u_j^{(1)} = \sum_{I=1}^{6}\sum_{n=1}^{4}\alpha_I^{(n)}(\xi,\eta,\tau)a_j^{(n)}\mathrm{e}^{\mathrm{i}q_Is^{(n)}y}\mathrm{e}^{\mathrm{i}q_I\psi} \quad + \quad \text{c.c.}\,. \qquad (7.2.12)$$

	q_1	q_2	q_3	q_4	q_5	q_6
q_1	q_3	q_5	–	–	–	–
q_2	q_5	q_4	–	–	–	q_1
q_3	–	–	–	–	–	–
q_4	–	–	–	–	–	q_5
q_5	–	–	–	–	–	q_3
q_6	–	q_1	–	q_5	q_3	–
$\bar{q}_1$	–	$\bar{q}_6$	q_1	–	q_2	$\bar{q}_2$
$\bar{q}_2$	q_6	–	–	q_2	q_1	–
$\bar{q}_3$	$\bar{q}_1$	–	–	–	$\bar{q}_6$	$\bar{q}_5$
$\bar{q}_4$	–	$\bar{q}_2$	–	–	q_6	–
$\bar{q}_5$	$\bar{q}_2$	$\bar{q}_1$	q_6	$\bar{q}_6$	–	$\bar{q}_4$
$\bar{q}_6$	q_2	–	q_5	–	q_4	–

Table 7.2.1 Modal interactions. The top row and left column indicate the two interacting modes

This solution must fulfil the first-order boundary conditions (7.2.4) and therefore it is necessary to satisfy

$$\sum_{n=1}^{4} \hat{M}_{kn} \alpha_I^{(n)} = 0\,, \quad \text{on } y = \eta = 0\,, \tag{7.2.13}$$

where

$$\hat{M}_{kn} = \left(\hat{c}_{k2j1} + \hat{c}_{k2j2} s^{(n)}\right) a_j^{(n)}\,. \tag{7.2.14}$$

In the above and for the remainder of this chapter I takes the values $1, 2, \ldots, 6$.

To ensure a non-trivial solution of equation (7.2.13), we require $\left|\hat{M}_{kn}\right| = 0$. The latter allows the determination of the Rayleigh wave speed, which must be calculated iteratively with equation (7.2.8). Denoting a particular solution of equation (7.2.8) by $\beta^{(n)}$ we can write

$$\alpha_I^{(n)} = \beta^{(n)} \gamma_I\,, \quad \text{on } y = \eta = 0\,, \tag{7.2.15}$$

where γ_I is related to the linear surface amplitude through

$$u_j^{(1)}(x, 0, \xi, \tau) = \sum_{I=1}^{6} \sum_{n=1}^{4} \gamma_I(\xi, \tau) \beta^{(n)} a_j^{(n)} \mathrm{e}^{\mathrm{i} q_I \psi} \quad + \quad \text{c.c.}\,. \tag{7.2.16}$$

7.2.2 Second-Order System

The linear solution (7.2.12) can now be substituted into equations (7.2.3) and (7.2.5) to yield a coupled second-order system satisfied by $u_j^{(2)}$. Taking the six linear modes, represented by q_I, $I = 1, 2, \ldots, 6$ and categorizing them as Types 1 to 6, a table of possible interaction modes, Table 7.2.1, may be drawn up. Here the dash denotes an interaction frequency of higher order than those considered here.

Using Table 7.2.1 the coupled second-order system can be written in the form

$$
\begin{aligned}
&\hat{c}_{ijkl}u^{(2)}_{k,lj} - \rho\hat{\delta}_{ij}\ddot{u}^{(2)}_{j} = \\
&\sum_{n=1}^{4}\Bigg[F^{(n)}_{i11}(y)\alpha^{(n)}_{1,\xi} + F^{(n)}_{i12}(y)\alpha^{(n)}_{1,\eta} + F^{(n)}_{i13}(y)\alpha^{(n)}_{1,\tau} + \sum_{m=1}^{4}\Big\{G^{(m,n)}_{i13}(y)\bar{\alpha}^{(n)}_{1}\alpha^{(m)}_{3} \\
&\qquad + G^{(m,n)}_{i25}(y)\bar{\alpha}^{(n)}_{2}\alpha^{(m)}_{5} + H^{(m,n)}_{i26}(y)\alpha^{(n)}_{2}\alpha^{(m)}_{6}\Big\}\Bigg]\, e^{iq_1\psi} \\
&+\sum_{n=1}^{4}\Bigg[F^{(n)}_{i21}(y)\alpha^{(n)}_{2,\xi} + F^{(n)}_{i22}(y)\alpha^{(n)}_{2,\eta} + F^{(n)}_{i23}(y)\alpha^{(n)}_{2,\tau} + \sum_{m=1}^{4}\Big\{G^{(m,n)}_{i24}(y)\bar{\alpha}^{(n)}_{2}\alpha^{(m)}_{4} \\
&\qquad + G^{(m,n)}_{i15}(y)\bar{\alpha}^{(n)}_{1}\alpha^{(m)}_{5} + G^{(m,n)}_{i61}(y)\bar{\alpha}^{(n)}_{6}\alpha^{(m)}_{1}\Big\}\Bigg]\, e^{iq_2\psi} \\
&+\sum_{n=1}^{4}\Bigg[F^{(n)}_{i31}(y)\alpha^{(n)}_{3,\xi} + F^{(n)}_{i32}(y)\alpha^{(n)}_{3,\eta} + F^{(n)}_{i33}(y)\alpha^{(n)}_{3,\tau} + \sum_{m=1}^{4}\Big\{H^{(m,n)}_{i11}(y)\alpha^{(n)}_{1}\alpha^{(m)}_{1} \\
&\qquad + H^{(m,n)}_{i56}(y)\alpha^{(n)}_{5}\alpha^{(m)}_{6}\Big\}\Bigg]\, e^{iq_3\psi} \\
&+\sum_{n=1}^{4}\Bigg[F^{(n)}_{i41}(y)\alpha^{(n)}_{4,\xi} + F^{(n)}_{i42}(y)\alpha^{(n)}_{4,\eta} + F^{(n)}_{i43}(y)\alpha^{(n)}_{4,\tau} + \sum_{m=1}^{4}\Big\{H^{(m,n)}_{i22}(y)\alpha^{(n)}_{2}\alpha^{(m)}_{2} \\
&\qquad + G^{(m,n)}_{i65}(y)\bar{\alpha}^{(n)}_{6}\alpha^{(m)}_{5}\Big\}\Bigg]\, e^{iq_4\psi} \\
&+\sum_{n=1}^{4}\Bigg[F^{(n)}_{i51}(y)\alpha^{(n)}_{5,\xi} + F^{(n)}_{i52}(y)\alpha^{(n)}_{5,\eta} + F^{(n)}_{i53}(y)\alpha^{(n)}_{5,\tau} + \sum_{m=1}^{4}\Big\{H^{(m,n)}_{i12}(y)\alpha^{(n)}_{1}\alpha^{(m)}_{2} \\
&\qquad + H^{(m,n)}_{i46}(y)\alpha^{(n)}_{4}\alpha^{(m)}_{6} + G^{(m,n)}_{i63}(y)\bar{\alpha}^{(n)}_{6}\alpha^{(m)}_{3}\Big\}\Bigg]\, e^{iq_5\psi} \\
&+\sum_{n=1}^{4}\Bigg[F^{(n)}_{i61}(y)\alpha^{(n)}_{6,\xi} + F^{(n)}_{i62}(y)\alpha^{(n)}_{6,\eta} + F^{(n)}_{i63}(y)\alpha^{(n)}_{6,\tau} + \sum_{m=1}^{4}\Big\{G^{(m,n)}_{i21}(y)\bar{\alpha}^{(n)}_{2}\alpha^{(m)}_{1} \\
&\qquad + G^{(m,n)}_{i53}(y)\bar{\alpha}^{(n)}_{5}\alpha^{(m)}_{3} + G^{(m,n)}_{i45}(y)\bar{\alpha}^{(n)}_{4}\alpha^{(m)}_{5}\Big\}\Bigg]\, e^{iq_6\psi} \\
&+ \text{c.c.}\ , \qquad (7.2.17)
\end{aligned}
$$

with the boundary conditions

$$
\begin{aligned}
&\hat{c}_{i2kl}u^{(2)}_{k,l} = \\
&\sum_{n=1}^{4}\Bigg[f^{(n)}_{i1}\alpha^{(n)}_{1,\xi} + f^{(n)}_{i2}\alpha^{(n)}_{1,\eta} + \sum_{m=1}^{4}\Big\{g^{(m,n)}_{i13}\bar{\alpha}^{(n)}_{1}\alpha^{(m)}_{3} + g^{(m,n)}_{i25}\bar{\alpha}^{(n)}_{2}\alpha^{(m)}_{5} \\
&\qquad + h^{(m,n)}_{i26}\alpha^{(n)}_{2}\alpha^{(m)}_{6}\Big\}\Bigg]\, e^{iq_1\psi} \\
&+\sum_{n=1}^{4}\Bigg[f^{(n)}_{i1}\alpha^{(n)}_{2,\xi} + f^{(n)}_{i2}\alpha^{(n)}_{2,\eta} + \sum_{m=1}^{4}\Big\{g^{(m,n)}_{i24}\bar{\alpha}^{(n)}_{2}\alpha^{(m)}_{4} + g^{(m,n)}_{i15}\bar{\alpha}^{(n)}_{1}\alpha^{(m)}_{5} \\
&\qquad + g^{(m,n)}_{i61}\bar{\alpha}^{(n)}_{6}\alpha^{(m)}_{1}\Big\}\Bigg]\, e^{iq_2\psi}
\end{aligned}
$$

$$+\sum_{n=1}^{4}\left[f_{i1}^{(n)}\alpha_{3,\xi}^{(n)}+f_{i2}^{(n)}\alpha_{3,\eta}^{(n)}+\sum_{m=1}^{4}\left\{h_{i11}^{(m,n)}\alpha_1^{(n)}\alpha_1^{(m)}+h_{i56}^{(m,n)}\alpha_5^{(n)}\alpha_6^{(m)}\right\}\right]\mathrm{e}^{\mathrm{i}q_3\psi}$$
$$+\sum_{n=1}^{4}\left[f_{i1}^{(n)}\alpha_{4,\xi}^{(n)}+f_{i2}^{(n)}\alpha_{4,\eta}^{(n)}+\sum_{m=1}^{4}\left\{h_{i22}^{(m,n)}\alpha_2^{(n)}\alpha_2^{(m)}+g_{i65}^{(m,n)}\bar{\alpha}_6^{(n)}\alpha_5^{(m)}\right\}\right]\mathrm{e}^{\mathrm{i}q_4\psi}$$
$$+\sum_{n=1}^{4}\left[f_{i1}^{(n)}\alpha_{5,\xi}^{(n)}+f_{i2}^{(n)}\alpha_{5,\eta}^{(n)}+\sum_{m=1}^{4}\left\{h_{i12}^{(m,n)}\alpha_1^{(n)}\alpha_2^{(m)}+h_{i46}^{(m,n)}\alpha_4^{(n)}\alpha_6^{(m)}\right.\right.$$
$$\left.\left.+g_{i63}^{(m,n)}\bar{\alpha}_6^{(n)}\alpha_3^{(m)}\right\}\right]\mathrm{e}^{\mathrm{i}q_5\psi}$$
$$+\sum_{n=1}^{4}\left[f_{i1}^{(n)}\alpha_{6,\xi}^{(n)}+f_{i2}^{(n)}\alpha_{6,\eta}^{(n)}+\sum_{m=1}^{4}\left\{g_{i21}^{(m,n)}\bar{\alpha}_2^{(n)}\alpha_1^{(m)}+g_{i53}^{(m,n)}\bar{\alpha}_5^{(n)}\alpha_3^{(m)}\right.\right.$$
$$\left.\left.+g_{i45}^{(m,n)}\bar{\alpha}_4^{(n)}\alpha_5^{(m)}\right\}\right]\mathrm{e}^{\mathrm{i}q_6\psi}$$

$$+\text{ c.c. }, \tag{7.2.18}$$

on $y=\eta=0$. By comparing with the results in earlier chapters, the values of the coefficients may be expressed

$$F_{jIw}^{(n)}(y)=-(\mathrm{i}q_I)\left[(\hat{c}_{jwk2}+\hat{c}_{j2kw})s^{(n)}+(\hat{c}_{jwk1}+\hat{c}_{j1kw})\right]a_k^{(n)}\mathrm{e}^{\mathrm{i}q_I s^{(n)}y}\ ,\ w=1,2\,, \tag{7.2.19}_1$$

$$F_{jI3}^{(n)}(y)=-2\mathrm{i}q_I\rho\hat{\delta}_{jk}a_k^{(n)}\mathrm{e}^{\mathrm{i}q_I s^{(n)}y}\,, \tag{7.2.19}_2$$

$$G_{jJK}^{(m,n)}(y)=2\mathrm{i}q_J q_K\hat{d}_{jklmno}\left[q_J\bar{a}_n^{(n)}a_l^{(m)}\bar{\nu}_k^{(n)}\nu_m^{(m)}\bar{\nu}_o^{(n)}\right.$$
$$\left.-q_K\bar{a}_l^{(n)}a_n^{(m)}\nu_k^{(m)}\bar{\nu}_m^{(n)}\nu_o^{(m)}\right]\mathrm{e}^{\mathrm{i}(q_K s^{(m)}-q_J\bar{s}^{(n)})y}\,, \tag{7.2.19}_3$$

$$H_{jJK}^{(m,n)}(y)=2\mathrm{i}q_J q_K\hat{d}_{jklmno}\left[q_J a_n^{(n)}a_l^{(m)}\nu_k^{(n)}\nu_m^{(m)}\nu_o^{(n)}\right.$$
$$\left.+(1-\delta_{JK})q_K a_l^{(n)}a_n^{(m)}\nu_k^{(m)}\nu_m^{(n)}\nu_o^{(m)}\right]\mathrm{e}^{\mathrm{i}(q_K s^{(m)}+q_J s^{(n)})y}\,, \tag{7.2.19}_4$$

and

$$f_{jw}^{(n)}=-\hat{c}_{j2kw}a_k^{(n)}\ ,\ w=1,2\,, \tag{7.2.19}_5$$

$$g_{jJK}^{(m,n)}=-2q_J q_K\hat{d}_{j2klmn}\bar{a}_m^{(n)}a_k^{(m)}\nu_l^{(m)}\bar{\nu}_n^{(n)}\,, \tag{7.2.19}_6$$

$$h_{jJK}^{(m,n)}=q_J q_K\hat{d}_{j2klmn}a_m^{(n)}a_k^{(m)}\nu_l^{(m)}\nu_n^{(n)}(2-\delta_{JK})\,, \tag{7.2.19}_7$$

where

$$\nu_1^{(n)} = 1 \quad , \quad \nu_2^{(n)} = s^{(n)} \quad , \quad \nu_3^{(n)} = \nu_4^{(n)} = 0\,. \qquad (7.2.19)_8$$

Second-Order Solution

We now seek a solution to equations (7.2.17) and (7.2.18) in the form

$$u_j^{(2)} = \sum_{I=1}^{6} Q_{jI}(y,\xi,\eta,\tau)\mathrm{e}^{\mathrm{i}q_I\psi} + \text{ c.c.}\,. \qquad (7.2.20)$$

Substituting the representation (7.2.20) into equations (7.2.17) and (7.2.18) yields six systems; one for each Q_{jI}, $I = 1, 2, \ldots, 6$. Each system is of an essentially similar structure and thus we only investigate a solution for Q_{j1}, but we present more general expressions for various coefficients where convenient.

From equations (7.2.17) and (7.2.18), Q_{k1} must satisfy, ,

$$\begin{aligned}&(\mathrm{i}q_1)^2(\hat{c}_{j1k1} - \rho\ \ \hat{\delta}_{jk})Q_{k1} + (\mathrm{i}q_1)(\hat{c}_{j2k1} + \hat{c}_{j1k2})Q_{k1,y} + \hat{c}_{j2k2}Q_{k1,yy} = \\ &\sum_{n=1}^{4}\Big[F_{j11}^{(n)}(y)\alpha_{1,\xi}^{(n)} + F_{j12}^{(n)}(y)\alpha_{1,\eta}^{(n)} + F_{j13}^{(n)}(y)\alpha_{1,\tau}^{(n)} + \sum_{m=1}^{4}\Big\{G_{j13}^{(m,n)}(y)\bar{\alpha}_1^{(n)}\alpha_3^{(m)} \\ &\qquad + G_{j25}^{(m,n)}(y)\bar{\alpha}_2^{(n)}\alpha_5^{(m)} + H_{j26}^{(m,n)}(y)\alpha_2^{(n)}\alpha_6^{(m)}\Big\}\Big] \qquad (7.2.21)\end{aligned}$$

together with the boundary conditions,

$$\begin{aligned}&(\mathrm{i}q_1)\hat{c}_{j2k1}Q_{k1} + \hat{c}_{j2k2}Q_{k1,y} = \\ &\sum_{n=1}^{4}\left[f_{j1}^{(n)}\alpha_{1,\xi}^{(n)} + f_{j2}^{(n)}\alpha_{1,\eta}^{(n)} + \sum_{m=1}^{4}\left\{g_{j13}^{(m,n)}\bar{\alpha}_1^{(n)}\alpha_3^{(m)} + g_{j25}^{(m,n)}\bar{\alpha}_2^{(n)}\alpha_5^{(m)} + h_{j26}^{(m,n)}\alpha_2^{(n)}\alpha_6^{(m)}\right\}\right] \qquad (7.2.22)\end{aligned}$$

on $y = \eta = 0$.

We seek a solution for Q_{k1} in the form

$$\begin{aligned}Q_{k1} = \sum_{n=1}^{4}\Big[&b_{k1}^{(n)}(\xi,\eta,\tau)\mathrm{e}^{\mathrm{i}q_1 s^{(n)}y} + \sum_{m=1}^{4}\Big\{W_{k113}^{(m,n)}(\xi,\eta,\tau)\mathrm{e}^{\mathrm{i}q_1 T_{113}^{(m,n)}y} \\ &+ W_{k125}^{(m,n)}(\xi,\eta,\tau)\mathrm{e}^{\mathrm{i}q_1 T_{125}^{(m,n)}y} + V_{k126}^{(m,n)}(\xi,\eta,\tau)\mathrm{e}^{\mathrm{i}q_1 R_{126}^{(m,n)}y}\Big\}\Big]\,, \qquad (7.2.23)\end{aligned}$$

where, in generality,

$$
\begin{aligned}
T_{IJK}^{(m,n)} &= (q_K s^{(m)} - q_J \bar{s}^{(n)})/q_I\,, \\
R_{IJK}^{(m,n)} &= (q_K s^{(m)} + q_J s^{(n)})/q_I\,, \quad n \neq m\,, \\
V_{kIJK}^{(m,n)} &= 0\,, \quad n = m\,.
\end{aligned}
\tag{7.2.24}
$$

As in earlier chapters, this form of solution avoids secular terms of the type $y\mathrm{e}^{\mathrm{i}Ks^{(n)}y}$ and the absence of such terms will lead to conditions upon the function $\alpha_I^{(n)}$.

Substituting the representation (7.2.23) into equations (7.2.21) and comparing first the coefficients of $\mathrm{e}^{\mathrm{i}q_1 s^{(n)}y}$, we obtain

$$
(\mathrm{i}q_1)^2 \hat{\mathrm{L}}_{jk}(s^{(n)}) b_{k1}^{(n)} = P_{j1}^{(n)}\,,
\tag{7.2.25}
$$

where

$$
P_{j1}^{(n)} = F_{j11}^{(n)}(0)\alpha_{1,\xi}^{(n)} + F_{j12}^{(n)}(0)\alpha_{1,\eta}^{(n)} + F_{j13}^{(n)}(0)\alpha_{1,\tau}^{(n)} + H_{j26}^{(n,n)}(0)\alpha_2^{(n)}\alpha_6^{(n)}\,.
\tag{7.2.26}
$$

The matrix $\hat{\mathrm{L}}_{jk}(s^{(n)})$ is singular and symmetric, and therefore the consistency condition becomes

$$
\Gamma_1^{(n)}\alpha_{1,\xi}^{(n)} + \Delta_1^{(n)}\alpha_{1,\eta}^{(n)} + \Theta_1^{(n)}\alpha_{1,\tau}^{(n)} + \Lambda_{26}^{(n)}\alpha_2^{(n)}\alpha_6^{(n)} = 0\,,
\tag{7.2.27}
$$

where, in general,

$$
\begin{aligned}
\Gamma_J^{(n)} &= a_k^{(n)} F_{kJ1}^{(n)}(0)\,, \\
\Delta_J^{(n)} &= a_k^{(n)} F_{kJ2}^{(n)}(0)\,, \\
\Theta_J^{(n)} &= a_k^{(n)} F_{kJ3}^{(n)}(0)\,, \\
\Lambda_{IJ}^{(n)} &= a_k^{(n)} H_{kIJ}^{(n,n)}(0)\,.
\end{aligned}
\tag{7.2.28}
$$

We assume that the general solution to

$$
(\mathrm{i}q_I)^2 \hat{\mathrm{L}}_{jk}(s^{(n)}) b_{kI}^{(n)} = P_{jI}^{(n)}
\tag{7.2.29}
$$

can be written as

$$
b_{kI}^{(n)} = \chi_I^{(n)} a_k^{(n)} + \frac{1}{(\mathrm{i}q_I)^2} \hat{\mathrm{U}}_{kj}^{(n)} P_{jI}^{(n)}\,,
\tag{7.2.30}
$$

where $\hat{\mathrm{U}}_{kj}^{(n)}$, defined through (4.7.28), is the inverse of $\hat{\mathrm{L}}_{jk}(s^{(n)})$ restricted to the subspace orthogonal to $a_k^{(n)}$.

Next, by comparing the coefficients of $e^{iq_1 T_{IJK}^{(m,n)} y}$ and $e^{iq_1 R_{IJK}^{(m,n)} y}$, we find, introducing the inverse matrix $\hat{L}_{jk}^{-1}(s^{(n)})$, that in general

$$W_{kIJK}^{(m,n)} = \frac{1}{(iq_I)^2} \hat{L}_{jk}^{-1}(T_{IJK}^{(m,n)}) G_{jJK}^{(m,n)}(0) \bar{\alpha}_J^{(n)} \alpha_K^{(m)} \tag{7.2.31}$$

and

$$V_{kIJK}^{(m,n)} = \frac{1}{(iq_I)^2} \hat{L}_{jk}^{-1}(R_{IJK}^{(m,n)}) H_{jJK}^{(m,n)}(0) \alpha_J^{(n)} \alpha_K^{(m)} \tag{7.2.32}$$

Finally we substitute the representation (7.2.23) into the second-order boundary conditions (7.2.22) to obtain

$$\begin{aligned}
&\sum_{n=1}^{4} iq_1 \left\{ \hat{c}_{j2k2} s^{(n)} + \hat{c}_{j2k1} \right\} b_{k1}^{(n)} + \sum_{n=1}^{4} \sum_{m=1}^{4} iq_1 \left\{ \hat{c}_{j2k2} T_{113}^{(m,n)} + \hat{c}_{j2k1} \right\} W_{k113}^{(m,n)} \\
&+ \sum_{n=1}^{4} \sum_{m=1}^{4} iq_1 \left\{ \hat{c}_{j2k2} T_{125}^{(m,n)} + \hat{c}_{j2k1} \right\} W_{k125}^{(m,n)} + \sum_{n=1}^{4} \sum_{\substack{m=1 \\ m \neq n}}^{4} iq_1 \left\{ \hat{c}_{j2k2} R_{126}^{(m,n)} + \hat{c}_{j2k1} \right\} V_{k126}^{(m,n)} = \\
&\sum_{n=1}^{4} \left[f_{j1}^{(n)} \alpha_{1,\xi}^{(n)} + f_{j2}^{(n)} \alpha_{1,\eta}^{(n)} + \sum_{m=1}^{4} \left\{ g_{j13}^{(m,n)} \bar{\alpha}_1^{(n)} \alpha_3^{(m)} + g_{j25}^{(m,n)} \bar{\alpha}_2^{(n)} \alpha_5^{(m)} + h_{j26}^{(m,n)} \alpha_2^{(n)} \alpha_6^{(m)} \right\} \right],
\end{aligned} \tag{7.2.33}$$

where all quantities are evaluated on $y = \eta = 0$.

Substituting the expressions (7.2.30) to (7.2.32) into equations (7.2.33), we obtain

$$\begin{aligned}
&\sum_{n=1}^{4} iq_1 \hat{M}_{jn} \chi_1^{(n)} + \sum_{n=1}^{4} \frac{1}{iq_1} \left\{ \hat{c}_{j2k2} s^{(n)} + \hat{c}_{j2k1} \right\} \hat{U}_{kl}^{(n)} P_{l1}^{(n)} \\
&+ \sum_{n=1}^{4} \sum_{m=1}^{4} \frac{1}{iq_1} \left\{ \hat{c}_{j2k2} T_{113}^{(m,n)} + \hat{c}_{j2k1} \right\} L_{kl}^{-1}(T_{113}^{(m,n)}) G_{l13}^{(m,n)}(0) \bar{\alpha}_1^{(n)} \alpha_3^{(m)} \\
&+ \sum_{n=1}^{4} \sum_{m=1}^{4} \frac{1}{iq_1} \left\{ \hat{c}_{j2k2} T_{125}^{(m,n)} + \hat{c}_{j2k1} \right\} L_{kl}^{-1}(T_{125}^{(m,n)}) G_{l25}^{(m,n)}(0) \bar{\alpha}_2^{(n)} \alpha_5^{(m)} \\
&+ \sum_{n=1}^{4} \sum_{\substack{m=1 \\ m \neq n}}^{4} \frac{1}{iq_1} \left\{ \hat{c}_{j2k2} R_{126}^{(m,n)} + \hat{c}_{j2k1} \right\} L_{kl}^{-1}(R_{126}^{(m,n)}) H_{l26}^{(m,n)}(0) \alpha_2^{(n)} \alpha_6^{(m)} = \\
&\sum_{n=1}^{4} \left[f_{j1}^{(n)} \alpha_{1,\xi}^{(n)} + f_{j2}^{(n)} \alpha_{1,\eta}^{(n)} + \sum_{m=1}^{4} \left\{ g_{j13}^{(m,n)} \bar{\alpha}_1^{(n)} \alpha_3^{(m)} + g_{j25}^{(m,n)} \bar{\alpha}_2^{(n)} \alpha_5^{(m)} + h_{j26}^{(m,n)} \alpha_2^{(n)} \alpha_6^{(m)} \right\} \right],
\end{aligned} \tag{7.2.34}$$

where we recall that $\hat{M}_{kn}$ are given by equations (7.2.14).

These matrix equations for $\chi_1^{(n)}$ are singular and, denoting by λ_j a particular solution of $\lambda_j \hat{M}_{jn} = 0$, we obtain the consistency condition for the existence of

a solution by premultiplying equations (7.2.34) by λ_j. Use may then be made of equations (7.2.15) and (7.2.27) to substitute for $\alpha_I^{(n)}$ and $\alpha_{I,\eta}^{(n)}$ and we finally obtain the equation

$$N_1\gamma_{1,\xi} + P_1\gamma_{1,\tau} + \Delta'_{113}\bar{\gamma}_1\gamma_3 + \Delta'_{125}\bar{\gamma}_2\gamma_5 + \Pi'_{126}\gamma_2\gamma_6 = 0 \tag{7.2.35}$$

where

$$N_I = \sum_{n=1}^{4} \lambda_j \left(\frac{1}{iq_I} \left\{ \hat{c}_{j2k2} s^{(n)} + \hat{c}_{j2k1} \right\} \hat{U}_{kl}^{(n)} F_{lI1}^{(n)}(0) - f_{j1}^{(n)} \right.$$
$$\left. - \frac{\Gamma_I^{(n)}}{\Delta_I^{(n)}} \left[\frac{1}{iq_I} \left\{ \hat{c}_{j2k2} s^{(n)} + \hat{c}_{j2k1} \right\} \hat{U}_{kl}^{(n)} F_{lI2}^{(n)}(0) - f_{j2}^{(n)} \right] \right) \beta^{(n)} \tag{7.2.36}$$

and

$$P_I = \sum_{n=1}^{4} \lambda_j \left(\frac{1}{iq_I} \left\{ \hat{c}_{j2k2} s^{(n)} + \hat{c}_{j2k1} \right\} \hat{U}_{kl}^{(n)} F_{lI3}^{(n)}(0) \right.$$
$$\left. - \frac{\Theta_I^{(n)}}{\Delta_I^{(n)}} \left[\frac{1}{iq_I} \left\{ \hat{c}_{j2k2} s^{(n)} + \hat{c}_{j2k1} \right\} \hat{U}_{kl}^{(n)} F_{lI2}^{(n)}(0) - f_{j2}^{(n)} \right] \right) \beta^{(n)} . \tag{7.2.37}$$

Further, we deduce from equations (4.7.28) and $(7.2.19)_2$ that

$$\hat{U}_{kj}^{(n)} F_{jI3}^{(n)} = 0 ,$$

and

$$N_I = cP_I .$$

Hence (7.2.35) reduces to

$$\gamma_{1,\xi} + \frac{1}{c}\gamma_{1,\tau} + \Delta_{113}\bar{\gamma}_1\gamma_3 + \Delta_{125}\bar{\gamma}_2\gamma_5 + \Pi_{126}\gamma_2\gamma_6 = 0 , \tag{7.2.38}$$

where, in generality,

$$\Delta_{IJK} = \frac{1}{N_I} \sum_{n=1}^{4} \sum_{m=1}^{4} \left[\frac{1}{iq_I} \left\{ \hat{c}_{j2k2} T_{IJK}^{(m,n)} + \hat{c}_{j2k1} \right\} \hat{L}_{kl}^{-1}(T_{IJK}^{(m,n)}) G_{lJK}^{(m,n)}(0) - g_{jJK}^{(m,n)} \right] \lambda_j \bar{\beta}^{(n)} \beta^{(m)} \tag{7.2.39}$$

$$\Pi_{IJK} = \frac{1}{N_I}\sum_{n=1}^{4}\sum_{\substack{m=1\\ m\neq n}}^{4}\left[\frac{1}{\mathrm{i}q_I}\left\{\hat{c}_{j2k2}R_{IJK}^{(m,n)} + \hat{c}_{j2k1}\right\}\hat{\mathrm{L}}_{kl}^{-1}(R_{IJK}^{(m,n)})H_{lJK}^{(m,n)}(0) - h_{jJK}^{(m,n)}\right]\lambda_j\beta^{(n)}\beta^{(m)}$$
$$+\sum_{n=1}^{4}\frac{1}{\mathrm{i}q_I}\left\{\hat{c}_{j2k2}s^{(n)} + \hat{c}_{j2k1}\right\}\hat{\mathrm{U}}_{kl}^{(n)}H_{lJK}^{(n,n)}(0)\lambda_j\beta^{(n)}\beta^{(n)}$$
$$-\sum_{n=1}^{4}\frac{\Lambda_{JK}^{(n)}}{\Delta_I^{(n)}}\left[\frac{1}{\mathrm{i}q_I}\left\{\hat{c}_{j2k2}s^{(n)} + \hat{c}_{j2k1}\right\}\hat{\mathrm{U}}_{kl}^{(n)}F_{lI2}^{(n)}(0) - f_{j2}^{(n)}\right]\lambda_j\beta^{(n)}\beta^{(n)}\,. \qquad (7.2.40)$$

Similar analyses on the remaining five systems produce the coupled system of partial differential equations

$$\begin{aligned}
&\gamma_{1,\xi} + \frac{1}{c}\gamma_{1,\tau} + \Delta_{113}\bar{\gamma}_1\gamma_3 + \Delta_{125}\bar{\gamma}_2\gamma_5 + \Pi_{126}\gamma_2\gamma_6 = 0\,,\\
&\gamma_{2,\xi} + \frac{1}{c}\gamma_{2,\tau} + \Delta_{224}\bar{\gamma}_2\gamma_4 + \Delta_{215}\bar{\gamma}_1\gamma_5 + \Delta_{261}\bar{\gamma}_6\gamma_1 = 0\,,\\
&\gamma_{3,\xi} + \frac{1}{c}\gamma_{3,\tau} + \Pi_{311}\gamma_1\gamma_1 + \Pi_{356}\gamma_5\gamma_6 = 0\,,\\
&\gamma_{4,\xi} + \frac{1}{c}\gamma_{4,\tau} + \Pi_{422}\gamma_2\gamma_2 + \Delta_{456}\bar{\gamma}_5\gamma_6 = 0\,,\\
&\gamma_{5,\xi} + \frac{1}{c}\gamma_{5,\tau} + \Pi_{512}\gamma_1\gamma_2 + \Pi_{546}\gamma_4\gamma_6 + \Delta_{563}\bar{\gamma}_6\gamma_3 = 0\,,\\
&\gamma_{6,\xi} + \frac{1}{c}\gamma_{6,\tau} + \Delta_{621}\bar{\gamma}_2\gamma_1 + \Delta_{653}\bar{\gamma}_5\gamma_3 + \Delta_{645}\bar{\gamma}_4\gamma_5 = 0\,,
\end{aligned} \qquad (7.2.41)$$

where all the coefficients that appear have been defined by equations (7.2.39) and (7.2.40).

Equations (7.2.41) are easily seen to be similar in form to equations (4.7.31) of Chapter 4, and thus admit similar solutions. Again the coefficients are generally complex and may only be evaluated numerically through the linear iterative procedures of Section 3.4.

7.3 RESULTS AND CONCLUSIONS

This chapter has so far presented the derivation of coupled amplitude equations for the propagation of two co-directional surface acoustic waves on the surface of a piezoelectric substrate. As was the case in Chapters 4 and 6, the derivation of these equations would be identical for both piezoelectric and anisotropic elastic materials. We may thus present results for the growth and decay of the harmonic amplitudes based upon the amplitude equations (7.2.41) for the two different classes of materials by merely adjusting the level of implicit summation.

If, as in earlier chapters, we consider excitation by two monochromatic signals, we may take γ_I, $I = 1,\ldots,6$, to be independent of τ and thereby reduce equations (7.2.41) to ordinary differential equations. These may then be solved either numerically by finite difference methods or analytically by considering a series solution in ξ.

We adopt the monochromatic signalling conditions of Kalyanasundaram [1981] for ease of comparison, namely

$$\gamma_1(0) = a \quad , \quad \gamma_2(0) = as \quad , \quad \gamma_I(0) = 0\,, (I = 3,\ldots,6)\,. \tag{7.3.1}$$

Let us first consider the cubically anisotropic elastic materials considered in Chapter 3.

Using finite differences, solutions to equations (7.2.41) for the material MgO subject to the signalling conditions (7.3.1) are plotted in Figures 7.3.1 to 7.3.12 for the amplitude ratio $s = \frac{1}{2}$. Results are presented for a selection of angles of propagation on the Y-cut surface of the material. The first is that utilised by Lardner and Tupholme [1986] for their analytical solution, when the plane $y = 0$ is taken to be a plane of material symmetry and the x-axis an axis of symmetry. The three different frequency ratios, $r = 0.1$, 0.5 and 0.9, shown by Kalyanasundaram are again utilised for ease of comparison.

The graphs bear remarkable similarity to those presented by Kalyanasundaram [1981] as well as those of Chapter 3 for a single elastic wave although the level of decay appears to be lower.

If we consider the series solutions

$$
\begin{aligned}
\tilde{\gamma}_1 &= 1 - w_1\xi_1^2 + \dots \\
\tilde{\gamma}_2 &= s - w_2\xi_1^2 + \dots \\
\tilde{\gamma}_3 &= w_3\xi_1 + \dots \\
\tilde{\gamma}_4 &= w_4\xi_1 + \dots \\
\tilde{\gamma}_5 &= w_5\xi_1 + \dots \\
\tilde{\gamma}_6 &= w_6\xi_1 + \dots ,
\end{aligned}
\tag{7.3.2}
$$

to equations (7.2.41), where $\xi_1 = a\xi$ and $\tilde{\gamma}_I = \gamma_I/a$, we may easily obtain the representations

$$
\begin{aligned}
w_1 &= -\tfrac{1}{2}\left(\Delta_{113}\Pi_{311} + s^2\Delta_{125}\Pi_{512} + s^2\Pi_{126}\Delta_{621}\right) \\
w_2 &= -\tfrac{1}{2}s\left(s^2\Delta_{224}\Pi_{422} + \Delta_{215}\Pi_{512} + \Delta_{261}\bar{\Delta}_{621}\right) \\
w_3 &= -\Pi_{311} \\
w_4 &= -s^2\,\Pi_{422} \\
w_5 &= -s\Pi_{512} \\
w_6 &= -s\Delta_{621} .
\end{aligned}
\tag{7.3.3}
$$

This solution, known as the near-field solution, is only valid for small values of ξ, but may give valuable qualitative information about the initial behaviour of the harmonics. A plot of the variation of the linear growth coefficients w_5 and w_1 with angle of propagation away from the axis of symmetry on Y-cut MgO is given in Figure 7.3.13.

As discussed earlier, the growth of the interaction frequencies is a significant factor in devices such as SAW filters, since it may introduce noise in the external circuit (IMD). This effect can be significant at levels as low as -20db. Using the near-field solution (7.3.2) and (7.3.3), we may assess the development of the interactions to a critical noise level, chosen to be 10% of the amplitude of the input waves.

Let x_{10} denote the distance from the source at which the amplitudes γ_I reach 10% of the input amplitude a. It simply follows from equations $(7.3.3)_3$ and $(7.3.3)_4$ and Lardner and Tupholme [1986] that

$$
x_{10} = \frac{0.1}{\pi w e_m} ,
$$

where $e_m = 2\epsilon aK$ is the maximum longitudinal strain on the surface, here assumed to be $O(10^{-3})$, and w represents w_5 or w_6.

Numerical calculations for the material MgO show that the interactions become significant at distances varying between about 35 and 3500 wavelengths. The upper

limit of this distance arise because directions of propagation on the crystal may be chosen for which there is extremely slow growth of the interaction frequencies, particularly the difference frequency as can be seen from Figure 7.3.13.

An interesting phenomenon may be observed in the amplitude plot Figure 7.3.7, for the case of propagation 30° away from the axis of symmetry and $r = 0.1$. The fundamental of the smaller amplitude wave initially grows in amplitude. Calculations of the wave power show that energy is conserved for relatively large propagation distances and that the amplitude peaks after about 500 wavelengths' propagation. This behaviour is present for a small range of angle about the 30° rotation and it was at first considered to arise through truncation of the series (7.2.9). Later results will show that third-order study verifies the existence of this phenomenon.

Figures 7.3.14 to 7.3.22 display the amplitude growth and decay for various configurations and frequency ratios on the material lithium nibate. These configurations and frequency ratios correspond to the Figures 7.4.1 to 7.4.12 and it is clear that similar characteristics are being displayed. It is noted that the growth and decay of the interaction of piezoelectric waves is far steeper than for the single piezoelectric wave and that at 40° away from the axis of symmetry (Figures 7.3.17 to 7.3.19) the results are comparable to those for the purely elastic material magnesium oxide. Figure 7.3.23 gives the variation of the growth and decay coefficients w_1 and w_5 for a range of angles of propagation on the surface of lithium niobate. This corresponds to Figure 4.8.16 for the case of a single propagating piezoelectric wave and it can be seen that the overall form is preserved.

Again performing the estimate of the 10% critical noise level we find that x_{10} varies between 80 and 3000 wavelengths.

Note that care must be taken when $r = 0.5$ since in this case some of the values of q_I become identical, meaning that the frequencies of these individual modes become equal. In this situation the amplitudes for the constituent modes remain unaltered but the interpretation of the results requires careful attention since the amplitude of the wave of a particular frequency, for these special modes, becomes the sum of the constituent amplitudes.

Key to Figures

- ■ Fundamental amplitude, $\tilde{\gamma}_1$.
- □ Fundamental amplitude, $\tilde{\gamma}_2$.
- ▲ Interaction amplitude, $\tilde{\gamma}_5$.
- △ Interaction amplitude, $\tilde{\gamma}_6$.

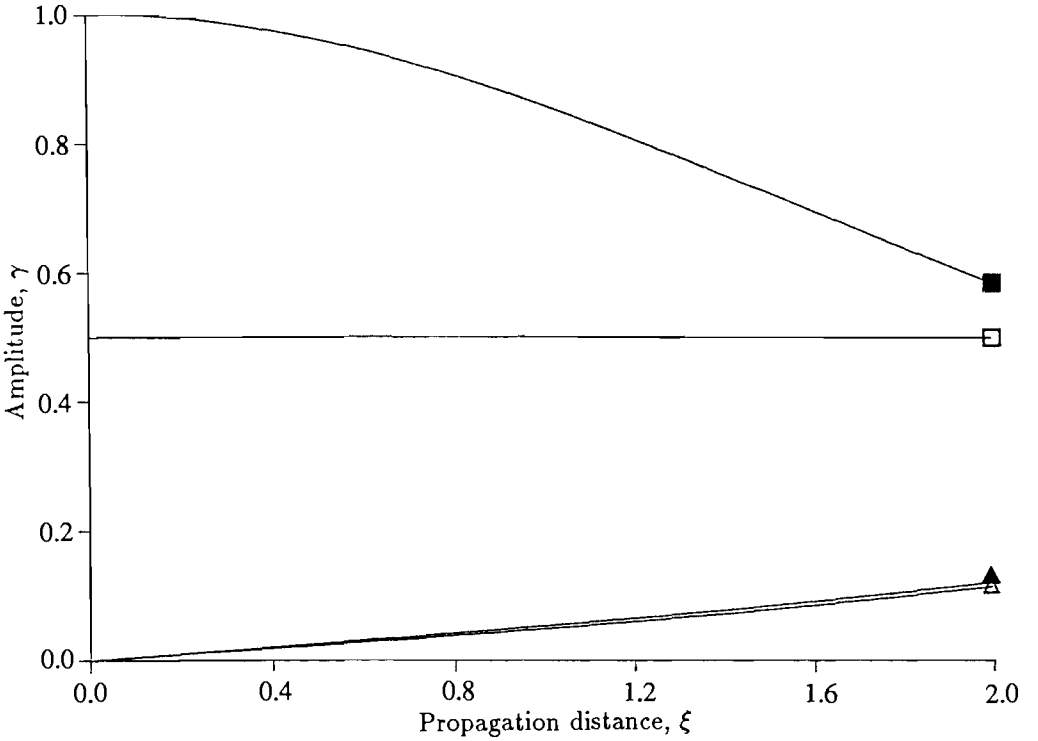

Figure 7.3.1 Growth and decay of the amplitudes $\tilde{\gamma}_I$, for I = 1, 2, 5 and 6, with propagation distance ξ_1 for X-propagation on Y-cut MgO, amplitude ratio $s = \frac{1}{2}$,frequency ratio $r = 0.1$

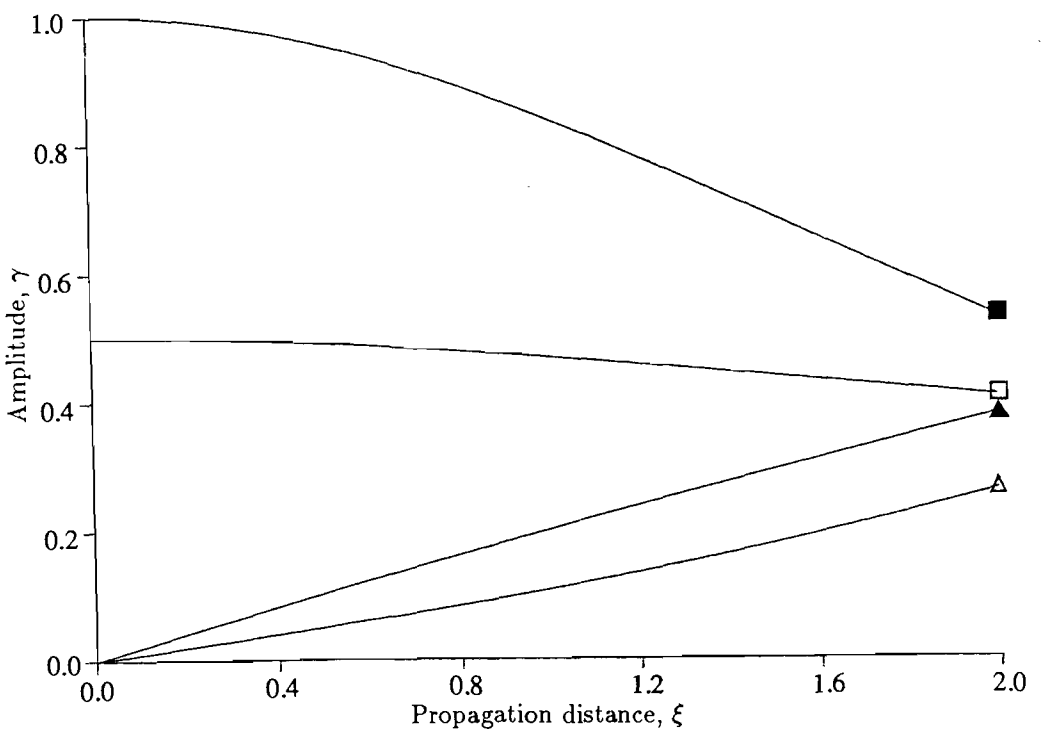

Figure 7.3.2 Growth and decay of the amplitudes $\tilde{\gamma}_I$, for I = 1, 2, 5 and 6, with propagation distance ξ_1 for X-propagation on Y-cut MgO, amplitude ratio $s = \frac{1}{2}$, frequency ratio $r = 0.5$

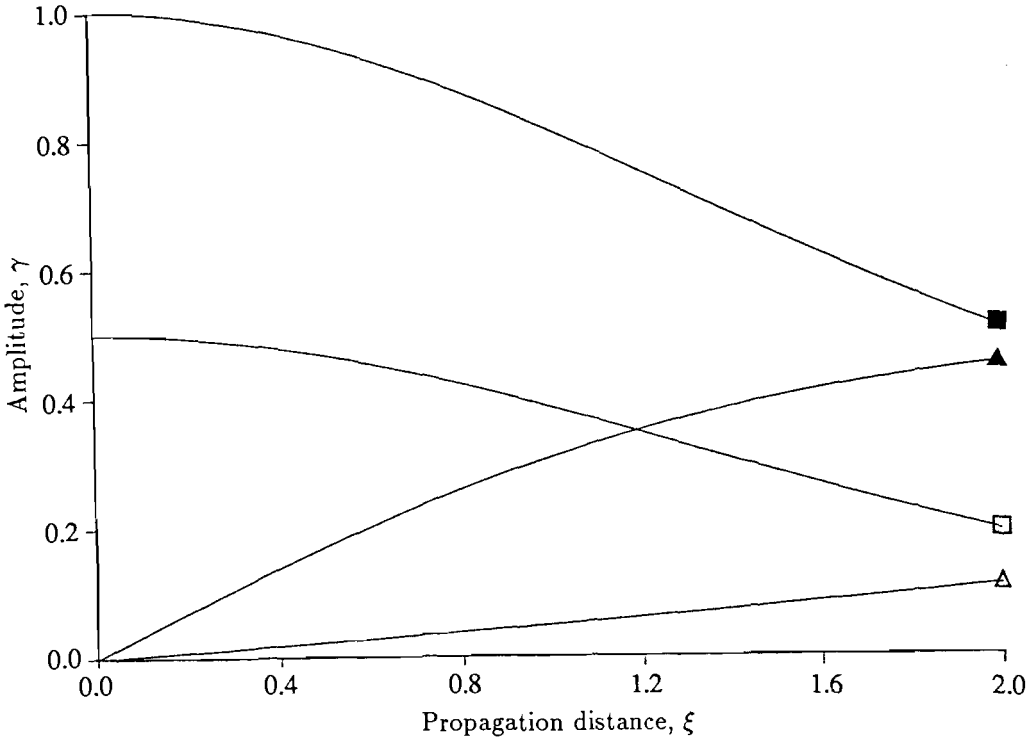

Figure 7.3.3 Growth and decay of the amplitudes $\tilde{\gamma}_I$, for I = 1, 2, 5 and 6, with propagation distance ξ_1 for X-propagation on Y-cut MgO, amplitude ratio $s = \frac{1}{2}$, frequency ratio $r = 0.9$

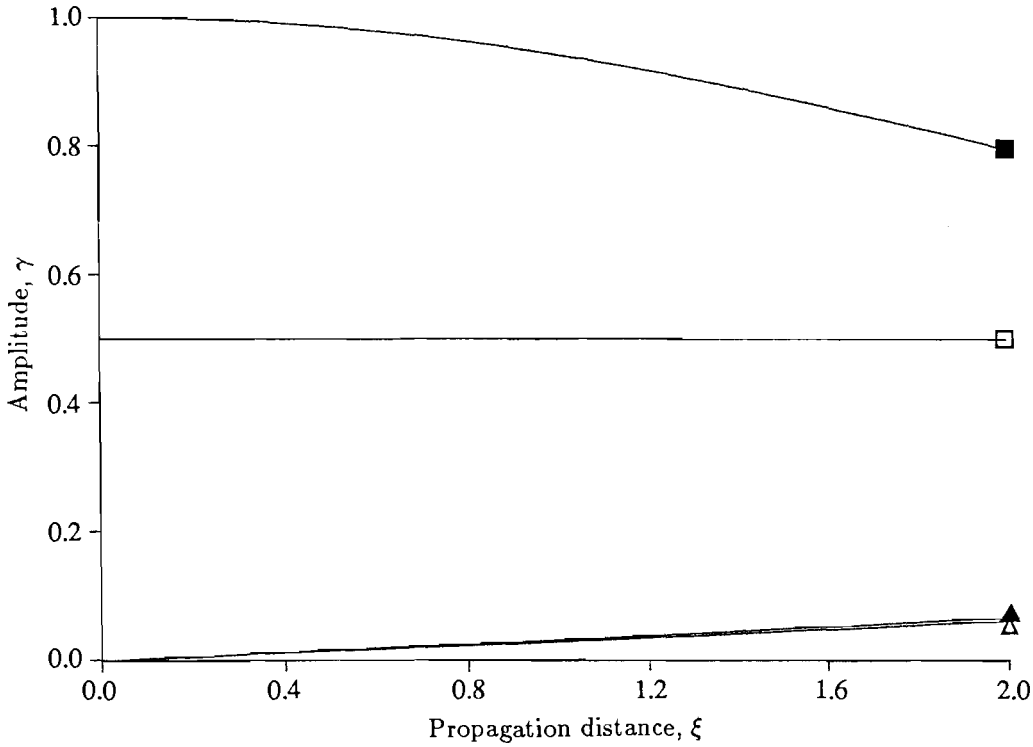

Figure 7.3.4 Growth and decay of the amplitudes $\tilde{\gamma}_I$, for I = 1, 2, 5 and 6, with propagation distance ξ_1 for propagation 20° from the X-axis on Y-cut MgO, amplitude ratio $s = \frac{1}{2}$, frequency ratio $r = 0.1$

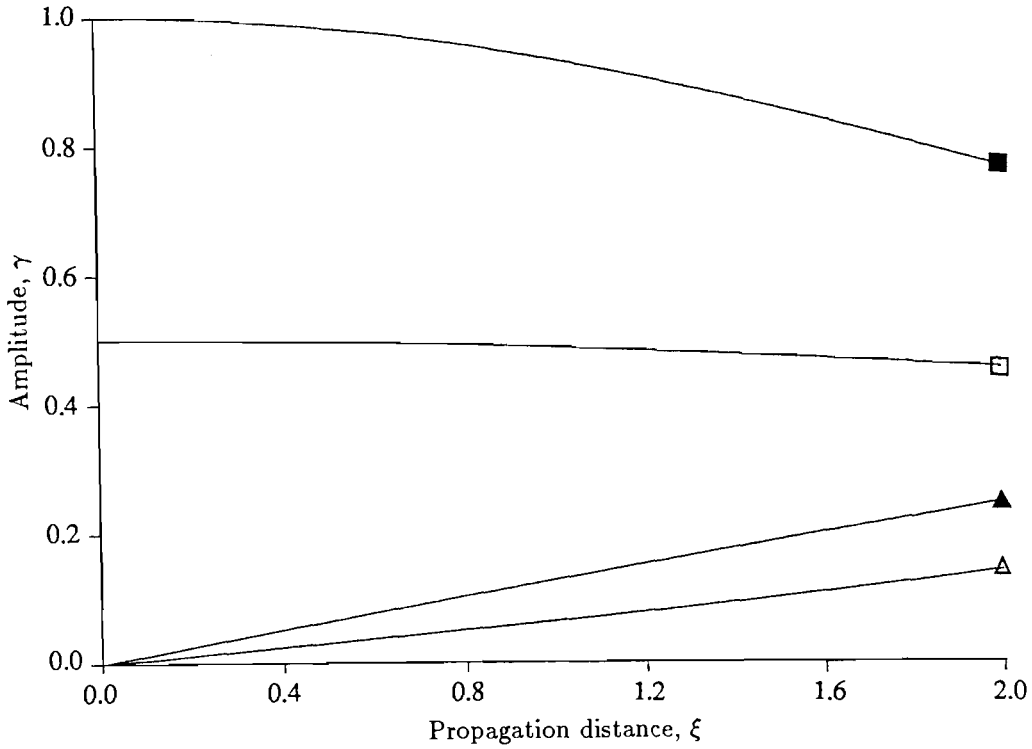

Figure 7.3.5 Growth and decay of the amplitudes $\tilde{\gamma}_I$, for I = 1, 2, 5 and 6, with propagation distance ξ_1 for propagation 20° from the X-axis on Y-cut MgO, amplitude ratio $s = \frac{1}{2}$, frequency ratio $r = 0.5$

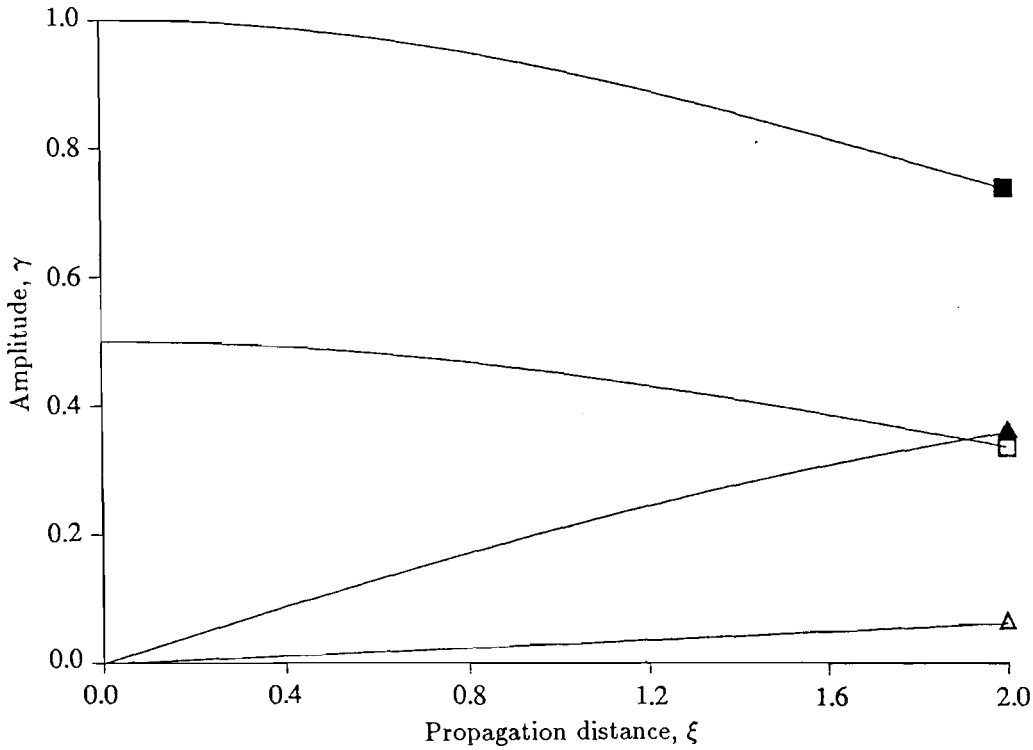

Figure 7.3.6 Growth and decay of the amplitudes $\tilde{\gamma}_I$, for I = 1, 2, 5 and 6, with propagation distance ξ_1 for propagation 20° from the X-axis on Y-cut MgO, amplitude ratio $s = \frac{1}{2}$, frequency ratio $r = 0.9$

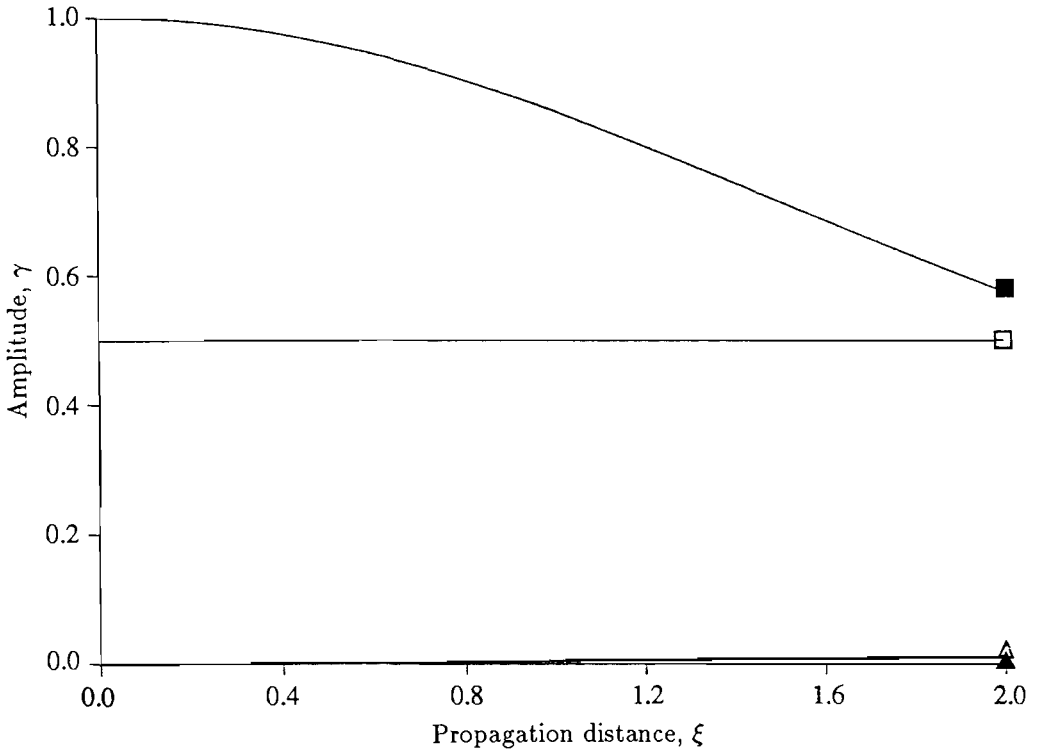

Figure 7.3.7 Growth and decay of the amplitudes $\tilde{\gamma}_I$, for I = 1, 2, 5 and 6, with propagation distance ξ_1 for propagation 30° from the X-axis on Y-cut MgO, amplitude ratio $s = \frac{1}{2}$, frequency ratio $r = 0.1$

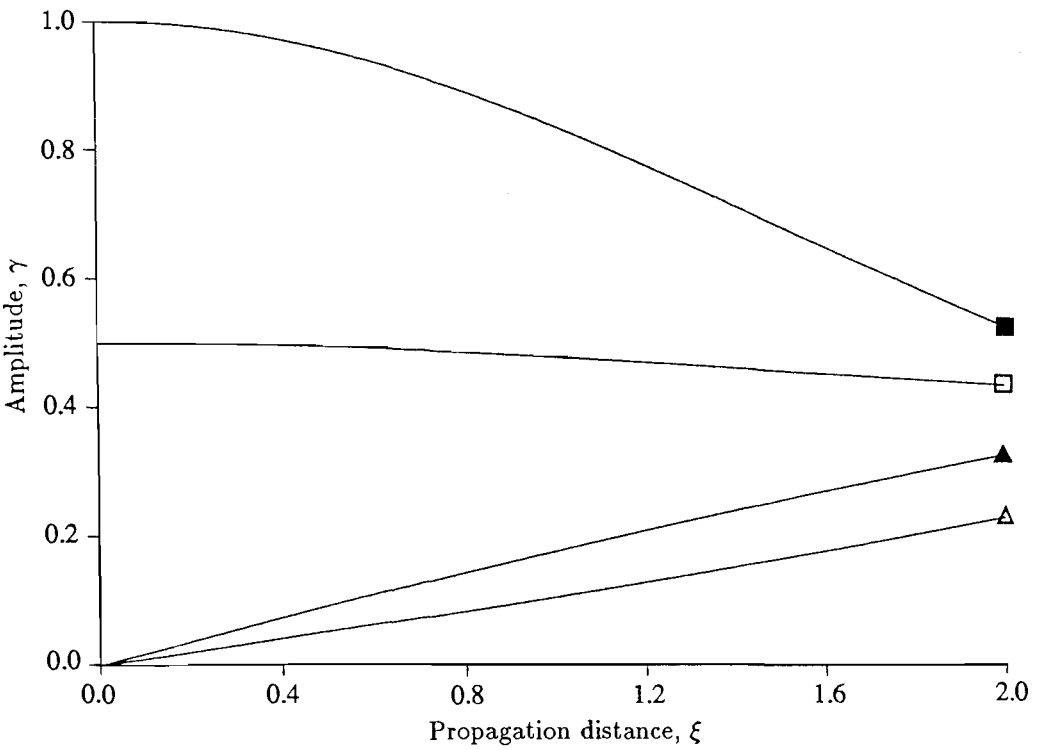

Figure 7.3.8 Growth and decay of the amplitudes $\tilde{\gamma}_I$, for I = 1, 2, 5 and 6, with propagation distance ξ_1 for propagation 30° from the X-axis on Y-cut MgO, amplitude ratio $s = \frac{1}{2}$, frequency ratio $r = 0.5$

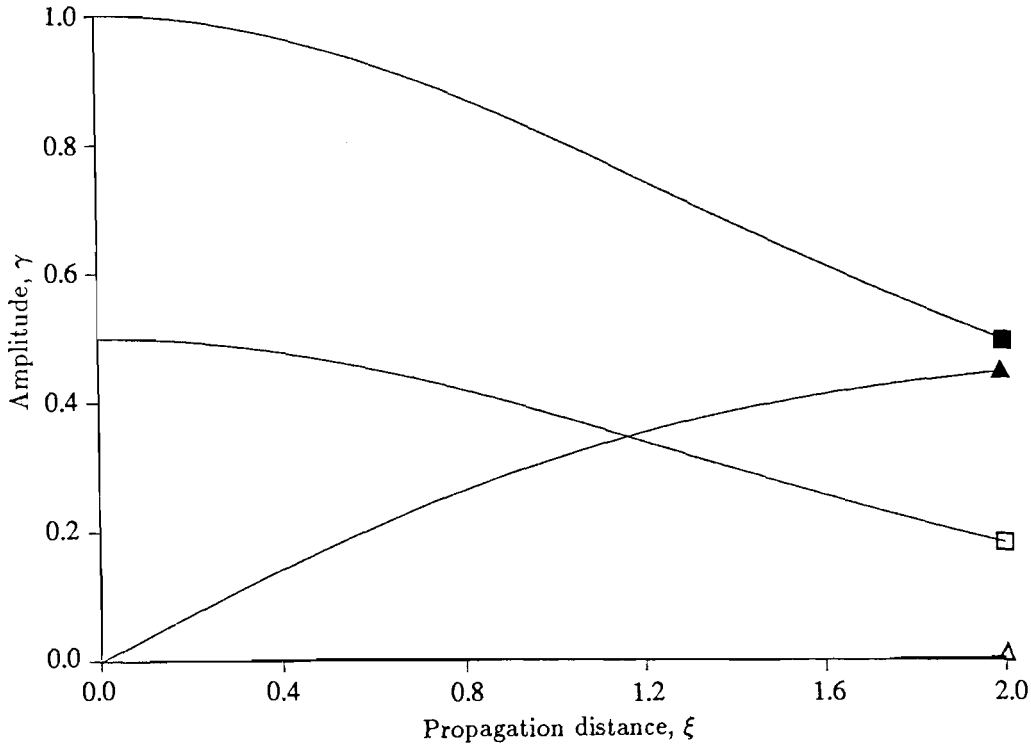

Figure 7.3.9 Growth and decay of the amplitudes $\tilde{\gamma}_I$, for I = 1, 2, 5 and 6, with propagation distance ξ_1 for propagation 30° from the X-axis on Y-cut MgO, amplitude ratio $s = \frac{1}{2}$, frequency ratio $r = 0.9$

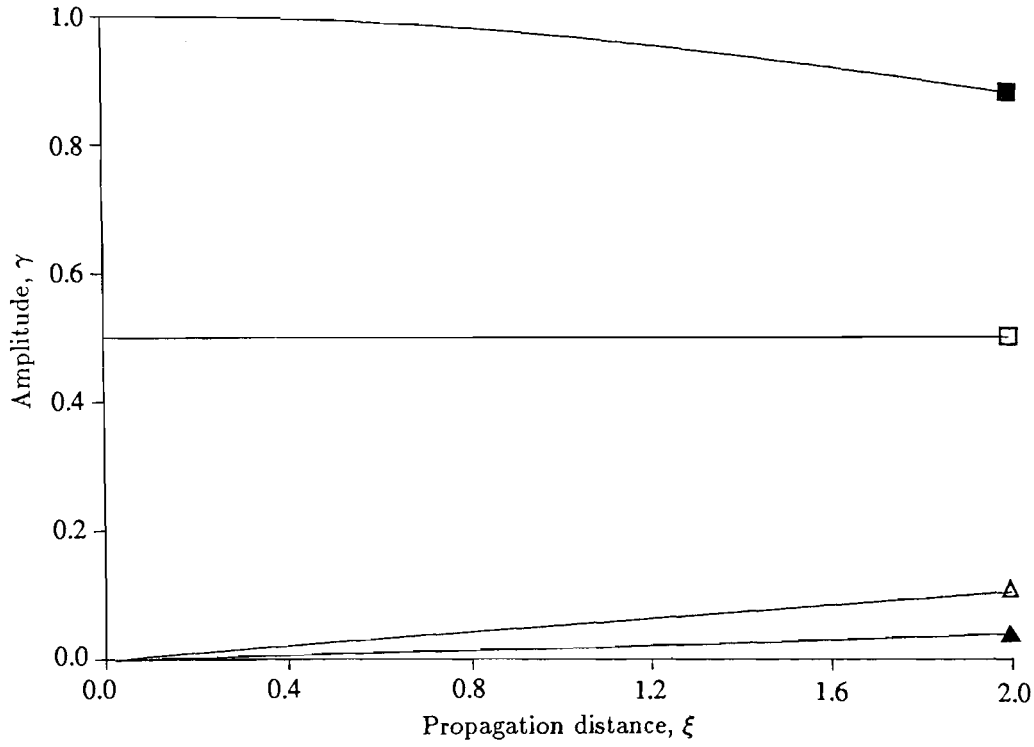

Figure 7.3.10 Growth and decay of the amplitudes $\tilde{\gamma}_I$, for I = 1, 2, 5 and 6, with propagation distance ξ_1 for propagation 40° from the X-axis on Y-cut MgO, amplitude ratio $s = \frac{1}{2}$, frequency ratio $r = 0.1$

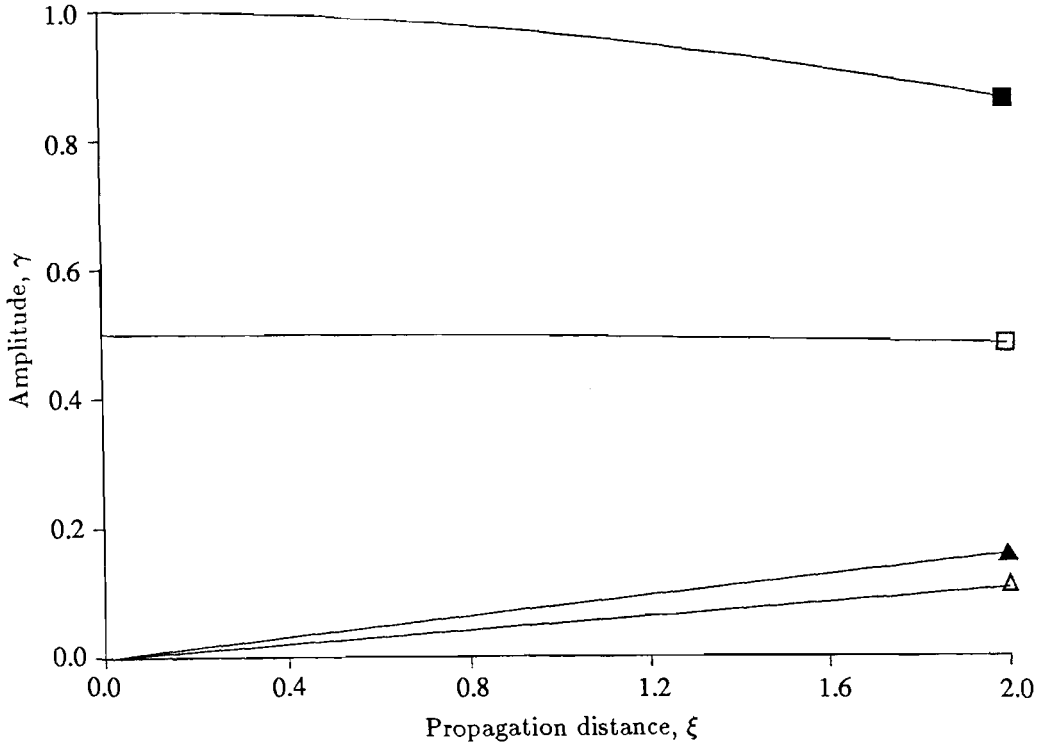

Figure 7.3.11 Growth and decay of the amplitudes $\tilde{\gamma}_I$, for I = 1, 2, 5 and 6, with propagation distance ξ_1 for propagation 40° from the X-axis on Y-cut MgO, amplitude ratio $s = \frac{1}{2}$, frequency ratio $r = 0.5$

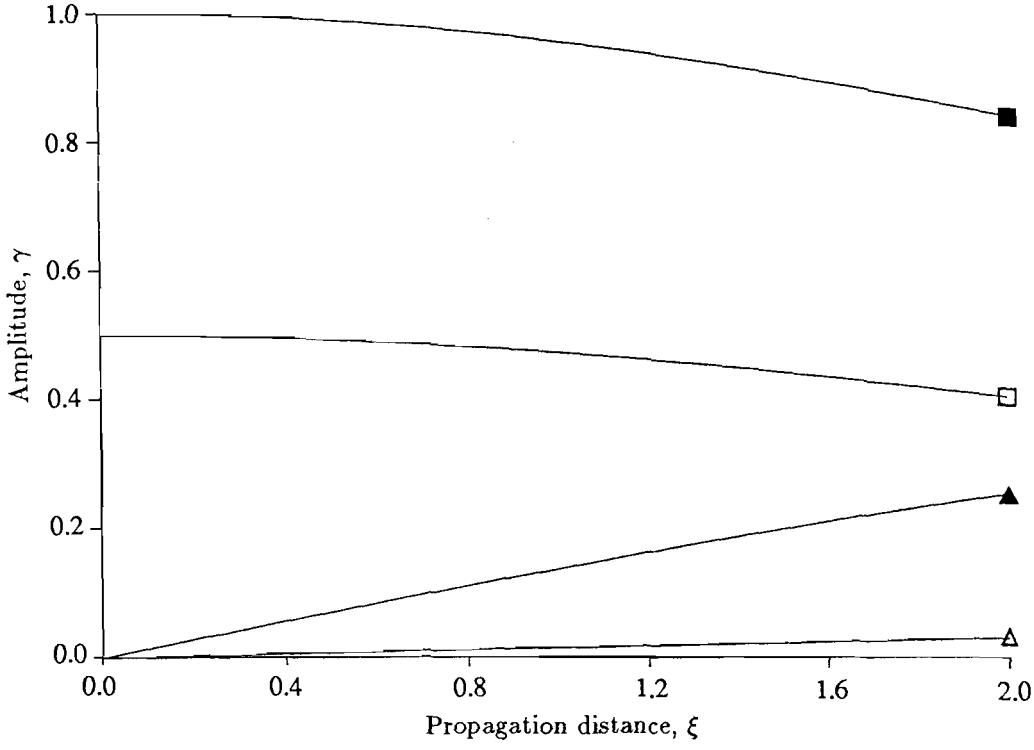

Figure 7.3.12 Growth and decay of the amplitudes $\tilde{\gamma}_I$, for I = 1, 2, 5 and 6, with propagation distance ξ_1 for propagation 40° from the X-axis on Y-cut MgO, amplitude ratio $s = \frac{1}{2}$, frequency ratio $r = 0.9$

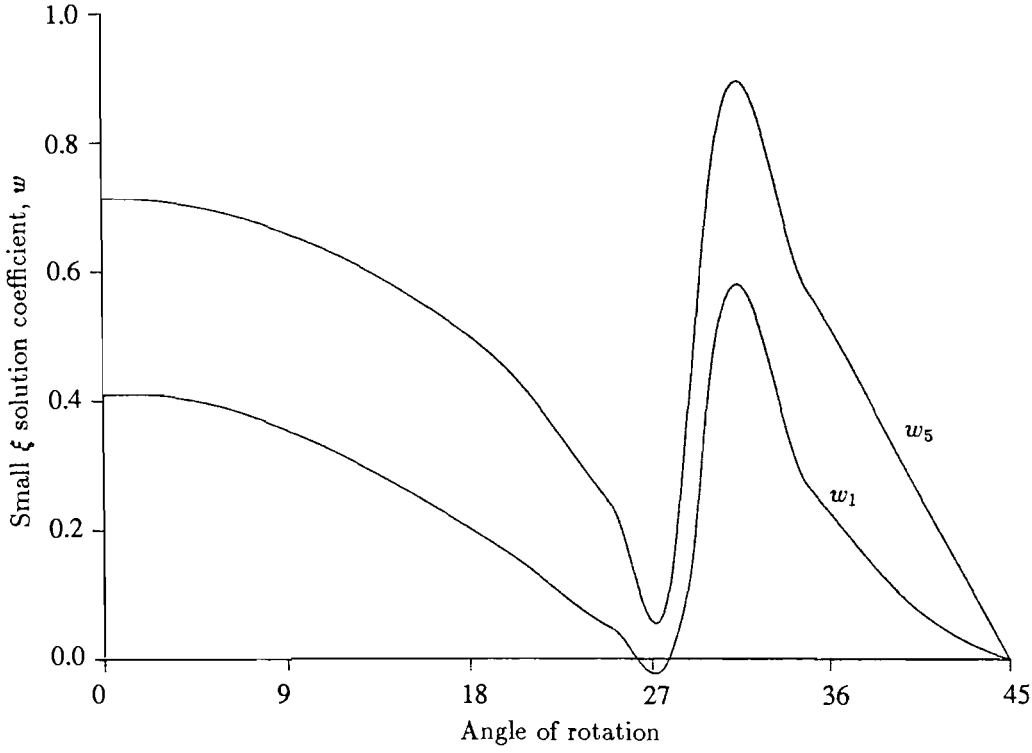

Figure 7.3.13 Variation of w_5 and w_1 with angle of propagation on the surface of Y-cut MgO, amplitude ratio $s = \frac{1}{2}$, frequency ratio $r = 0.1$

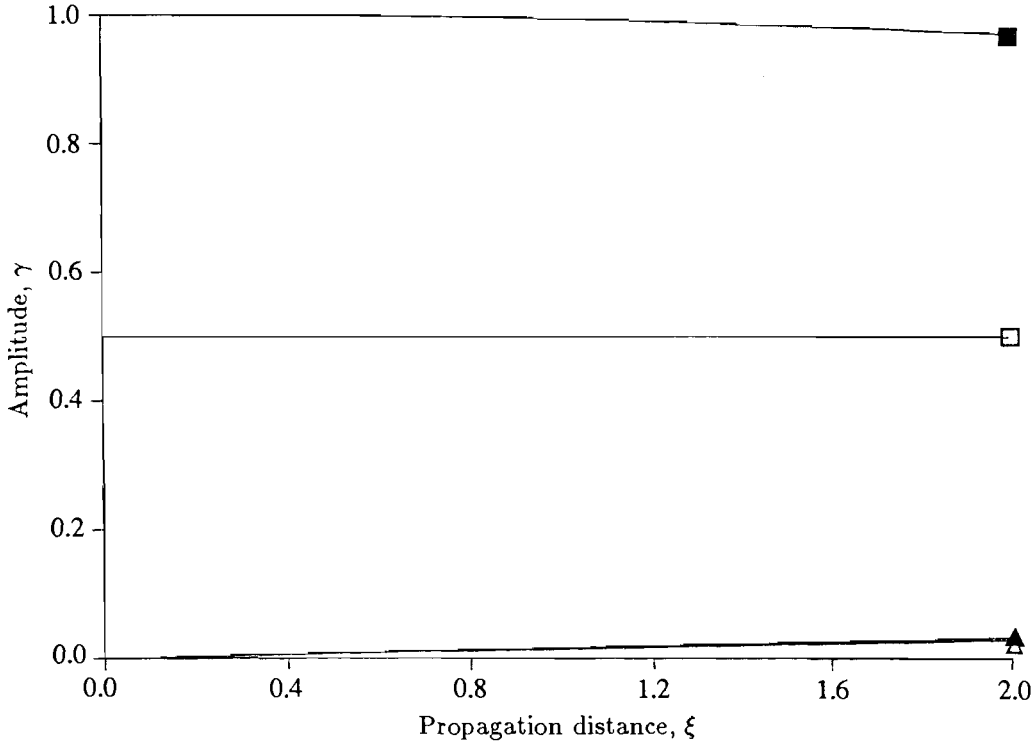

Figure 7.3.14 Growth and decay of the amplitudes $\tilde{\gamma}_I$, for $I = 1, 2, 5$ and 6, with propagation distance ξ_1 for X-propagation on Y-cut $LiNbO_3$, amplitude ratio $s = \frac{1}{2}$, frequency ratio $r = 0.1$

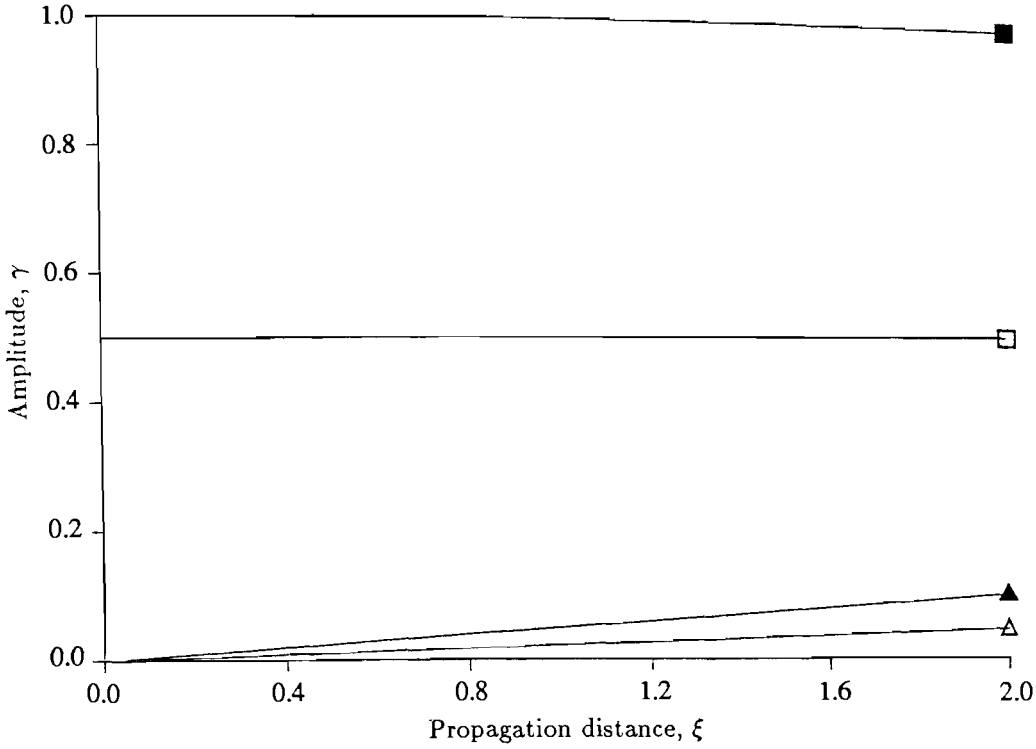

Figure 7.3.15 Growth and decay of the amplitudes $\tilde{\gamma}_I$, for I = 1, 2, 5 and 6, with propagation distance ξ_1 for X-propagation on Y-cut $LiNbO_3$, amplitude ratio $s = \frac{1}{2}$, frequency ratio $r = 0.5$

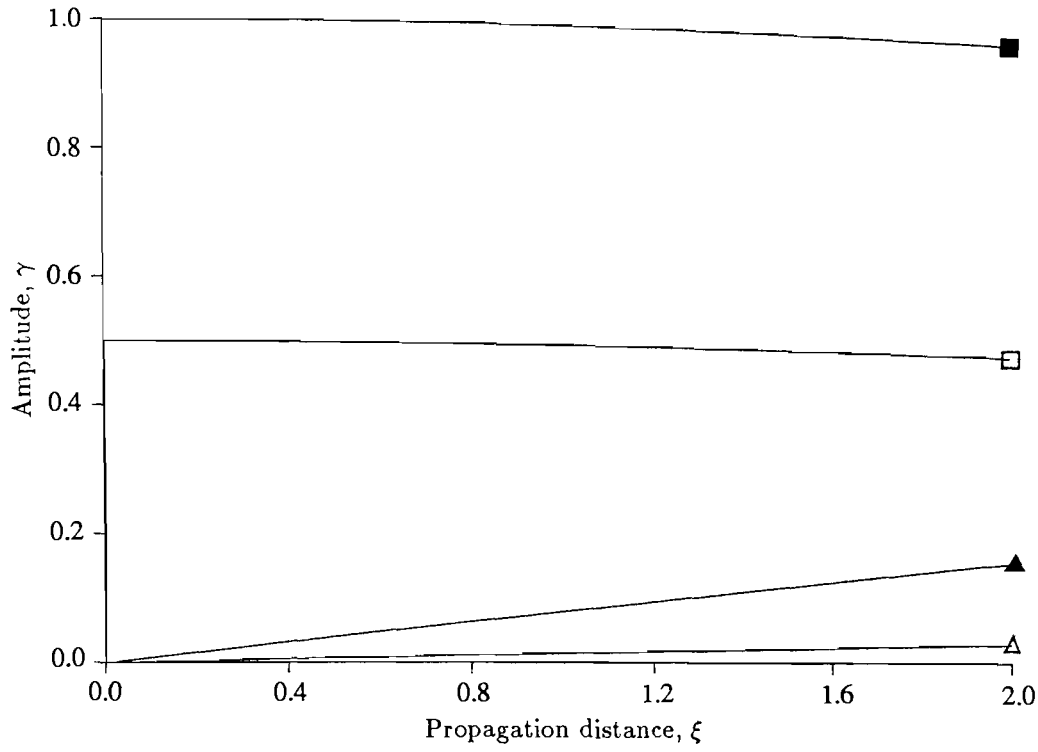

Figure 7.3.16 Growth and decay of the amplitudes $\tilde{\gamma}_I$, for I = 1, 2, 5 and 6, with propagation distance ξ_1 for X-propagation on Y-cut $LiNbO_3$, amplitude ratio $s = \frac{1}{2}$, frequency ratio $r = 0.9$

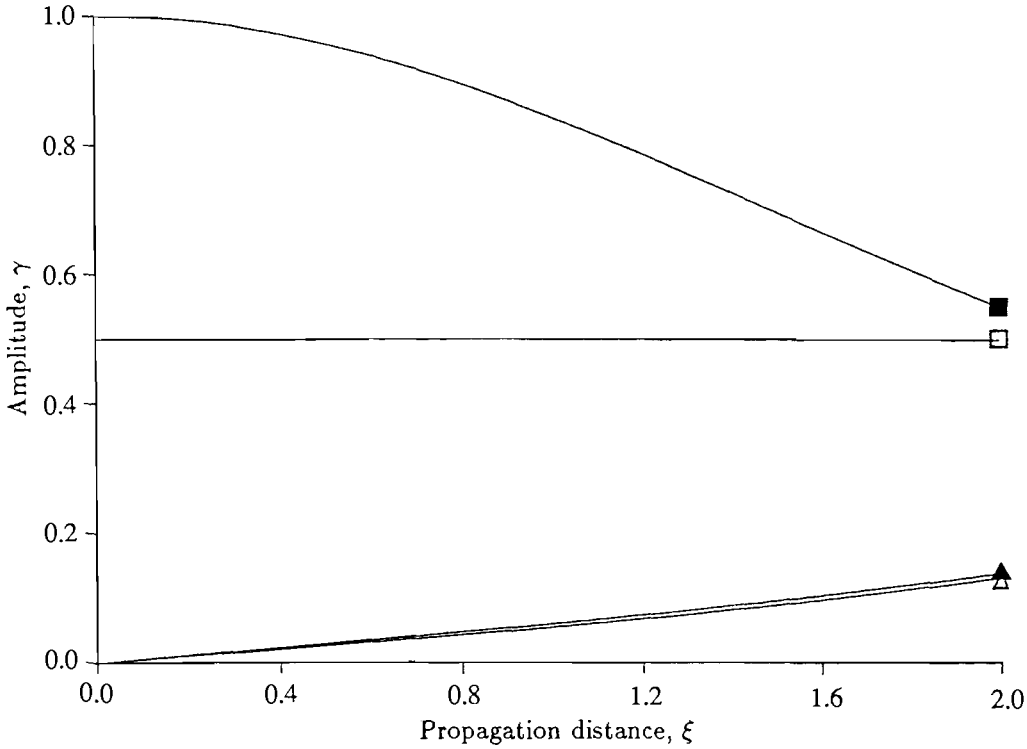

Figure 7.3.17 Growth and decay of the amplitudes $\tilde{\gamma}_I$, for I = 1, 2, 5 and 6, with propagation distance ξ_1 for propagation 40° from the X-axis on Y-cut $LiNbO_3$, amplitude ratio $s = \frac{1}{2}$, frequency ratio $r = 0.1$

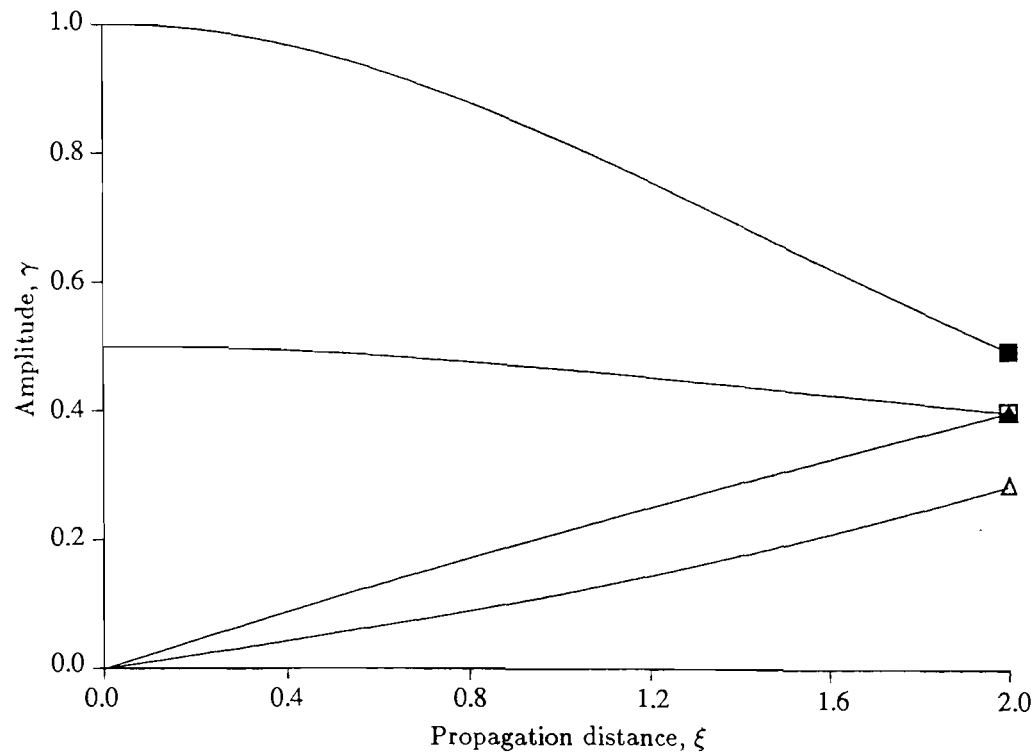

Figure 7.3.18 Growth and decay of the amplitudes $\tilde{\gamma}_I$, for I = 1, 2, 5 and 6, with propagation distance ξ_1 for propagation 40° from the X-axis on Y-cut $LiNbO_3$, amplitude ratio $s = \frac{1}{2}$, frequency ratio $r = 0.5$

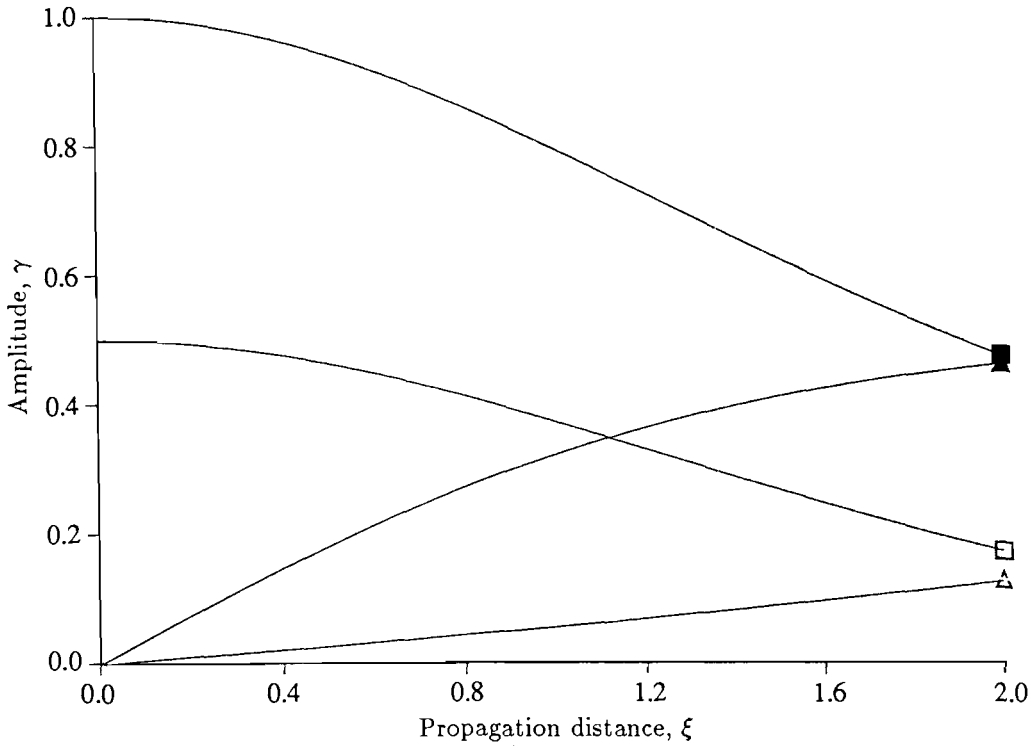

Figure 7.3.19 Growth and decay of the amplitudes $\tilde{\gamma}_I$, for I = 1, 2, 5 and 6, with propagation distance ξ_1 for propagation 40° from the X-axis on Y-cut $LiNbO_3$, amplitude ratio $s = \frac{1}{2}$, frequency ratio $r = 0.9$

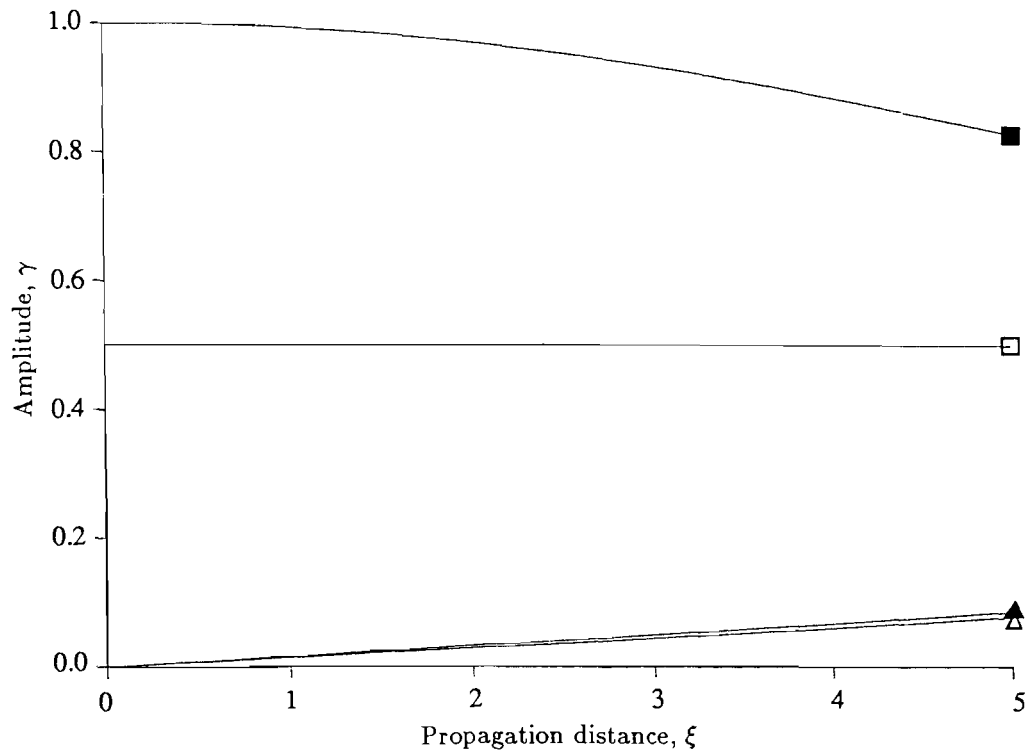

Figure 7.3.20 Growth and decay of the amplitudes $\tilde{\gamma}_I$, for I = 1, 2, 5 and 6, with propagation distance ξ_1 for Z-propagation on X-cut $LiNbO_3$, amplitude ratio $s = \frac{1}{2}$, frequency ratio $r = 0.1$

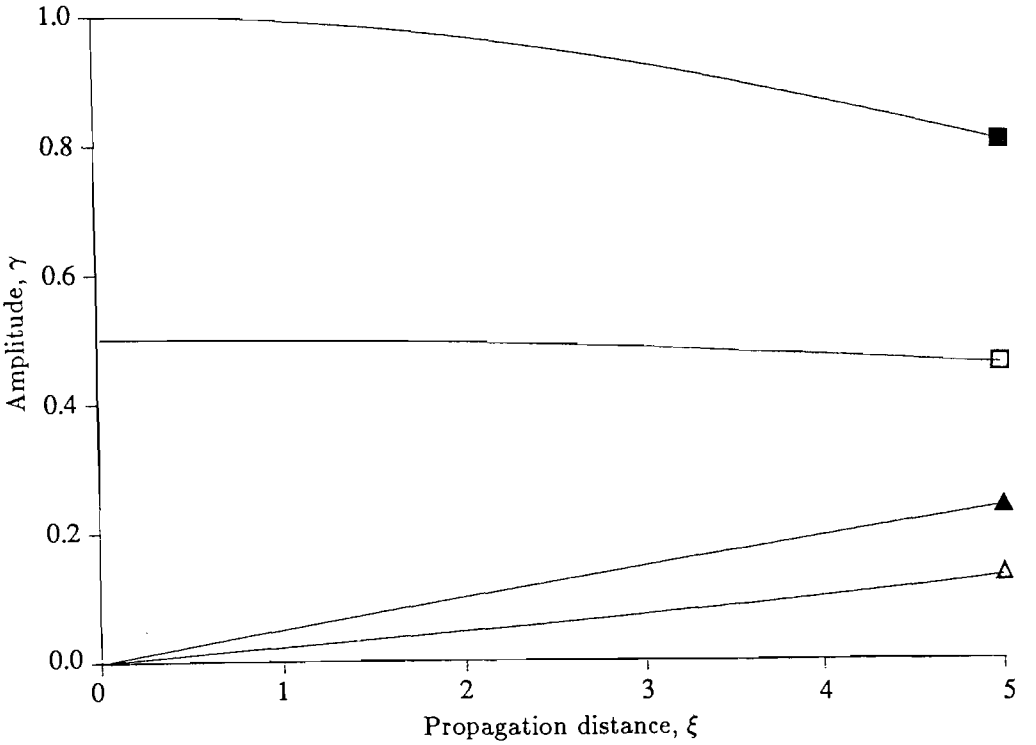

Figure 7.3.21 Growth and decay of the amplitudes $\tilde{\gamma}_I$, for I = 1, 2, 5 and 6, with propagation distance ξ_1 for Z-propagation on X-cut $LiNbO_3$, amplitude ratio $s = \frac{1}{2}$, frequency ratio $r = 0.5$

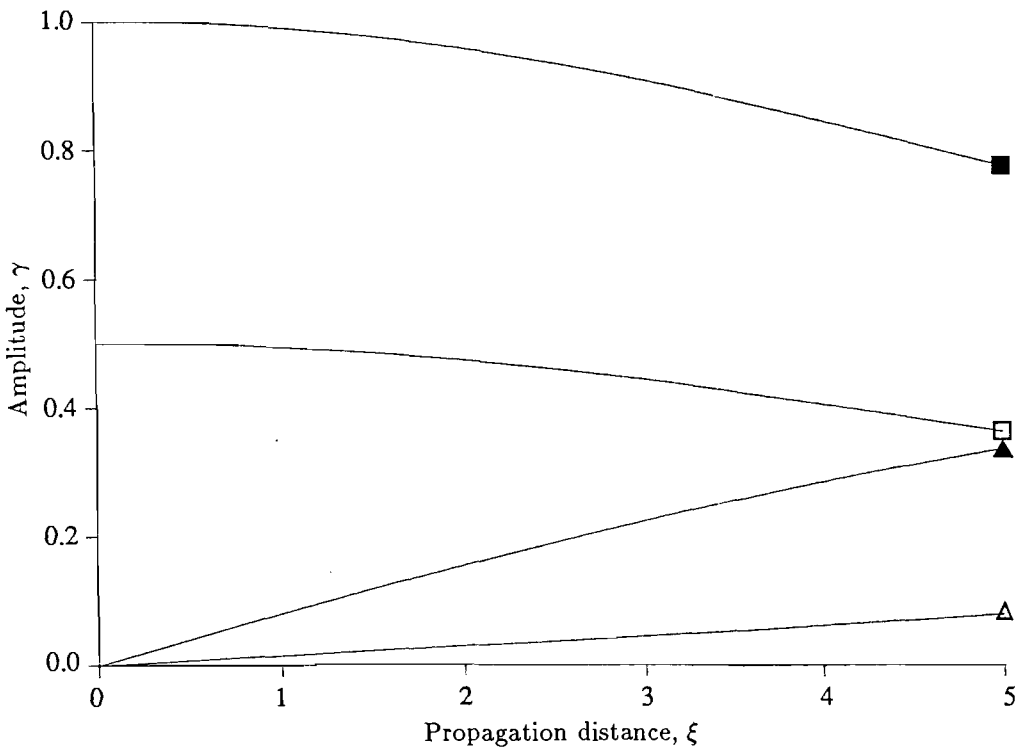

Figure 7.3.22 Growth and decay of the amplitudes $\tilde{\gamma}_I$, for I = 1, 2, 5 and 6, with propagation distance ξ_1 for Z-propagation on X-cut $LiNbO_3$, amplitude ratio $s = \frac{1}{2}$, frequency ratio $r = 0.9$

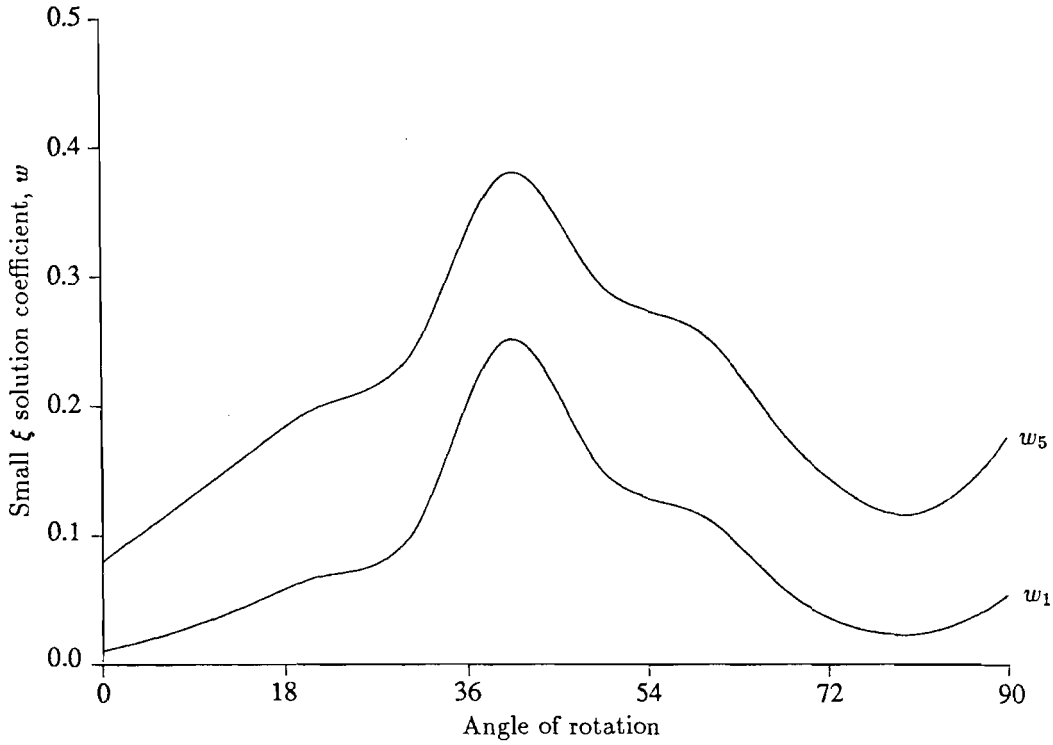

Figure 7.3.23 Vartiation of w_1 and w_5 with angle of propagation on Y-cut $LiNbO_3$, amplitude ratio $s = \frac{1}{2}$, frequency ratio $r = 0.1$

7.4 EXTENSIONS

As outlined in the introduction to this chapter, the most important distortion effect is third-order IMD. The theory presented so far in this chapter only enables us to predict second-order IMD, however all coefficients have been defined in a wholly general manner and it is thus easy to extend the analysis to cover the interaction of second harmonics.

The linear expansion of equation (7.2.9) was truncated, following the approximation of Kalyanasundaram [1981], to consider only those terms involving $A_K^{(n)}$, $B_K^{(n)}$, $K = 1, 2$, and $C_{KL}^{(n)}$, $D_{KL}^{(n)}$, $K = L = 1$, and the notational simplification

$$q_1 = 1 \quad , \quad q_2 = r \quad , \quad q_3 = 2 \quad , \quad q_4 = 2r \quad , \quad q_5 = 1+r \quad , \quad q_6 = 1-r \, , \tag{7.4.1}$$

was also introduced.

To accurately model third-order IMD it is clear that we must also include those terms representing the interaction of the second harmonic and fundamental as well as the second and third harmonics of the input waves. We thus require consideration of terms involving $A_K^{(n)}$, $B_K^{(n)}$, $K = 1, 2, 3$ and $C_{KL}^{(n)}$, $D_{KL}^{(n)}$, $K = L = 1, 2$. For this purpose we introduce the notational simplification

$$\begin{aligned} &q_1 = r \, , \; q_2 = 2r \, , \; q_3 = 1 - 2r \, , \; q_4 = 1 - r \, , \; q_5 = 1 \, , \\ &q_6 = 1 + r \, , \; q_7 = 1 + 2r \, , \; q_8 = 2 - 2r \, , \; q_9 = 2 - r \, , \; q_{10} = 2 \, , \\ &q_{11} = 2 + r \, , \; q_{12} = 2 + 2r \, , \; q_{13} = 3 \, , \; q_{14} = 3r \, . \end{aligned} \tag{7.4.2}$$

We thus derive the table of possible interactions, analogous to Table 7.2.1, presented in Table 7.4.1.

Using this table the complete second-order field equations may be deduced, however they are not reproduced in full here for the sake of brevity.

Using the method of solution for a particular frequency prescribed earlier, we may deduce the coupled amplitude equations for third-order IMD to be

$$\begin{aligned} &\gamma_{1,\xi} + \frac{1}{c}\gamma_{1,\tau} + \Delta_{1\,1\,2}\bar{\gamma}_1\gamma_2 + \Delta_{1\,3\,4}\bar{\gamma}_3\gamma_4 + \Delta_{1\,4\,5}\bar{\gamma}_4\gamma_5 + \Delta_{1\,5\,6}\bar{\gamma}_5\gamma_6 + \Delta_{1\,6\,7}\bar{\gamma}_6\gamma_7 \\ &\qquad + \Delta_{1\,8\,9}\bar{\gamma}_8\gamma_9 + \Delta_{1\,9\,10}\bar{\gamma}_9\gamma_{10} + \Delta_{1\,10\,11}\bar{\gamma}_{10}\gamma_{11} + \Delta_{1\,11\,12}\bar{\gamma}_{11}\gamma_{12} + \Delta_{1\,2\,14}\bar{\gamma}_2\gamma_{14} = 0 \, , \\ &\gamma_{2,\xi} + \frac{1}{c}\gamma_{2,\tau} + \Delta_{2\,3\,5}\bar{\gamma}_3\gamma_5 + \Delta_{2\,4\,6}\bar{\gamma}_4\gamma_6 + \Delta_{2\,5\,7}\bar{\gamma}_5\gamma_7 + \Delta_{2\,8\,10}\bar{\gamma}_8\gamma_{10} + \Delta_{2\,9\,11}\bar{\gamma}_9\gamma_{11} \\ &\qquad + \Delta_{2\,10\,12}\bar{\gamma}_{10}\gamma_{12} + \Delta_{2\,1\,14}\bar{\gamma}_1\gamma_{14} + \Pi_{2\,1\,1}\gamma_1\gamma_1 = 0 \, , \end{aligned}$$

	q_1	q_2	q_3	q_4	q_5	q_6	q_7	q_8	q_9	q_{10}	q_{11}	q_{12}	q_{13}	q_{14}
q_1	q_2	q_{14}	q_4	q_5	q_6	q_7	–	q_9	q_{10}	q_{11}	q_{12}	–	–	–
q_2	q_{14}	–	q_5	q_6	q_7	–	–	q_{10}	q_{11}	q_{12}	–	–	–	–
q_3	q_4	q_5	–	–	q_8	q_9	q_{10}	–	–	–	–	q_{13}	–	q_6
q_4	q_5	q_6	–	q_8	q_9	q_{10}	q_{11}	–	–	–	q_{13}	–	–	q_7
q_5	q_6	q_7	q_8	q_9	q_{10}	q_{11}	q_{12}	–	–	q_{13}	–	–	–	–
q_6	q_7	–	q_9	q_{10}	q_{11}	q_{12}	–	–	q_{13}	–	–	–	–	–
q_7	–	–	q_{10}	q_{11}	q_{12}	–	–	q_{13}	–	–	–	–	–	–
q_8	q_9	q_{10}	–	–	–	–	q_{13}	–	–	–	–	–	–	q_{11}
q_9	q_{10}	q_{11}	–	–	–	q_{13}	–	–	–	–	–	–	–	q_{12}
q_{10}	q_{11}	q_{12}	–	–	q_{13}	–	–	–	–	–	–	–	–	–
q_{11}	q_{12}	–	–	q_{13}	–	–	–	–	–	–	–	–	–	–
q_{12}	–	–	q_{13}	–	–	–	–	–	–	–	–	–	–	–
q_{13}	–	–	–	–	–	–	–	–	–	–	–	–	–	–
q_{14}	–	–	q_6	q_7	–	–	–	q_{11}	q_{12}	–	–	–	–	–
$\bar{q}_1$	–	q_1	–	q_3	q_4	q_5	q_6	–	q_8	q_9	q_{10}	q_{11}	–	q_2
$\bar{q}_2$	$\bar{q}_1$	–	–	–	q_3	q_4	q_5	–	–	q_8	q_9	q_{10}	–	q_1
$\bar{q}_3$	–	–	–	q_1	q_2	q_{14}	–	q_5	q_6	q_7	–	–	q_{12}	–
$\bar{q}_4$	$\bar{q}_3$	–	q_1	–	q_1	q_2	q_{14}	q_4	q_5	q_6	q_7	–	q_{11}	–
$\bar{q}_5$	$\bar{q}_4$	$\bar{q}_3$	$\bar{q}_2$	$\bar{q}_1$	–	q_1	q_2	q_3	q_4	q_5	q_6	q_7	q_{10}	–
$\bar{q}_6$	$\bar{q}_5$	$\bar{q}_4$	$\bar{q}_{14}$	$\bar{q}_2$	$\bar{q}_1$	–	q_1	–	q_3	q_4	q_5	q_6	q_9	$\bar{q}_3$
$\bar{q}_7$	$\bar{q}_6$	$\bar{q}_5$	–	$\bar{q}_{14}$	$\bar{q}_2$	$\bar{q}_1$	–	–	–	q_3	q_4	q_5	q_8	$\bar{q}_4$
$\bar{q}_8$	–	–	$\bar{q}_5$	$\bar{q}_4$	$\bar{q}_3$	–	–	–	q_1	q_2	q_{14}	–	q_7	–
$\bar{q}_9$	$\bar{q}_8$	–	$\bar{q}_6$	$\bar{q}_5$	$\bar{q}_4$	$\bar{q}_3$	–	$\bar{q}_1$	–	q_1	q_2	q_{14}	q_6	–
$\bar{q}_{10}$	$\bar{q}_9$	$\bar{q}_8$	$\bar{q}_7$	$\bar{q}_6$	$\bar{q}_5$	$\bar{q}_4$	$\bar{q}_3$	$\bar{q}_2$	$\bar{q}_1$	–	q_1	q_2	q_5	–
$\bar{q}_{11}$	$\bar{q}_{10}$	$\bar{q}_9$	–	$\bar{q}_7$	$\bar{q}_6$	$\bar{q}_5$	$\bar{q}_4$	$\bar{q}_{14}$	$\bar{q}_2$	$\bar{q}_1$	–	q_1	q_4	$\bar{q}_8$
$\bar{q}_{12}$	$\bar{q}_{11}$	$\bar{q}_{10}$	–	–	$\bar{q}_7$	$\bar{q}_6$	$\bar{q}_5$	–	$\bar{q}_{14}$	$\bar{q}_2$	$\bar{q}_1$	–	q_3	$\bar{q}_9$
$\bar{q}_{13}$	–	–	$\bar{q}_{12}$	$\bar{q}_{11}$	$\bar{q}_{10}$	$\bar{q}_9$	$\bar{q}_8$	$\bar{q}_7$	$\bar{q}_6$	$\bar{q}_5$	$\bar{q}_4$	$\bar{q}_3$	–	–
$\bar{q}_{14}$	$\bar{q}_2$	$\bar{q}_1$	–	–	–	q_3	q_4	–	–	–	q_8	q_9	–	–

Table 7.4.1 Modal interactions. The top row and left column represent the two interacting modes

$$\gamma_{3,\xi} + \frac{1}{c}\gamma_{3,\tau} + \Delta_{3\,1\,4}\bar{\gamma}_1\gamma_4 + \Delta_{3\,2\,5}\bar{\gamma}_2\gamma_5 + \Delta_{3\,5\,8}\bar{\gamma}_5\gamma_8 + \Delta_{3\,6\,9}\bar{\gamma}_6\gamma_9 + \Delta_{3\,7\,10}\bar{\gamma}_7\gamma_{10} + \Delta_{4\,6\,10}\bar{\gamma}_6\gamma_{10} + \Delta_{3\,12\,13}\bar{\gamma}_{12}\gamma_{13} + \Delta_{3\,14\,6}\bar{\gamma}_{14}\gamma_6 = 0\,,$$

$$\gamma_{4,\xi} + \frac{1}{c}\gamma_{4,\tau} + \Delta_{4\,1\,5}\bar{\gamma}_1\gamma_5 + \Delta_{4\,2\,6}\bar{\gamma}_2\gamma_6 + \Delta_{4\,4\,8}\bar{\gamma}_4\gamma_8 + \Delta_{4\,5\,9}\bar{\gamma}_5\gamma_9 + \Delta_{4\,7\,11}\bar{\gamma}_7\gamma_{11} + \Delta_{4\,11\,13}\bar{\gamma}_{11}\gamma_{13} + \Delta_{4\,14\,7}\bar{\gamma}_{14}\gamma_7 + \Pi_{4\,1\,3}\gamma_1\gamma_3 = 0\,,$$

$$\gamma_{5,\xi} + \frac{1}{c}\gamma_{5,\tau} + \Delta_{5\,1\,6}\bar{\gamma}_1\gamma_6 + \Delta_{5\,2\,7}\bar{\gamma}_2\gamma_7 + \Delta_{5\,3\,8}\bar{\gamma}_3\gamma_8 + \Delta_{5\,4\,9}\bar{\gamma}_4\gamma_9 + \Delta_{5\,5\,10}\bar{\gamma}_5\gamma_{10} + \Delta_{5\,6\,11}\bar{\gamma}_6\gamma_{11} + \Delta_{5\,7\,12}\bar{\gamma}_7\gamma_{12} + \Delta_{5\,10\,13}\bar{\gamma}_{10}\gamma_{13} + \Pi_{5\,1\,4}\gamma_1\gamma_4 + \Pi_{5\,2\,3}\gamma_2\gamma_3 = 0\,,$$

$$\gamma_{6,\xi} + \frac{1}{c}\gamma_{6,\tau} + \Delta_{6\,1\,7}\bar{\gamma}_1\gamma_7 + \Delta_{6\,3\,9}\bar{\gamma}_3\gamma_9 + \Delta_{6\,4\,10}\bar{\gamma}_4\gamma_{10} + \Delta_{6\,5\,11}\bar{\gamma}_5\gamma_{11} + \Delta_{6\,6\,12}\bar{\gamma}_6\gamma_{12} + \Delta_{6\,9\,13}\bar{\gamma}_9\gamma_{13} + \Pi_{6\,1\,5}\gamma_1\gamma_5 + \Pi_{6\,2\,4}\gamma_2\gamma_4 + \Pi_{6\,3\,14}\gamma_3\gamma_{14} = 0\,,$$

$$\gamma_{7,\xi} + \frac{1}{c}\gamma_{7,\tau} + \Delta_{7\,3\,10}\bar{\gamma}_3\gamma_{10} + \Delta_{7\,4\,11}\bar{\gamma}_4\gamma_{11} + \Delta_{7\,5\,12}\bar{\gamma}_5\gamma_{12} + \Delta_{7\,8\,13}\bar{\gamma}_8\gamma_{13} + \Pi_{7\,1\,6}\gamma_1\gamma_6 + \Pi_{7\,2\,5}\gamma_2\gamma_5 + \Pi_{7\,4\,14}\gamma_4\gamma_{14} = 0\,,$$

$$\gamma_{8,\xi} + \frac{1}{c}\gamma_{8,\tau} + \Delta_{8\,1\,9}\bar{\gamma}_1\gamma_9 + \Delta_{8\,2\,10}\bar{\gamma}_2\gamma_{10} + \Delta_{8\,7\,13}\bar{\gamma}_7\gamma_{13} + \Delta_{8\,14\,11}\bar{\gamma}_{14}\gamma_{11} + \Pi_{8\,3\,5}\gamma_3\gamma_5$$

$$+\Pi_{844}\gamma_4\gamma_4 = 0\,,$$

$$\gamma_{9,\xi} + \frac{1}{c}\gamma_{9,\tau} + \Delta_{9110}\bar{\gamma}_1\gamma_{10} + \Delta_{9211}\bar{\gamma}_2\gamma_{11} + \Delta_{9613}\bar{\gamma}_6\gamma_{13} + \Delta_{91412}\bar{\gamma}_{14}\gamma_{12} + \Pi_{936}\gamma_3\gamma_6$$
$$+\Pi_{945}\gamma_4\gamma_5 + \Pi_{918}\gamma_1\gamma_8 = 0\,,$$

$$\gamma_{10,\xi} + \frac{1}{c}\gamma_{10,\tau} + \Delta_{10111}\bar{\gamma}_1\gamma_{11} + \Delta_{10212}\bar{\gamma}_2\gamma_{12} + \Delta_{10513}\bar{\gamma}_5\gamma_{13} + \Pi_{1019}\gamma_1\gamma_9 + \Pi_{1028}\gamma_2\gamma_8$$
$$+\Pi_{1037}\gamma_3\gamma_7 + \Pi_{1046}\gamma_4\gamma_6 + \Pi_{1055}\gamma_5\gamma_5 = 0\,,$$

$$\gamma_{11,\xi} + \frac{1}{c}\gamma_{11,\tau} + \Delta_{11112}\bar{\gamma}_1\gamma_{12} + \Delta_{11413}\bar{\gamma}_4\gamma_{13} + \Pi_{11110}\gamma_1\gamma_{10} + \Pi_{1129}\gamma_2\gamma_9 + \Pi_{1147}\gamma_4\gamma_7$$
$$+\Pi_{1156}\gamma_5\gamma_6 + \Pi_{11814}\gamma_8\gamma_{14} = 0\,,$$

$$\gamma_{12,\xi} + \frac{1}{c}\gamma_{12,\tau} + \Delta_{12313}\bar{\gamma}_3\gamma_{13} + \Pi_{12111}\gamma_1\gamma_{11} + \Pi_{12210}\gamma_2\gamma_{10} + \Pi_{1257}\gamma_5\gamma_7 + \Pi_{1266}\gamma_6\gamma_6$$
$$+\Pi_{12914}\gamma_9\gamma_{14} = 0$$

$$\gamma_{13,\xi} + \frac{1}{c}\gamma_{13,\tau} + \Pi_{13312}\gamma_3\gamma_{12} + \Pi_{13411}\gamma_4\gamma_{11} + \Pi_{13510}\gamma_5\gamma_{10} + \Pi_{1369}\gamma_6\gamma_9 + \Pi_{1378}\gamma_7\gamma_8 = 0$$

$$\gamma_{14,\xi} + \frac{1}{c}\gamma_{14,\tau} + \Delta_{14367}\bar{\gamma}_3\gamma_6 + \Delta_{14477}\bar{\gamma}_4\gamma_7 + \Delta_{14811}\bar{\gamma}_8\gamma_{11} + \Delta_{14912}\bar{\gamma}_9\gamma_{12} + \Pi_{1412}\gamma_1\gamma_2 = 0\,. \tag{7.4.3}$$

The finite difference method solutions to equations (7.4.3) for the signalling conditions (7.3.1) and $s = 1/2$ are given in Figures 7.4.1 to 7.4.9 for the cubically anisotropic elastic material MgO. It is seen that the growth of the third-order interaction terms is far slower than that of second-order terms, as may have been predicted. Figures 7.4.10 to 7.4.12 present the growth and decay of the second-order IMD amplitudes for comparison with the results of Section 7.3. These results are a partial verification of our procedure and numerical routines.

The particular case of propagation 30° away from the axis of symmetry for the frequency ratio $r = 0.1$ has again been considered and the fundamental of the smaller amplitude wave found to grow in amplitude whilst conserving energy. This phenomenon could possibly prove useful in amplification applications.

Figures 7.4.13 to 7.4.18 give the corresponding results for the piezoelectric substrate lithium niobate whilst Figures 7.4.19 to 7.4.21 present the second-order IMD amplitudes for comparison with Section 7.3. The third-order graphs again exhibit similar features to those of second-order IMD and single propagating piezoelectric waves.

No small ξ solution is attempted for the system (7.4.3), however the value of x_{10} for third-order IMD effects may be estimated from the Figures 7.4.1 to 7.4.9 and 7.4.13 to 7.4.18. It is found to vary between 120 and well over 5000 wavelengths for magnesium oxide, and betweeen 80 and over 8000 wavelengths for lithium niobate. As can be seen from the figures presented in this section, many surfaces

exist for which one interaction frequency remains negligible. However, this appears to correspond to cases in which the other interaction frequency grows at a faster rate and hence some compromise must be made.

Key to Figures

- ■ Fundamental amplitude, $\tilde{\gamma}_5$.
- □ Fundamental amplitude, $\tilde{\gamma}_1$.
- ▲ Interaction amplitude, $\tilde{\gamma}_3$.
- △ Interaction amplitude, $\tilde{\gamma}_9$.

Except Figures 7.4.10 to 7.4.12 and 7.4.19 to 7.4.21, where the convention of Section 7.3 is used.

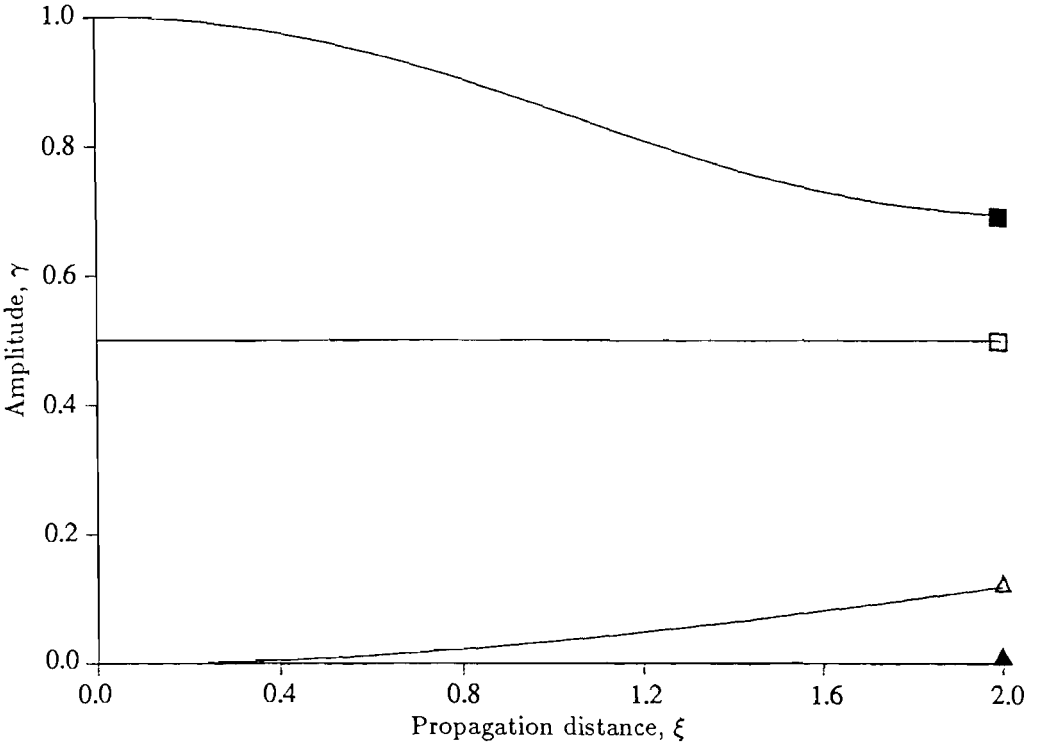

Figure 7.4.1 Growth and decay of the amplitudes $\tilde{\gamma}_I$ with propagation distance ξ_1 for X-propagation on Y-cut MgO, amplitude ratio $s = \frac{1}{2}$,frequency ratio $r = 0.1$

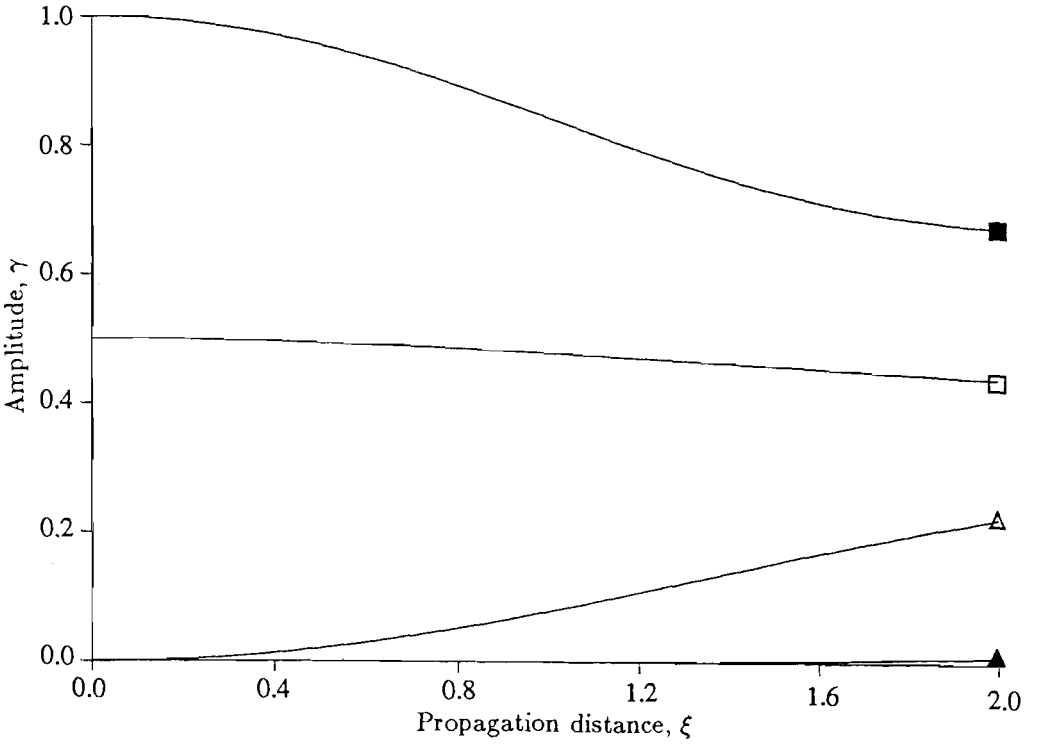

Figure 7.4.2 Growth and decay of the amplitudes $\tilde{\gamma}_I$ with propagation distance ξ_1 for X-propagation on Y-cut MgO, amplitude ratio $s = \frac{1}{2}$, frequency ratio $r = 0.5$

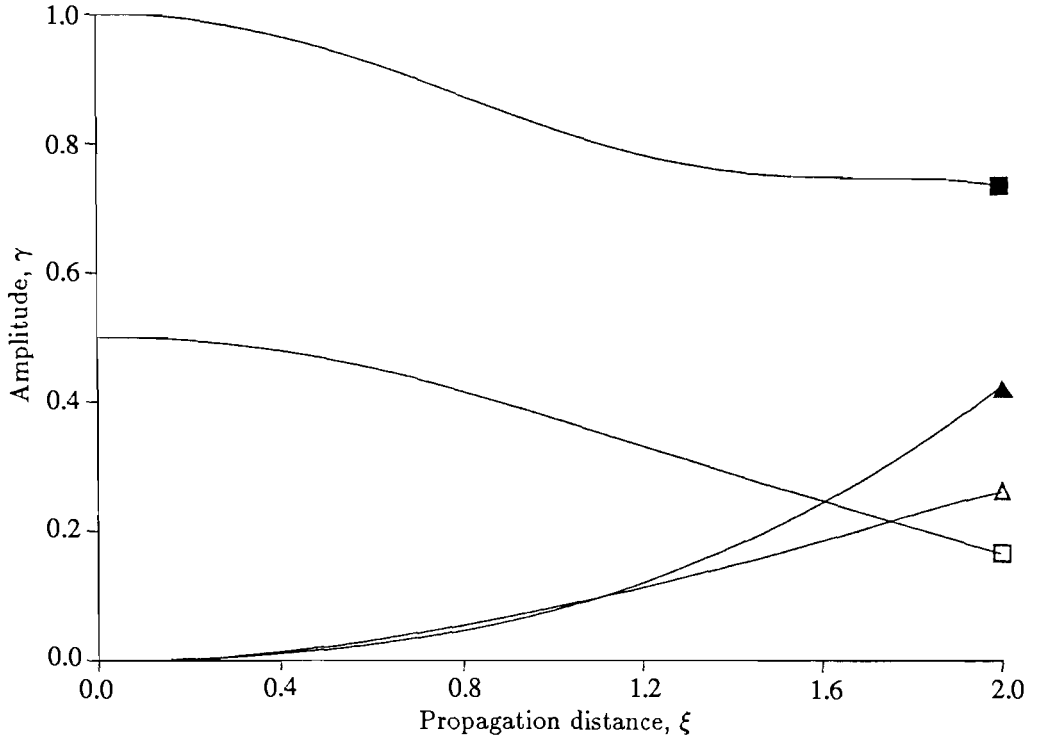

Figure 7.4.3 Growth and decay of the amplitudes $\tilde{\gamma}_I$ with propagation distance ξ_1 for X-propagation on Y-cut MgO, amplitude ratio $s = \frac{1}{2}$, frequency ratio $r = 0.9$

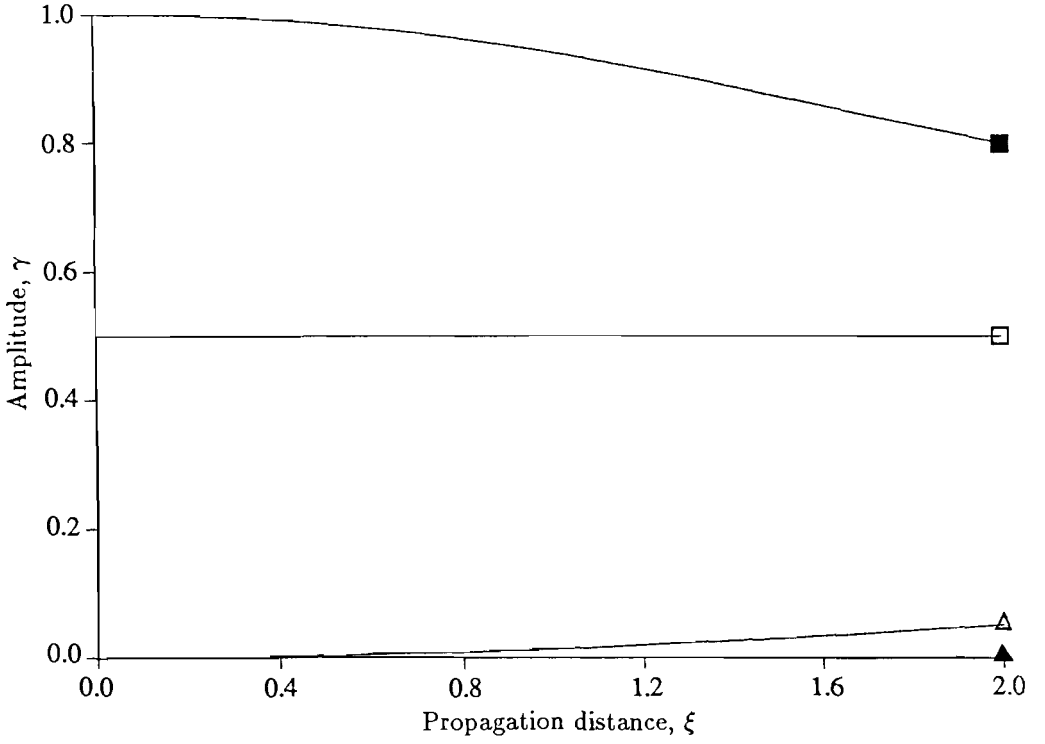

Figure 7.4.4 Growth and decay of the amplitudes $\tilde{\gamma}_I$ with propagation distance ξ_1 for propagation 20° from the X-axis on Y-cut MgO, amplitude ratio $s = \frac{1}{2}$, frequency ratio $r = 0.1$

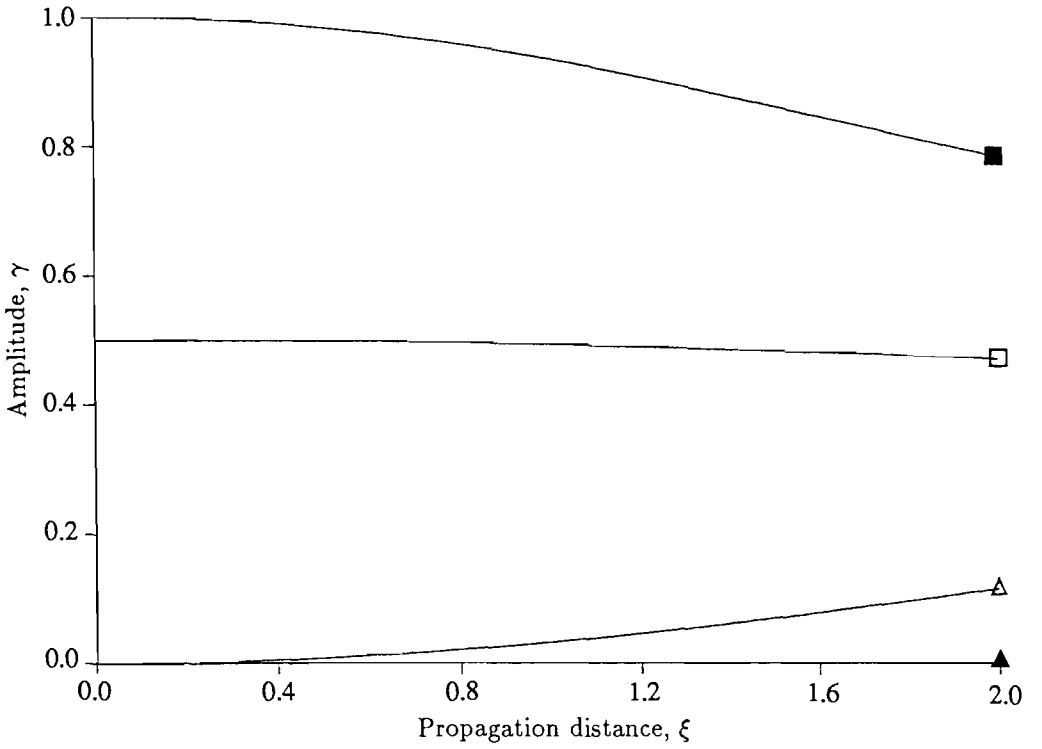

Figure 7.4.5 Growth and decay of the amplitudes $\tilde{\gamma}_I$ with propagation distance ξ_1 for propagation 20° from the X-axis on Y-cut MgO, amplitude ratio $s = \frac{1}{2}$, frequency ratio $r = 0.5$

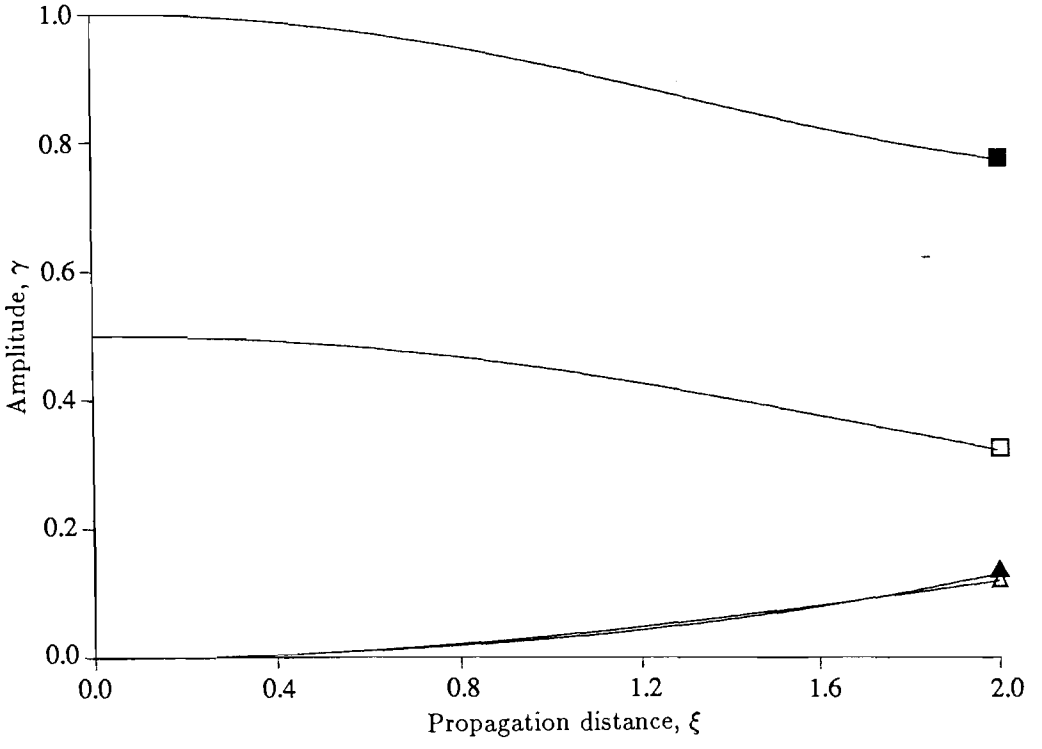

Figure 7.4.6 Growth and decay of the amplitudes $\tilde{\gamma}_I$ with propagation distance ξ_1 for propagation 20° from the X-axis on Y-cut MgO, amplitude ratio $s = \frac{1}{2}$, frequency ratio $r = 0.9$

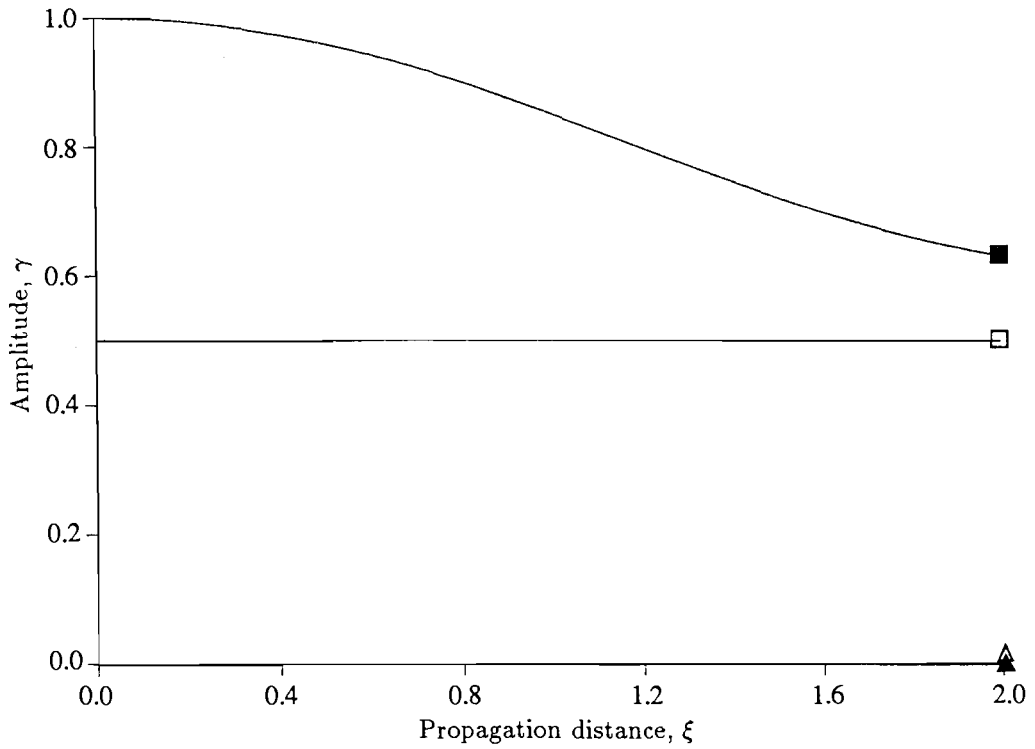

Figure 7.4.7 Growth and decay of the amplitudes $\tilde{\gamma}_I$ with propagation distance ξ_1 for propagation 30° from the X-axis on Y-cut MgO, amplitude ratio $s = \frac{1}{2}$, frequency ratio $r = 0.1$

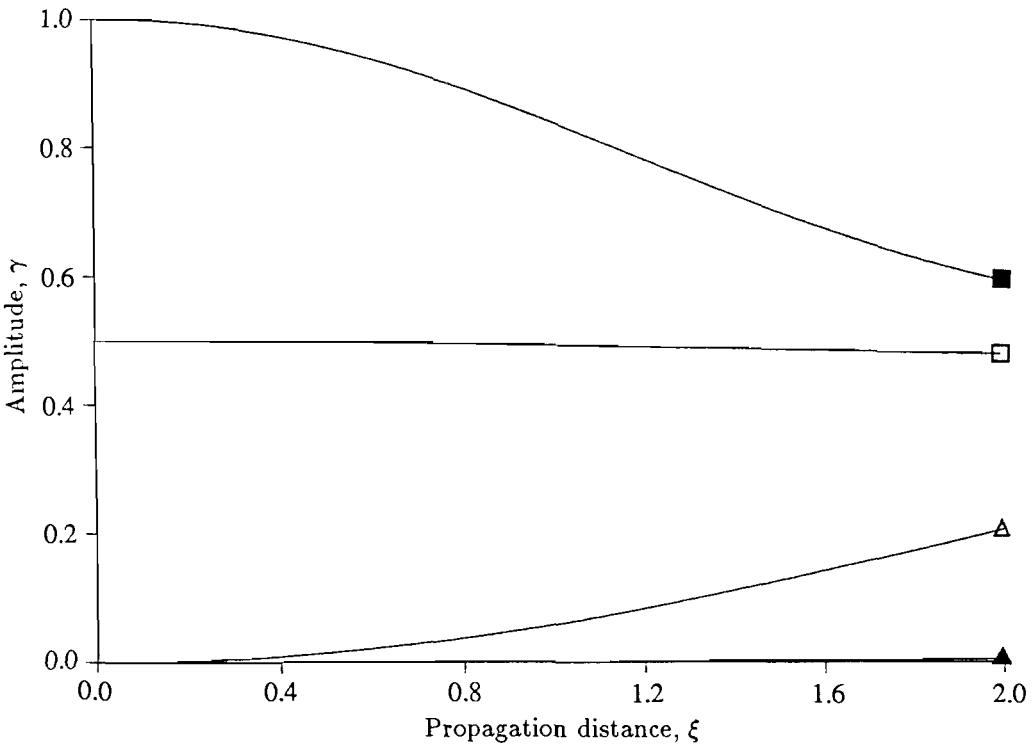

Figure 7.4.8 Growth and decay of the amplitudes $\tilde{\gamma}_I$ with propagation distance ξ_1 for propagation 30° from the X-axis on Y-cut MgO, amplitude ratio $s = \frac{1}{2}$, frequency ratio $r = 0.5$

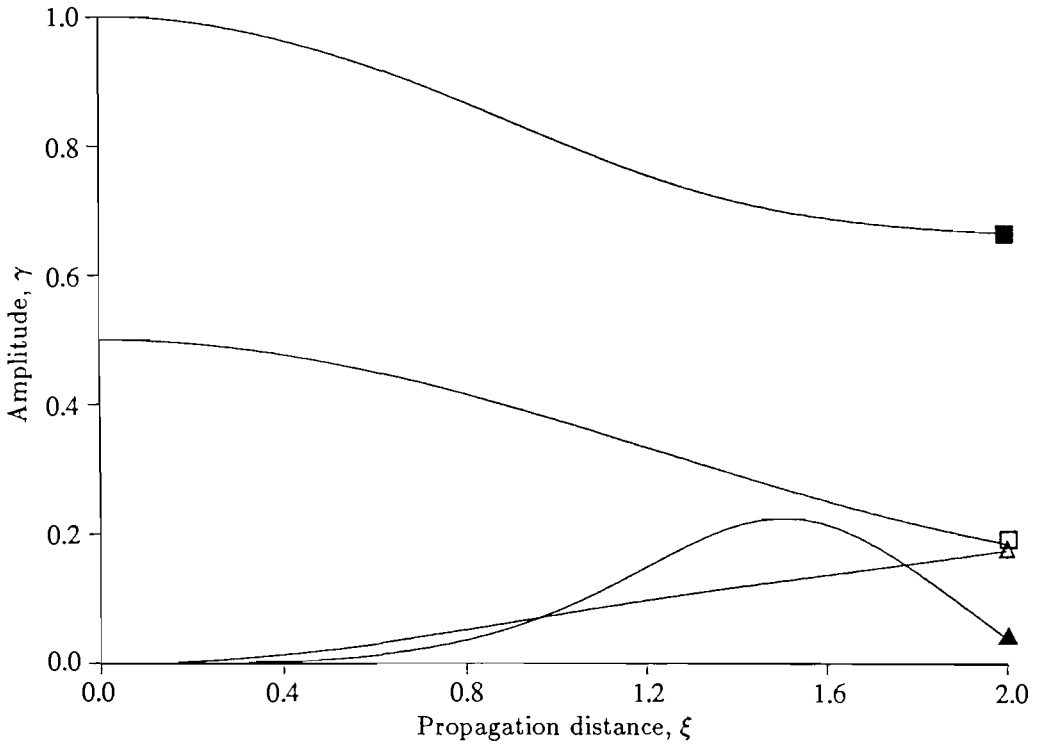

Figure 7.4.9 Growth and decay of the amplitudes $\tilde{\gamma}_I$ with propagation distance ξ_1 for propagation 30° from the X-axis on Y-cut MgO, amplitude ratio $s = \frac{1}{2}$, frequency ratio $r = 0.9$

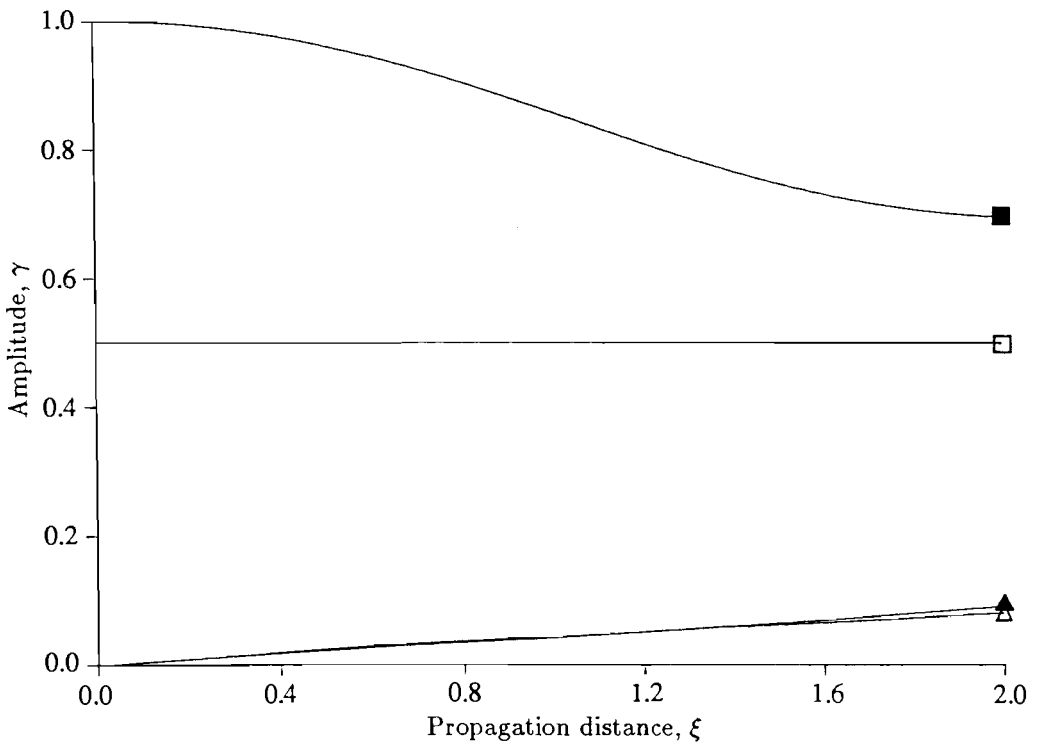

Figure 7.4.10 Growth and decay of the amplitudes $\tilde{\gamma}_I$ with propagation distance ξ_1 for X-propagation on Y-cut MgO displaying second-order IMD, amplitude ratio $s = \frac{1}{2}$, frequency ratio $r = 0.1$

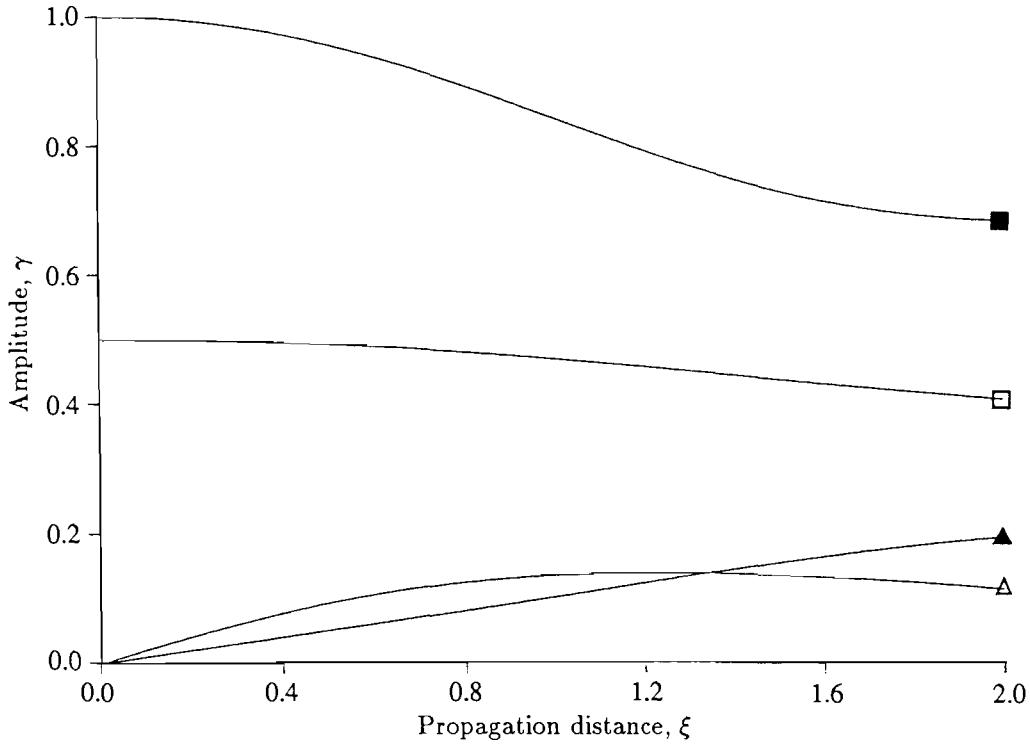

Figure 7.4.11 Growth and decay of the amplitudes $\tilde{\gamma}_I$ with propagation distance ξ_1 for X-propagation on Y-cut MgO displaying second-order IMD, amplitude ratio $s = \frac{1}{2}$, frequency ratio $r = 0.5$

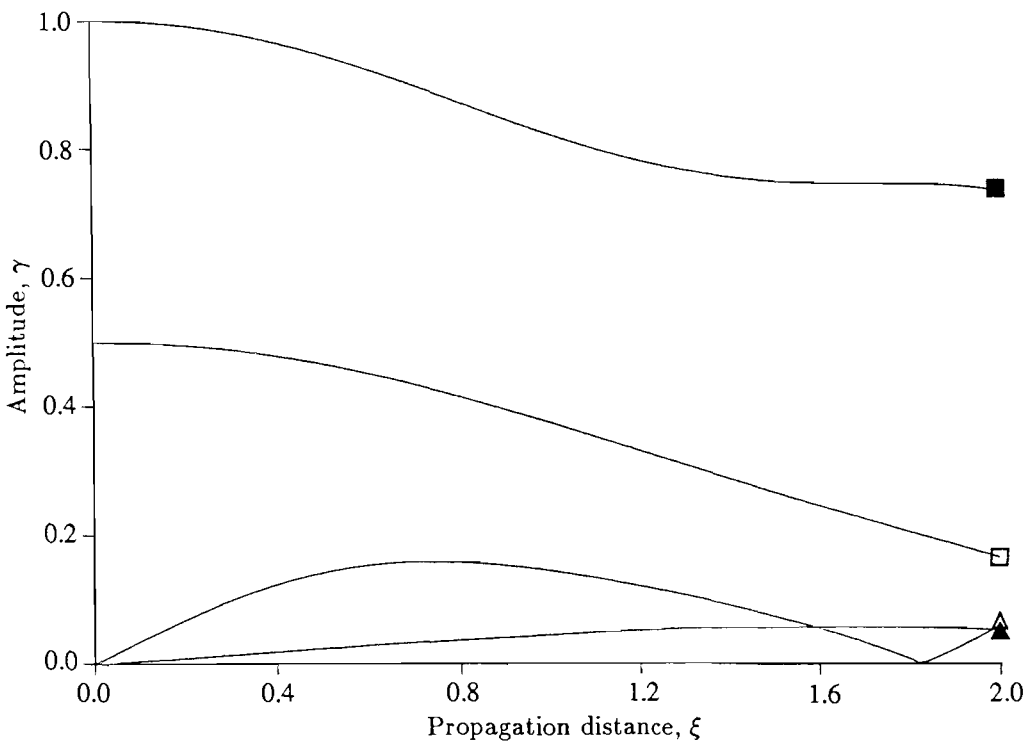

Figure 7.4.12 Growth and decay of the amplitudes $\tilde{\gamma}_I$ with propagation distance ξ_1 for X-propagation on Y-cut MgO displaying second-order IMD, amplitude ratio $s = \frac{1}{2}$, frequency ratio $r = 0.9$

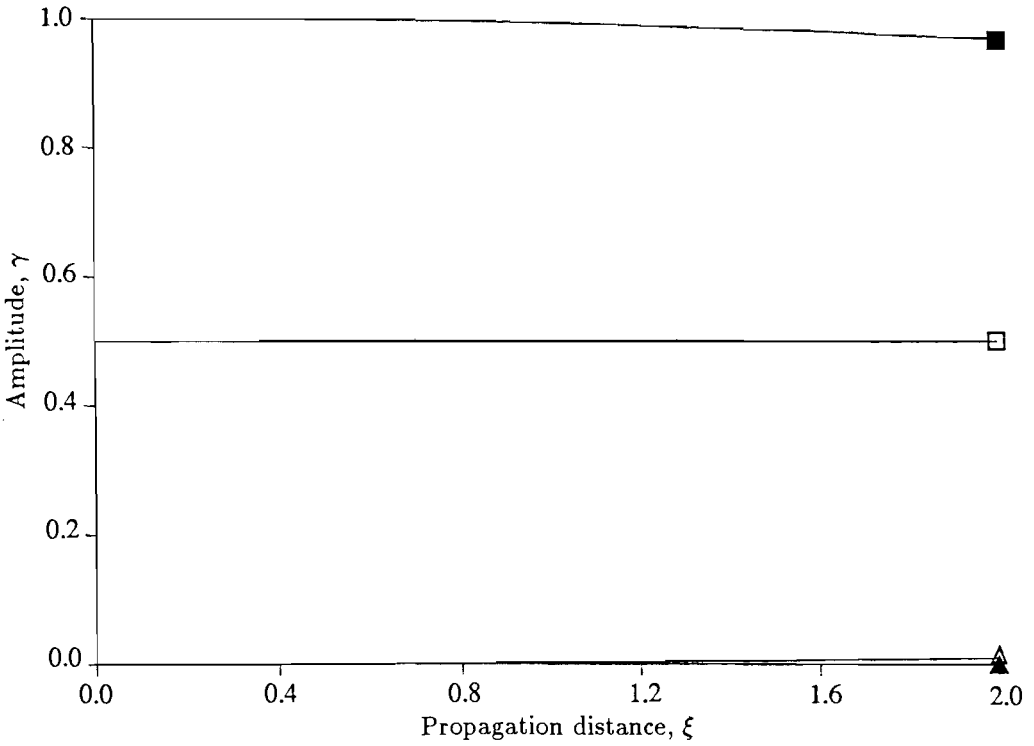

Figure 7.4.13 Growth and decay of the amplitudes $\tilde{\gamma}_I$ with propagation distance ξ_1 for X-propagation on Y-cut $LiNbO_3$, amplitude ratio $s = \frac{1}{2}$, frequency ratio $r = 0.1$

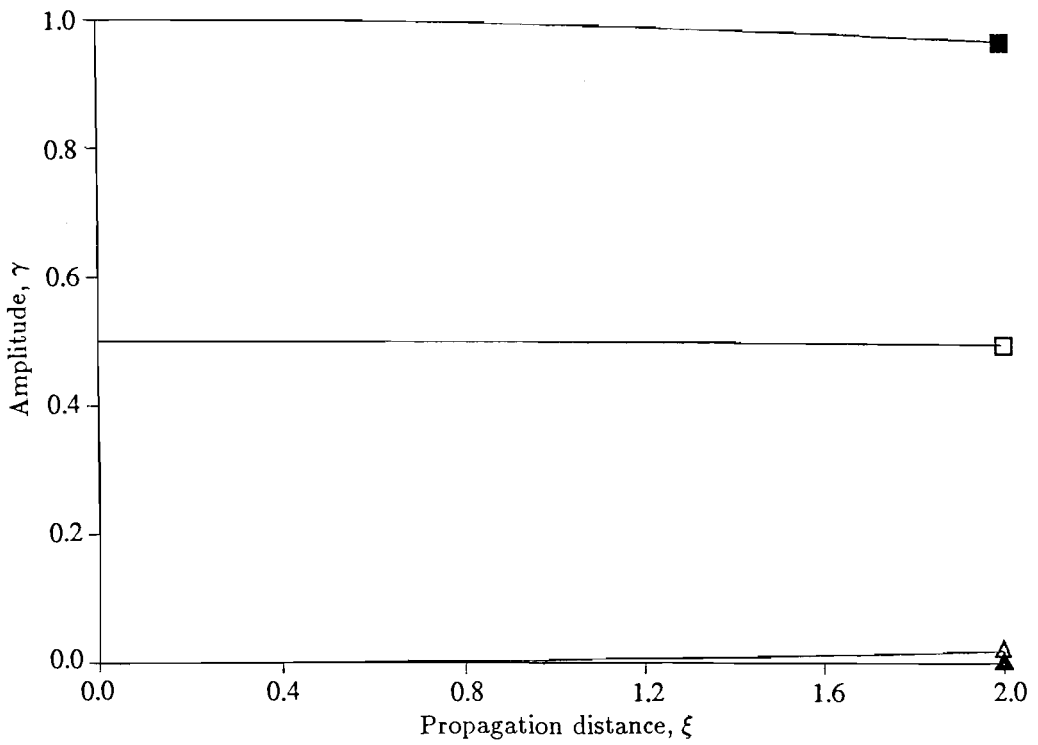

Figure 7.4.14 Growth and decay of the amplitudes $\tilde{\gamma}_I$ with propagation distance ξ_1 for X-propagation on Y-cut $LiNbO_3$, amplitude ratio $s = \frac{1}{2}$, frequency ratio $r = 0.5$

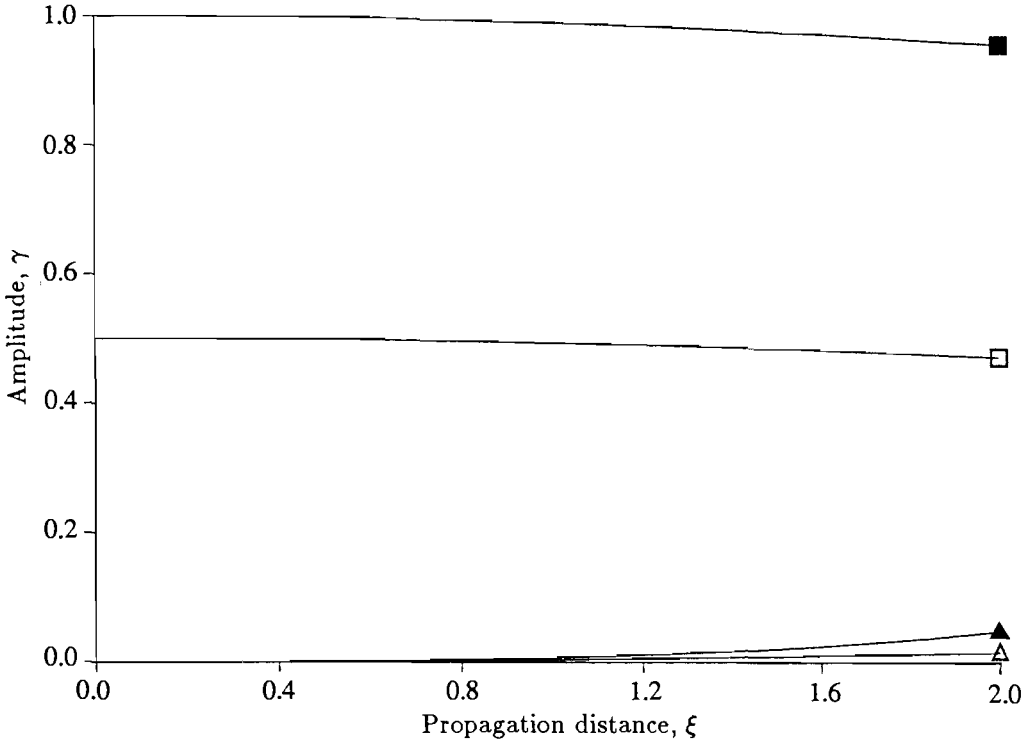

Figure 7.4.15 Growth and decay of the amplitudes $\tilde{\gamma}_I$ with propagation distance ξ_1 for X-propagation on Y-cut $LiNbO_3$, amplitude ratio $s = \frac{1}{2}$, frequency ratio $r = 0.8$

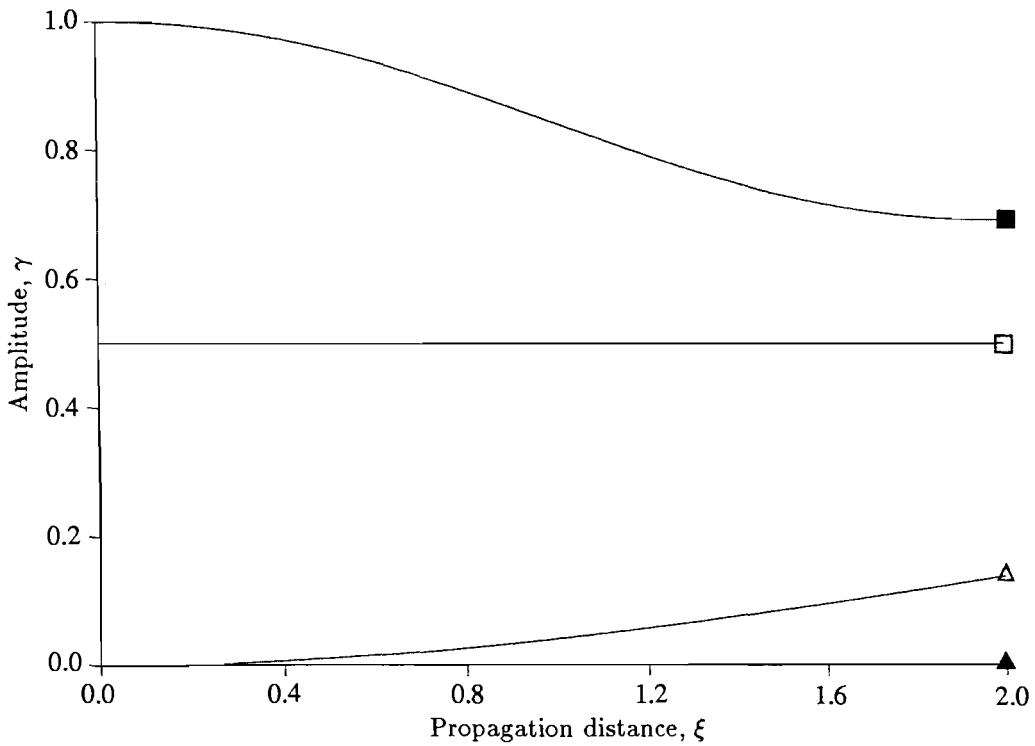

Figure 7.4.16 Growth and decay of the amplitudes $\tilde{\gamma}_I$ with propagation distance ξ_1 for propagation 40° from the X-axis on Y-cut $LiNbO_3$, amplitude ratio $s = \frac{1}{2}$, frequency ratio $r = 0.1$

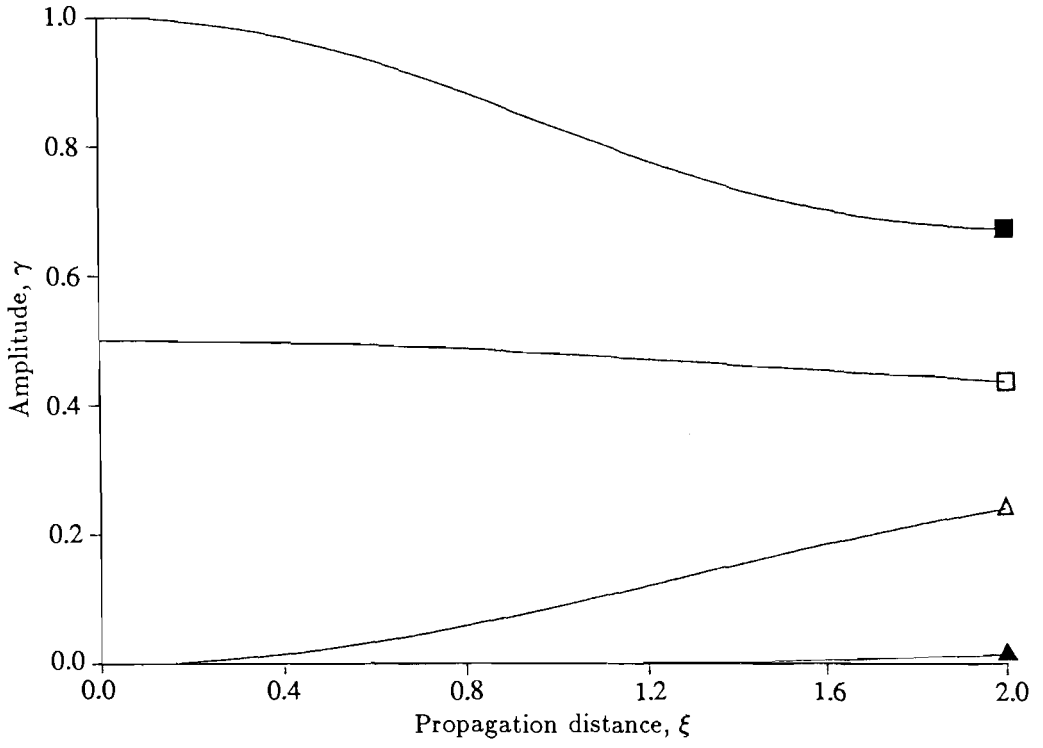

Figure 7.4.17 Growth and decay of the amplitudes $\tilde{\gamma}_I$ with propagation distance ξ_1 for propagation 40° from the X-axis on Y-cut $LiNbO_3$, amplitude ratio $s = \frac{1}{2}$, frequency ratio $r = 0.5$

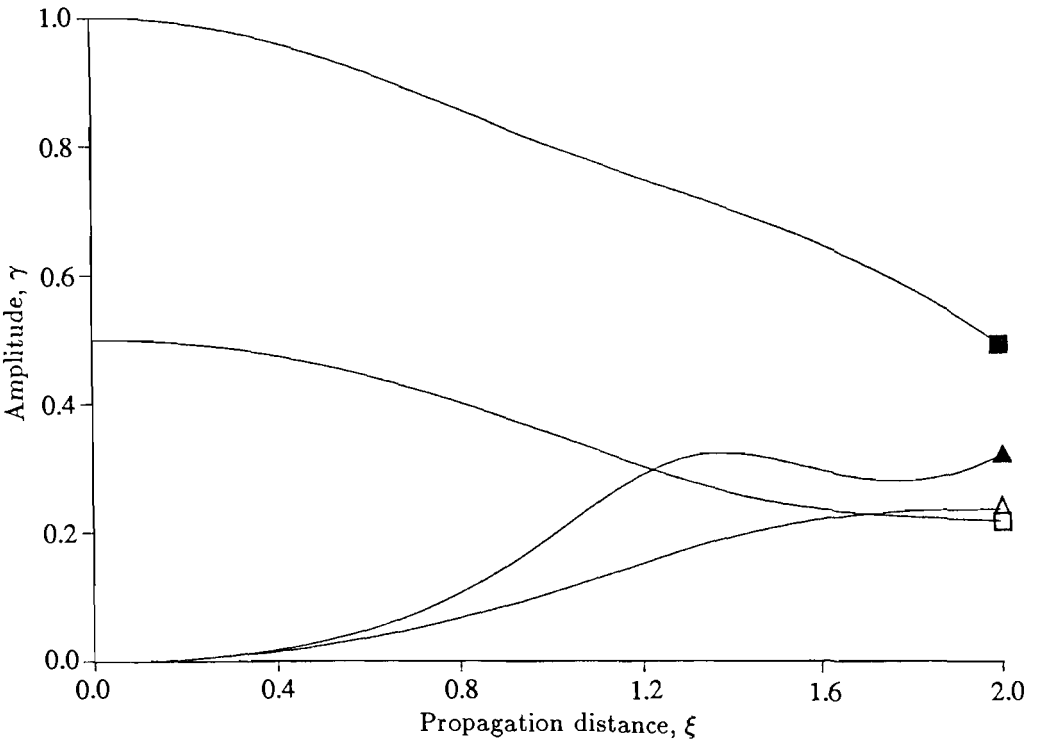

Figure 7.4.18 Growth and decay of the amplitudes $\tilde{\gamma}_I$ with propagation distance ξ_1 for propagation 40° from the X-axis on Y-cut $LiNbO_3$, amplitude ratio $s = \frac{1}{2}$, frequency ratio $r = 0.9$

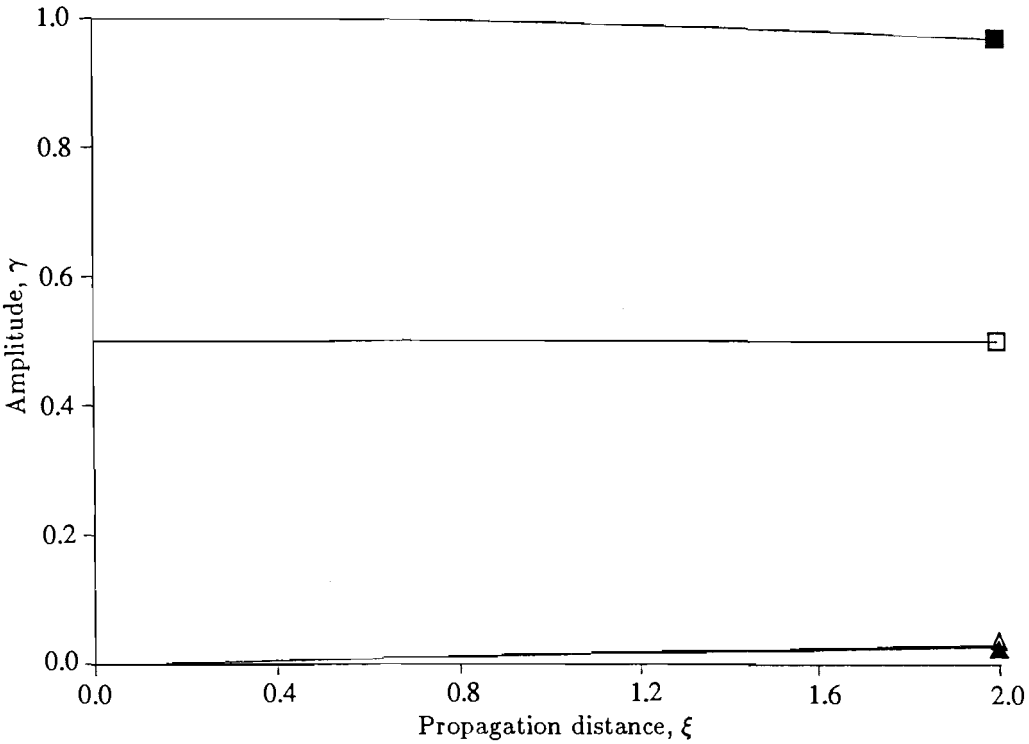

Figure 7.4.19 Growth and decay of the amplitudes $\tilde{\gamma}_I$ with propagation distance ξ_1 for X-propagation on Y-cut $LiNbO_3$ displaying second-order IMD, amplitude ratio $s = \frac{1}{2}$, frequency ratio $r = 0.1$

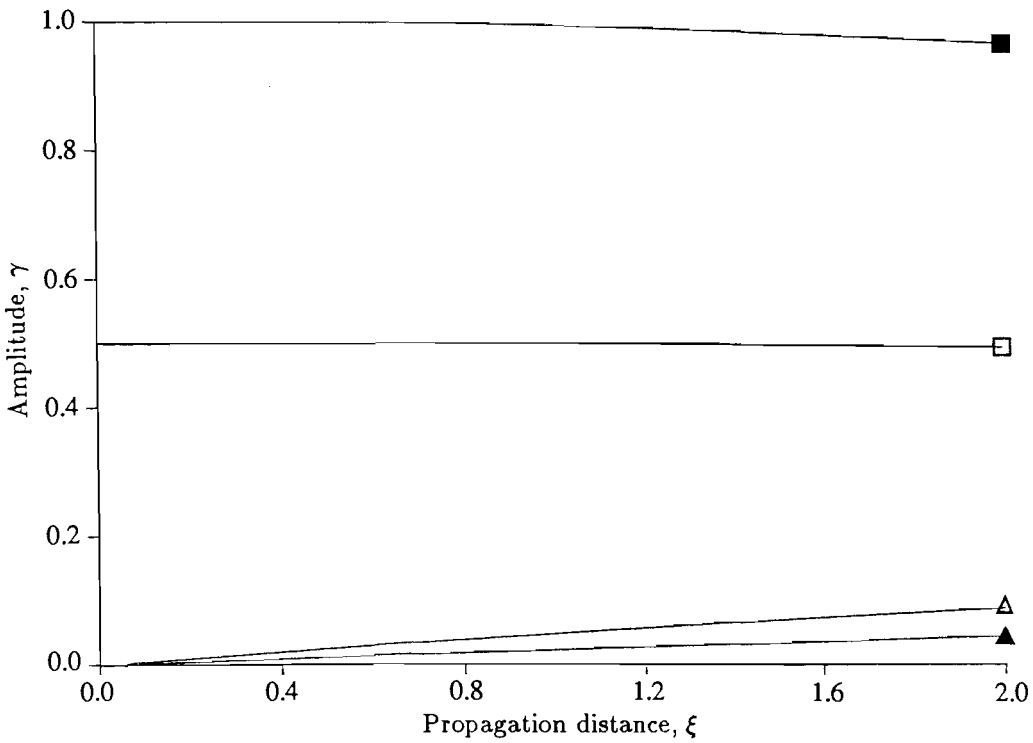

Figure 7.4.20 Growth and decay of the amplitudes $\tilde{\gamma}_I$ with propagation distance ξ_1 for X-propagation on Y-cut $LiNbO_3$ displaying second-order IMD, amplitude ratio $s = \frac{1}{2}$, frequency ratio $r = 0.5$

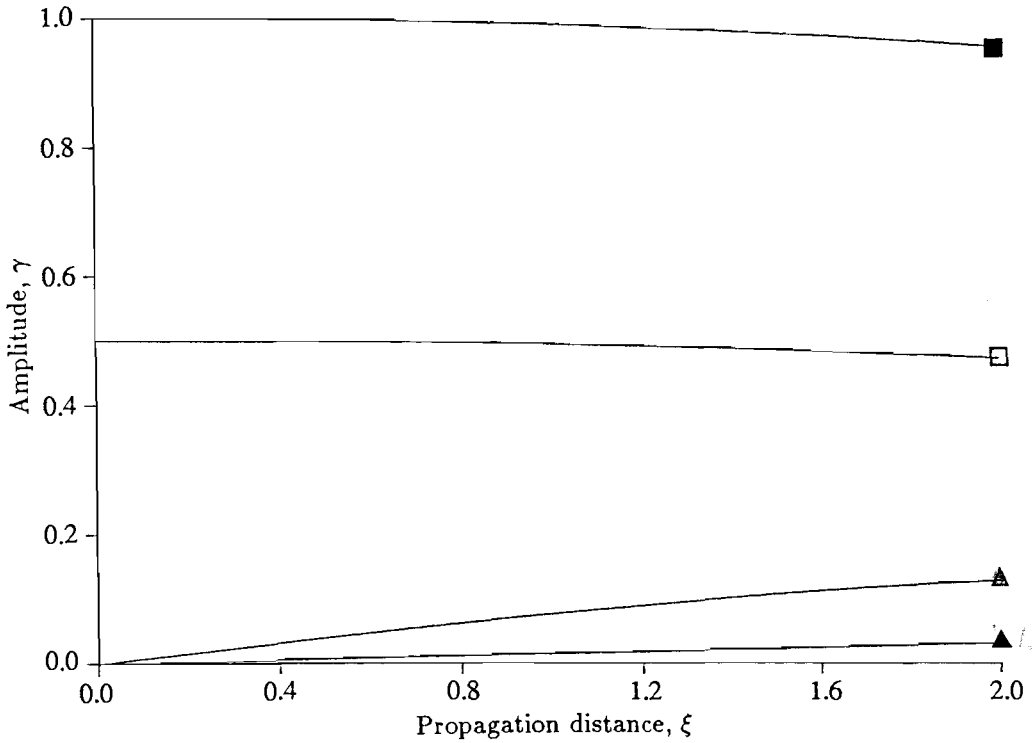

Figure 7.4.21 Growth and decay of the amplitudes $\tilde{\gamma}_I$ with propagation distance ξ_1 for X-propagation on Y-cut $LiNbO_3$ displaying second-order IMD, amplitude ratio $s = \frac{1}{2}$, frequency ratio $r = 0.9$

8 Concluding Discussion

The aim of this thesis has been to mathematically model the nonlinear propagation and interaction of surface acoustic waves on a variety of substrates and thus to predict the behaviour of two particular acoustic wave devices. This task has been achieved by separating the problem into its two constitutive parts: the propagation of surface acoustic waves on anisotropic and piezoelectric media and the interaction of surface acoustic waves under specific boundary conditions. In the present chapter the advances made will be highlighted and shortcomings discussed. Unresolved problems will also be presented and possible extensions of the present work noted.

The material presented in Chapter 3 has received considerable attention in recent years, Lardner [1986], Lardner and Tupholme [1986], Parker [1988]. The shortcomings of the multiple scales technique have been discussed in detail by Parker and Talbot [1985] and Parker [1988] and resolve around the necessity of considering the secularity of the second-order system. It is noted here that small perturbations about the linear solution can lead to bounded solutions to the nonlinear equations of motion as presented by Parker [1988], and that a generalised harmonic function formulation for the material displacement allows consideration of waves that propagate at speeds other than the Rayleigh wave speed and that are non-distorting. For the purposes of this thesis, however, and bearing in mind the goal of modelling an idealised acoustic device, it was felt that the method of multiple scales was able to provide a straightforward derivation of the bounded evolution equations, closely comparable to a perturbation expansion, and thus lead to results accessible to designers of devices.

The results presented for the material magnesium oxide give a general representation of the behaviour of the growth and decay parameters governing the evolution of surface waves with changing material symmetry. As noted in earlier chapters, the form of this behaviour could not have been predicted through symmetry considerations alone and it would be constructive to introduce some parameter denoting

the level of material symmetry of any particular crystallographic orientation. It is felt that comparison of the growth and decay parameters, introduced through the series expansion in the slow distance parameter, ξ, would lead to a greater insight into the mechanisms involved and how to tailor them to the device designer's advantage.

The problems encountered obtaining reliable estimates for the numerical values of the third-order elastic and electric constants for materials of classes other than the simple case of cubically anisotropic elasticity must be considered as the most serious problem faced in the application of the theory presented in this thesis to any "real" application. In many cases it has not proved possible even to predict the sign of particular constants by the stress–loading techniques commonly applied. The results of statistical errors in the constants is briefly discussed in Chapter 4 and implies that surface acoustic wave propagation could be efficiently employed in the evaluation of certain constants.

It is hoped that the analysis of Chapter 7 will prove to be a reliable estimate of the level of distortion in particular filter designs and an improvement upon the intercept point convention currently employed. A systematic study of the growth and decay parameters is now possible for any particular cut of crystal and could efficiently be utilised by designers.

There are many problems raised in this thesis that cannot satisfactorily be answered in the space and time allocated for a doctoral thesis. Some of particular interest are here noted in the hope that they may be considered by future researchers.

In Section 3.4 the particular case of cubic symmetry was discussed and linear solutions presented for rotations within a plane of symmetry. Analytical solutions were sought but not found for rotation to a general angle θ, although such solutions are obtainable through consideration of the slowness surface, Chadwick and Smith [1982]. It is felt that decompositions are available for other classes of restricted symmetry and that consideration of such cases may lead to more general observations regarding the behaviour of surface waves with varying levels of symmetry.

A justification of the simplification (4.1.19) has been presented in Chapter 5 based upon a transformation of the free space coordinate system. Results show that the errors introduced through this assumption are negligible in comparison to the high level of statistical error present in the numerical data employed. It is possible that

such rigorous techniques may be employed in the study of the effects of transducer placement on the free surface.

The notational simplifications of Chapter 4, noted also by Parker and David $[1989]_a$, lead one to suppose that any piezoelectric half-space problem may now be reduced to its anisotropic elastic equivalent and solved through techniques developed for the study of elasticity. Problems posed could include shock development, crack propagation, diffraction and non-destructive testing.

Bibliography

Alippi, A., Palma, A., Palmieri, L. and Socino, G. [1977] "Phase and amplitude relations between fundamental and second harmonic acoustic surface waves on silicon dioxide and lithium niobate" *J. Appl. Phys.* **48(6)** 2182

Atkin, R. and Fox, N. [1980] *An introduction to the theory of elasticity,* Longman

Auld, B.A. [1973] *Acoustic Fields and Waves in Solids, Vols 1 and 2,* Wiley New York

Barnett, D.M. and Lothe, J. [1974] "Consideration of the existence of surface wave solutions in anisotropic elastic crystals" *J. Phys. F: Metal Phys.* **4** 671

Barnett, D.M., Lothe, J., Nishioka, K. and Saro, R.J. [1973] "Elastic surface waves in anisotropic crystals" *J. Phys. F: Metal Phys.* **3** 1083

Bechtel, S.E. and Bogy, D.B. [1984] "Interaction of a piezoelectric transducer with an elastic half-space" *Int. J. Solids Structures* **20(9/10)** 809

Bender, C.M. and Orszag, S.A. [1978] *See end of bibliography*

Brugger, K. [1965] "Pure modes for elastic waves in crystals" *J. Appl. Phys.* **36(3)** 759

Buchwald, V.T. [1961] "Rayleigh waves in transversely isotropic media" *Quart. Journ. Mech. and Applied Math.* **XIV** pt.3

Buchwald, V.T. and Davis, A. [1963] "Surface waves in elastic media with cubic symmetry" *Quart. Journ. Mech. and Applied Math.* **XVI** pt.3 293

Burridge, R. [1970] "The directions in which Rayleigh waves may be propagated on crystals" *Quart. Journ. Mech. and Applied Math.* **XXIII** pt.2 217

Campbell, J.J. and Jones, W.R. [1968] "A method for estimating optimal crystal cuts and propagation directions for excitation of piezoelectric surface waves" *IEEE Trans. Sonics and Ultrasonics* SU-**15** 209

Chadwick, P. [1976] "The existence of pure surface modes in elastic materials with orthorhombic symmetry" *J. Sound and Vib.* **47(1)** 39

Chadwick, P. and Smith, G.D. [1982] "Surface waves in cubic elastic materials" in *Mechanics of Solids* (Hopkins, H.G. and Sewell, M.J. eds.) Pergamon

Chambers, Turner and Mason [1972] "Acoustic surface wave convolution" *Electron. Letts.* **8(12)** 314

Cho, Y. and Yamanouchi, K. [1987] "Nonlinear elastic, piezoelectric, electrostrictive and dielectric constants of lithium niobate" *J. Appl. Phys.* **61** 875

Cho, Y. and Yamanouchi, K. [1987] "Theoretical and experimental studies of transverse–horizontal convolvers" *J. Appl. Phys.* **61** 1728

Cole, J.D. and Kevorkian, X.X. [1968] *Perturbation methods in applied mathematics,* Ginn and Co.

Cowin, S.C. and Mehrabadi, M.M. [1987] "On the identification of material symmetry for anisotropic elastic materials" *Quart. Journ. Mech. and Applied Math.* **40** pt.4 451

Currie, P.K. [1974] "Rayleigh waves on elastic crystals" *Quart. Journ. Mech. and Applied Math.* **XXVII** pt.4 489

David, E.A. [1985] "Uniform asymptotic solution for nonlinear surface acoustic waves" *Int. J. Engng. Sci.* **16** 699

David, E.A. and Parker, D.F. [1990] "Nondistorting waveforms of electroelastic surface waves" Wave Motion

Eringen, A.C. [1962] *Nonlinear theory of continuous media,* McGraw-Hill

Eringen, A.C. [1967] *Mechanics of continua,* Wiley

Eringen, A.C. [1974] *Elastodynamics,* Academic Press

Farnell, G.W. [1970] in *Physical Acoustics* Mason, W.P. and Thurston, R.N. eds., Volume IV Chapter 3, Academic Press, New York

Ganguly, A.K. and Davis, K.L. [1980] "Nonlinear interactions in degenerate surface acoustic wave elastic convolvers" *J. Appl. Phys.* **51** 920

Gazis, D.C., Herman, R. and Wallis, R.F. [1960] "Surface elastic waves in cubic crystals" *Physical review* **119** no. 2 533

Graham, R.A. [1977] "Second- and third-order piezoelectric stress constants of lithium niobate as determined by the impact-loading technique" *J. Appl. Phys.* **48(6)** 2153

Grassl, H. *et al* [1988] *See end of bibliography*

Harvey, A.P., Craine, R.E. and Syngellakis, S. [1988] "Nonlinear piezoelectric surface acoustic waves using the multiple scales technique" in *Recent Developments in Surface Acoustic Waves,* (Maugin, G.A. and Parker, D.F. eds.) Series on Wave Phenomena, Springer-Verlag

Harvey, A.P. and Tupholme, G.E. [1990] "Nonlinear mode coupling of two co-directional surface acoustic waves on a piezoelectric solid" *Int. J. Engng. Sci.* (submitted for publication)

Hearmon, R.F.S. [1953] "Third-order elastic coefficients" *Acta Crystallographica* **6** 331

Hearmon, R.F.S. [1961] *Introduction to applied anisotropic elasticity,* Oxford

Hellwege, K.-H. [1979] *Landolt–Börnstein. Numerical data and functional relationships in science and technology. New series. Group III: Crystal and solid state Physics, Volume 11, Elastic, Piezoelectric, Pyroelectric, Piezooptic, Electrooptic constants, and nonlinear dielectric susceptibilities of crystals,* Springer-Verlag

I.R.E. [1949] "Standards on piezoelectric crystals, 1949" *Proceedings of the I.R.E.* **37** 1378

Jacobi, J.H. [1986] "IMD: Still unclear after 20 years" *Microwaves and RF* 119, November

Kakutani, T., Inoue, Y. and Kan, T. [1974] *J. Phys. Soc. Japan* **37** 529

Kalyanasundaram, N. $[1981]_a$ "Nonlinear surface acoustic waves on an isotropic solid" *Int. J. Engng. Sci.* **19** 279

Kalyanasundaram, N. $[1981]_b$ "Nonlinear mode coupling of surface acoustic waves on an isotropic solid" *Int. J. Engng. Sci.* **19** 435

Kalyanasundaram, N. [1983] "Nonlinear mixing of surface acoustic waves propagating in opposite directions" *J. Acoust. Soc. Am.* **73** 1956

Kalyanasundaram, N. [1984] "Nonlinear propagation characteristics of Bleustein-Gulyaev waves" *J. Sound Vib.* **96(4)** 411

Kalyanasundaram, N. and Anand, G.V. [1980] "Surface acoustic waves of finite amplitude excited by a monochromatic line source" *J. Acoust. Soc. Am.* **68(2)**

Kalyanasundaram, N. and Anand, G.V. [1982] "Periodic Rayleigh waves of finite amplitude on an isotropic solid" *J. Acoust. Soc. Am.* **72(5)** 1518

Kalyanasundaram, N. Ravindran, R. and Prasad, P. [1982] "Coupled amplitude theory of nonlinear surface acoustic waves" *J. Acoust. Soc. Am.* **72(2)** 488

Korobov, A.I. and Lyamov, V.E. [1975] "Nonlinear piezoelectric coefficients of lithium niobate" *Sov. Phys. Solid State* **17(5)** 932

Kraut, E.A., Lim, T.C. and Tittmann, B.R. [1972] "Application of nonlinear interactions in ferroelectric ceramics to microwave signal processing" *Ferroelectrics* **3** 247

Lardner, R.W. [1983] "Nonlinear surface waves on an elastic solid" *Int. J. Engng. Sci.* **21** 1331

Lardner, R.W. [1984] "Nonlinear Rayleigh waves: Harmonic generation, parametric amplification and thermoviscous damping" *J. Appl. Phys.* **55(9)** 3251

Lardner, R.W. [1985] "Nonlinear effects on transverse shear waves in an elastic medium" *J. Elast.* **15** 53

Lardner, R.W. [1985] "Waveform distortion and shock development in nonlinear Rayleigh waves" *Int. J. Engng. Sci.* **23(1)** 113

Lardner, R.W. [1986] "Nonlinear surface acoustic waves on an elastic solid of general anisotropy" *J. Elast.* **16** 63

Lardner, R.W. and Tupholme, G.E. [1986] "Nonlinear surface waves on cubic materials" *J. Elast.* **16** 251

Lean, E.G. and Tseng, C.C. [1970] "Nonlinear effects in surface acoustic waves" *J. Appl. Phys.* **41(10)** 3912

Lee, Wang and Markenscoff [1975] "Vibrations of crystal plates" *J. Acoust. Soc. Am.* **57(1)** 98

Lim, T.C., Kraut, E.A. and Thompson, R.B. [1972] "Nonlinear materials for acoustic surface wave convolvers" *Appl. Phys. Lett.* **20(3)** 127

Luukkala, M.V. and Kino, G.S. [1971] "Convolution and time-inversion using parametric interactions of acoustic surface waves" *Appl. Phys. Letts.* **18** 393

Mathews, H. [1977] *Surface wave filters,* Wiley, New York

Maugin, G.A. [1985] *Nonlinear electromechanical effects and their applications,* World Scientific Publishing

Miller, R.C. [1964] "Optical second harmonic generation in piezoelectric crystals" *Appl. Phys. Lett.* **5(1)** 17

Monks, T., Paige, E.G.S. and Woods, R.C. [1983] "SAW convolvers using the transverse–horizontal bilinear field" *Electr. Letts.* **19** 466

Morgan, D.P. [1973] "Surface acoustic wave devices and applications: 1. Introductory review" *Ultrasonics* **11** 121

Morgan, D.P. [1974] "Surface acoustic wave devices and applications: 5. Signal processing using programmable nonlinear convolvers" *Ultrasonics* **12** 74

Morgan, D.P [1985] *Surface wave devices for signal processing,* Elsevier

Motz, I.M. and Mason, M.D. [1971] "Nonlinear interaction of microwave electric fields in lithium niobate" *J. Appl. Phys.* **42(3)** 907

Musgrave, M.J.P. [1970] *Crystal acoustics,* Holden-Day, San Francisco, USA

Nakagawa, Y., Yamanouchi, K. and Shibayama, K. [1973] "Third-order elastic constants of lithium niobate" *J. Appl. Phys.* **44(9)** 3969

Nayfeh, A.H. [1973] *Perturbation methods,* Wiley, New York

Nelson, D.F. [1978] "Theory of nonlinear electroacoustics of dielectric, piezoelectric and pyroelectric crystals" *J. Acoust. Soc. Am.* **63(6)** 1738

Nelson, D.F. [1979] *Electric, optic and acoustic interactions in dielectrics,* Wiley, New York

Nye, J.F. [1957] *Physical properties of crystals,* Clarendon Press, Oxford

Parker, D.F. [1985] "Nonlinear dispersion of Rayleigh waves" *Physica* **16D** 385

Parker, D.F. [1988] "Waveform evolution for nonlinear surface acoustic waves" *Int. J. Engng. Sci.* **26** 59

Parker, D.F. and David, E.A. $[1989]_a$ "Nonlinear piezoelectric surface waves" *Int. J. Engng. Sci.* 27 565

Parker, D.F. and David, E.A. $[1989]_b$ "Spreading of nonlinear surface waves" in *Elastic wave propagation* (McCarthy, M.F. and Hayes, M.A., eds) Elsevier Science Publishers

Parker, D.F. and Talbot, D. [1985] "Analysis and computation for nonlinear elastic surface waves of permanent form" *J. Elast.* **15** 389

Planat, M. [1985] "Multiple scale analysis of the nonlinear surface acoustic wave propagation in anisotropic crystals" *J. Appl. Phys.* **57(11)** 4911

Planat, M., Vanderborck, G., Gautier, H. and Maerfield, C. [1985] "Finite element analysis of the piezoelectric waveguide convolver" *IEEE Trans. Sonics and Ultrasonics* SU-**32** 428

Rayleigh, L. [1896] *Theory of Sound,* 2nd Ed. Vol. 2, Macmillan, London

Ristic, V. [1983] *Principles of acoustic devices,* Wiley, New York

Royer, D. and Dieulesaint, E. [1984] "Rayleigh wave velocity and displacement in orthorhombic, tetragonal, hexagonal and cubic crystals" *J. Acoust. Soc. Am.* **76(5)** 1438

Shtykov, V.V., Mason, I.M. and Motz, M.D. [1975] "On the anisotropy of guided acoustic surface wave degenerate convolution" *IEEE Trans, Sonics and Ultrasonics* SU-**22(2)** 131

Smith, R.T. and Welsh, F.S. [1971] "Temporature dependence of elastic, piezoelectric and dielectric constants of lithium tantalate and lithium niobate" *J. Appl. Phys.* **42(6)** 2219

Solodov, I.Y. [1988] "Acoustic nonlinearity of a piezoelectric crystal surface" *J. Appl. Phys.* **64(6)** 2901

Stoneley, R. [1955] *Proc. Roy. Soc. A.* **232** 447

Stroh, A.N. [1962] "Steady state problems in anisotropic elasticity" *J. Math. Phys.* **41** 77

Svaasland, X.X. [1969] "Interaction between elastic surface waves in piezoelectric materials" *Appl. Phys. Letts.* **15(9)** 300

Synge, J.L. [1956] "Elastic waves in anisotropic media" *J. Math. Phys.* **35** 323

Taylor, D.B. and Crampin, S. [1978] "Surface waves in anisotropic media: propagation in a homogeneous piezoelectric halfspace" *Proc. R. Soc. Lond. A* **364** 161

Thompson, R.B. and Quate, C.F. [1971] "Nonlinear interaction of microwave electric fields and sound in lithium niobate" *J. Appl. Phys.* **42(3)** 907

Tiersten, H.F. and Baumhauer, J.C. [1974] "Second harmonic generation and parametric excitation of surface waves in elastic and piezoelectric solids" *J. Appl. Phys.* **45** 4272

Toupin, R.A. [1963] "A dynamical theory of elastic dielectrics" *Int. J. Engng. Sci.* **1** 101

Tupholme, G.E. [1988] "Multiple scale techniques applied to nonlinear elastic and piezoelectric surface waves" in *Recent Developments in Surface Acoustic Waves,*(Maugin, G.A. and Parker, D.F. eds.) Series on Wave Phenomena, Springer-Verlag

Tupholme, G.E. and Harvey, A.P. [1988] "Nonlinear surface acoustic waves on a pizoelectric solid" *Int. J. Engng. Sci.* **26** 1661

Warner, A.W., Onoe, M. and Coquin, G.A. [1967] "Determination of elastic and piezoelectric constants for crystals in class (*3m*)" *J. Acoust. Soc. Am.* **42(6)** 1223

Yashiro, K. and Goto, N. [1978] "Analysis of the generation of acoustic waves on the surface of a semi-infinite piezoelectric solid" *IEEE Trans. Sonics and Ultrasonics* SU-**25** 146

Bender, C.M. and Orszag, S.A. [1978] *Advanced mathematical methods for scientists and engineers,* McGraw-Hill

Grassl, H., Reindl, L. and Wörz, H.-W. [1988] "State-of-the-art elastic SAW convolvers" in *Recent Developments in Surface Acoustic Waves,* (Maugin, G.A. and Parker, D.F. eds.) Series on Wave Phenomena, Springer-Verlag